Report No. NPS 62-88 008

NAVAL POSTGRADUATE SCHOOL

Monterey, California

THESIS

A COMPUTER MODEL INVESTIGATION
OF A
HALF SQUARE LOG-PERIODIC ARRAY

by

Mustafa Erdeviren

December 1987

Thesis Advisor Richard W. Adler

Prepared for:
Naval Ocean Systems Center
San Diego, CA 92152

NAVAL POSTGRADUATE SCHOOL
MONTEREY, CALIFORNIA 93943

This thesis prepared in conjunction with research sponsored in part by Naval Ocean Systems Center.

REPORT DOCUMENTATION PAGE

a. REPORT SECURITY CLASSIFICATION UNCLASSIFIED	1b RESTRICTIVE MARKINGS
a. SECURITY CLASSIFICATION AUTHORITY b. DECLASSIFICATION / DOWNGRADING SCHEDULE	3 DISTRIBUTION / AVAILABILITY OF REPORT Approved for public release; distribution is unlimited
PERFORMING ORGANIZATION REPORT NUMBER(S) NPS-62-88-008	5 MONITORING ORGANIZATION REPORT NUMBER(S)
. NAME OF PERFORMING ORGANIZATION aval Postgraduate School | 6b OFFICE SYMBOL (If applicable) 62	7a NAME OF MONITORING ORGANIZATION Naval Postgraduate School
. ADDRESS (City, State, and ZIP Code) onterey, California 93943-5000	7b. ADDRESS (City, State, and ZIP Code) Monterey, California 93943-5000
. NAME OF FUNDING / SPONSORING ORGANIZATION aval Ocean Systems Center | 8b OFFICE SYMBOL (If applicable)	9 PROCUREMENT INSTRUMENT IDENTIFICATION NUMBER N6227186WR60125
. ADDRESS (City, State, and ZIP Code) San Diego, CA 92152	10 SOURCE OF FUNDING NUMBERS PROGRAM ELEMENT NO. | PROJECT NO | TASK NO | WORK UNIT ACCESSION NO

TITLE (Include Security Classification)
A COMPUTER MODEL INVESTIGATION OF A HALF SQUARE LOG-PERIODIC ARRAY

. PERSONAL AUTHOR(S)
ERDEVIREN, Mustafa

a. TYPE OF REPORT	13b TIME COVERED	14 DATE OF REPORT (Year, Month, Day)	15 PAGE COUNT
Master's Thesis	FROM ______ TO ______	December 1987	167

. SUPPLEMENTARY NOTATION

COSATI CODES			18 SUBJECT TERMS (Continue on reverse if necessary and identify by block number)
FIELD	GROUP	SUB-GROUP	Half Square Log-Periodic Array, Numerical Electromagnetic Code (NEC)

. ABSTRACT (Continue on reverse if necessary and identify by block number)

This thesis investigates the potential of a half square log-periodic array for use by the military over the frequency range of 2 to 30 MHz using a computer simulation technique by numerical methods. Using the Numerical Electromagnetics Code (NEC), a selected model was run in free space and over perfect ground to obtain data for radiation patterns and element currents on the array. After the evaluation of the NEC data, the results of the investigation show that half square log-periodic array with dual feed and switched transmission line has characteristics of a successful log-periodic structure with a unidirectional radiation pattern, over the design frequency range of 2 to 30 MHz, showing promise for military applications.

DISTRIBUTION / AVAILABILITY OF ABSTRACT ☒ UNCLASSIFIED/UNLIMITED ☐ SAME AS RPT ☐ DTIC USERS	21 ABSTRACT SECURITY CLASSIFICATION UNCLASSIFIED
a NAME OF RESPONSIBLE INDIVIDUAL R. W. Adler	22b TELEPHONE (Include Area Code) 408-646-2352 | 22c. OFFICE SYMBOL 62Ab

D FORM 1473, 84 MAR   83 APR edition may be used until exhausted
All other editions are obsolete

SECURITY CLASSIFICATION OF THIS PAGE

Approved for public release; distribution is unlimited.

A Computer Model Investigation
of A
Half Square Log-Periodic Array

by

Mustafa Erdeviren
Captain, Turkish Army
B.S., Naval Postgraduate School, 1987

Submitted in partial fulfillment of the
requirements for the degree of

MASTER OF SCIENCE IN ELECTRICAL ENGINEERING

from the

NAVAL POSTGRADUATE SCHOOL
December 1987

ABSTRACT

This thesis investigates the potential of a half square log-periodic array for use by the military over the frequency range of 2 to 30 MHz using a computer simulation technique by numerical methods. Using the Numerical Electromagnetics Code (NEC), a selected model was run in free space and over perfect ground to obtain data for radiation patterns and element currents on the array. After the evaluation of the NEC data, the results of the investigation show that half square log-periodic array with dual feed and switched transmission line has characteristics of a successful log-periodic structure with a unidirectional radiation pattern, over the design frequency range of 2 to 30 MHz, showing promise for military applications.

TABLE OF CONTENTS

LIST OF TABLES

LIST OF FIGURES

I. INTRODUCTION

A. THE EMERGENCE OF A HALF SQUARE LOG-PERIODIC ARRAY

In order to meet military communications needs, today's military uses a wide variety of communication systems. Military high frequency (HF) communication systems provide different kinds of short, medium, and long range communications capability. The users of military HF communications vary from special teams to high level headquarters. These different requirements necessitate finding a solution to meet all these needs. In this respect, major important design factors for a military HF antenna are a frequency range of 2 to 30 MHz and practicability; that is the ease of deployment of the antenna under the combat conditions.

To meet these requirements, D.V. Campbell and his associates at Fort Monmouth, New Jersey designed a lightweight wire array consisting of half square elements arranged in a log-periodic configuration with dual feed. A prototype of the half square log-periodic antenna was constructed at Fort Monmouth for testing at a frequency range of 8 to 30 MHz. Test results gave an impedance behavior common to a log-periodic antenna thus warranting further investigation. [Ref. 1]

J.R. Johnsen, in his thesis research [Ref. 2] investigated near magnetic fields of a uniformly periodic half square array with dual feed in order to be able to determine the potential of the structure as a half square log-periodic array (HLPA) for use by the military. Taking 2 to 30 MHz as the design frequency range for his model, Johnsen chose 8 MHz as mid-frequency resonance (which is 2 octaves above the lowest and almost 2 octaves below the highest frequency). He modeled a uniformly periodic half square array of 10 elements with double feed. Using the Numerical Electromagnetics Code (NEC) [Ref. 3] he simulated the model on the computer for free space and perfect ground environments with in-phase and anti-phase feed options to obtain data for near magnetic fields and radiation patterns. After collecting the data for near magnetic fields, Johnsen used these data to obtain the k-β relationship of the array. By inspecting the k-β diagrams he tried to identify the frequency regions where backward radiation occurred. Since backward radiation is an important characteristic of successful log-periodic antennas, he ran the model on the computer for the frequencies for which backward radiation on the k-β diagram was observed and obtained radiation patterns. The results of his research led to the conclusion that the potential of designing a successful half square log-periodic antenna with dual feed is good.

The purpose of this thesis is to model a half square log-periodic antenna (HLPA) for different scaling and spacing factors and by using a computer simulation technique to investigate the characteristics of the antenna in order to be able to determine its applicability as a broadband military HF antenna.

B. BROADBAND ANTENNAS

In many applications an antenna must operate effectively over a wide range of frequencies. Generally an antenna with wide bandwidth is referred to as a broadband antenna. In this sense the term " broadband " is a relative measure of bandwidth and varies with the circumstances [Ref. 4]. In practice, a broadband antenna is considered to be the one which retains certain desired or specified radiation pattern, polarization, or impedance characteristics over more than an octave.

C. THE FREQUENCY INDEPENDENT CONCEPT AND LOG-PERIODIC ANTENNAS

The research work which led to the development of antennas whose performance is almost independent of frequency was carried out mainly at the University of Illinois in the period from 1955 to 1958. The work, along with several other projects was sponsored by the Air Force in order to relieve the problems associated with the increasing numbers of different electromagnetic systems and equipment being carried on high-speed military aircraft. So many different antennas were required that finding locations for the antennas was a serious problem. It was recognized that the problem would be relieved if a given antenna could serve several systems and frequencies, and consequently the Air Force sponsored a research program on the general subject of broadband antennas.

In connection with the sponsored research work on broadband antennas, Professor V.H. Rumsey, then antenna laboratory director at the University of Illinois realized that the features which introduce frequency dependence are the characteristic lengths of the structure. Antenna performance is generally a function of length/wavelength. On the other hand, by the principle of modeling or scaling, to ensure that a given type of structure has the same performance at different frequencies, it is only necessary to scale the size of the structure in the ratio of frequencies. Thus, Rumsey concluded that the structural feature required for frequency independent operation is the absence of characteristic lengths. With this feature a structure could be self-scaling. But what kind of physical structure is there that has no characteristic lengths ? Rumsey's answer was that the structure should be completely described by angles. Thus he put forward the "angle concept," which said, essentially, that a structure whose shape is defined by angles alone, with no characteristic length, should be a frequency-independent structure.

In looking for structures that can be defined by angles alone, the first that come to mind are the infinite biconical antenna and the infinite bifin (bow-tie) antenna. However, practical versions of these structures are obviously finite in size, and although these structures do have comparatively broadband tendencies, the truncation to a finite size introduces a characteristic length and this destroys the frequency-independent behavior. [Ref. 5]

Next, R.H. DuHamel (then a research assistant professor at the University of Illinois) continued with the design of a broadband antenna with linear polarization. He realized that the bifin or bow-tie antenna could be constructed in a self complementary fashion and of course that it radiates linear polarization. But he also realized that the bandwidth of the bifin was limited because of the truncation, or more particularly, because the currents were not negligible at the point of truncation. Consequently, the problem was to somehow alter the bow-tie structure in such a way as to cause the currents to fall off with distance from the feed point more rapidly than usual. His method of accomplishing this was to introduce discontinuities, for example, teeth, into the fins in an attempt to increase the radiation and speed up the decay of current. But the question was,"How should the teeth be designed?" DuHamel decided to adhere to Rumsey's angle concept and to cut the teeth along circular arcs and let the length of the arcs be determined by an angle (see Figure 1.1).

However, this did not fix the tooth spacing, since the latter could not be specified by angles alone. In trying to solve the spacing problem, DuHamel noticed that on the equiangular structure (a successful structure), along a line drawn from the center outward, the spacings from one conductor to the next were in a constant ratio. He therefore considered spacing the teeth in the bifin such that the spacings were in a constant ratio. He accomplished this by choosing the radii of the circular arcs forming the corresponding parts of the successive teeth such that they were in a constant ratio, $R_{n+1} / R_n = \tau$. He recognized that the structure would not necessarily be frequency independent but that, on the other hand, the performance on an infinite structure

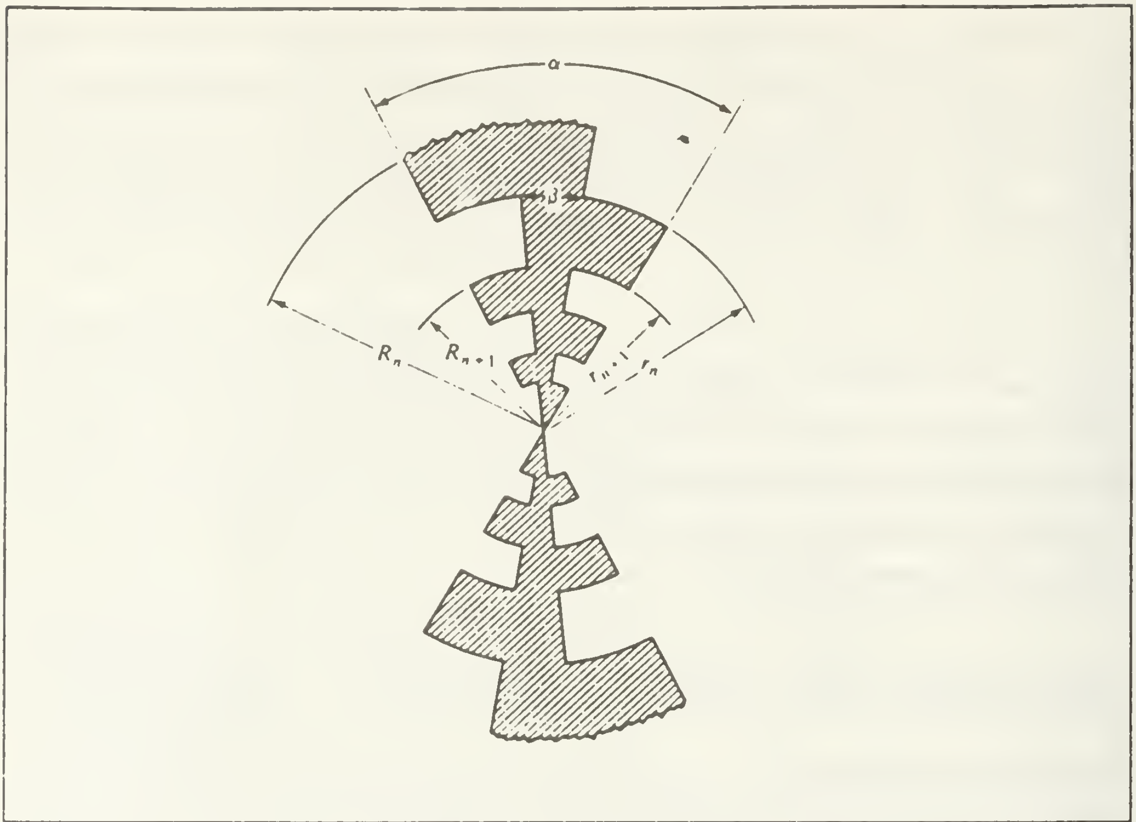

Figure 1.1 Log-periodic toothed structure (self complementary).

would be identical at a discrete number of frequencies. In fact, if the structure has a performance at frequency f_1, the performance should be identical at frequencies τf_1, $\tau^2 f_1$, $\tau^3 f_1$, and so on as long as the structure is modeled accurately at the feed point and is effectively infinite in size (i.e., current zero at the point of truncation). Again τ is the common ratio of distances. The frequencies at which the performance should be identical are related by the equation $f_n = f_{n+1}\tau$, or $\log f_{n+1} = \log f_n + \log (1/\tau)$. Inspection of this latter equation shows that the performance is a periodic function of the logarithm of the frequency (i.e., the frequencies at which the performance is the same are spaced equally when plotted on log paper). Thus, these types of structures were subsequently named *log-periodic* antennas.

After DuHamel's findings many structures of this type were built and tested. Some were less successful than others.

The next major step came with Isbell's invention of the log-periodic dipole array. His work was motivated by the desire to develop broadband arrays of more conventional construction. Thus he decided to build and test an antenna array constructed of conventional wirelike elements; however, the length of the elements were determined by an angle α as before, and the spacings were such as to give the log-periodic type of behavior; that is successive distances between the apex and the elements were in a constant ratio, $R_{n+1} / R_n = \tau$ (Figure 1.2).

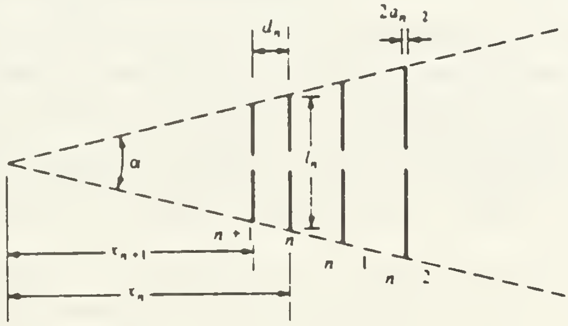

Figure 1.2 Log-periodic dipole construction.

The experiments with the structure demonstrated that in a certain range of values for τ and α, the structure was indeed a broadband log-periodic structure with a unidirectional pattern. Isbell also demonstrated experimentally that most of the radiation was coming from those dipole elements which were in the vicinity of a half wavelength long and that the currents and voltages at the large end of the structure were negligible within the operating band of frequencies. Finally, it was shown once again that the operating band of frequencies was bounded on the high side by frequencies corresponding to the size of the smallest elements and on the low side by the frequencies at which the largest dipole element is about a half wavelength long.

A careful and extremely valuable analysis of the log-periodic dipole array was made by R.L. Carrel in a doctoral dissertation. The physical makeup of the log-periodic array is such that an analysis of it may be based on more or less conventional theory of linear antennas and transmission lines. The main difficulty is the inherent complication. Carrel's analysis consisted of breaking the overall problem into parts, each of which was programmed for the digital computer. First, making the assumption that the element currents were sinusoidally distributed, he computed in the conventional way the mutual impedances between the dipole elements and the self-impedance of each element. In the second part of the problem, Carrel focused his attention on the parallel-wire transmission line, fed at one end shunt-loaded with impedances corresponding to the dipole antenna elements having sizes and spacings characteristic of log-periodic arrays; of course, the impedance values came from the first part of his computer program. He carried out (on a digital computer) a circuit analysis to find the input impedance, voltages, and the currents on the loaded transmission line, together with the base (i.e., input) currents at each antenna element. As the last part of the problem, with the specific values for the magnitude and phase of the currents in the antenna elements, he calculated the radiation patterns. Having developed a systematic computer program, Carrel completed calculations on more than 100 different log-periodic dipole designs. He then compared the results of several of these with corresponding experimental models. The measurements included not only impedances and radiation patterns but also the voltage and current distributions in the structure. The agreement between the computer output and the experimental results was excellent. Carrel's work provided a set of design curves which show how to adjust the dimensions of a structure in order to meet specified design objectives.

D. GENERAL CHARACTERISTICS OF SUCCESSFUL LOG-PERIODIC ANTENNAS

From the results of successful log-periodic antennas, some general characteristics can be cited as follows :

* Log-periodic antennas have a special kind of repetitiveness in their physical structure which results in a repetitive behavior of the electrical characteristics. The impedance is a logarithmically periodic function of frequency. That is, if a plot is made of the input impedance as a function of logarithm of the frequency, the variation will be periodic. Radiation patterns vary in the same manner, along with such parameters as the directive gain, beamwidth, and side-lobe level. [Ref. 6]
* Excitation of the antenna or array is from the high frequency or small end.

* Backfire radiation (in the case of unidirectional radiators) occurs, so that the antenna "fires" through the small part of the structure, with the radiation in the forward direction being zero or at least very small. For bidirectional antennas the backfire requirement is replaced by a requirement for broadside radiation. In any case the radiation in the forward direction along the surface of the antenna (which theoretically extends to infinity) must be zero or very small.
* A transmission region is formed by the inactive portion of the antenna between the feed point and the active region. This transmission line region should have the proper characteristic impedance and negligible radiation.
* An active region exists from which antenna radiates strongly because of a proper combination of current magnitudes and phasings. The position and phasing of these radiating currents produce a very small radiation field along the surface of the antenna or array in the forward direction, and a maximum radiation field in the backward direction.
* An inactive or reflection region exists beyond the active region. All successful frequency independent antennas must exhibit a rapid decay of current within and beyond the active region, so that operation will not be affected by truncation of the structure. A major cause of the rapid current decay is, of course, the large radiation of energy from the active region. [Ref. 7]

II. NUMERICAL CONSIDERATIONS AND PROCEDURE

A. SELECTED METHOD OF INVESTIGATION

The method of investigation of the Half Square Log-Periodic Array was planned in two steps. The first step was to design several computer models of the Half Square Log-Periodic Array with different scaling and spacing factors and to compare the performances of these models in terms of the antenna parameters, such as radiation patterns, half-power beamwidth, front-to-back ratio, and input impedance, and depending on the results, to determine the most promising model. The second step was to run the selected model on the computer by using NEC to get data both for radiation patterns and near magnetic fields. Examination of the radiation patterns is the most effective way to see the performance of log-periodic antennas. The purpose of getting near magnetic fields data in addition to radiation fields data was for an attempt to obtain the k-β diagrams of the half square log-periodic array by using near magnetic fields data and to see the relation between the radiation patterns and the k-β diagram. The importance of the k-β diagram comes from the fact that in uniformly periodic arrays it is possible to identify the frequency regions where backward radiation occurs by examining the k-β diagram. A uniformly periodic array is one in which all the elements, dimensions and, spacing between the elements are the same. Since backward radiation is an important characteristic of successful log-periodic antennas, a k-β diagram is a very useful tool in determining the potential of a candidate log-periodic structure by analyzing the k-β diagram of its uniformly periodic counterpart. For the log-periodic case it is not easy to obtain the k-β diagram. The k-β diagram approach used in the analysis of the uniformly periodic structures is based on the analysis of infinite length structures. Since practical structures are of finite length, their current distribution usually will be different than that of the infinite length structures and some deviations in behavior may occur even in uniformly periodic structures. For example, the boundary lines between the various length regions are not sharply defined. Effective radiation may occur from a finite structure at frequencies where the phase constant lies within the slow-wave region [Ref. 8]. Secondly, in the uniformly periodic case, d is constant and k is the controlled variable in obtaining the k-β diagram. For the log-periodic case, the period, d, continually increases as one moves away from the feed with the frequency fixed. By fixing k and making d variable, a k-β diagram for the log-periodic structure may be obtained. With this approach, it is assumed that β on the log-periodic structure is determined only by local behavior of the structure [Ref. 9]. Also, since a log-periodic structure is not uniform, at a given frequency different space harmonic phase constants are found for each cell along the structure. For these reasons different approaches, other than the k-β diagram approach, are generally used in the analysis of log-periodic structures. One of the methods used in this thesis is evaluation of amplitude and phase plots of element currents to determine regions which create backfire radiation and comparison of this information with radiation patterns.

For accuracy, a double precision version of the Numerical Electromagnetics Code (NEC) was used throughout the simulation process.

B. NUMERICAL ELECTROMAGNETICS CODE (NEC)

Half square log-periodic arrays used in this thesis were modeled on the IBM system 370 main-frame computer by using the Numerical Electromagnetics Code (NEC), version three. NEC has been developed at the Lawrence Livermore Laboratory, Livermore, California, under the sponsorship of the Naval Ocean Systems Center and The Air Force Weapons Laboratory.

It is a user oriented computer code for analyzing the electromagnetic response of antennas and other metal structures by evaluating the numerical solutions of integral equations for currents induced on the structure by incident fields or sources.

The code can handle models with nonradiating networks and transmission lines connecting parts of the structure, imperfect or perfect conductors, and lumped element loading. Structures may also be modeled in free space or over a ground plane that may be either a perfect or imperfect conducter.

Structures may be excited either by voltage sources on the structure or by an incident plane wave which may be linearly or elliptically polarized. NEC outputs may include currents and charges, radiated fields and near electric or magnetic fields. For better accuracy calculations double precision versions are also available to the user.

C. DEVELOPMENT OF THE COMPUTER MODEL

The major consideration in selection of computer model was the tradeoff between antenna performance and deployment capability. As the number of the elements in the array increases, the performance of the antenna also increases, but, construction of the antenna will require more time and manpower, which are crucial factors under battle conditions. Therefore a computer model must be chosen which is operationally practical.

Because the performance of the antenna can be determined from its far field radiation patterns, originally an array of 10 elements was modeled and run on the computer for radiation pattern evaluation. Far field radiation patterns for a 10-element half square log-periodic array did not show good performance. Following this, a 13-element array was modeled. The performance was better than that of the 10-element array, but was not good enough.

After observing the results of the 13-element half square log-periodic array the final model was designed. At the start of the design the only parameter available was the required operational frequency range of 2 to 30 MHz. Since the radiating elements are to be approximately half wavelength long at the operating frequency, the length of the longest element was 75 M. Considering that the length of the array should be around one wavelength long at the lowest frequency, the distance from the apex to the longest element was 150 M. From these parameters the apex angle α was found as 28.14 ° from $\tan \alpha/2 = L_n/2R_n$. Here L_n is the length of the longest element and R_n is the distance from apex to the longest element. The selection of the scale factor, τ, was somewhat arbitrary. Since, higher values of τ require more elements in the array Carrel's design curves for dipoles were examined (although it is not known whether his information is applicable to the half square or not) and a value of 0.84 was chosen. Using this scale factor and the length of the longest element, lengths of other elements were determined. Seventeen elements were required to cover the 2-30 MHz frequency range. Figure 2.1 shows the structural geometry of the half square log-periodic array. For ease of computer modeling, the structure was placed on the X-Y plane, the shortest element being at the origin and the array extending along the X axis. The lengths of the elements and their distances from the origin along with their corresponding resonant frequencies are shown in Table 1.

Based on Johnsen's findings for the uniformly periodic array, an implicit transmission line of 300 Ohms was used in the NEC model. An implicit transmission line model is one in which the currents on the wire segments which are connected to the ends of the transmission line are modified by using ideal, non-radiating transmission line equations. This neglects transmission line attenuation due to radiation, conductor and dielectric losses and assumes balanced currents. Johnsen showed that the half square log-periodic array is a balanced structure and NEC allows transmission lines on balanced structures to be modeled by implicit transmission line equations. The use of implicit transmission line equations allows the treatment of transmission lines as two port networks by defining characteristic impedance and length and calculating response. Implicit transmission lines reduce the number of wire segments in a model, thus the size of the matrix necessary to evaluate currents is reduced.

Since the half square log-periodic array is constructed with half square elements and each element consists of two quarter square elements connected together by an insulated connector on the horizontal wire, to make the model precise to the highest degree possible the lengths of the insulators between the elements were scaled by scale factor. The insulators were modeled as open circuits. In order to see the effect of the scaling on element wire thickness, model was run for scaled wire diameters but no significant variation on performance was observed. Both "in-phase" and "anti-phase" excitation were tested to establish the usefulness of each. In-phase excitation is where both sets of corners on a half square element are fed with the same phase. In anti-phase excitation, the phase difference between corners is 180° Anti-phase excitation was chosen because the desired unidirectional azimuth radiation pattern is produced. With in-phase excitation, radiation from currents on the horizontal portion of the elements cancel producing azimuthal nulls on-axis, which are undesired.

Data sets used for the computer simulation are listed in Appendix A and Appendix B.

D. FAR-FIELD RADIATION PATTERNS

Since there is not a well established methodology for the analysis of log-periodic antennas, mostly the analysis of the performance is experimental. In this respect radiation patterns are one of the key parameters for evaluating the performance of log-periodic antennas. For this research, radiation patterns were calculated at the resonant, and also in-between frequencies in free space and on perfect ground environments with in-phase and anti-phase excitation options using NEC.

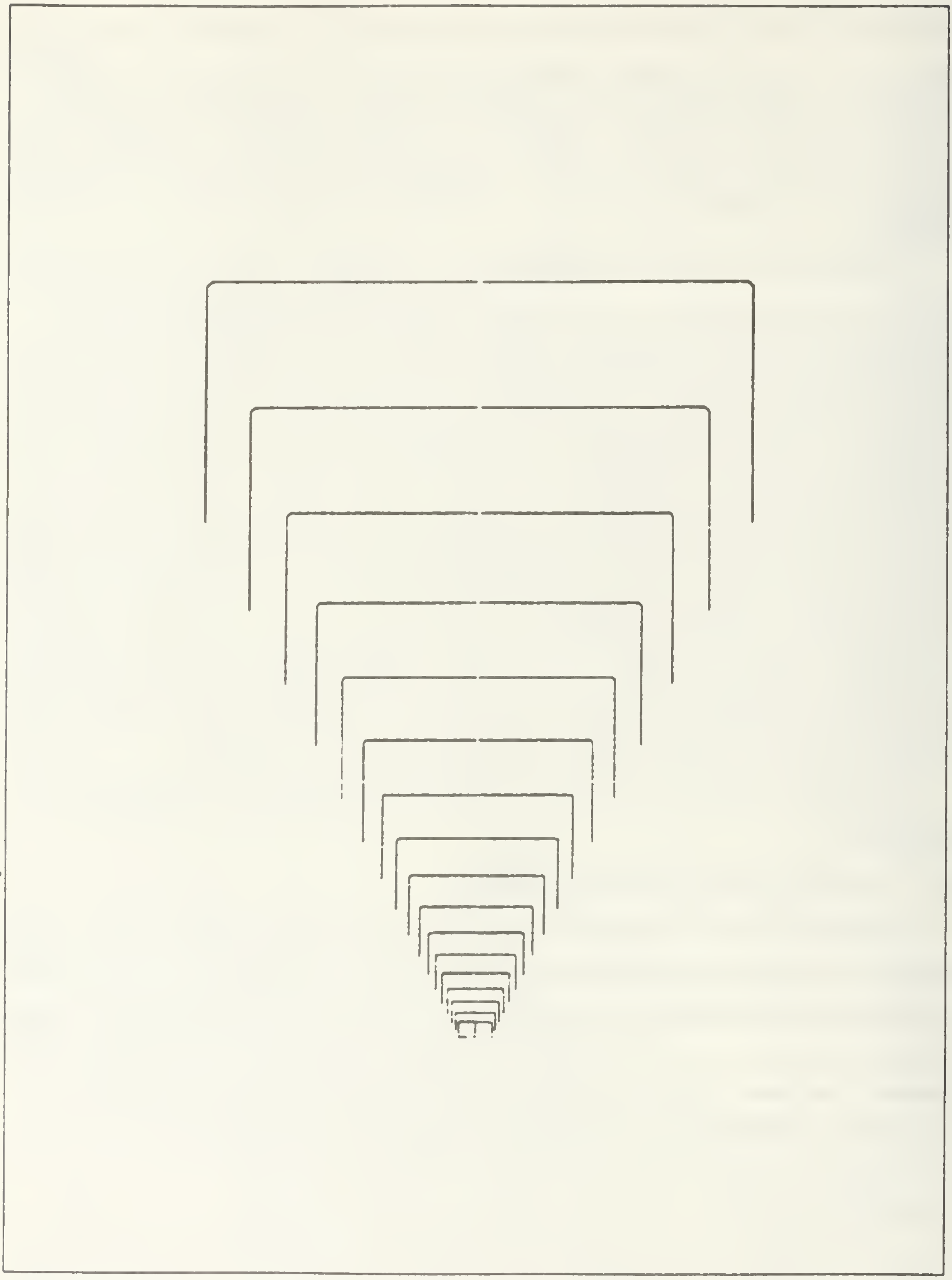

Figure 2.1 Half Square Log-Periodic Array.

TABLE 1

HLPA DESIGN PARAMETERS

Element No.	Frequency (MHz)	Distance (m)	Length (m)
1	32.55	0.0	4.61
2	27.34	1.76	5.49
3	22.96	3.85	6.53
4	19.29	6.33	7.77
5	16.20	9.29	9.25
6	13.61	12.82	11.02
7	11.43	17.02	13.12
8	9.60	22.02	15.62
9	8.06	27.96	18.59
10	6.77	35.05	22.13
11	5.69	43.48	26.34
12	4.78	53.52	31.37
13	4.01	65.46	37.34
14	3.37	79.68	44.45
15	2.83	96.62	52.92
16	2.38	116.78	63.00
17	2.00	140.78	75.00

III. EXPERIMENTAL RESULTS

The selected model was first run with in-phase and anti-phase excitation with a switched transmission line in free space, then over perfect ground. Switching is the transposition of the transmission line between adjacent elements as seen in Figure 1.2 to generate a 180° phase reversal. The data collected included radiation patterns and magnitude and phase plots of near magnetic fields.

A. RADIATION PATTERNS

Free space radiation patterns with anti-phase excitation showed the expected backfire radiation. (Backfire radiation is directed toward the point of excitation, a trait which appears to be inherent in most of the successful unidirectional log-periodic antennas, and is believed to be the result of a space wave traveling along the structure in the direction opposite to the phase progression of currents in the feed line.) The backward-traveling wave is due to the existence of backward space harmonics in the spectrum of the periodic structure. The periodic structure should be such as to produce only waves which are quite slow at the frequencies where radiation is not intended. At frequencies where radiation is intended, one or more of the space-harmonic waves should be "fast" or almost fast. Thus, for the log-periodic structure, a feeder wave progresses toward the active (radiating) region under slow wave conditions. According to this theory, the dominant space harmonic in the active region propagates in the backward direction [Ref. 8]. Between 2 and 5 MHz, although the main radiation is in the backfire direction, the front-to-back ratio is lower than that of for the rest of the frequency range. There seems to be one major reason for this, namely "truncation effect". If the structure were of infinite type the properties would repeat periodically and there would not be any performance variation. Near the low-frequency cutoff of 2 MHz, a sizable reflection of the fundamental wave (end effect) is produced by the rear truncation. This reflected wave then travels back along the structure in the opposite direction, passing through the active region a second time where it is partially radiated. The resulting radiation pattern from this second pass is a reduced mirror image of the main pattern from the first pass of the fundamental wave [Ref. 10]. As the frequency is increased the electrical properties of the truncated structure converge to characteristic values. So for our case 5 Mhz. presents a low-frequency limit; above this frequency the properties display fairly small variations. Figure 3.1 shows a sample radiation pattern in free space. Appendix C includes other radiation patterns calculated in free space. Patterns show an average half power beamwidth of 56° and an average gain of 4 dB. at resonant frequencies. In Table 2 the antenna parameters, power gain, half power beamwidth, and input impedance are shown for resonant frequencies in free space.

Radiation patterns taken over perfect ground showed similar results except for higher and more stable gain and half power beamwidth values. A sample radiation pattern plotted over perfect ground is shown in Figure 3.2 and the antenna parameters, half power beamwidth, power gain, and input impedance values for resonant frequencies are shown in Table 3. Appendix D contains other radiation patterns taken over perfect ground. As can be seen from radiation patterns as the frequency increases the back lobe gets smaller and radiation in the forward direction gets stronger. This is an indication of the smooth transfer of functions of one resonant element to the next.

B. AMPLITUDE AND PHASE DISTRIBUTIONS OF ELEMENT CURRENTS

Appendix E shows amplitude and phase plots of element currents for the half square log-periodic array in free space for resonant frequencies. Appendix F shows amplitude and phase plots of element currents for resonant frequencies over perfect ground. These plots clearly show the possibility of obtaining a leading phase shift along some portion of the structure that will produce backfire radiation. On the plots, the leftmost point corresponds to the smallest element which is half-wavelength long at the highest cut-off frequency. The feed line is connected to the array at this element. The rightmost point corresponds to the longest element which is half wavelength long at lowest cut-off frequency of 2 Mhz. From the amplitude and phase plots of element currents it can be observed that small contributions from those elements close to feed point tend to cancel each other because of the a phase difference of almost 180°. Currents are strongest mainly on a few elements in front of the element which is closer in length to a half wavelength of the operating frequency. These elements form the active region of the array. For these elements, the phase shift along the structure shows a leading phase condition. The leading phase condition corresponds to a backward traveling wave and leads to directivity which is predominantly backfire. Following the element closest in length to the resonant frequency, the current amplitude falls off suddenly showing a desired end-effect. As the operating frequency is increased or decreased the active region moves along the array but radiation patterns vary only slightly.

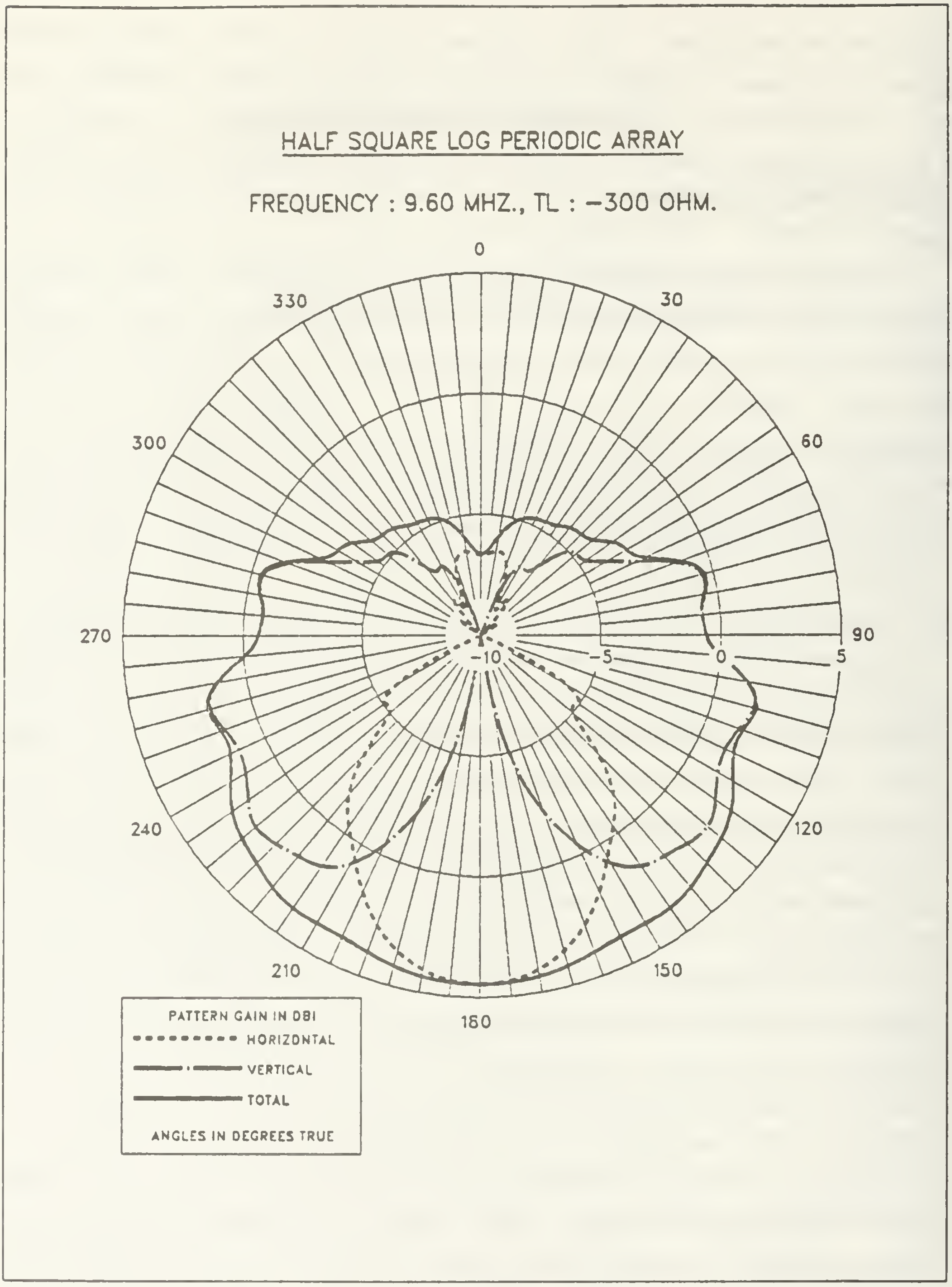

Figure 3.1 Horizontal Pattern, Frequency: 9.60 MHz.

TABLE 2

NUMERICAL RESULTS
IN FREE SPACE

Frequency (MHz)	HPBW (degrees)	Gain (dB)	Input impedance (real and imaginary)
2.0	68	2.15	236 -187
2.38	64	3.74	215 -180
2.83	66	3.26	256 -221
3.37	60	3.90	255 -189
4.07	58	4.08	333 -192
4.78	64	3.66	418 -195
5.69	58	4.20	462 -45.2
6.77	56	4.29	460 63
8.06	56	4.40	340 150
9.60	54	4.45	214 136
11.43	52	4.54	145 64.3
13.61	56	4.39	117 -22
16.20	54	4.41	151 -125
19.29	56	4.80	337 -193
22.96	58	4.26	219 38.8
27.34	54	3.65	77 -102

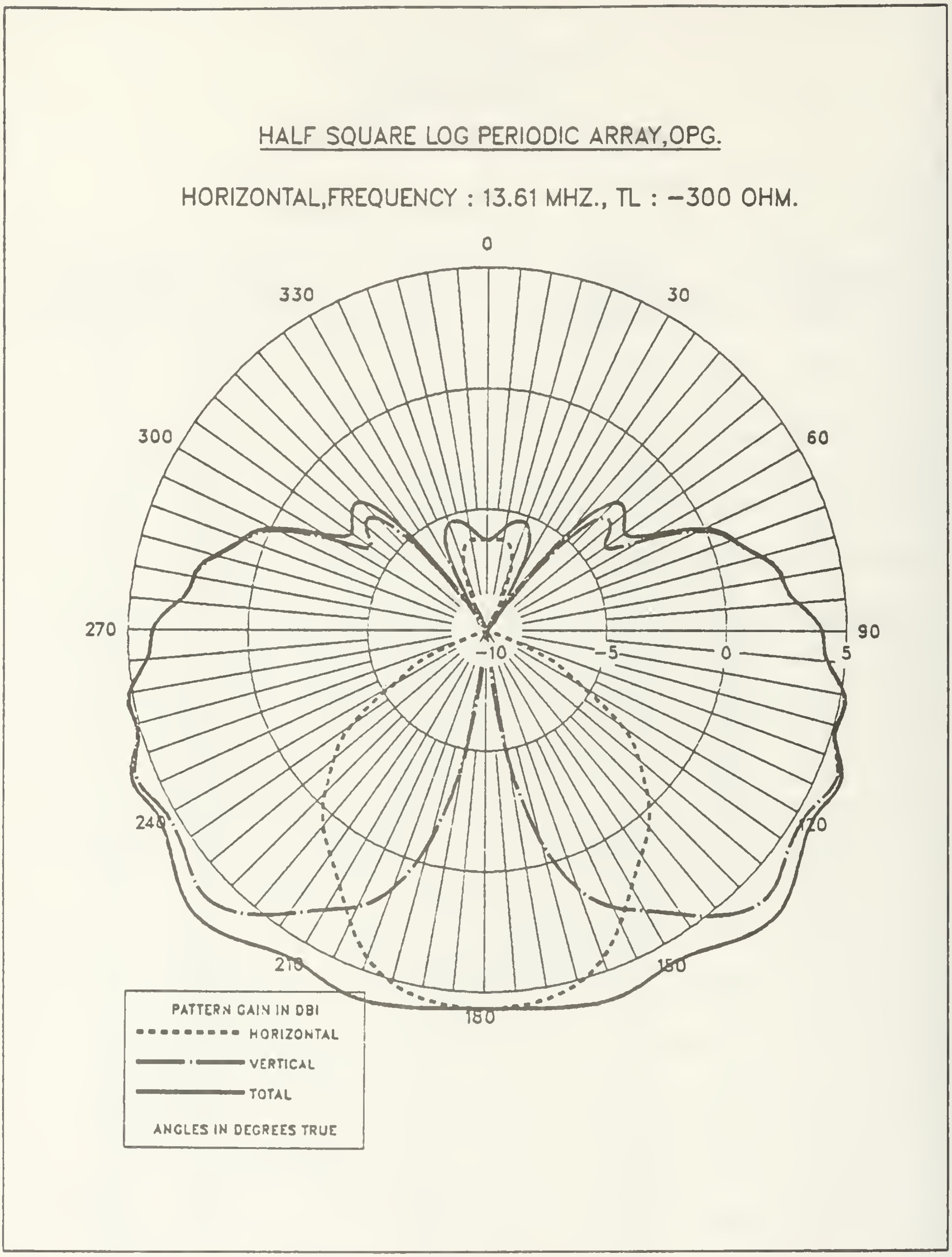

Figure 3.2 Horizontal Pattern, Frequency: 13.61 MHz.

TABLE 3

NUMERICAL RESULTS
OVER PERFECT GROUND

Frequency (MHz)	HPBW (degrees)	Gain (dB)	Input impedance (real and imaginary)
2.0	72	3.35	157 -47
2.38	66	5.31	135 -43.3
2.83	68	5.19	151 -83
3.37	62	5.14	136 -62
4.01	62	5.91	160 -79.1
4.78	70	6.28	186 -123
5.69	58	5.55	199 -118
6.77	58	5.56	239 -145
8.06	58	5.69	309 -143
9.60	56	5.66	387 -62
11.43	56	5.67	349 75
13.61	56	5.67	211 84
16.20	56	5.69	137 9.7
19.29	56	5.91	152 -110
22.96	60	5.21	257 -193
27.34	54	5.29	50 -37.5

IV. CONCLUSIONS AND RECOMMENDATIONS

A. CONCLUSIONS

This thesis investigated the potential of a half square log-periodic array for use by the military over the specific high frequency range of 2 to 30 MHz. Using the Numerical Electromagnetics Code (NEC) a computer model of half square log-periodic array with dual feed was used to obtain data for plotting radiation patterns and amplitude and phase plots of the element currents for evaluation of the performance of the array. The model was run with a transmission line impedance value of 300 Ohms which had been shown by Johnsen [Ref. 2] to be the optimum. The model was also run with impedance values below and above 300 Ohms verifying 300 Ohms as optimum.

The model was run in free space and over perfect ground with different combinations of switched and unswitched transmission line and in-phase and anti-phase feed options. Radiation patterns and amplitude and phase plots of the element currents were used to evaluate the performance of the antenna. Since there is not a well established method, examination of the radiation patterns was the major tool for determination of the performance of the array. The results can be listed as follows:

* The half square log-periodic array with dual feed shows the characteristics of a successful log-periodic structure. Structure shows a unidirectional "backfire" radiation pattern, radiation being directed towards the small end of the array.
* The structure keeps almost the same performance over the entire design frequency range with small variations. But, between 2 and 5 MHz, there is a performance degradation because of the truncation effect. As the frequency increases performance of the antenna is stabilized and variations get smaller.
* With these design parameters the array gives an average power gain of 5.2 dB. and an average half power beamwidth (HPBW) of 57°
* It can be said that it would be possible to get a more directive radiation pattern and higher gain from the structure using a higher scale factor, but this in turn would require more elements to cover the frequency range making the construction of the array unpractical when considered for military use. With these design parameters, although it is still a big structure, it would not be difficult to construct the array at high levels of command for this frequency.

The most important conclusion which can be drawn from this study is that the half square log-periodic array shows the characteristics of a successful log-periodic structure. When considered for use at much higher frequencies the dimensions of the elements will be much smaller making it possible to use higher scale factor values for higher gain and directivity.

B. RECOMMENDATIONS

Based on the results of the study, the following recommendations are made :

* This study investigated the half square log-periodic array in free space and over perfect ground. Although, the results show satisfactory performance, a study of the array should be done over lossy ground to see what additional effects occur because of the lossy ground.
* The study was limited by considerations of frequency range and military application. To satisfy these considerations a lower value of scale factor was used in order to make the array practical for the military. Although performance is satisfactory with these design parameters over this frequency range, it should be possible to get better performance at much higher frequencies using higher values of scale factor (since the overall dimensions of the array will be much smaller). Even at the 2 to 30 MHz range, when considered for civilian use at a fixed site, the array can be constructed with more elements for better gain and directivity.
* Following near magnetic field analysis of uniformly periodic half square array by Johnsen [Ref. 2], this thesis formed the second step in study of half square log-periodic array. Johnsen investigated near magnetic fields of uniformly periodic half square array and obtained k-β diagrams. From the k-β diagrams, he identified frequency regions showing backward radiation, suggesting that a log-periodic half square array would support backward radiation. In the absence of a well established theoretical approach for log-periodic antenna design, the method used in this combined study and first suggested by Mayes, Deschamps, and Patton [Ref. 8] has proven to be very successful and less time consuming. It is therefore recommended that before attacking log-periodic structures directly, a near field investigation of the uniformly periodic counterparts may give insight to log-periodic performance. Analysis of k-β diagrams of uniformly periodic structures can provide clues to the performance of log-periodic counterparts. If the study of uniformly periodic structures proves fruitful, it is highly probable that log-periodic counterparts will give good broadband performance. Near field analysis of uniformly periodic counterparts of many successful and unsuccessful structures shows this to be the case.

APPENDIX A
NEC DATA FILE FOR FREE SPACE

```
CM HALF SQUARE LOG PERIODIC ARRAY
CM 17 ELEMENTS, TL:-300 , ANTI PHASE DUAL FEED
CM TAU:0.84,SIGMA:0.16,ALPHA:28.072 DEGREE
CM ARRAY LENGTH:140.784 M.
CM IN FREE SPACE
CE FREQUENCY:10.0 MHZ.
GW 31,6, 0,-.02,2.349, 0,-2.304,2.349, .000814
GW 1,1, 0,-2.304,2.349, 0,-2.349,2.304, .000814
GW 51,6, 0,-2.349,2.304, 0,-2.349,0, .000814
GW 32,6, 1.756,-.024,2.797, 1.756,-2.743,2.797, .000814
GW 2,1, 1.756,-2.743,2.797, 1.756,-2.797,2.743, .000814
GW 52,6, 1.756,-2.797,2.743, 1.756,-2.797,0, .000814
GW 33,6, 3.845,-.028,3.33, 3.845,-3.265,3.33, .000814
GW 3,1, 3.845,-3.265,3.33, 3.845,-3.33,3.265, .000814
GW 53,6, 3.845,-3.33,3.265, 3.845,-3.33,0, .000814
GW 34,6, 6.333,-.034,3.964, 6.333,-3.887,3.964, .000814
GW 4,1, 6.333,-3.887,3.964, 6.333,-3.964,3.887, .000814
GW 54,6, 6.333,-3.964,3.887, 6.333,-3.964,0, .000814
GW 35,6, 9.295,-.04,4.719, 9.295,-4.628,4.719, .000814
GW 5,1, 9.295,-4.628,4.719, 9.295,-4.719,4.628, .000814
GW 55,6, 9.295,-4.719,4.628, 9.295,-4.719,0, .000814
GW 36,6, 12.821,-.048,5.618, 12.821,-5.509,5.618, .000814
GW 6,1, 12.821,-5.509,5.618, 12.821,-5.618,5.509, .000814
GW 56,6, 12.821,-5.618,5.509, 12.821,-5.618,0, .000814
GW 37,6, 17.019,-.057,6.688, 17.019,-6.559,6.688, .000814
GW 7,1, 17.019,-6.559,6.688, 17.019,-6.688,6.559, .000814
GW 57,6, 17.019,-6.688,6.559, 17.019,-6.688,0, .000814
GW 38,6, 22.016,-.068,7.961, 22.016,-7.808,7.961, .000814
GW 8,1, 22.016,-7.808,7.961, 22.016,-7.961,7.808, .000814
GW 58,6, 22.016,-7.961,7.808, 22.016,-7.961,0, .000814
GW 39,6, 27.965,-.081,9.478, 27.965,-9.295,9.478, .000814
GW 9,1, 27.965,-9.295,9.478, 27.965,-9.478,9.295, .000814
GW 59,6, 27.965,-9.478,9.295, 27.965,-9.478,0, .000814
GW 40,6, 35.047,-.096,11.283, 35.047,-11.066,11.283, .000814
GW 10,1, 35.047,-11.066,11.283, 35.047,-11.283,11.066, .000814
GW 60,6, 35.047,-11.283,11.066, 35.047,-11.283,0, .000814
GW 41,6, 43.478,-.114,13.303, 43.478,-13.174,13.303, .000814
GW 11,1, 43.478,-13.174,13.303, 43.478,-13.303,13.174, .000814
GW 61,6, 43.478,-13.303,13.174, 43.478,-13.303,0, .000814
GW 42,6, 53.515,-.136,15.991, 53.515,-15.683,15.991, .000814
GW 12,1, 53.515,-15.683,15.991, 53.515,-15.991,15.683, .000814
GW 62,6, 53.515,-15.991,15.683, 53.515,-15.991,0, .000814
GW 43,6, 65.464,-.162,19.037, 65.464,-18.670,19.037, .000814
GW 13,1, 65.464,-18.670,19.037, 65.464,-19.037,18.670, .000814
GW 63,6, 65.464,-19.037,18.670, 65.464,-19.037,0, .000814
GW 44,6, 79.689,-.193,22.663, 79.689,-22.226,22.663, .000814
GW 14,1, 79.689,-22.226,22.663, 79.689,-22.663,22.226, .000814
GW 64,6, 79.689,-22.663,22.226, 79.689,-22.663,0, .000814
GW 45,6, 96.624,-.23,26.980, 96.624,-26.460,26.980, .000814
GW 15,1, 96.624,-26.460,26.980, 96.624,-26.980,26.460, .000814
GW 65,6, 96.624,-26.980,26.460, 96.624,-26.980,0, .000814
GW 46,6, 116.784,-.273,32.119, 116.784,-31.5,32.119, .000814
GW 16,1, 116.784,-31.5,32.119, 116.784,-32.119,31.5, .000814
GW 66,6, 116.784,-32.119,31.5, 116.784,-32.119,0, .000814
GW 47,6, 140.784,-.326,38.237, 140.784,-37.5,38.237, .000814
GW 17,1, 140.784,-37.5,38.237, 140.784,-38.237,37.5, .000814
GW 67,6, 140.784,-38.237,37.5, 140.784,-38.237,0, .000814
GX 100,010
GE
TL 1,1,2,1, -300, 1.755
TL 2,1,3,1, -300, 2.09
```

```
TL 3,1,4,1, -300, 2.488
TL 4,1,5,1, -300, 2.962
TL 5,1,6,1, -300, 3.526
TL 6,1,7,1, -300, 4.198
TL 7,1,8,1, -300, 4.997
TL 8,1,9,1, -300, 5.949
TL 9,1,10,1, -300, 7.082
TL 10,1,11,1, -300, 8.431
TL 11,1,12,1, -300, 10.037
TL 12,1,13,1, -300, 11.949
TL 13,1,14,1, -300, 14.225
TL 14,1,15,1, -300, 16.934
TL 15,1,16,1, -300, 20.16
TL 16,1,17,1, -300, 24.0
TL 101,1,102,1, -300, 1.755
TL 102,1,103,1, -300, 2.09
TL 103,1,104,1, -300, 2.488
TL 104,1,105,1, -300, 2.962
TL 105,1,106,1, -300, 3.526
TL 106,1,107,1, -300, 4.198
TL 107,1,108,1, -300, 4.997
TL 108,1,109,1, -300, 5.949
TL 109,1,110,1, -300, 7.082
TL 110,1,111,1, -300, 8.431
TL 111,1,112,1, -300, 10.037
TL 112,1,113,1, -300, 11.949
TL 113,1,114,1, -300, 14.225
TL 114,1,115,1, -300, 16.934
TL 115,1,116,1, -300, 20.16
TL 116,1,117,1, -300, 24.0
EX 0,0,7,0,-1,0
EX 0,0,228,0,1,0
FR 1,1,,10.0,0,
PL 2,2,1,1
NH 0,1,1,1, 0,-2.327,2.327, 1,1,1
PL 2,2,1,1
NH 0,1,1,1, 1.756,-2.770,2.770, 1,1,1
PL 2,2,1,1
NH 0,1,1,1, 3.845,-3.298,3.298, 1,1,1
PL 2,2,1,1
NH 0,1,1,1, 6.333,-3.926,3.926, 1,1,1
PL 2,2,1,1
NH 0,1,1,1, 9.295,-4.673,4.673, 1,1,1
PL 2,2,1,1
NH 0,1,1,1, 12.821,-5.563,5.563, 1,1,1
PL 2,2,1,1
NH 0,1,1,1, 15.019,-6.118,6.118, 1,1,1
PL 2,2,1,1
NH 0,1,1,1, 17.019,-6.623,6.623, 1,1,1
PL 2,2,1,1
NH 0,1,1,1, 19.516,-7.254,7.254, 1,1,1
PL 2,2,1,1
NH 0,1,1,1, 22.016,-7.885,7.885, 1,1,1
PL 2,2,1,1
NH 0,1,1,1, 23.965,-8.377,8.377, 1,1,1
PL 2,2,1,1
NH 0,1,1,1, 25,965,-8.882,8.882, 1,1,1
PL 2,2,1,1
NH 0,1,1,1, 27.965,-9.387,9.387, 1,1,1
PL 2,2,1,1
NH 0,1,1,1, 30.347,-9.888,9.888, 1,1,1
PL 2,2,1,1
NH 0,1,1,1, 32.687,-10.579,10.579, 1,1,1
PL 2,2,1,1
NH 0,1,1,1, 35.047,-11.175,11.175, 1,1,1
PL 2,2,1,1
NH 0,1,1,1, 37.878,-11.889,11.889, 1,1,1
PL 2,2,1,1
NH 0,1,1,1, 40.678,-12.596,12.596, 1,1,1
PL 2,2,1,1
```

```
NH 0,1,1,1, 43.478,-13.303,13.303, 1,1,1
PL 2,2,1,1
NH 0,1,1,1, 46.815,-14.146,14.146, 1,1,1
PL 2,2,1,1
NH 0,1,1,1, 50.165,-14.991,14.991, 1,1,1
PL 2,2,1,1
NH 0,1,1,1, 53.515,-15.837,15.837, 1,1,1
PL 2,2,1,1
NH 0,1,1,1, 57.464,-16.181,16.181, 1,1,1
PL 2,2,1,1
NH 0,1,1,1, 61.464,-17.844,17.844, 1,1,1
PL 2,2,1,1
NH 0,1,1,1, 65.464,-18.854,18.854, 1,1,1
PL 2,2,1,1
NH 0,1,1,1, 68.889,-19.718,19.718, 1,1,1
PL 2,2,1,1
NH 0,1,1,1, 72.489,-21.536,21.536, 1,1,1
PL 2,2,1,1
NH 0,1,1,1, 76.089,-21.964,21.964, 1,1,1
PL 2,2,1,1
NH 0,1,1,1, 79.689,-22.445,22.445, 1,1,1
PL 2,2,1,1
NH 0,1,1,1, 83.874,-23.501,23.501, 1,1,1
PL 2,2,1,1
NH 0,1,1,1, 88.124,-24.574,24.574, 1,1,1
PL 2,2,1,1
NH 0,1,1,1, 92.374,-25.647,25.647, 1,1,1
PL 2,2,1,1
NH 0,1,1,1, 96.624,-26.72,26.72, 1,1,1
PL 2,2,1,1
NH 0,1,1,1, 100.784,-27.77,27.77, 1,1,1
PL 2,2,1,1
NH 0,1,1,1, 104.784,-28.779,28.779, 1,1,1
PL 2,2,1,1
NH 0,1,1,1, 108.784,-29.789,29.789, 1,1,1
PL 2,2,1,1
NH 0,1,1,1, 112.784,-30.799,30.799, 1,1,1
PL 2,2,1,1
NH 0,1,1,1, 116.784,-31.809,31.809, 1,1,1
PL 2,2,1,1
NH 0,1,1,1, 120.784,-32.819,32.819, 1,1,1
PL 2,2,1,1
NH 0,1,1,1, 124.784,-33.829,33.829, 1,1,1
PL 2,2,1,1
NH 0,1,1,1, 128.784,-34.839,34.839, 1,1,1
PL 2,2,1,1
NH 0,1,1,1, 132.784,-35.844,35.844, 1,1,1
PL 2,2,1,1
NH 0,1,1,1, 136.784,-36.858,36.858, 1,1,1
PL 2,2,1,1
NH 0,1,1,1, 140.784,-37.868,37.868, 1,1,1
XQ
PL 3, 2, 0, 4
RP 0, 1, 361, 1000, 90, 0, 0, 1     HORIZONTAL
XQ
PL 3, 1, 0, 4
RP 0, 181, 1, 1000, 90, 0, -1, 0      VERTICAL
XQ
EN
```

APPENDIX B

NEC DATA FILE FOR PERFECT GROUND

```
CM HALF SQUARE LOG PERIODIC ARRAY
CM 17 ELEMENTS, TL:-300 , ANTI PHASE DUAL FEED
CM TAU:0.84,SIGMA:0.16,ALPHA:28.072 DEGREE
CM ARRAY LENGTH:140.784 M.
CM OVER PERFECT GROUND
CE FREQUENCY: 30.0 MHZ.
GW 31,6, 0,-.02,2.349, 0,-2.304,2.349, .000814
GW 1,1, 0,-2.304,2.349, 0,-2.349,2.304, .000814
GW 51,6, 0,-2.349,2.304, 0,-2.349,0, .000814
GW 32,6, 1.756,-.024,2.797, 1.756,-2.743,2.797, .000814
GW 2,1, 1.756,-2.743,2.797, 1.756,-2.797,2.743, .000814
GW 52,6, 1.756,-2.797,2.743, 1.756,-2.797,0, .000814
GW 33,6, 3.845,-.028,3.33, 3.845,-3.265,3.33, .000814
GW 3,1, 3.845,-3.265,3.33, 3.845,-3.33,3.265, .000814
GW 53,6, 3.845,-3.33,3.265, 3.845,-3.33,0, .000814
GW 34,6, 6.333,-.034,3.964, 6.333,-3.887,3.964, .000814
GW 4,1, 6.333,-3.887,3.964, 6.333,-3.964,3.887, .000814
GW 54,6, 6.333,-3.964,3.887, 6.333,-3.964,0, .000814
GW 35,6, 9.295,-.04,4.719, 9.295,-4.628,4.719, .000814
GW 5,1, 9.295,-4.628,4.719, 9.295,-4.719,4.628, .000814
GW 55,6, 9.295,-4.719,4.628, 9.295,-4.719,0, .000814
GW 36,6, 12.821,-.048,5.618, 12.821,-5.509,5.618, .000814
GW 6,1, 12.821,-5.509,5.618, 12.821,-5.618,5.509, .000814
GW 56,6, 12.821,-5.618,5.509, 12.821,-5.618,0, .000814
GW 37,6, 17.019,-.057,6.688, 17.019,-6.559,6.688, .000814
GW 7,1, 17.019,-6.559,6.688, 17.019,-6.688,6.559, .000814
GW 57,6, 17.019,-6.688,6.559, 17.019,-6.688,0, .000814
GW 38,6, 22.016,-.068,7.961, 22.016,-7.808,7.961, .000814
GW 8,1, 22.016,-7.808,7.961, 22.016,-7.961,7.808, .000814
GW 58,6, 22.016,-7.961,7.808, 22.016,-7.961,0, .000814
GW 39,6, 27.965,-.081,9.478, 27.965,-9.295,9.478, .000814
GW 9,1, 27.965,-9.295,9.478, 27.965,-9.478,9.295, .000814
GW 59,6, 27.965,-9.478,9.295, 27.965,-9.478,0, .000814
GW 40,6, 35.047,-.096,11.283, 35.047,-11.066,11.283, .000814
GW 10,1, 35.047,-11.066,11.283, 35.047,-11.283,11.066, .000814
GW 60,6, 35.047,-11.283,11.066, 35.047,-11.283,0, .000814
GW 41,6, 43.478,-.114,13.303, 43.478,-13.174,13.303, .000814
GW 11,1, 43.478,-13.174,13.303, 43.478,-13.303,13.174, .000814
GW 61,6, 43.478,-13.303,13.174, 43.478,-13.303,0, .000814
GW 42,6, 53.515,-.136,15.991, 53.515,-15.683,15.991, .000814
GW 12,1, 53.515,-15.683,15.991, 53.515,-15.991,15.683, .000814
GW 62,6, 53.515,-15.991,15.683, 53.515,-15.991,0, .000814
GW 43,6, 65.464,-.162,19.037, 65.464,-18.670,19.037, .000814
GW 13,1, 65.464,-18.670,19.037, 65.464,-19.037,18.670, .000814
GW 63,6, 65.464,-19.037,18.670, 65.464,-19.037,0, .000814
GW 44,6, 79.689,-.193,22.663, 79.689,-22.226,22.663, .000814
GW 14,1, 79.689,-22.226,22.663, 79.689,-22.663,22.226, .000814
GW 64,6, 79.689,-22.663,22.226, 79.689,-22.663,0, .000814
GW 45,6, 96.624,-.23,26.980, 96.624,-26.460,26.980, .000814
GW 15,1, 96.624,-26.460,26.980, 96.624,-26.980,26.460, .000814
GW 65,6, 96.624,-26.980,26.460, 96.624,-26.980,0, .000814
GW 46,6, 116.784,-.273,32.119, 116.784,-31.5,32.119, .000814
GW 16,1, 116.784,-31.5,32.119, 116.784,-32.119,31.5, .000814
GW 66,6, 116.784,-32.119,31.5, 116.784,-32.119,0, .000814
GW 47,6, 140.784,-.326,38.237, 140.784,-37.5,38.237, .000814
GW 17,1, 140.784,-37.5,38.237, 140.784,-38.237,37.5, .000814
GW 67,6, 140.784,-38.237,37.5, 140.784,-38.237,0, .000814
GX 100,010
GE -1
GN 1
TL 1,1,2,1, -300, 1.755
```

```
TL 2,1,3,1, -300, 2.09
TL 3,1,4,1, -300, 2.488
TL 4,1,5,1, -300, 2.962
TL 5,1,6,1, -300, 3.526
TL 6,1,7,1, -300, 4.198
TL 7,1,8,1, -300, 4.997
TL 8,1,9,1, -300, 5.949
TL 9,1,10,1, -300, 7.082
TL 10,1,11,1, -300, 8.431
TL 11,1,12,1, -300, 10.037
TL 12,1,13,1, -300, 11.949
TL 13,1,14,1, -300, 14.225
TL 14,1,15,1, -300, 16.934
TL 15,1,16,1, -300, 20.16
TL 16,1,17,1, -300, 24.0
TL 101,1,102,1, -300, 1.755
TL 102,1,103,1, -300, 2.09
TL 103,1,104,1, -300, 2.488
TL 104,1,105,1, -300, 2.962
TL 105,1,106,1, -300, 3.526
TL 106,1,107,1, -300, 4.198
TL 107,1,108,1, -300, 4.997
TL 108,1,109,1, -300, 5.949
TL 109,1,110,1, -300, 7.082
TL 110,1,111,1, -300, 8.431
TL 111,1,112,1, -300, 10.037
TL 112,1,113,1, -300, 11.949
TL 113,1,114,1, -300, 14.225
TL 114,1,115,1, -300, 16.934
TL 115,1,116,1, -300, 20.16
TL 116,1,117,1, -300, 24.0
EX 0,0,7,0,-1,0
EX 0,0,228,0,1,0
FR 1,1,,30.0,0,
PL 2,2,1,1
NH 0,1,1,1, 0,-2.327,2.327, 1,1,1
PL 2,2,1,1
NH 0,1,1,1, 1.756,-2.770,2.770, 1,1,1
PL 2,2,1,1
NH 0,1,1,1, 3.845,-3.298,3.298, 1,1,1
PL 2,2,1,1
NH 0,1,1,1, 6.333,-3.926,3.926, 1,1,1
PL 2,2,1,1
NH 0,1,1,1, 9.295,-4.673,4.673, 1,1,1
PL 2,2,1,1
NH 0,1,1,1, 12.821,-5.563,5.563, 1,1,1
PL 2,2,1,1
NH 0,1,1,1, 15.019,-6.118,6.118, 1,1,1
PL 2,2,1,1
NH 0,1,1,1, 17.019,-6.623,6.623, 1,1,1
PL 2,2,1,1
NH 0,1,1,1, 19.516,-7.254,7.254, 1,1,1
PL 2,2,1,1
NH 0,1,1,1, 22.016,-7.885,7.885, 1,1,1
PL 2,2,1,1
NH 0,1,1,1, 23.965,-8.377,8.377, 1,1,1
PL 2,2,1,1
NH 0,1,1,1, 25,965,-8.882,8.882, 1,1,1
PL 2,2,1,1
NH 0,1,1,1, 27.965,-9.387,9.387, 1,1,1
PL 2,2,1,1
NH 0,1,1,1, 30.347,-9.888,9.888, 1,1,1
PL 2,2,1,1
NH 0,1,1,1, 32.687,-10.579,10.579, 1,1,1
PL 2,2,1,1
NH 0,1,1,1, 35.047,-11.175,11.175, 1,1,1
PL 2,2,1,1
NH 0,1,1,1, 37.878,-11.889,11.889, 1,1,1
PL 2,2,1,1
NH 0,1,1,1, 40.678,-12.596,12.596, 1,1,1
```

```
PL 2,2,1,1
NH 0,1,1,1, 43.478,-13.303,13.303, 1,1,1
PL 2,2,1,1
NH 0,1,1,1, 46.815,-14.146,14.146, 1,1,1
PL 2,2,1,1
NH 0,1,1,1, 50.165,-14.991,14.991, 1,1,1
PL 2,2,1,1
NH 0,1,1,1, 53.515,-15.837,15.837, 1,1,1
PL 2,2,1,1
NH 0,1,1,1, 57.464,-16.181,16.181, 1,1,1
PL 2,2,1,1
NH 0,1,1,1, 61.464,-17.844,17.844, 1,1,1
PL 2,2,1,1
NH 0,1,1,1, 65.464,-18.854,18.854, 1,1,1
PL 2,2,1,1
NH 0,1,1,1, 68.889,-19.718,19.718, 1,1,1
PL 2,2,1,1
NH 0,1,1,1, 72.489,-21.536,21.536, 1,1,1
PL 2,2,1,1
NH 0,1,1,1, 76.089,-21.964,21.964, 1,1,1
PL 2,2,1,1
NH 0,1,1,1, 79.689,-22.445,22.445, 1,1,1
PL 2,2,1,1
NH 0,1,1,1, 83.874,-23.501,23.501, 1,1,1
PL 2,2,1,1
NH 0,1,1,1, 88.124,-24.574,24.574, 1,1,1
PL 2,2,1,1
NH 0,1,1,1, 92.374,-25.647,25.647, 1,1,1
PL 2,2,1,1
NH 0,1,1,1, 96.624,-26.72,26.72, 1,1,1
PL 2,2,1,1
NH 0,1,1,1, 100.784,-27.77,27.77, 1,1,1
PL 2,2,1,1
NH 0,1,1,1, 104.784,-28.779,28.779, 1,1,1
PL 2,2,1,1
NH 0,1,1,1, 108.784,-29.789,29.789, 1,1,1
PL 2,2,1,1
NH 0,1,1,1, 112.784,-30.799,30.799, 1,1,1
PL 2,2,1,1
NH 0,1,1,1, 116.784,-31.809,31.809, 1,1,1
PL 2,2,1,1
NH 0,1,1,1, 120.784,-32.819,32.819, 1,1,1
PL 2,2,1,1
NH 0,1,1,1, 124.784,-33.829,33.829, 1,1,1
PL 2,2,1,1
NH 0,1,1,1, 128.784,-34.839,34.839, 1,1,1
PL 2,2,1,1
NH 0,1,1,1, 132.784,-35.844,35.844, 1,1,1
PL 2,2,1,1
NH 0,1,1,1, 136.784,-36.858,36.858, 1,1,1
PL 2,2,1,1
NH 0,1,1,1, 140.784,-37.868,37.868, 1,1,1
XQ
PL 3, 2, 0, 4
RP 0, 1, 361, 1000, 60, 0, 0, 1     HORIZONTAL
PL 3, 2, 0, 4
RP 0, 1, 361, 1000, 90, 0, 0, 1     HORIZONTAL
XQ
PL 3, 1, 0, 4
RP 0, 181, 1, 1000, 90, 0, -1, 0      VERTICAL
XQ
EN
```

APPENDIX C
RADIATION PATTERNS IN FREE SPACE

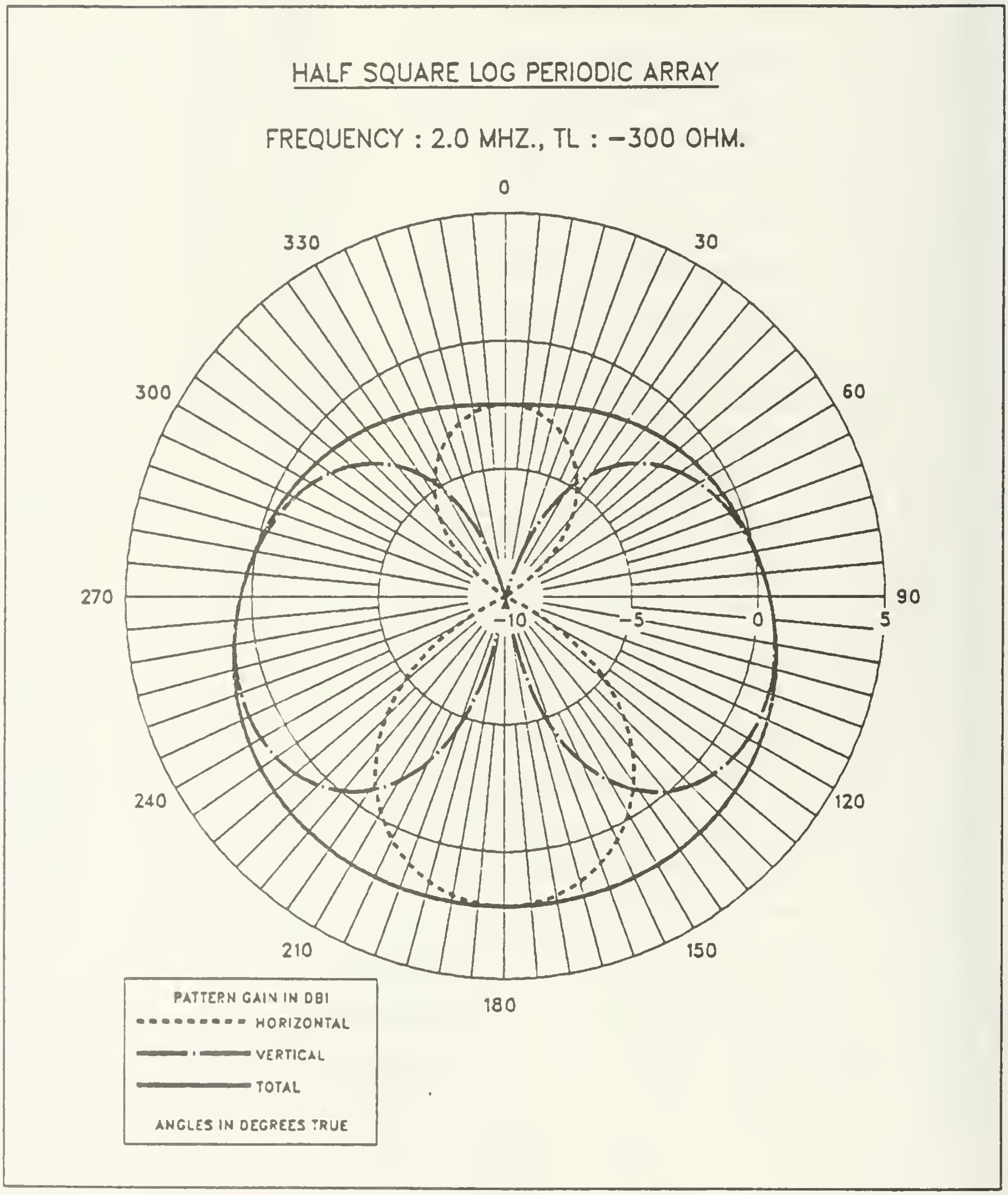

Figure C.1 Horizontal Pattern, Frequency: 2 MHz.

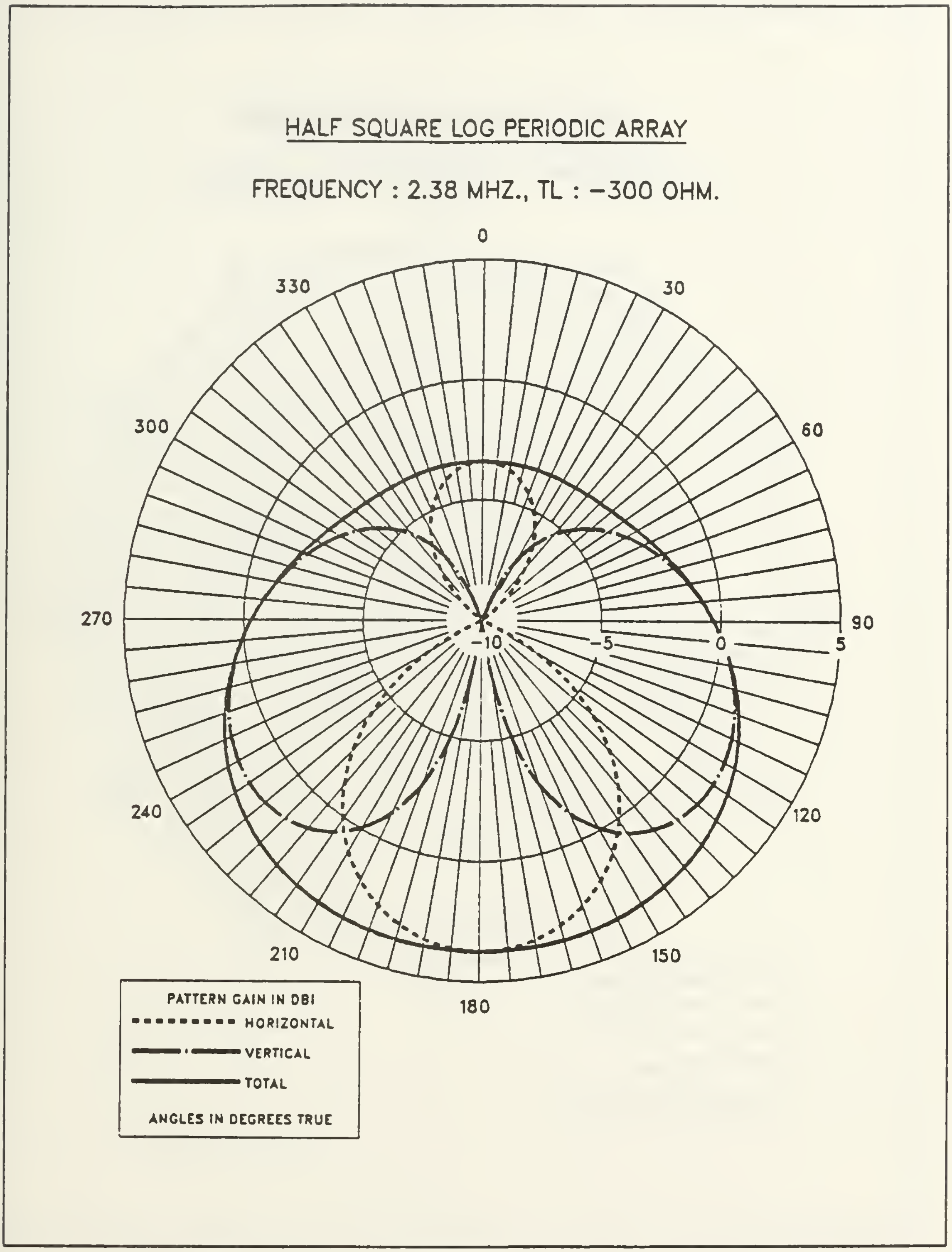

Figure C.2 Horizontal Pattern, Frequency: 2.38 MHz.

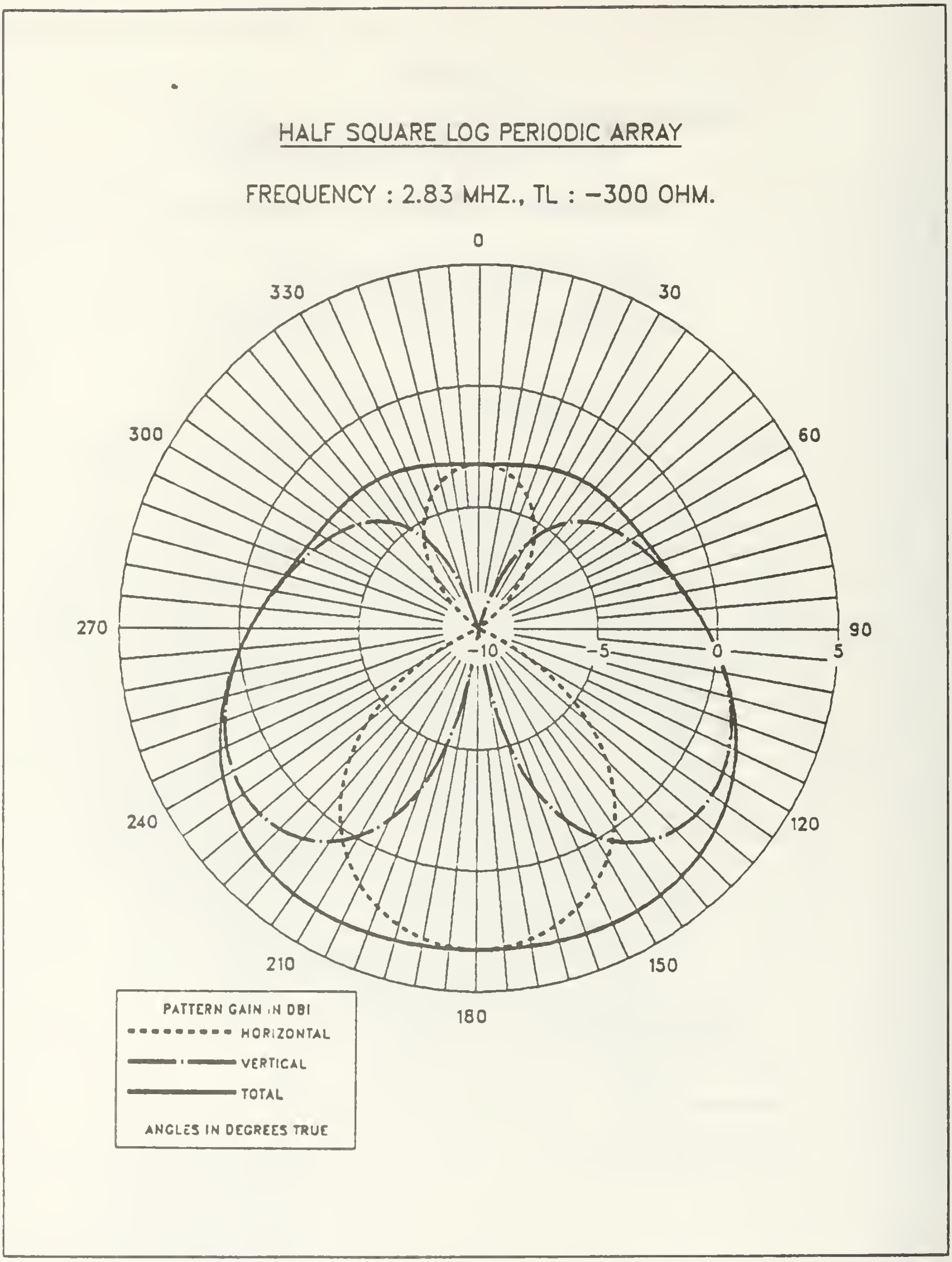

Figure C.3 Horizontal Pattern, Frequency: 2.83 MHz.

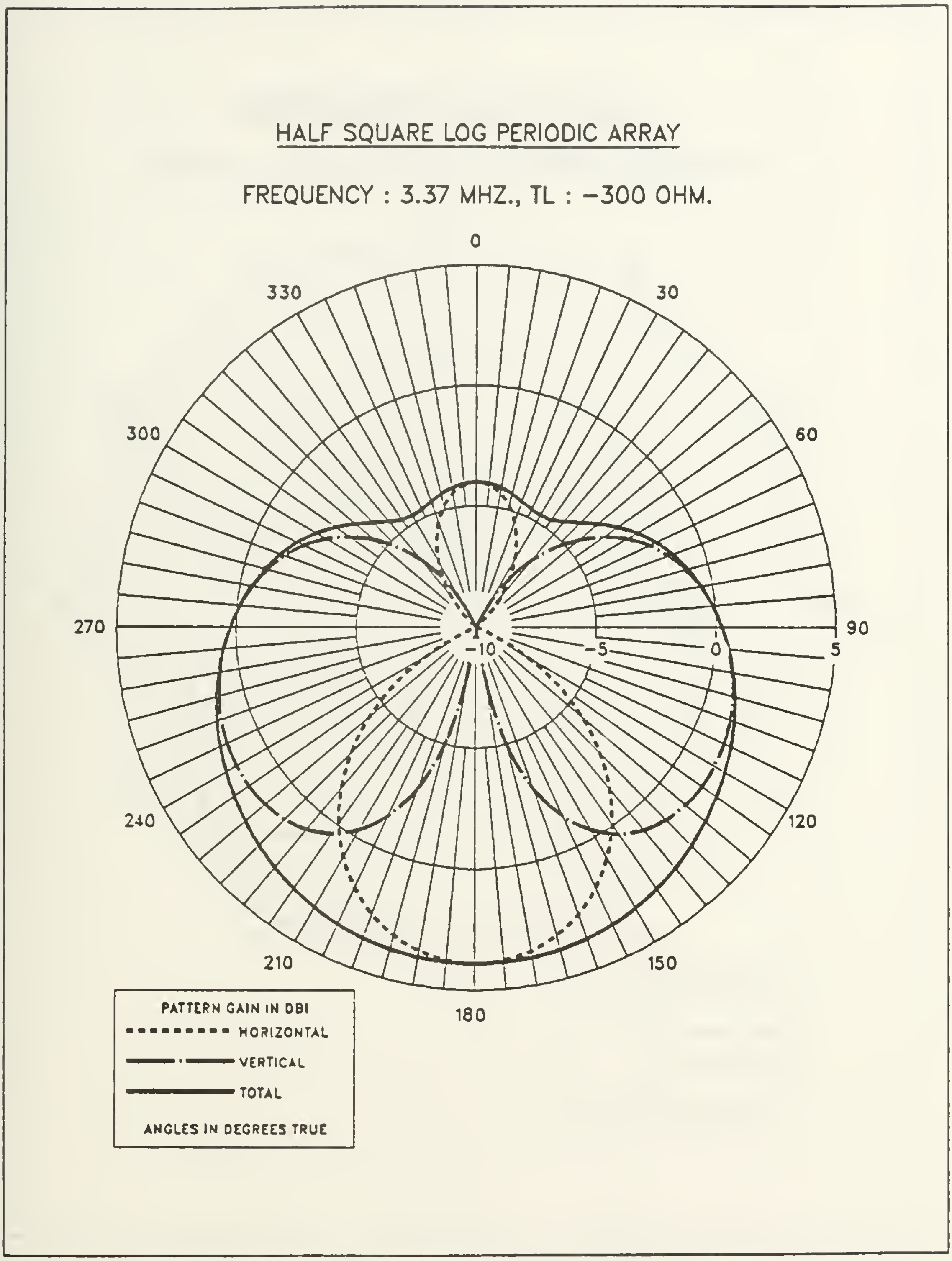

Figure C.4 Horizontal Pattern, Frequency: 3.37 MHz.

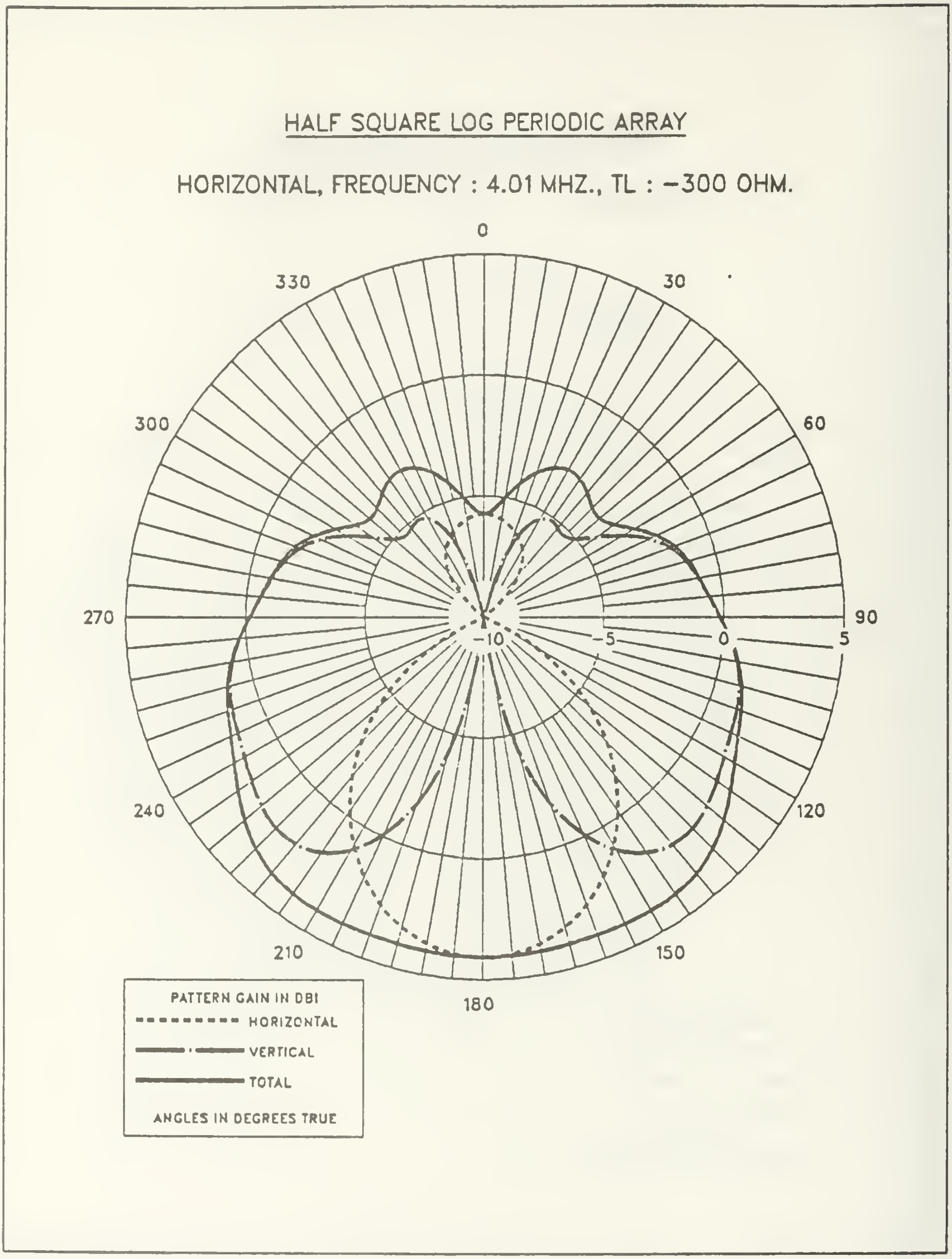

Figure C.5 Horizontal Pattern, Frequency: 4.01 MHz.

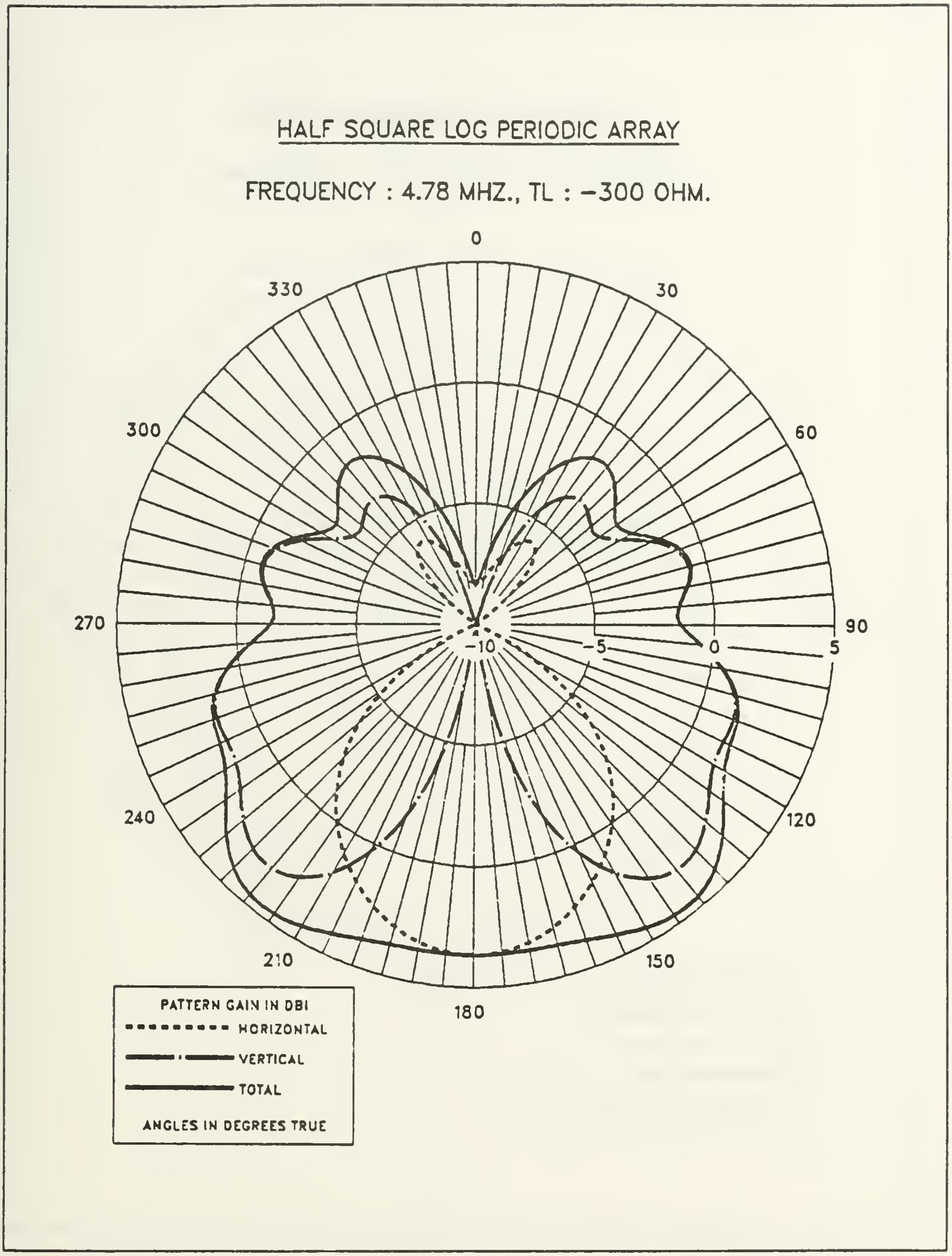

Figure C.6 Horizontal Pattern, Frequency: 4.78 MHz.

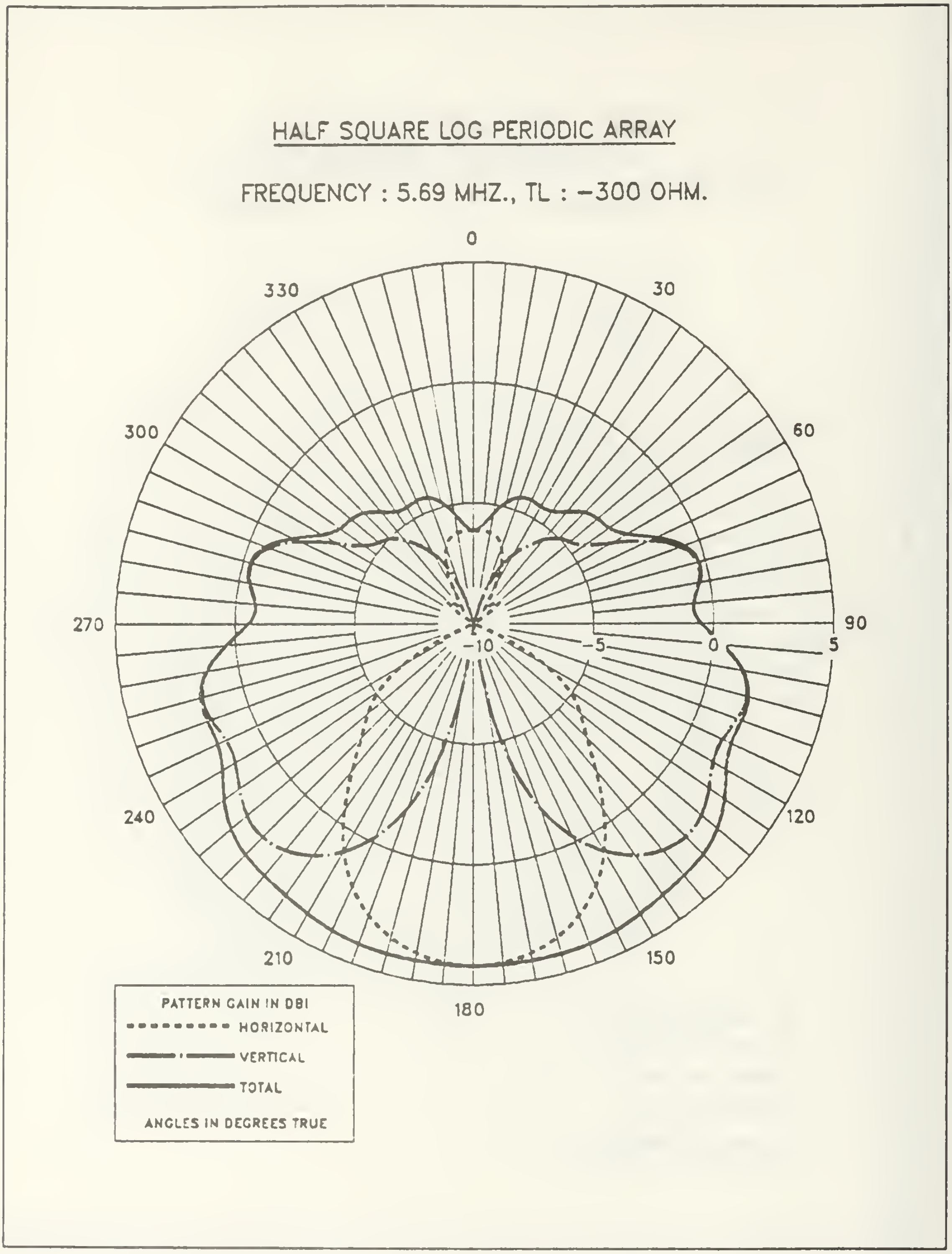

Figure C.7 Horizontal Pattern, Frequency: 5.69 MHz.

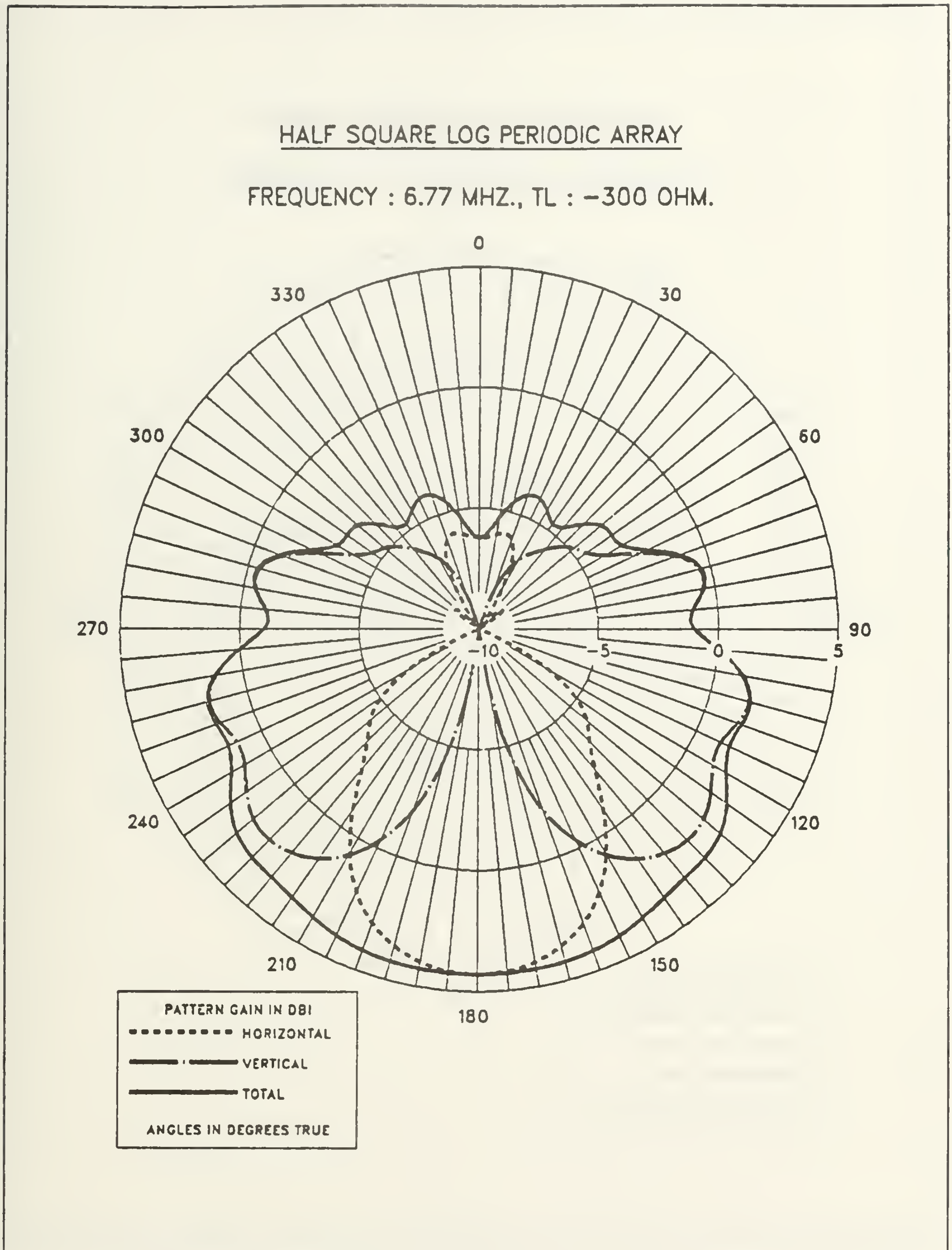

Figure C.8 Horizontal Pattern, Frequency: 6.77 MHz.

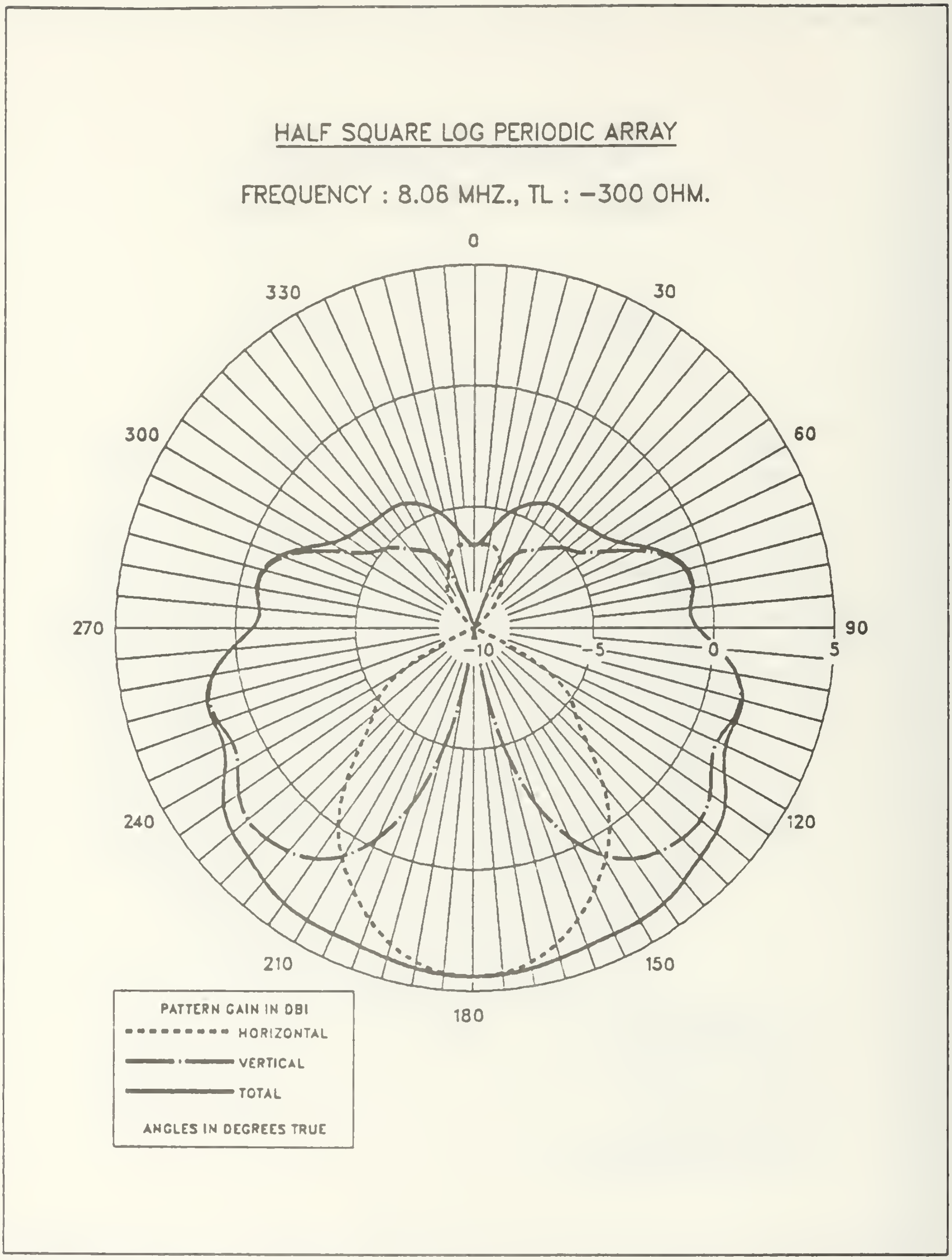

Figure C.9 Horizontal Pattern, Frequency: 8.06 MHz.

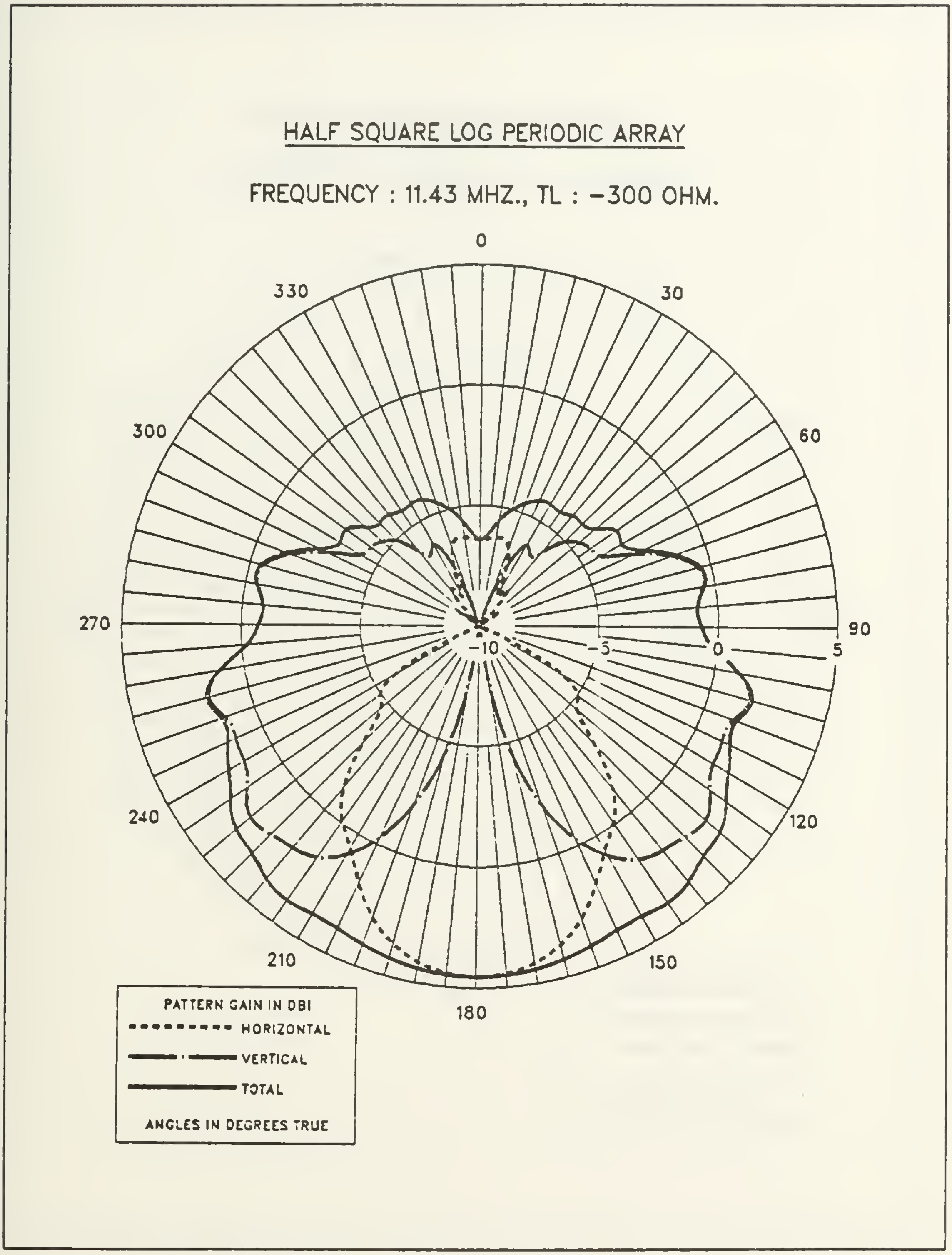

Figure C.10 Horizontal Pattern, Frequency: 11.43 MHz.

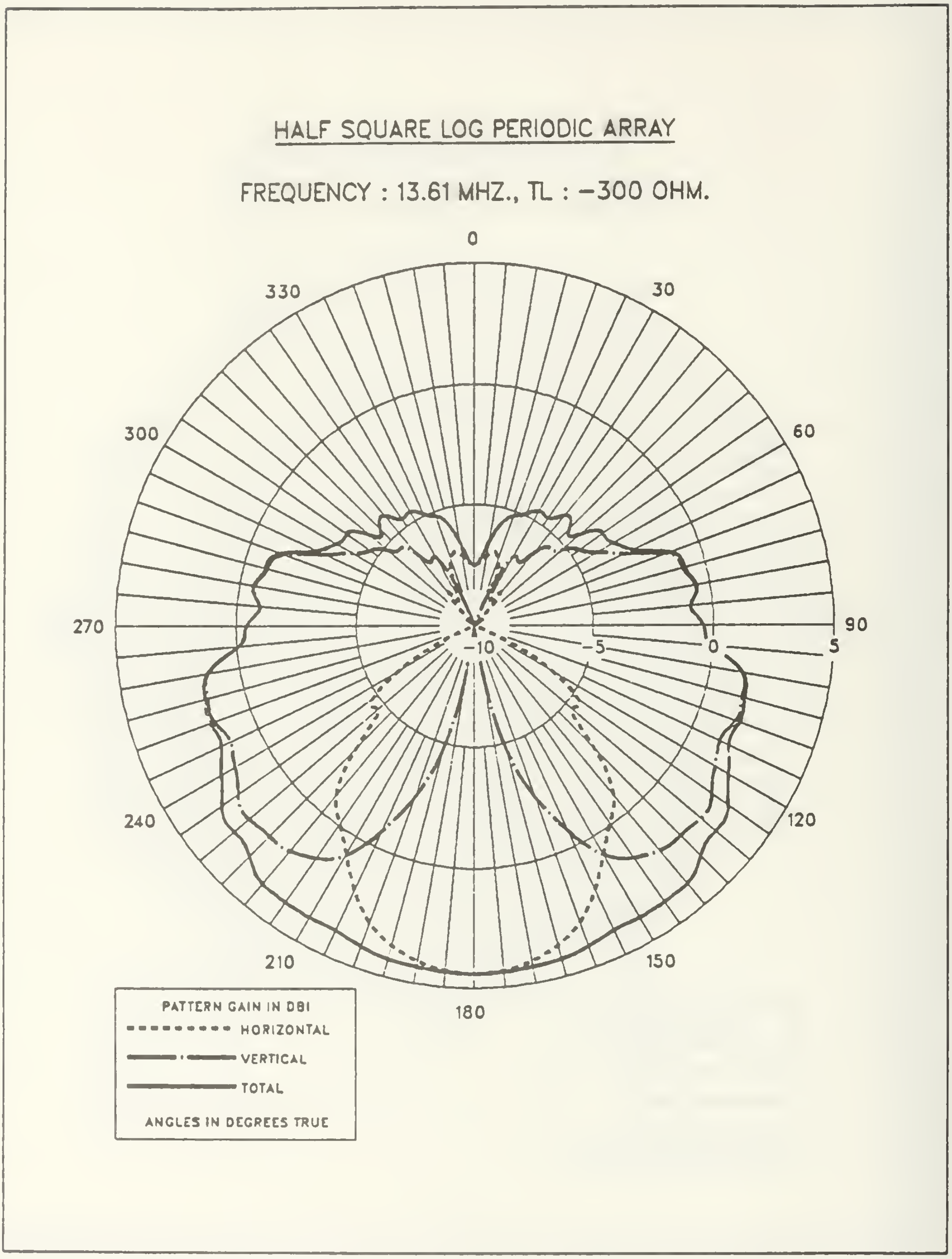

Figure C.11 Horizontal Pattern, Frequency: 13.61 MHz.

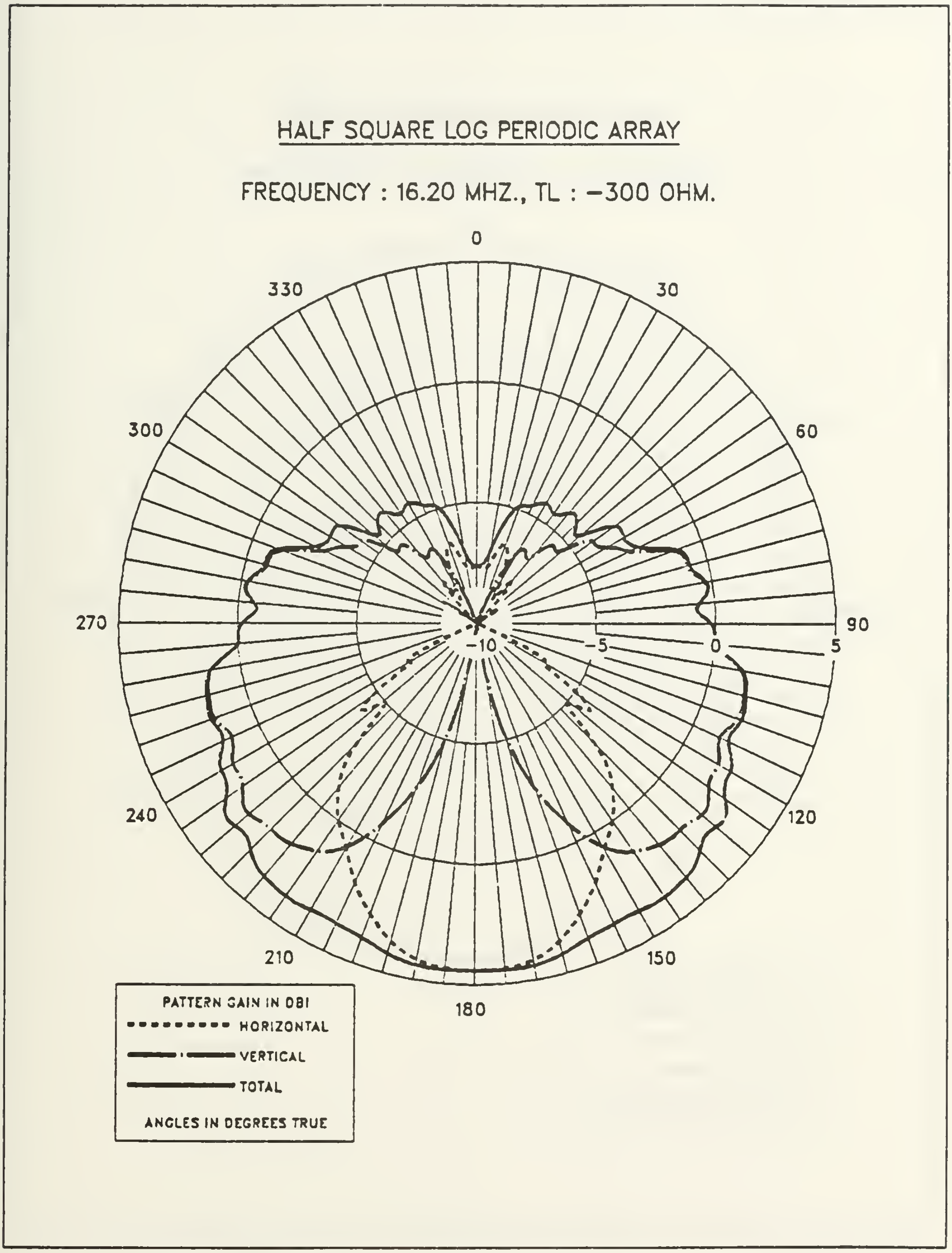

Figure C.12 Horizontal Pattern, Frequency: 16.20 MHz.

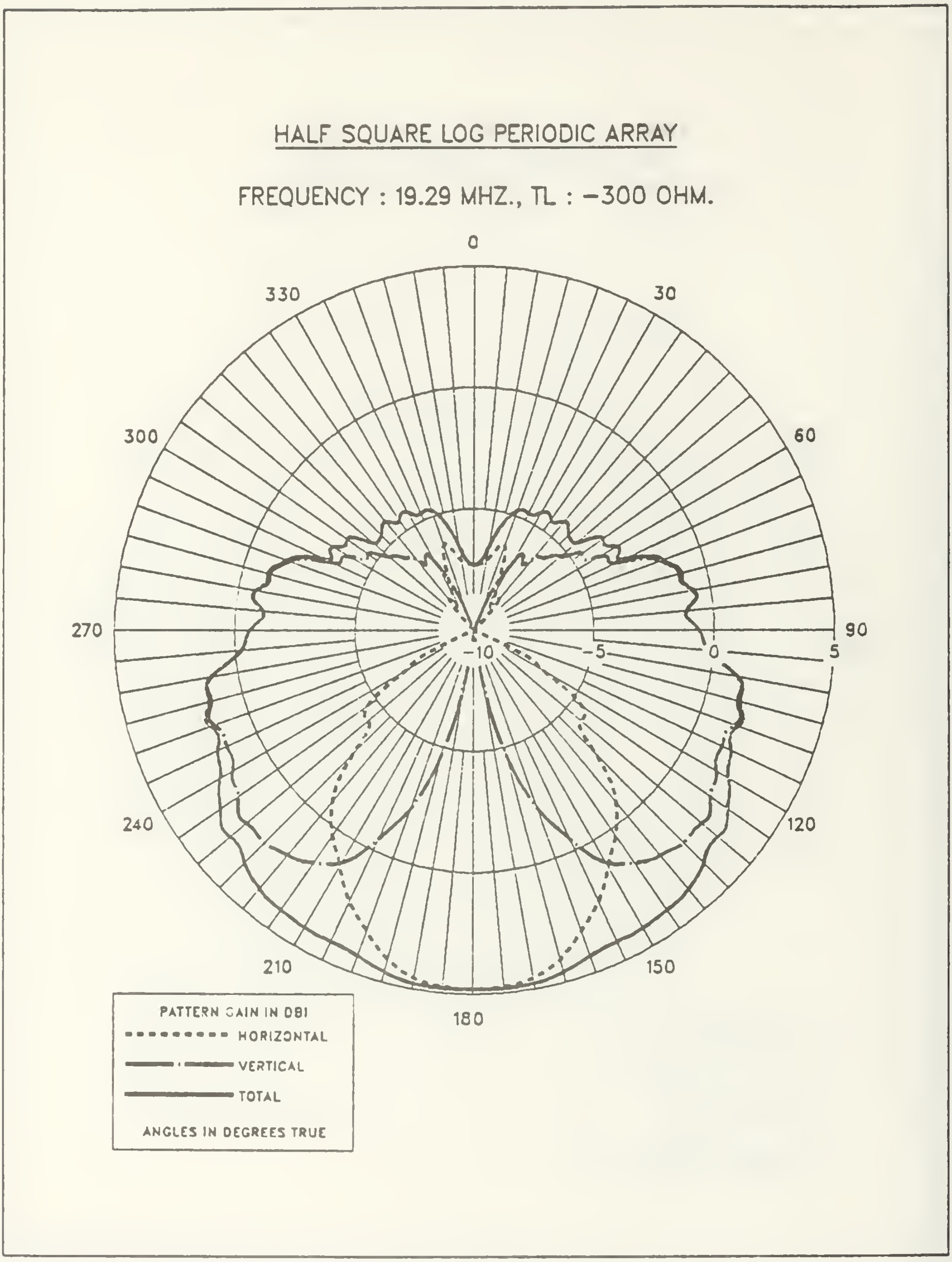

Figure C.13 Horizontal Pattern, Frequency: 19.29 MHz.

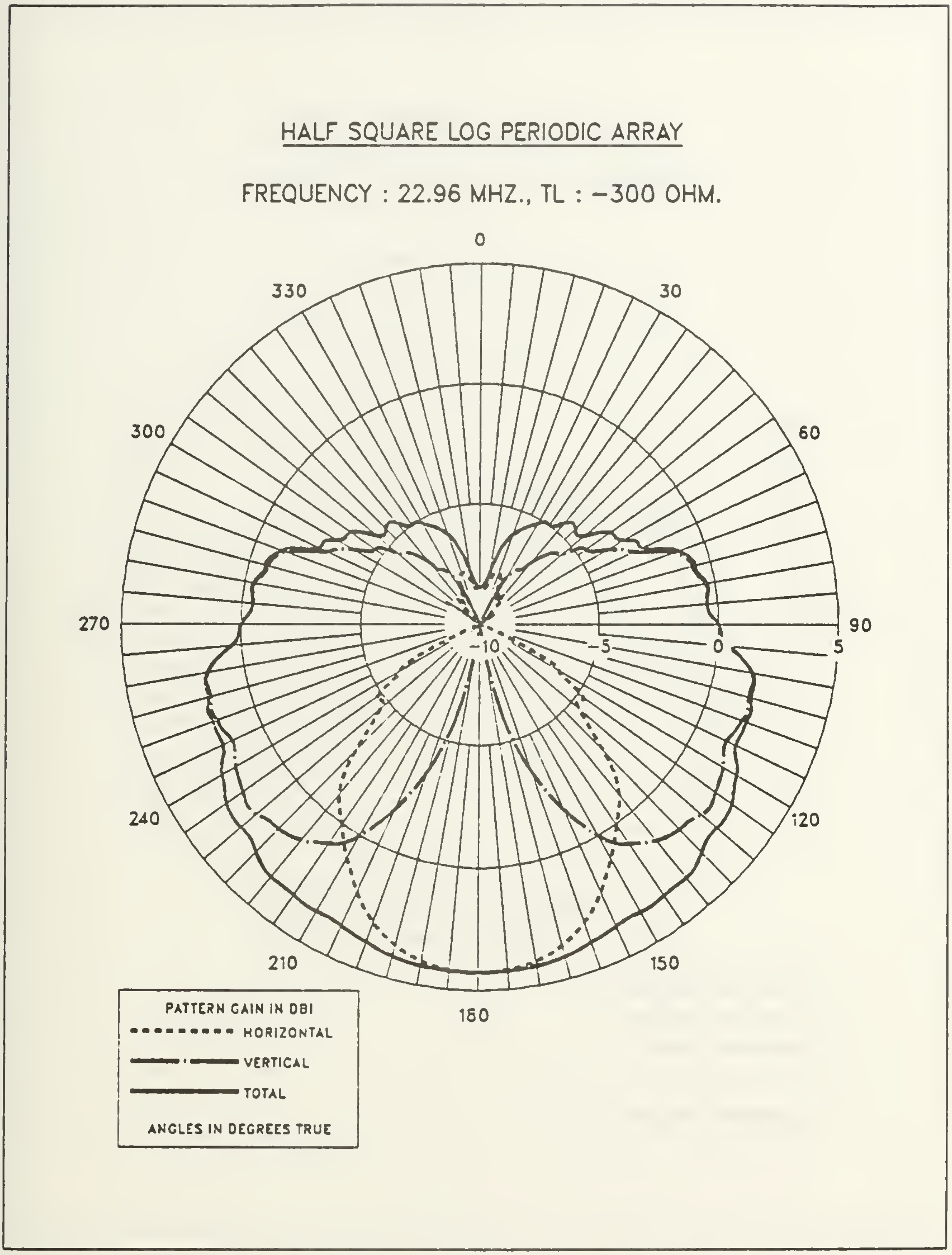

Figure C.14 Horizontal Pattern, Frequency: 22.96 MHz.

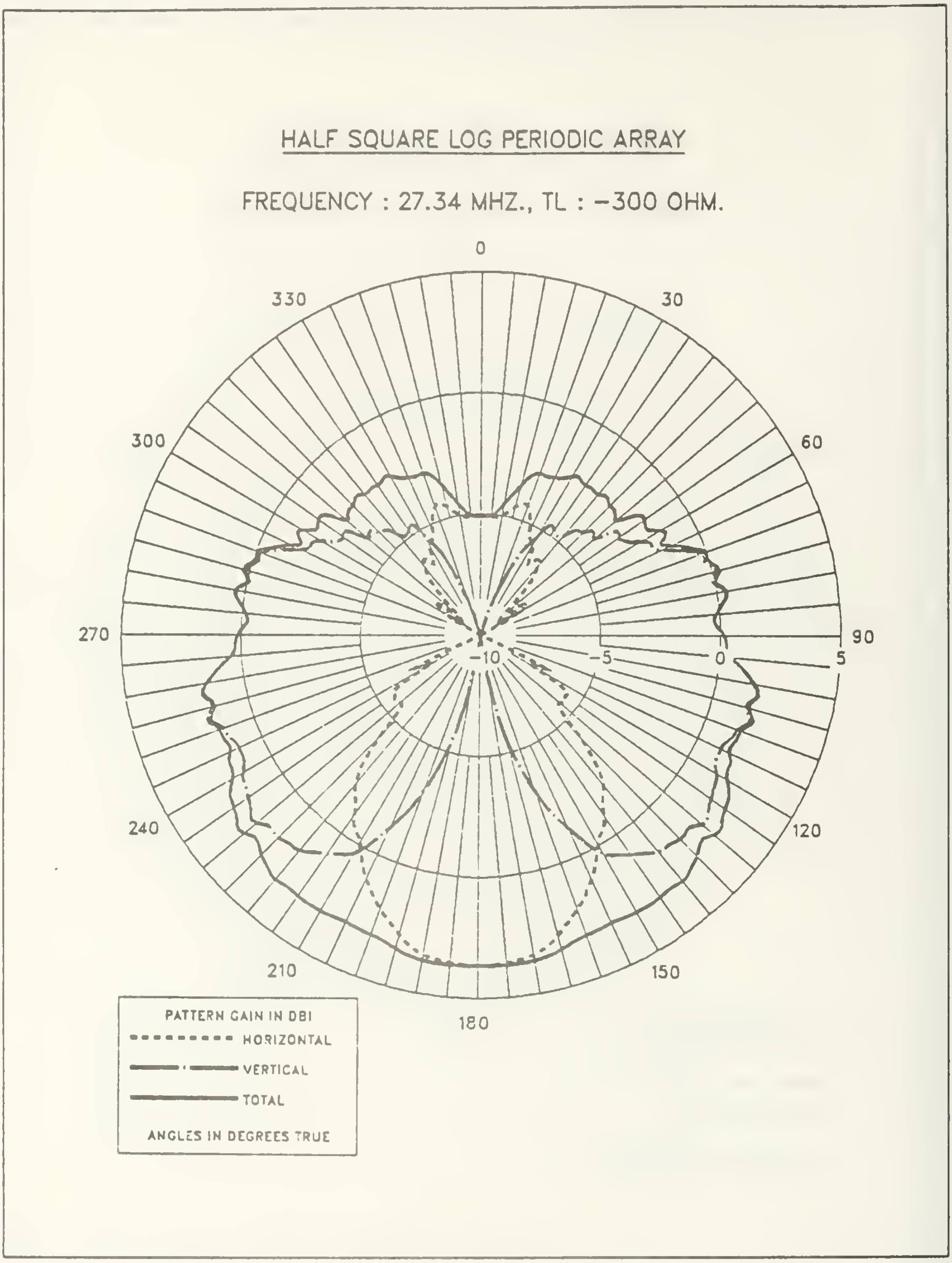

Figure C.15 Horizontal Pattern, Frequency: 27.34 MHz.

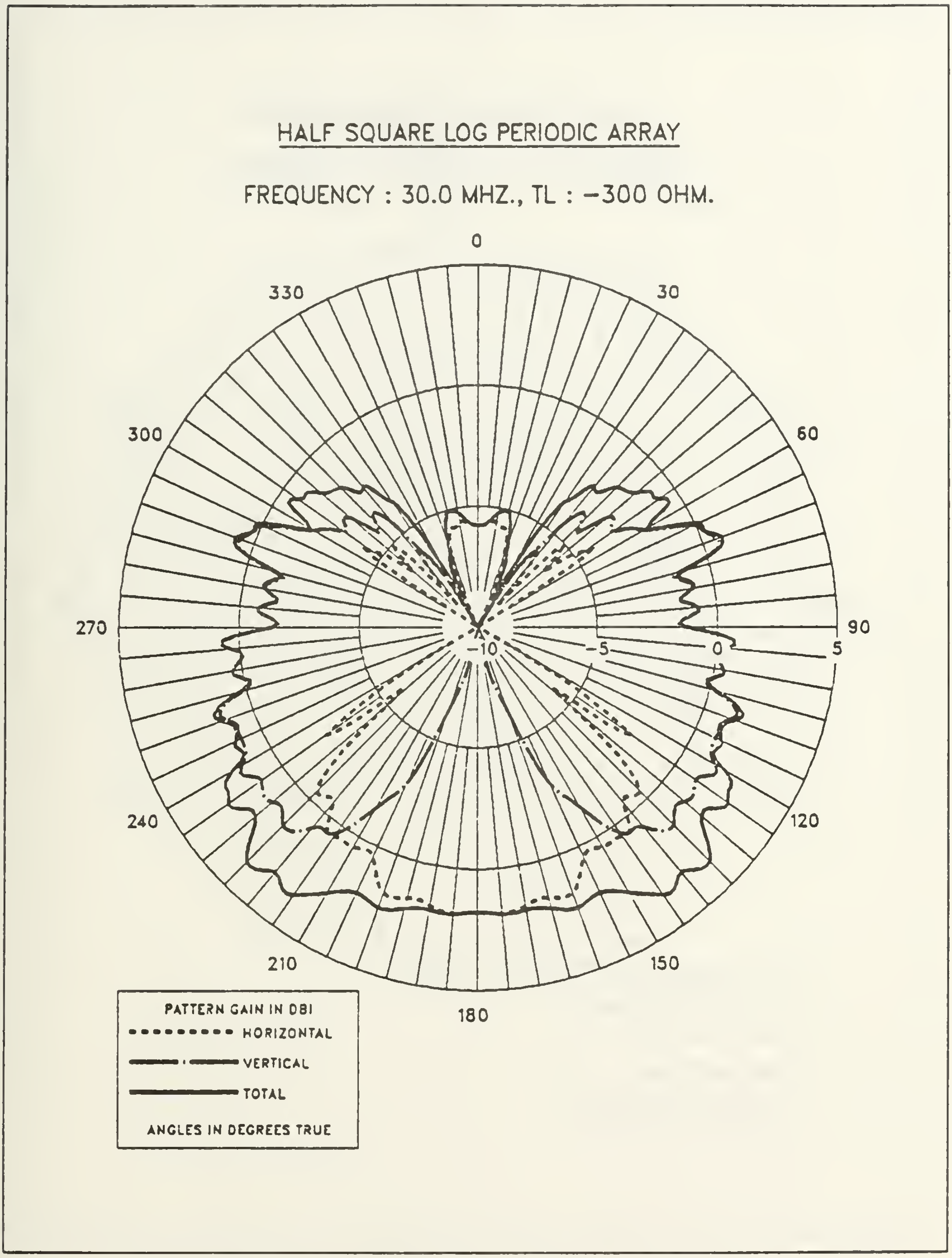

Figure C.16 Horizontal Pattern, Frequency: 30.0 MHz.

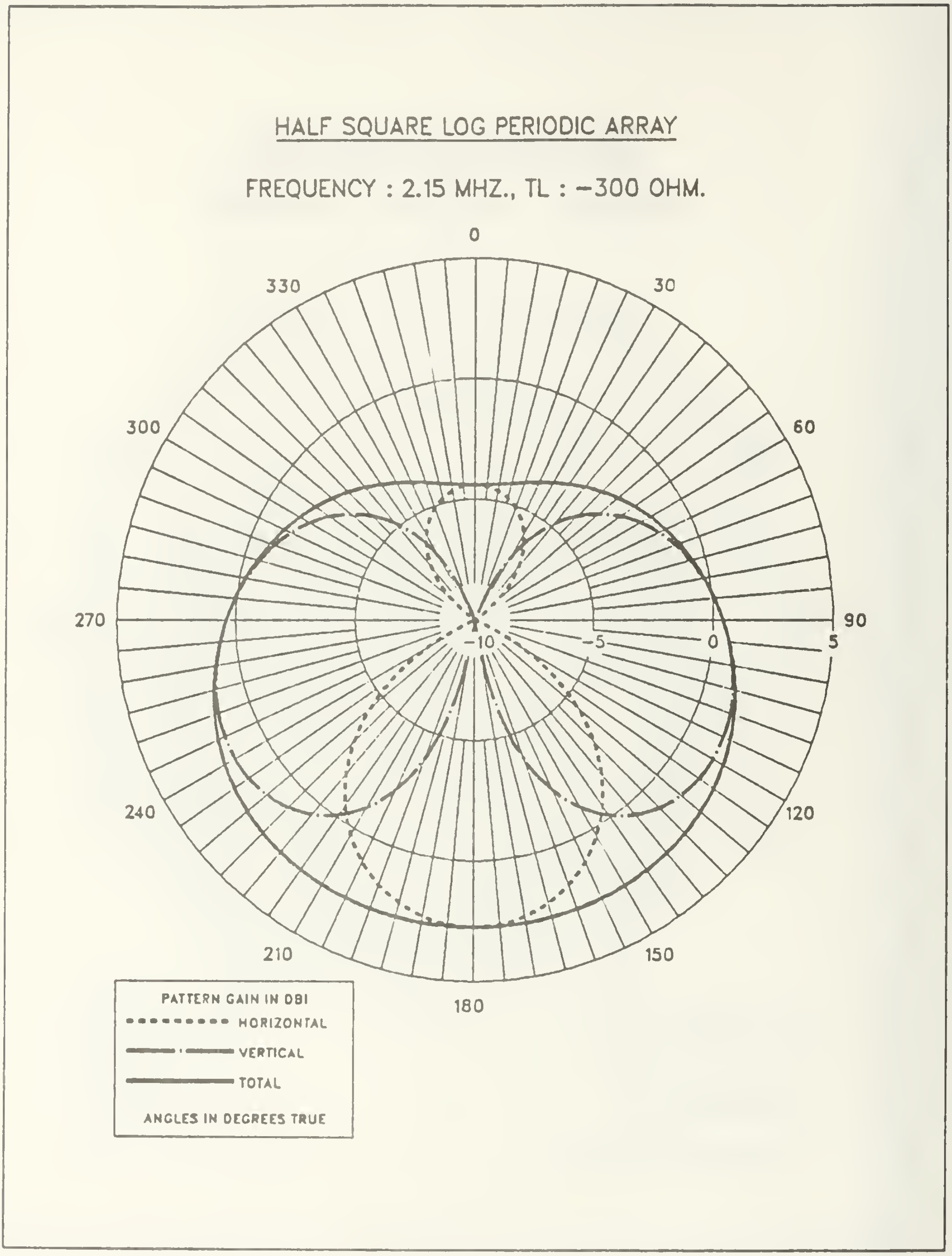

Figure C.17 Horizontal Pattern, Frequency: 2.15 MHz.

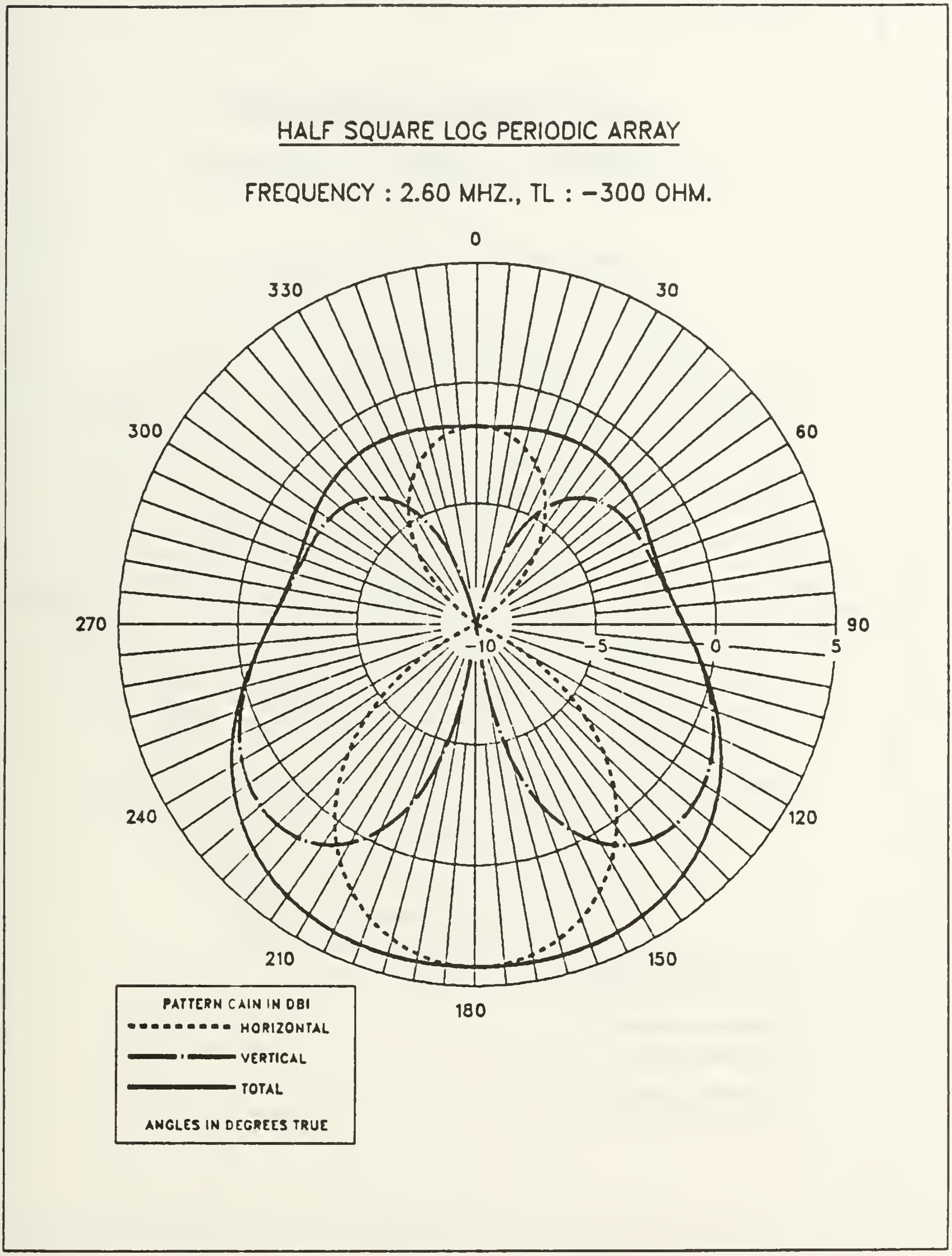

Figure C.18 Horizontal Pattern, Frequency: 2.60 MHz.

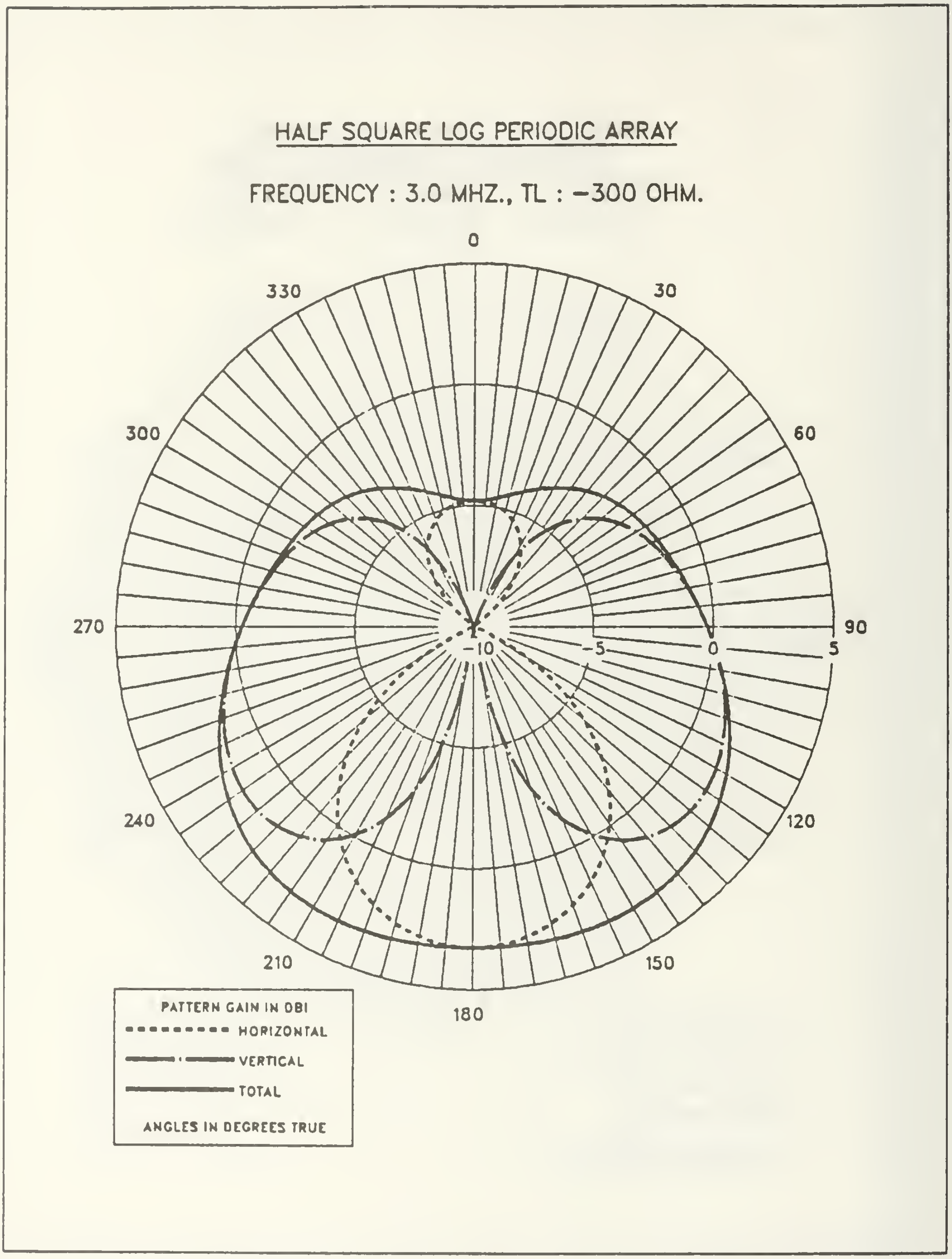

Figure C.19 Horizontal Pattern, Frequency: 3.0 MHz.

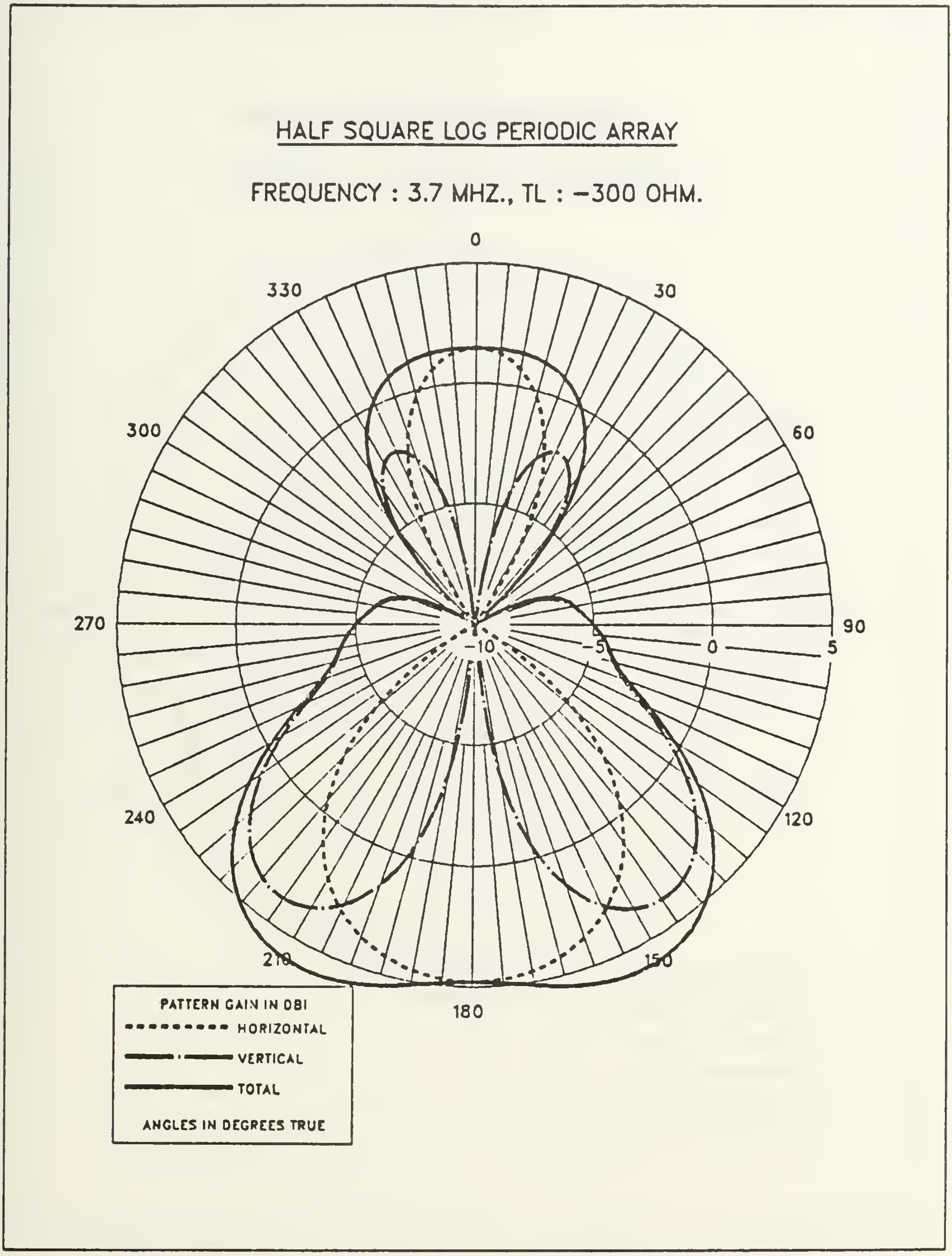

Figure C.20 Horizontal Pattern, Frequency: 3.7 MHz.

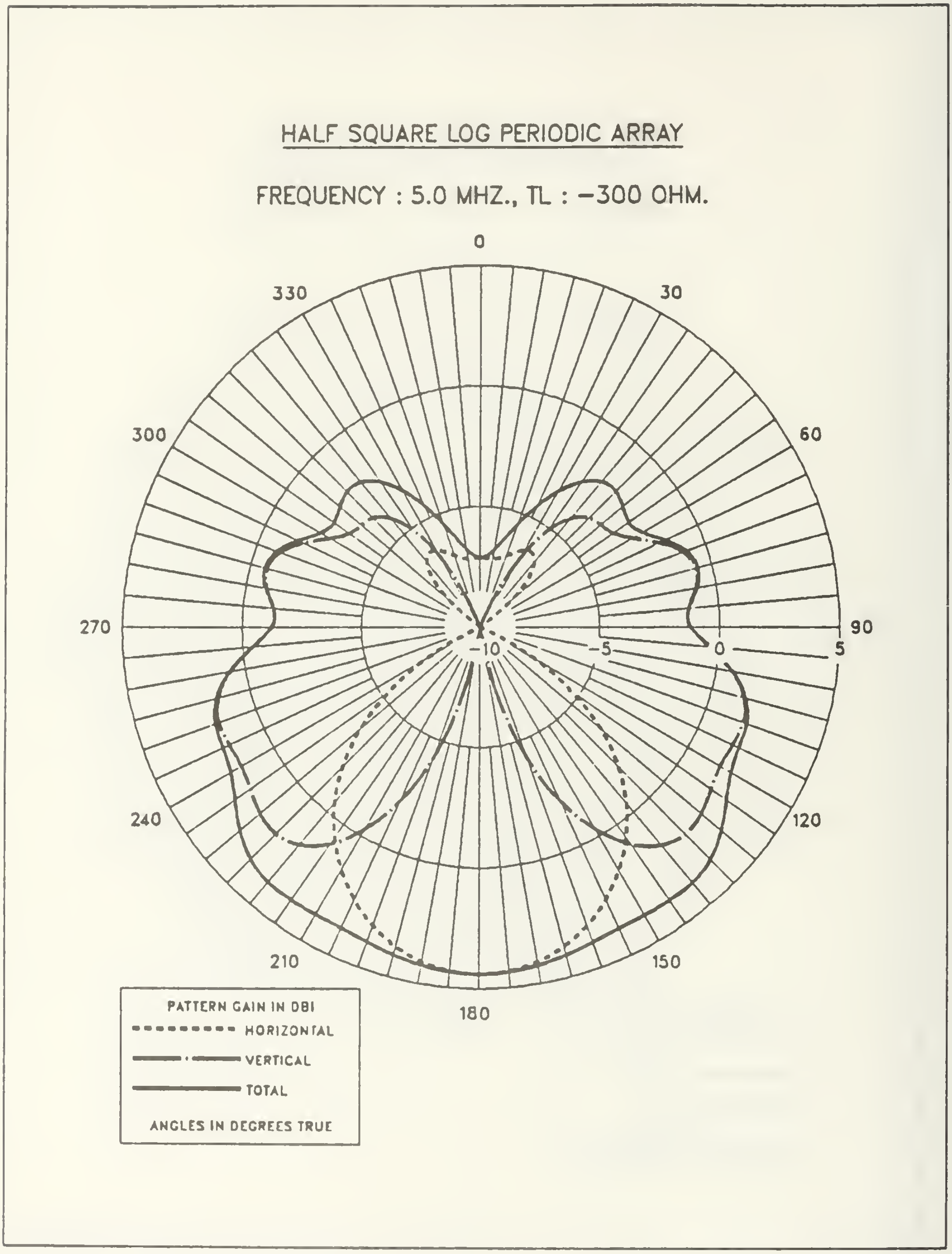

Figure C.21 Horizontal Pattern, Frequency: 5.0 MHz.

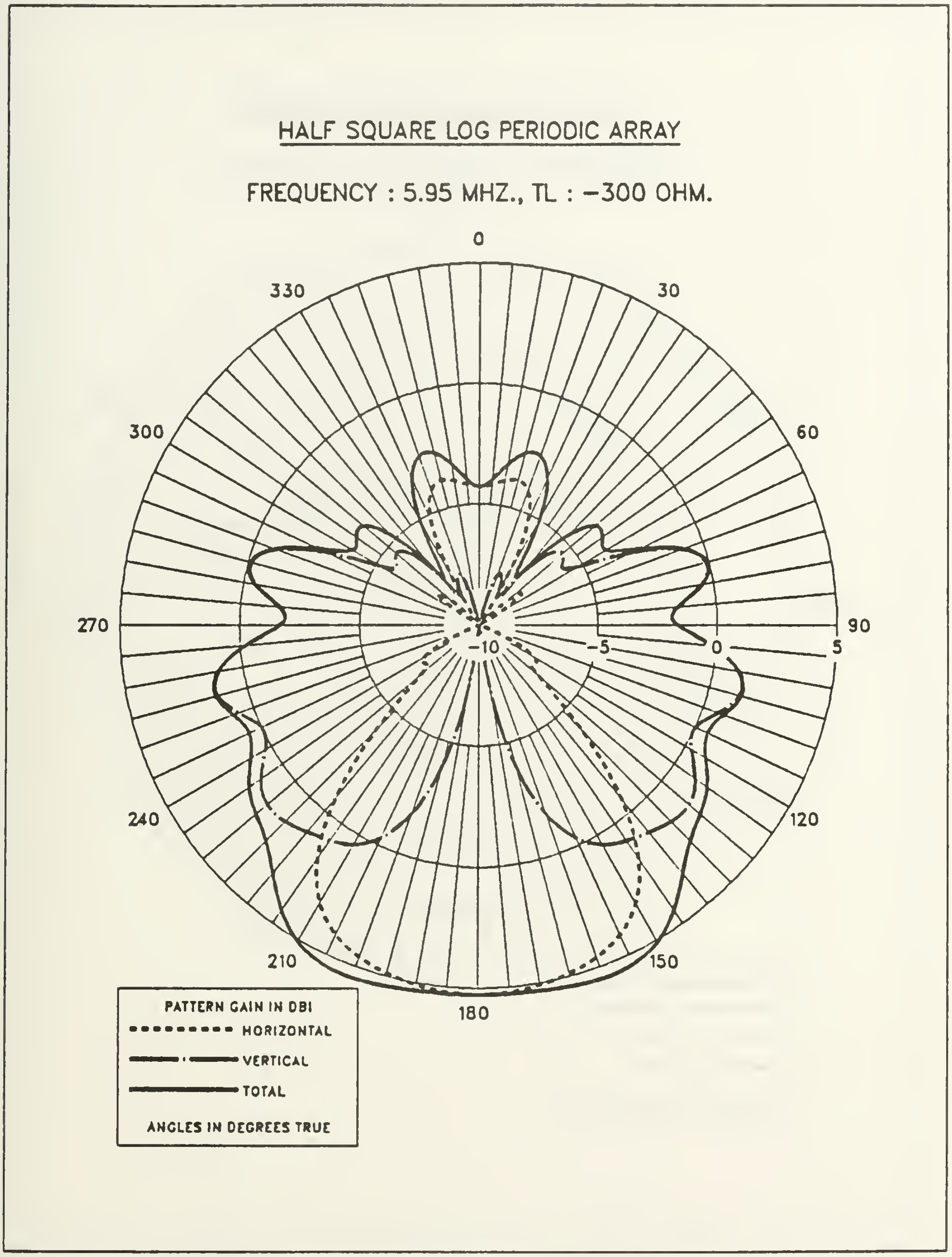

Figure C.22 Horizontal Pattern, Frequency: 5.95 MHz.

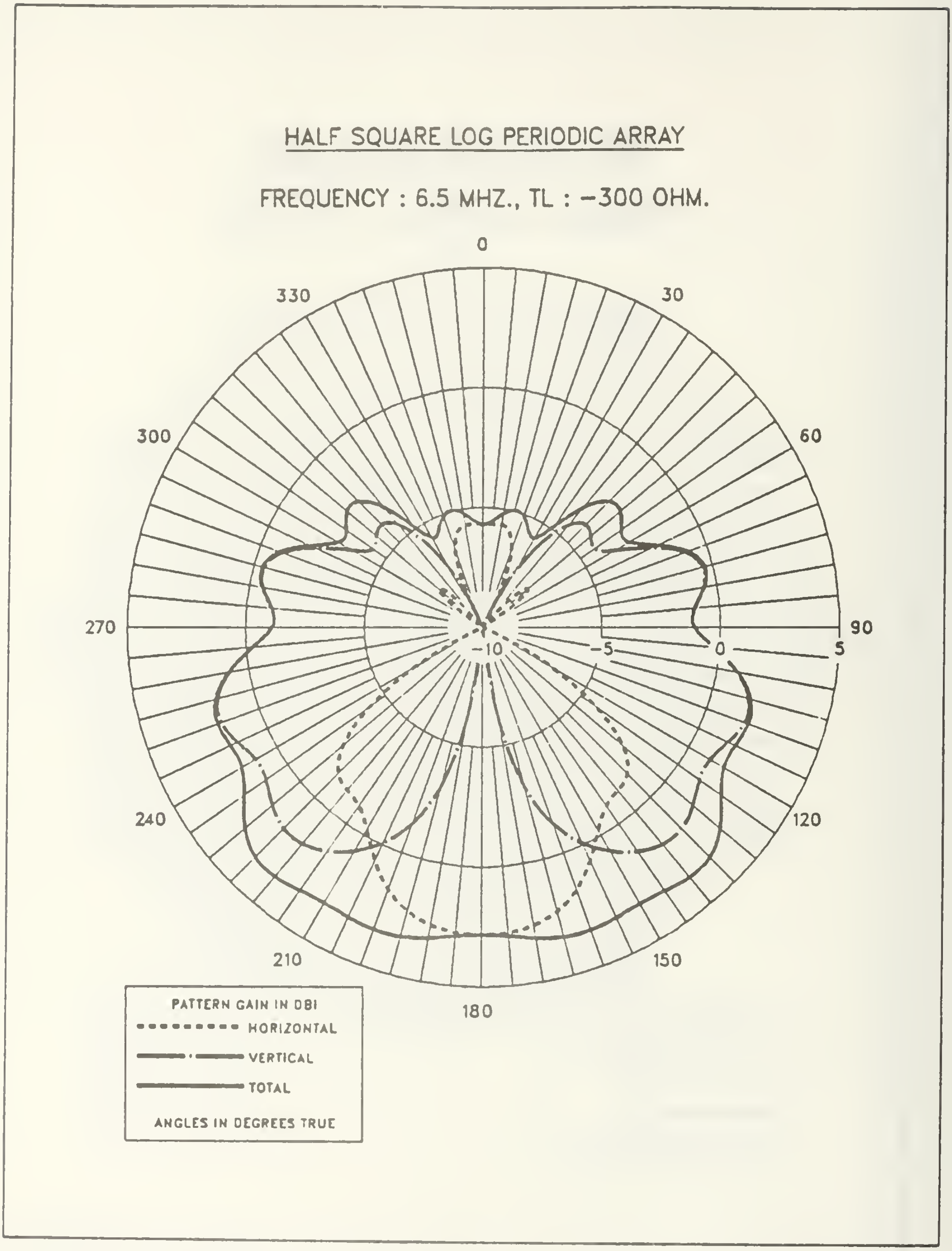

Figure C.23 Horizontal Pattern, Frequency: 6.5 MHz.

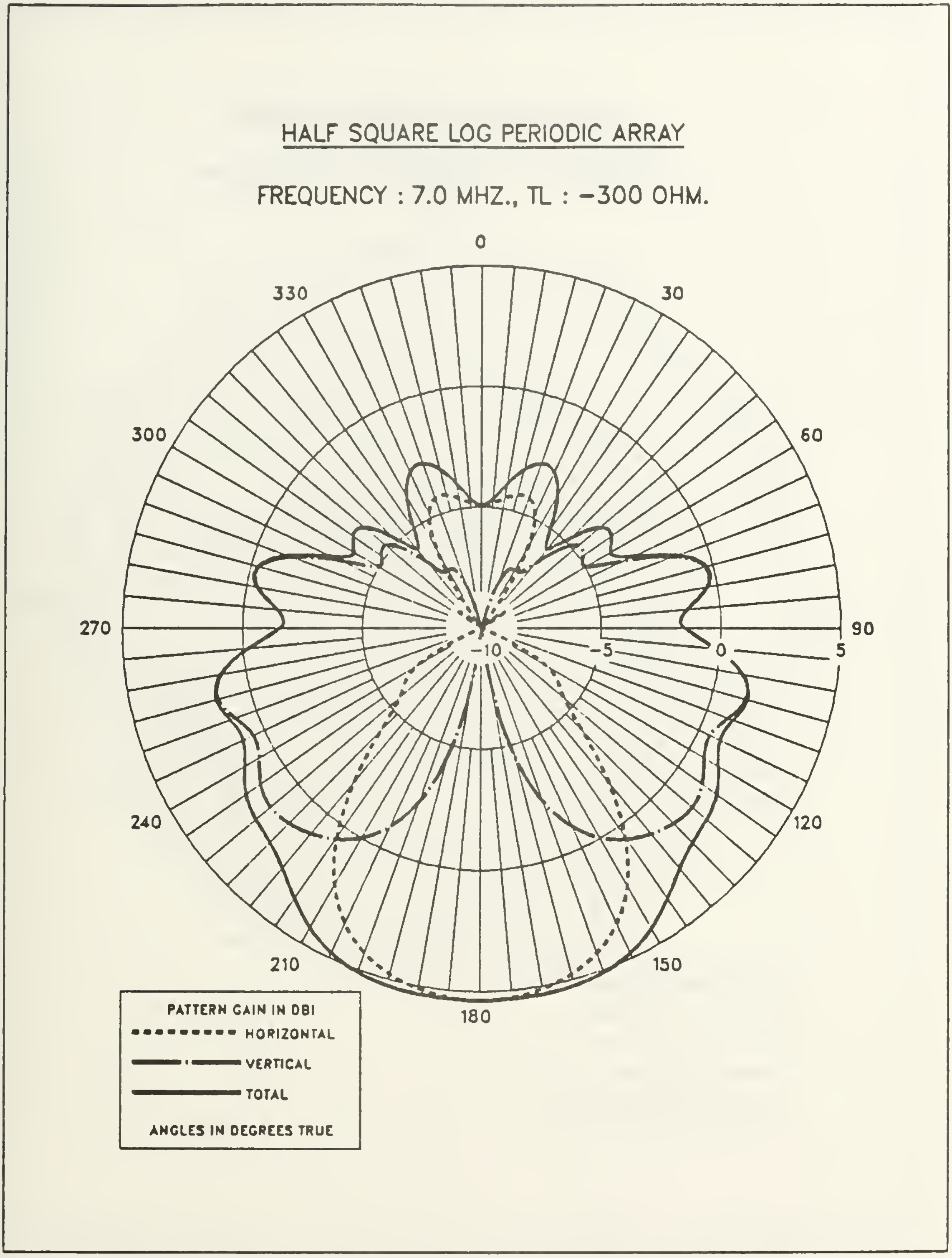

Figure C.24 Horizontal Pattern, Frequency: 7.0 MHz.

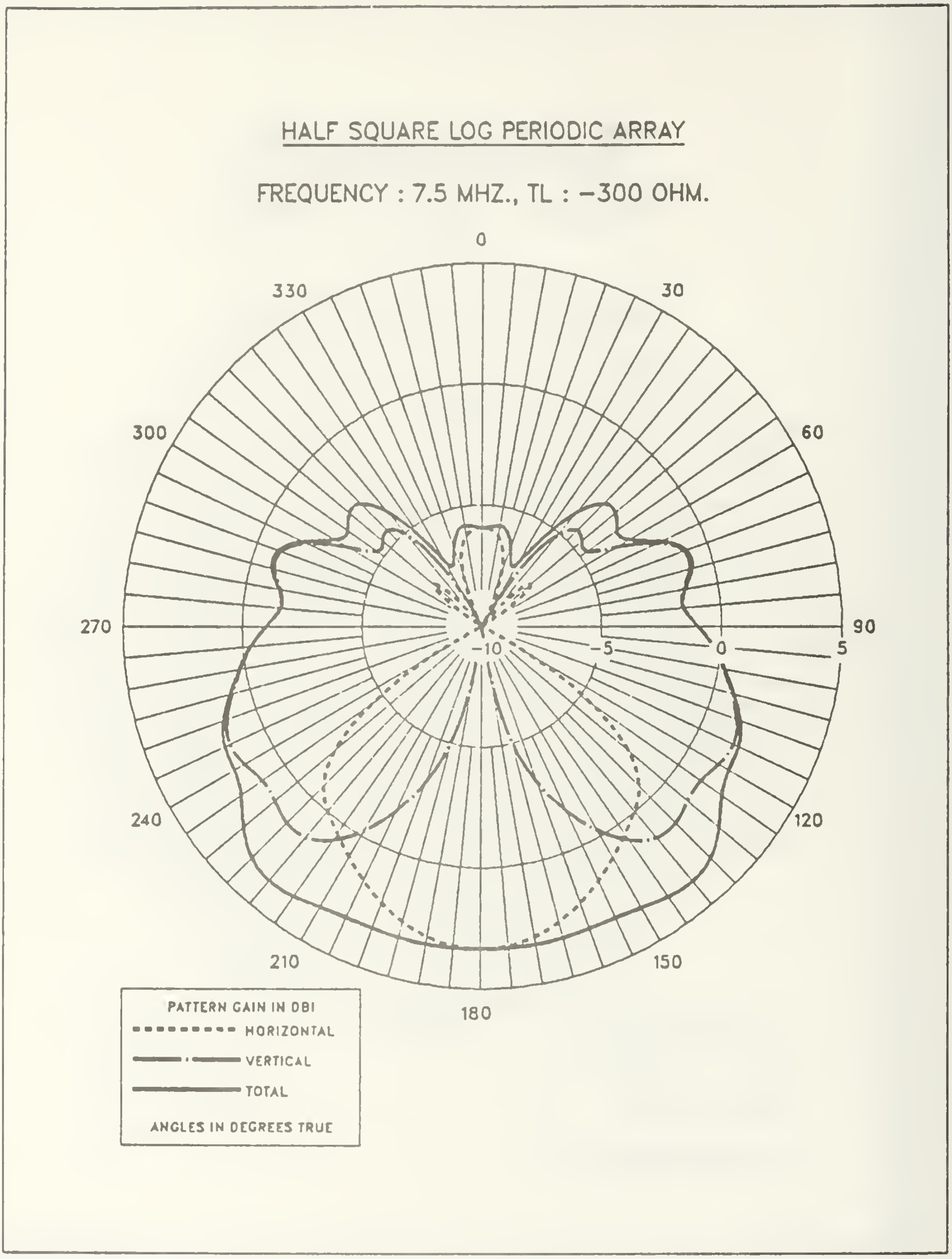

Figure C.25 Horizontal Pattern, Frequency: 7.5 MHz.

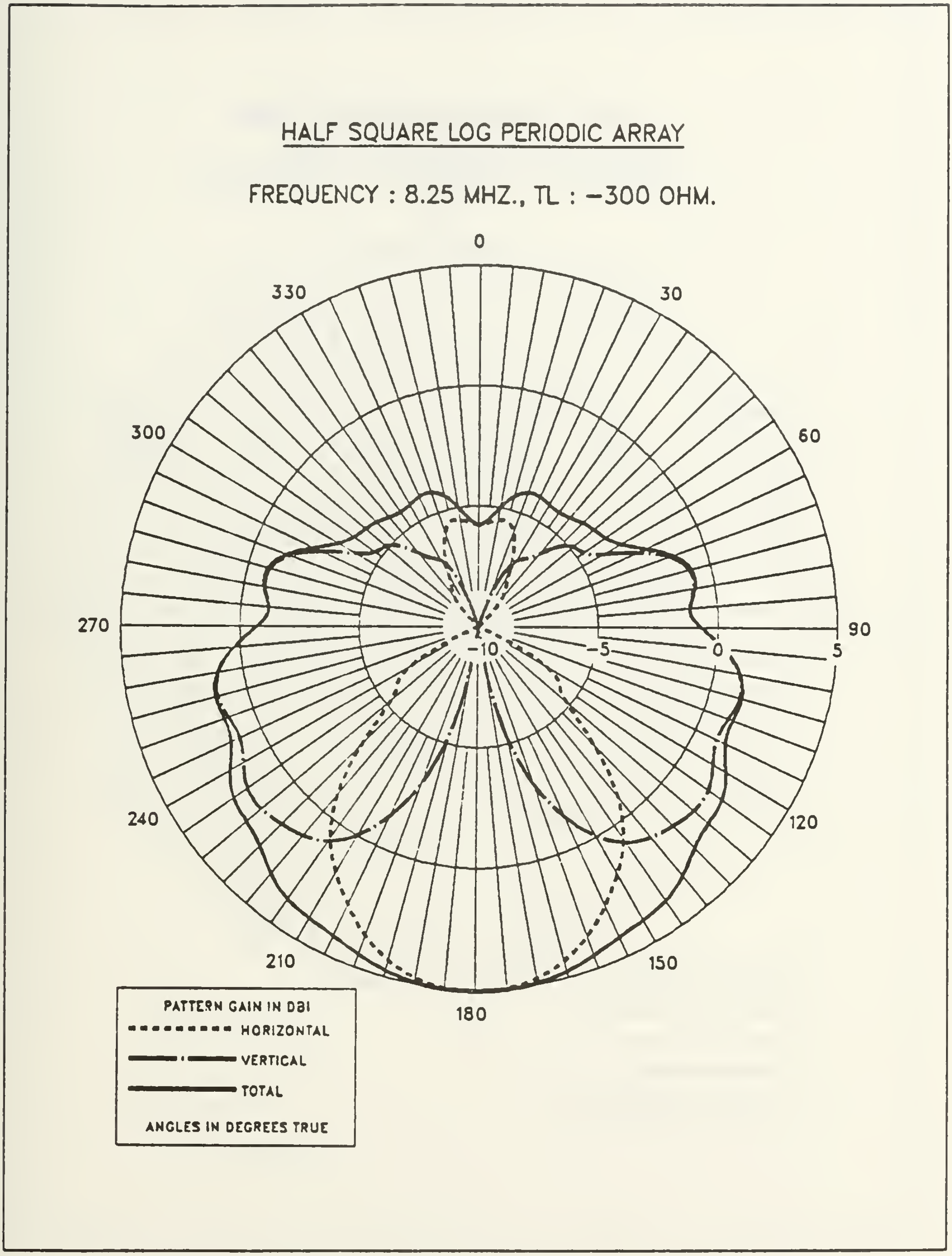

Figure C.26 Horizontal Pattern, Frequency: 8.25 MHz.

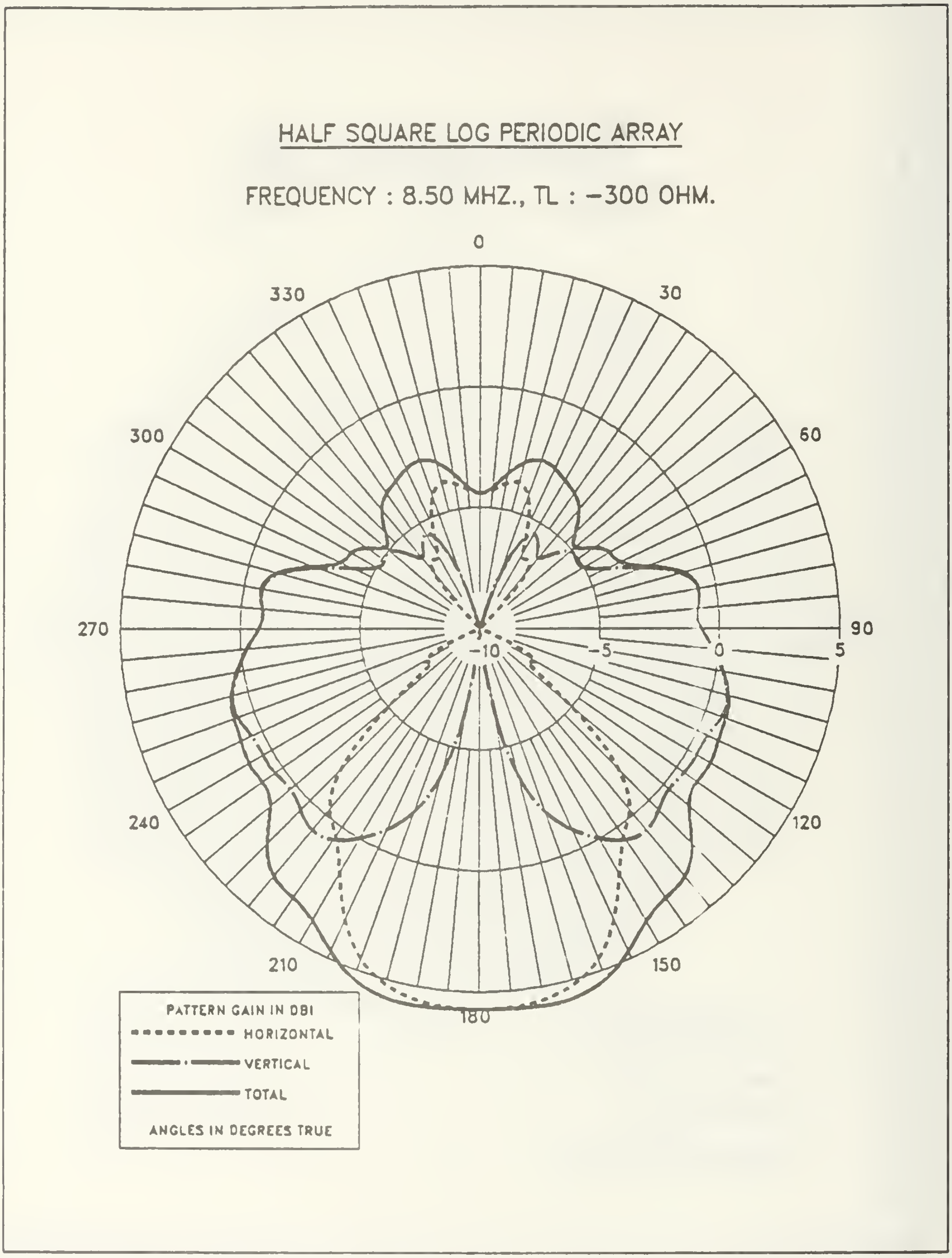

Figure C.27 Horizontal Pattern, Frequency: 8.5 MHz.

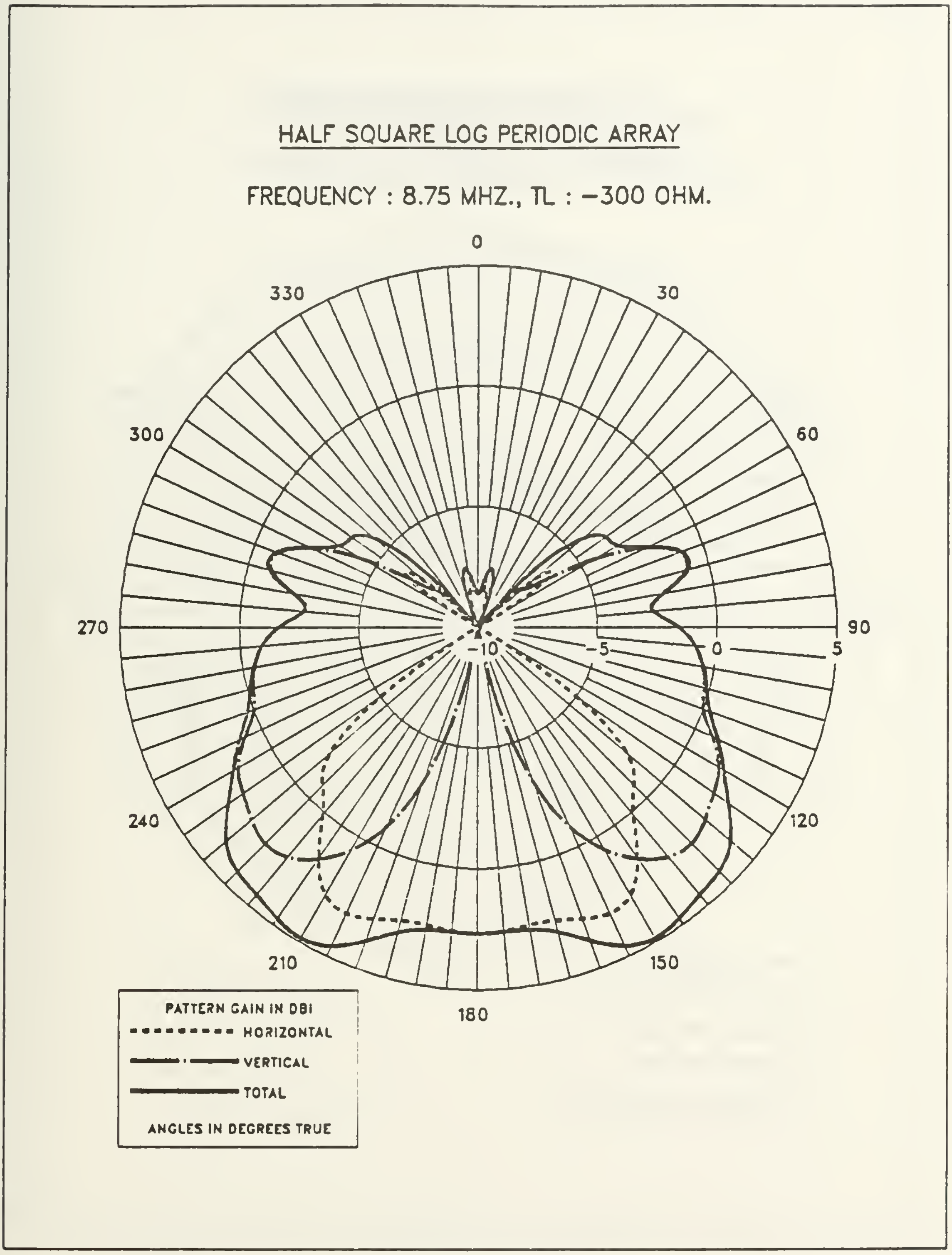

Figure C.28 Horizontal Pattern, Frequency: 8.75 MHz.

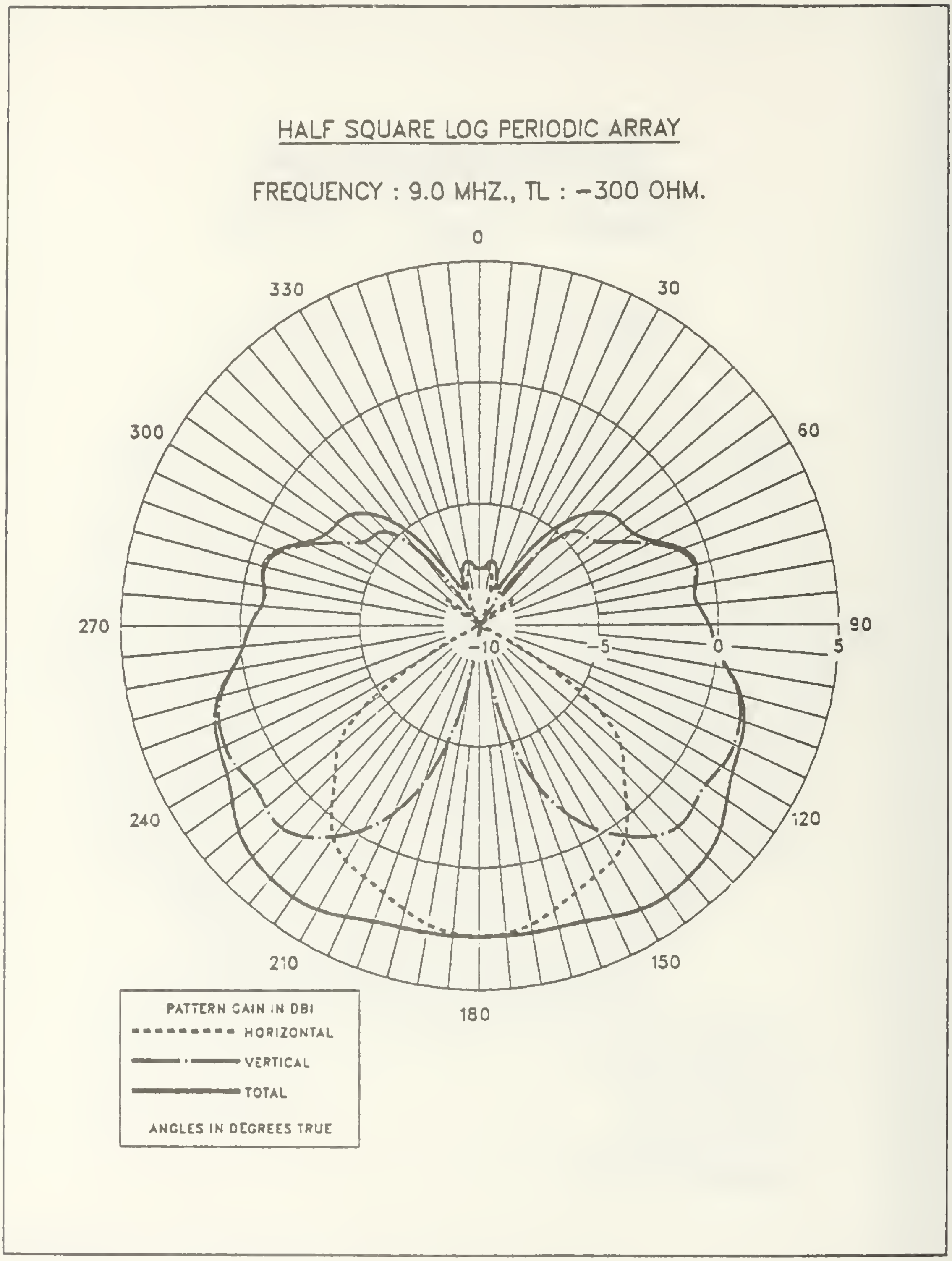

Figure C.29 Horizontal Pattern, Frequency: 9.0 MHz.

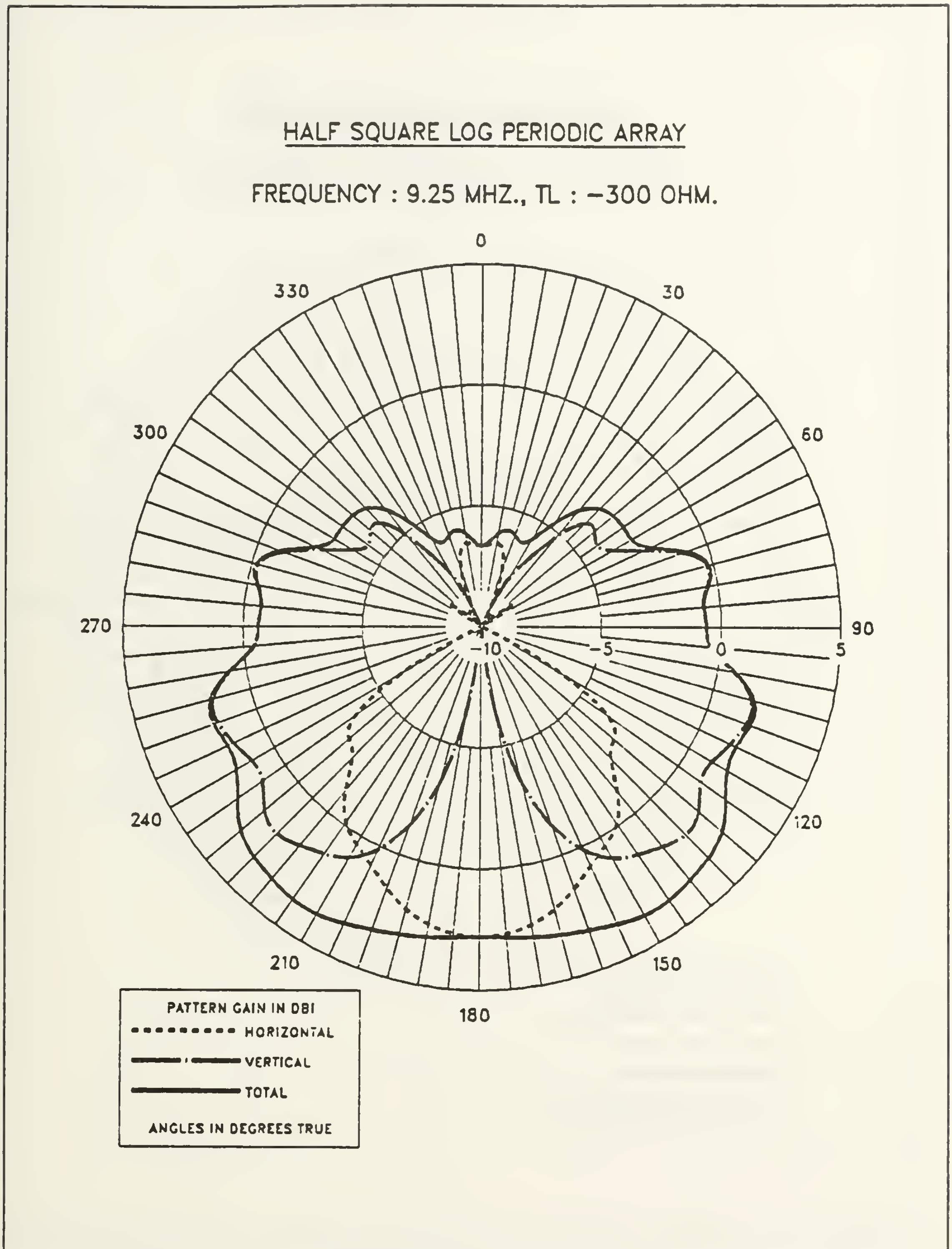

Figure C.30 Horizontal Pattern, Frequency: 9.25 MHz.

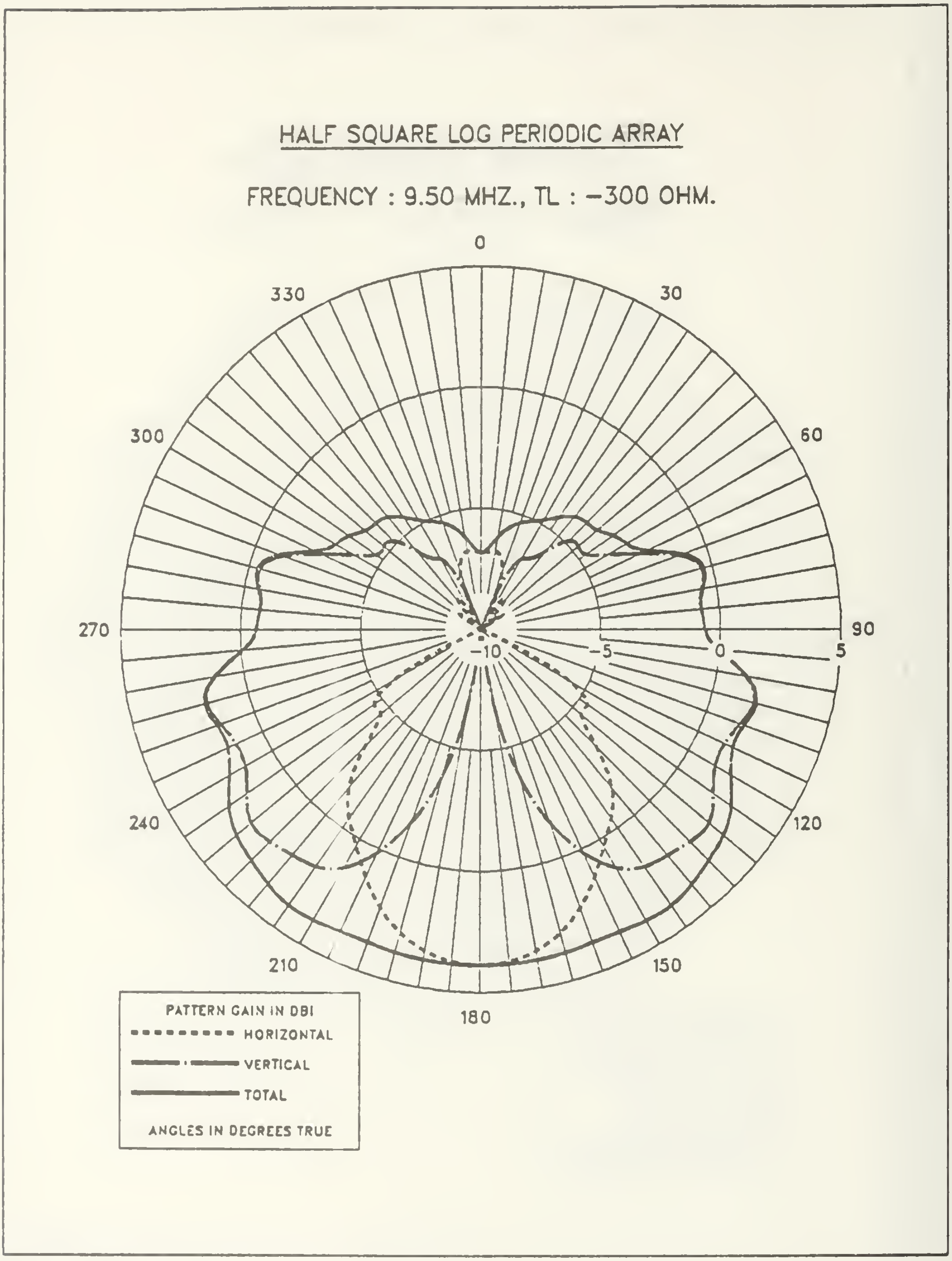

Figure C.31 Horizontal Pattern, Frequency: 9.5 MHz.

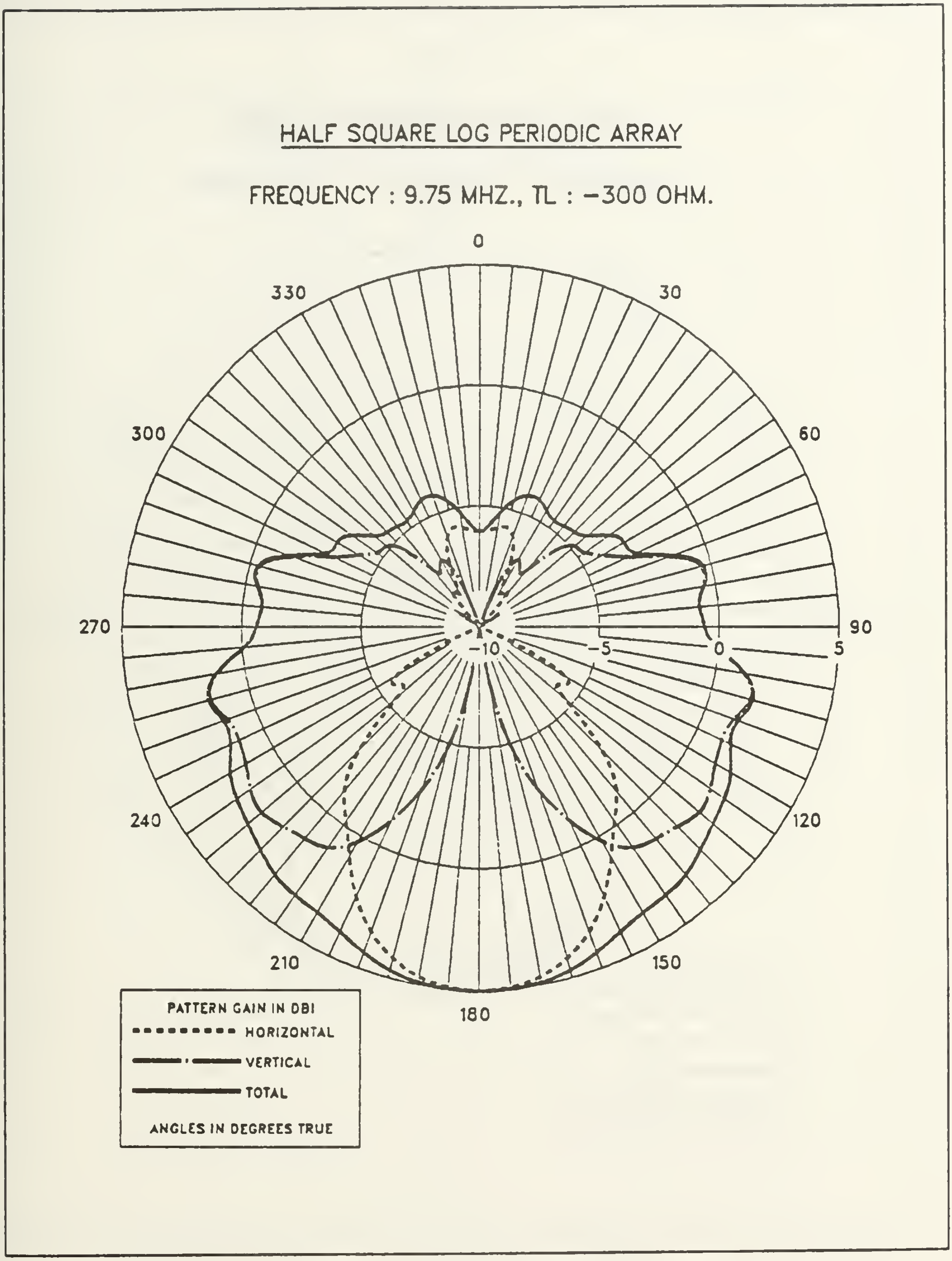

Figure C.32 Horizontal Pattern, Frequency: 9.75 MHz.

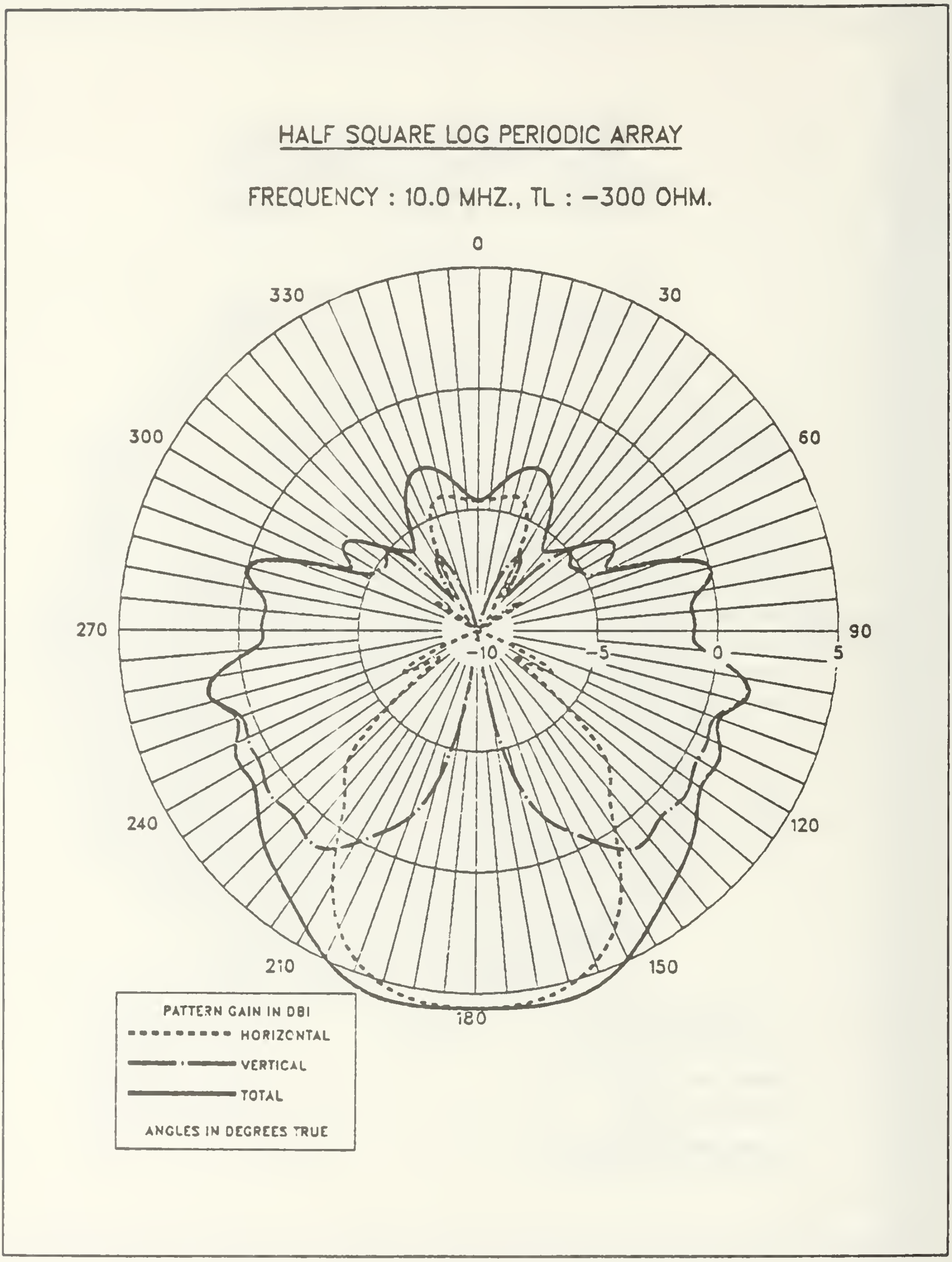

Figure C.33 Horizontal Pattern, Frequency: 10.0 MHz.

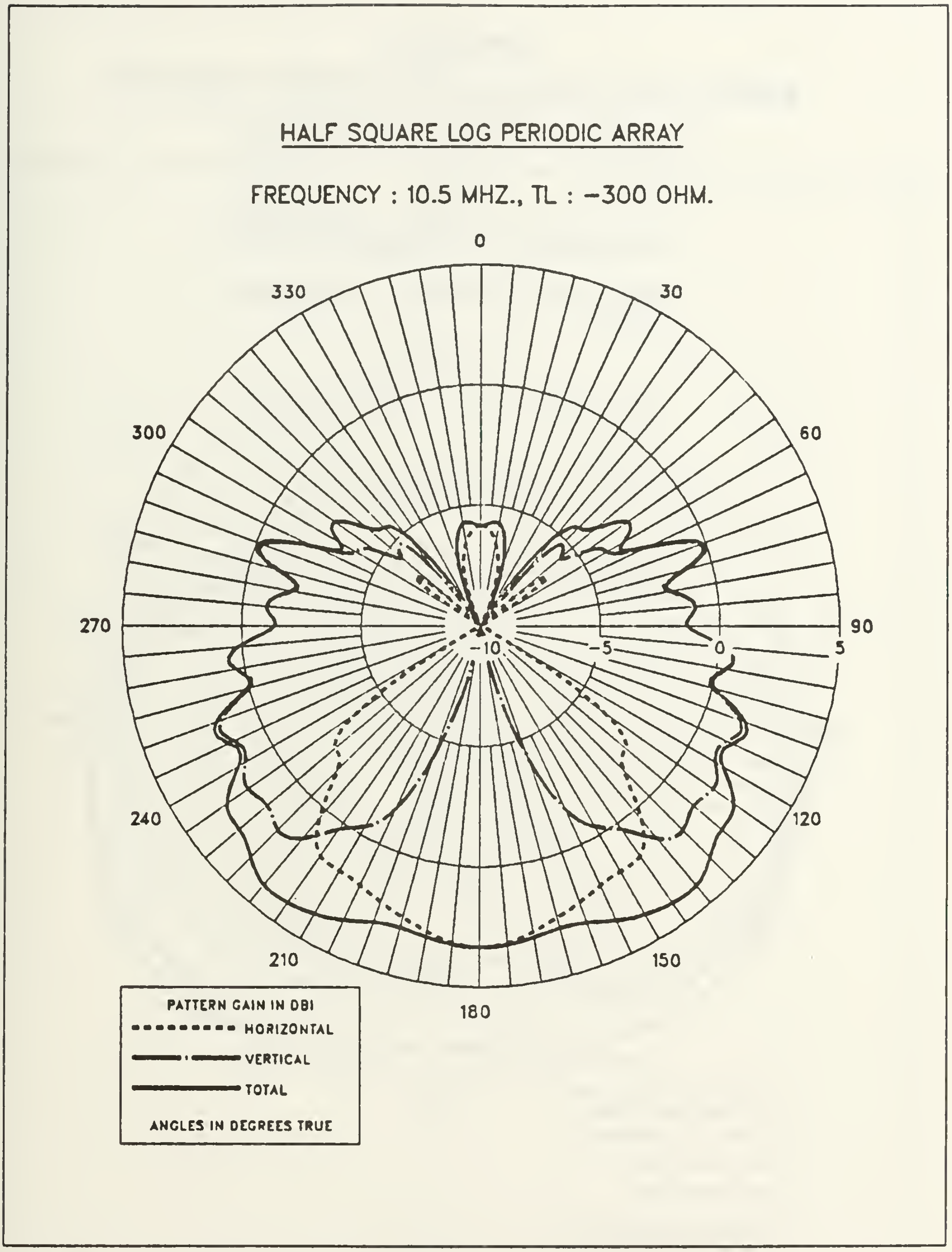

Figure C.34 Horizontal Pattern, Frequency: 10.5 MHz.

APPENDIX D
RADIATION PATTERNS OVER PERFECT GROUND

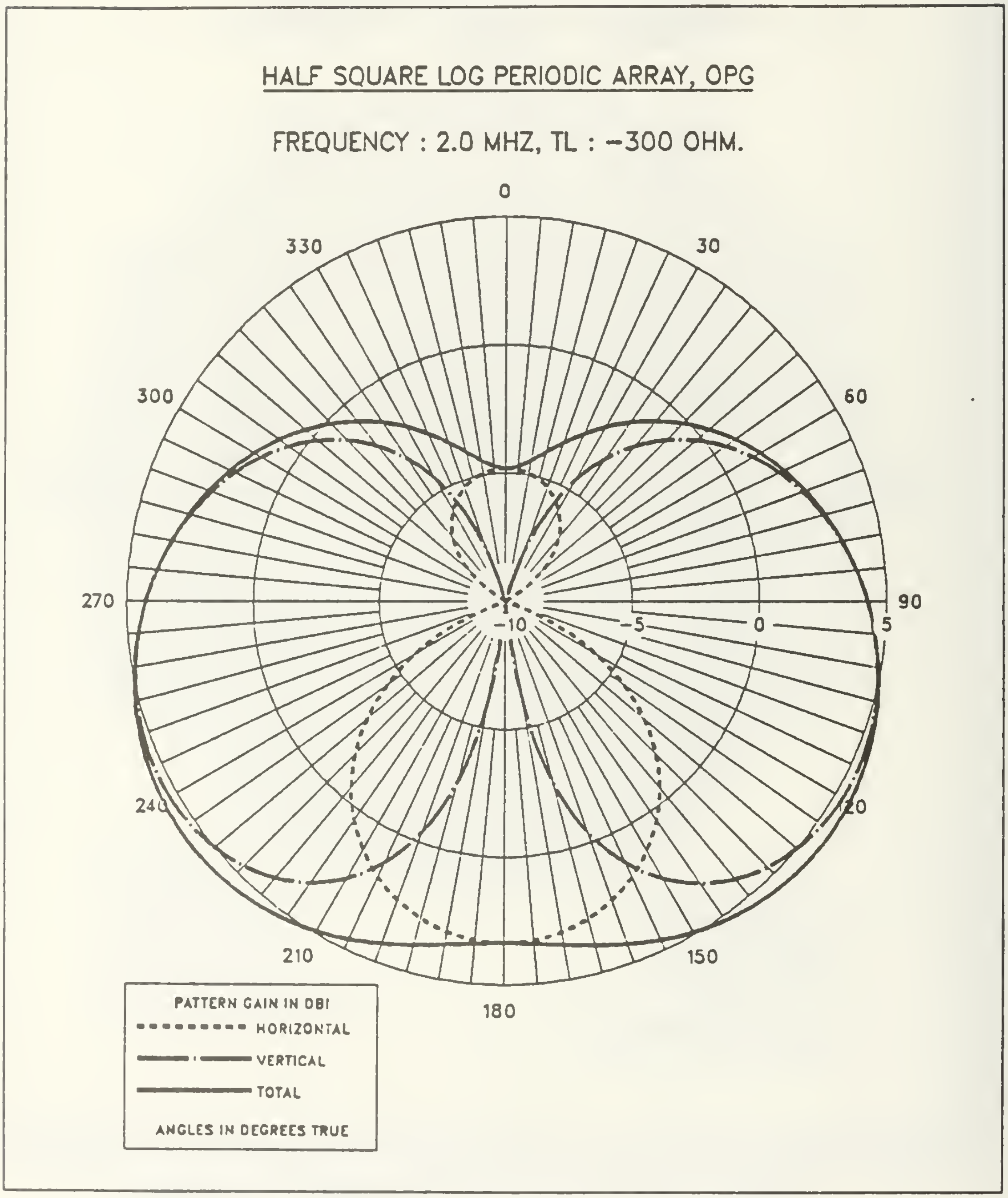

Figure D.1 Horizontal Pattern. Frequency: 2 MHz.

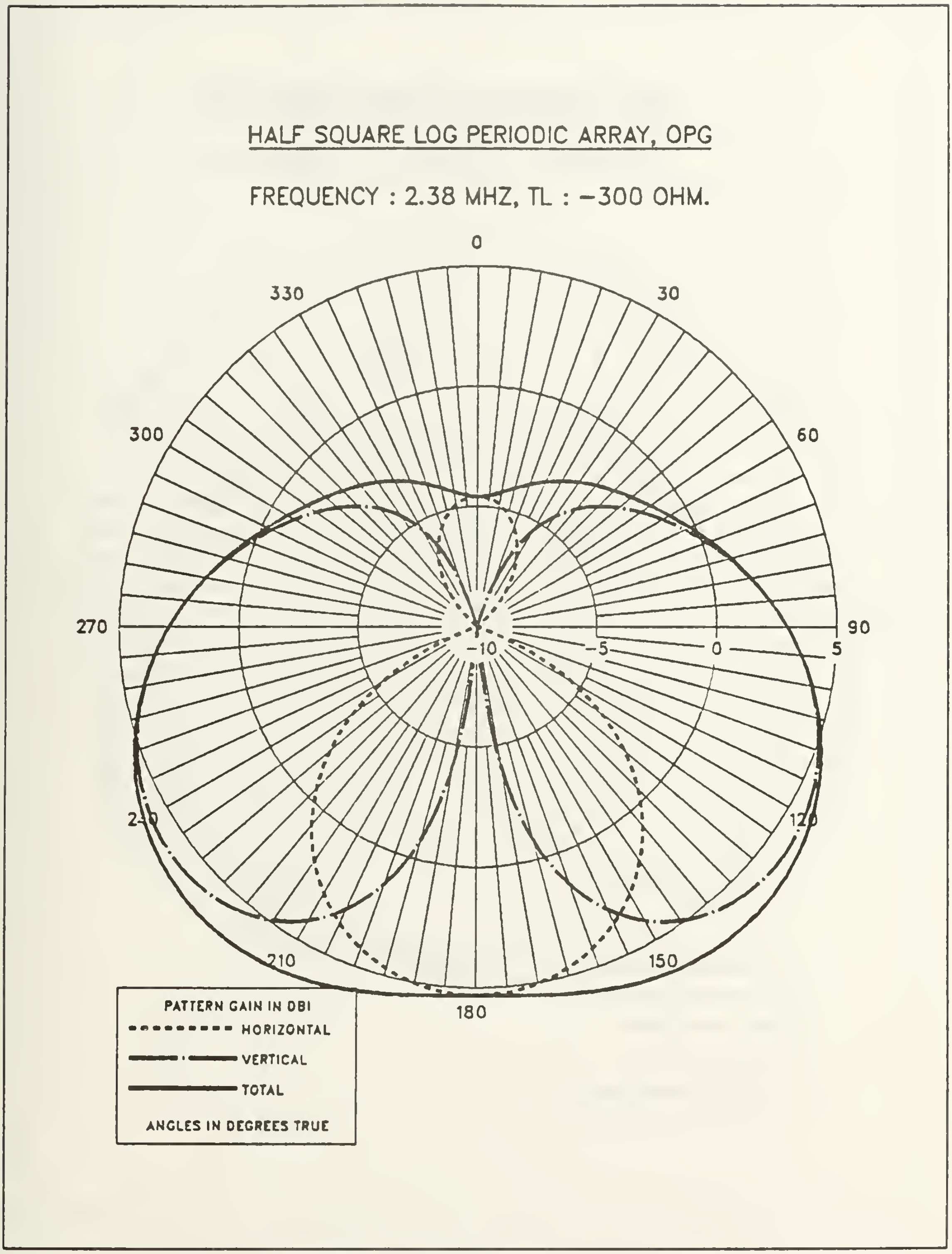

Figure D.2 Horizontal Pattern, Frequency: 2.38 MHz.

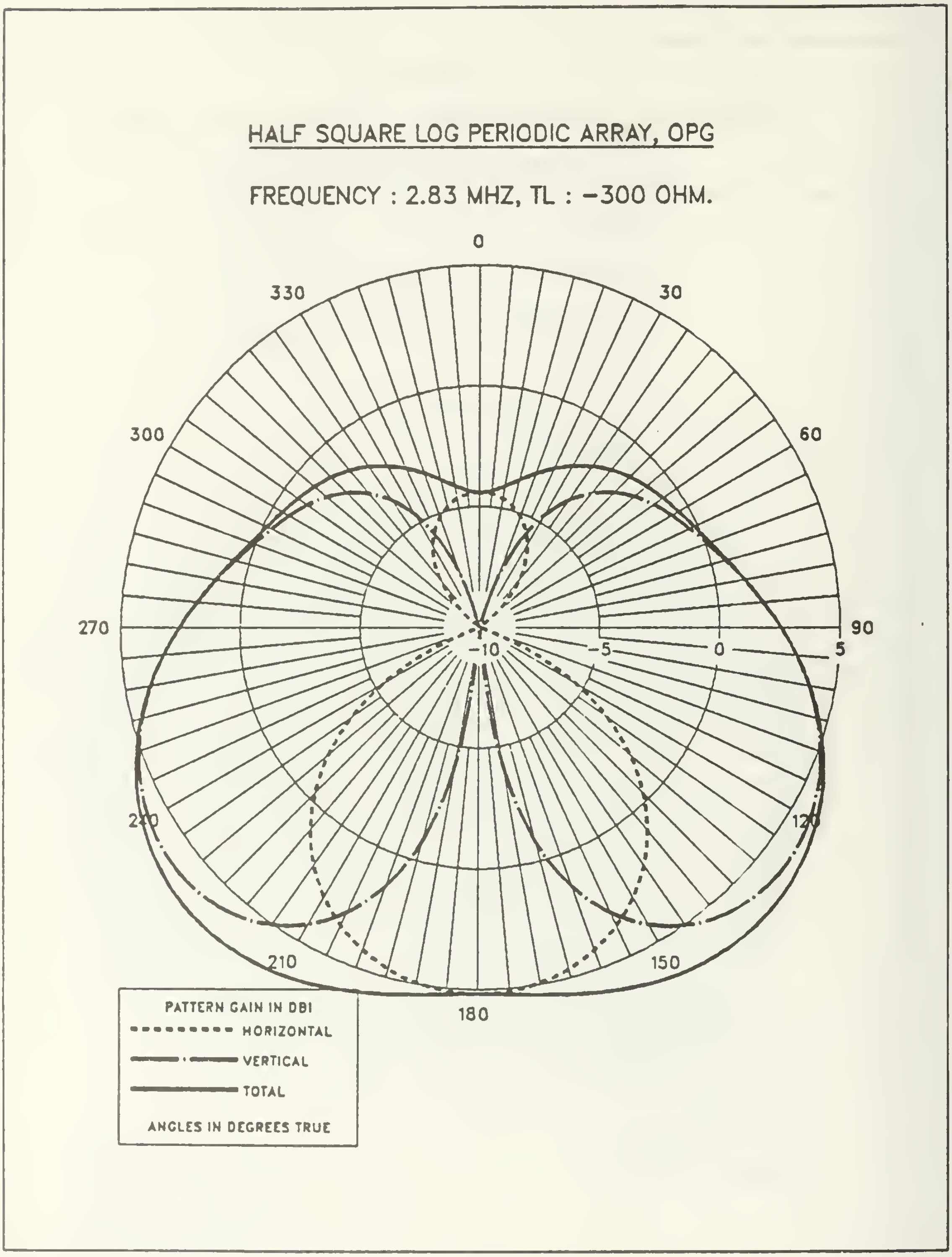

Figure D.3 Horizontal Pattern, Frequency: 2.83 MHz.

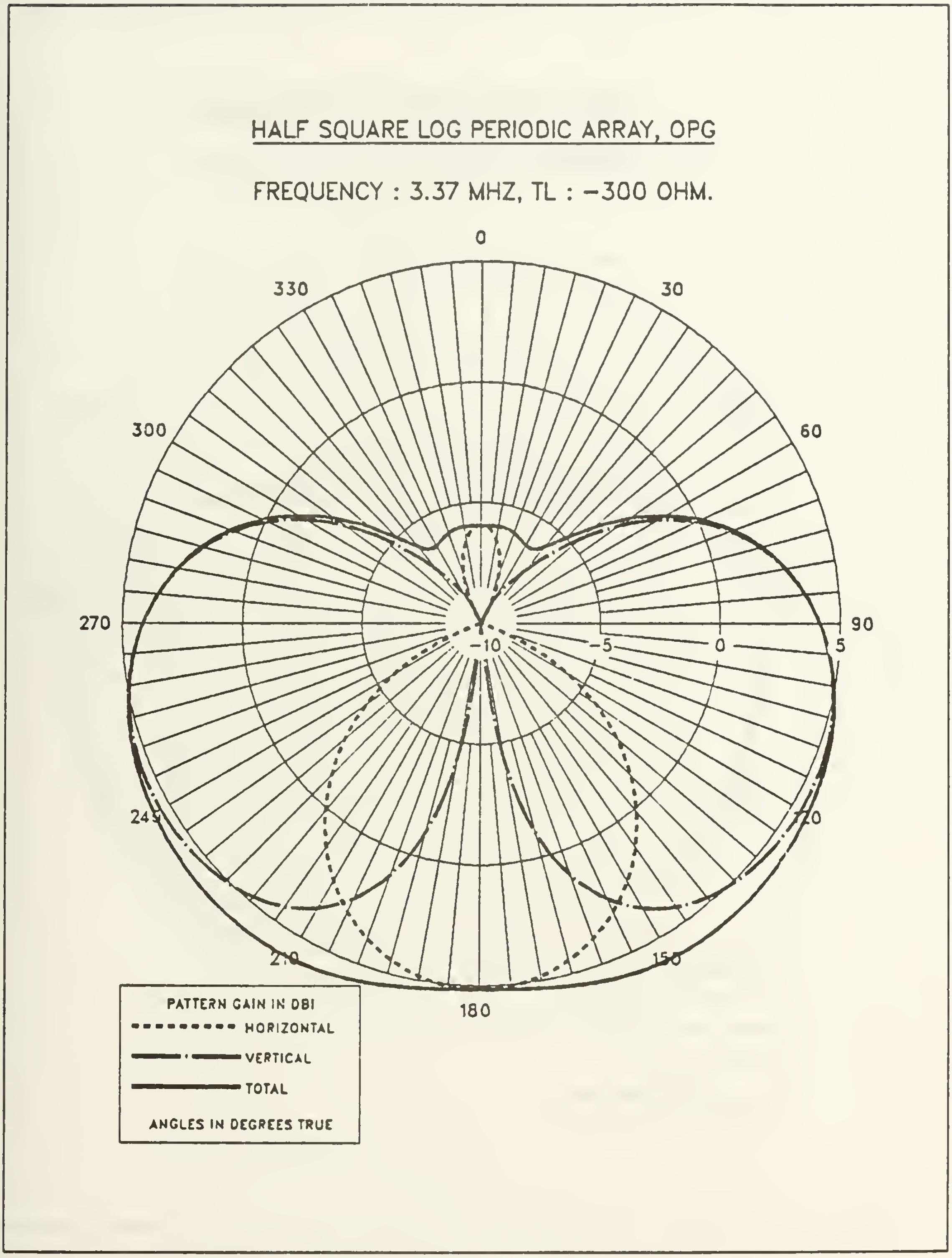

Figure D.4 Horizontal Pattern, Frequency: 3.37 MHz.

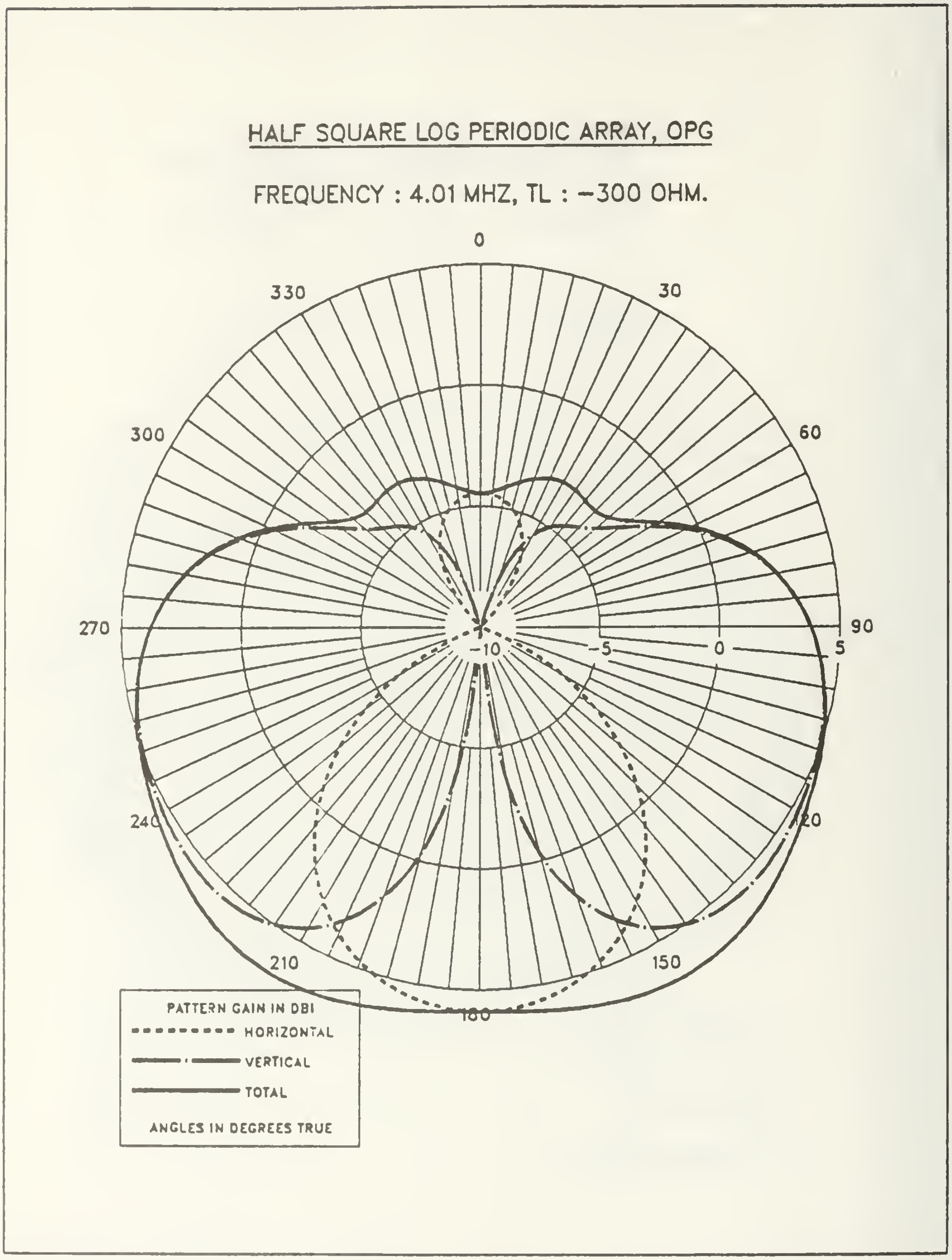

Figure D.5 Horizontal Pattern, Frequency: 4.07 MHz.

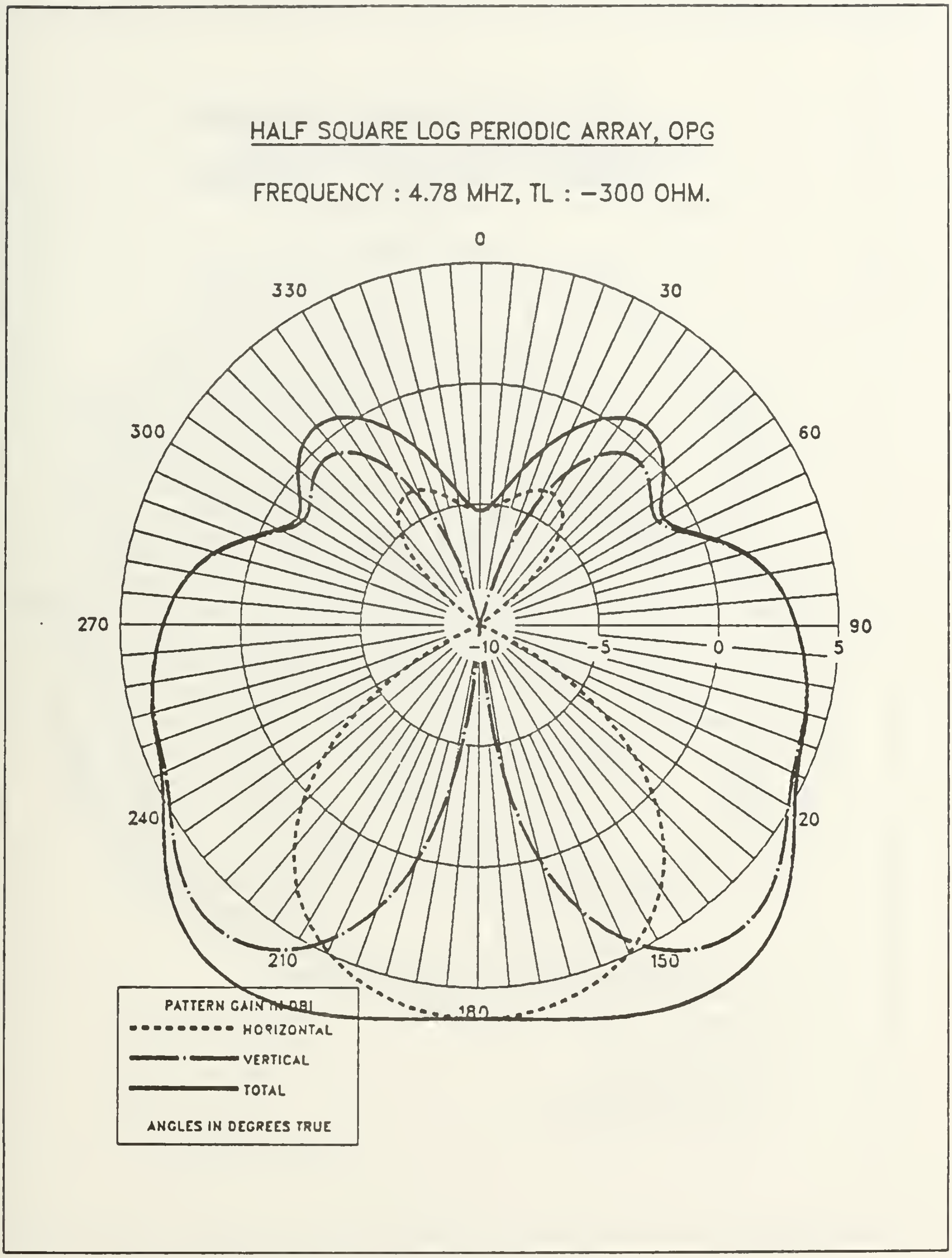

Figure D.6 Horizontal Pattern, Frequency: 4.78 MHz.

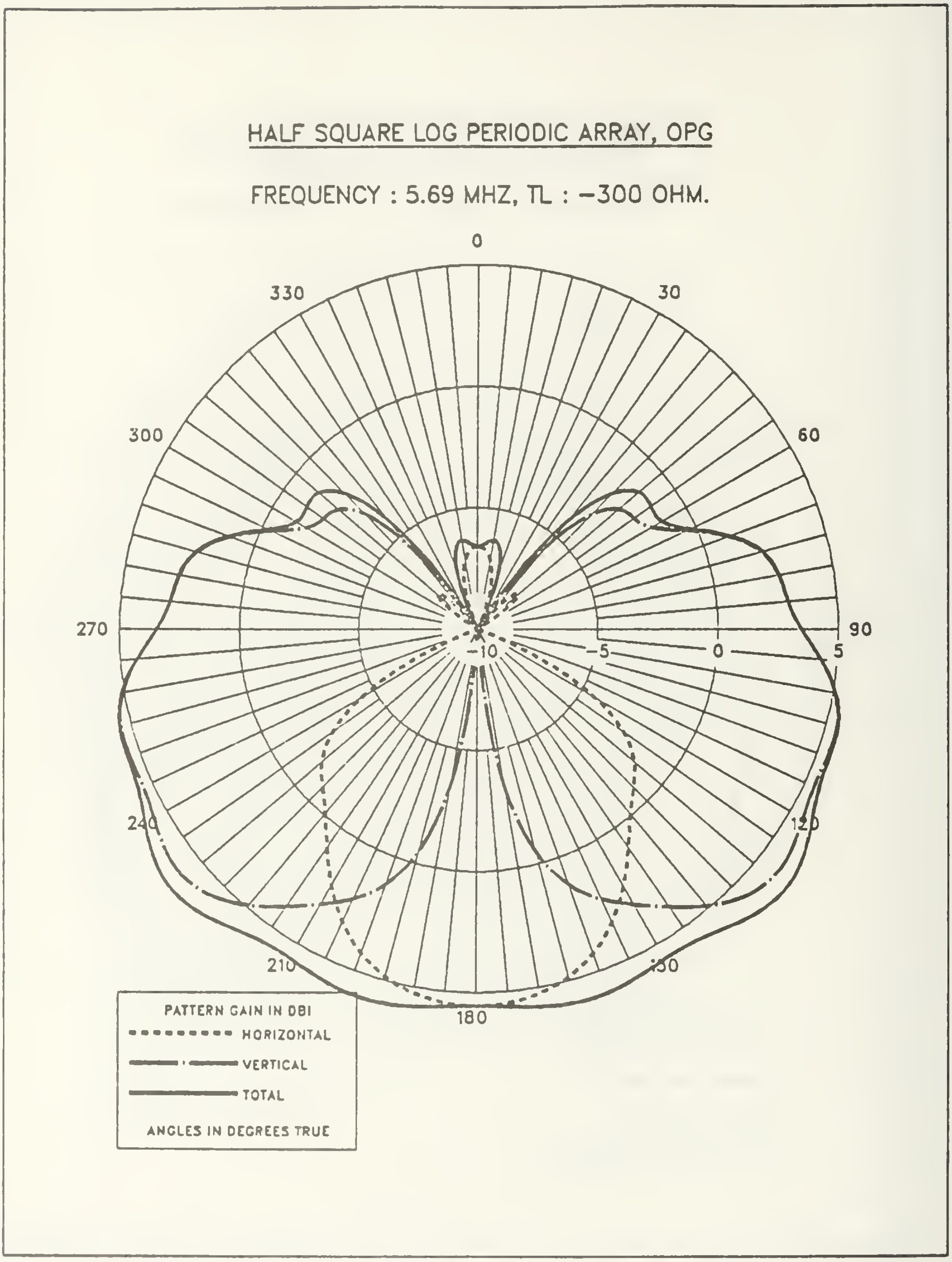

Figure D.7 Horizontal Pattern, Frequency: 5.69 MHz.

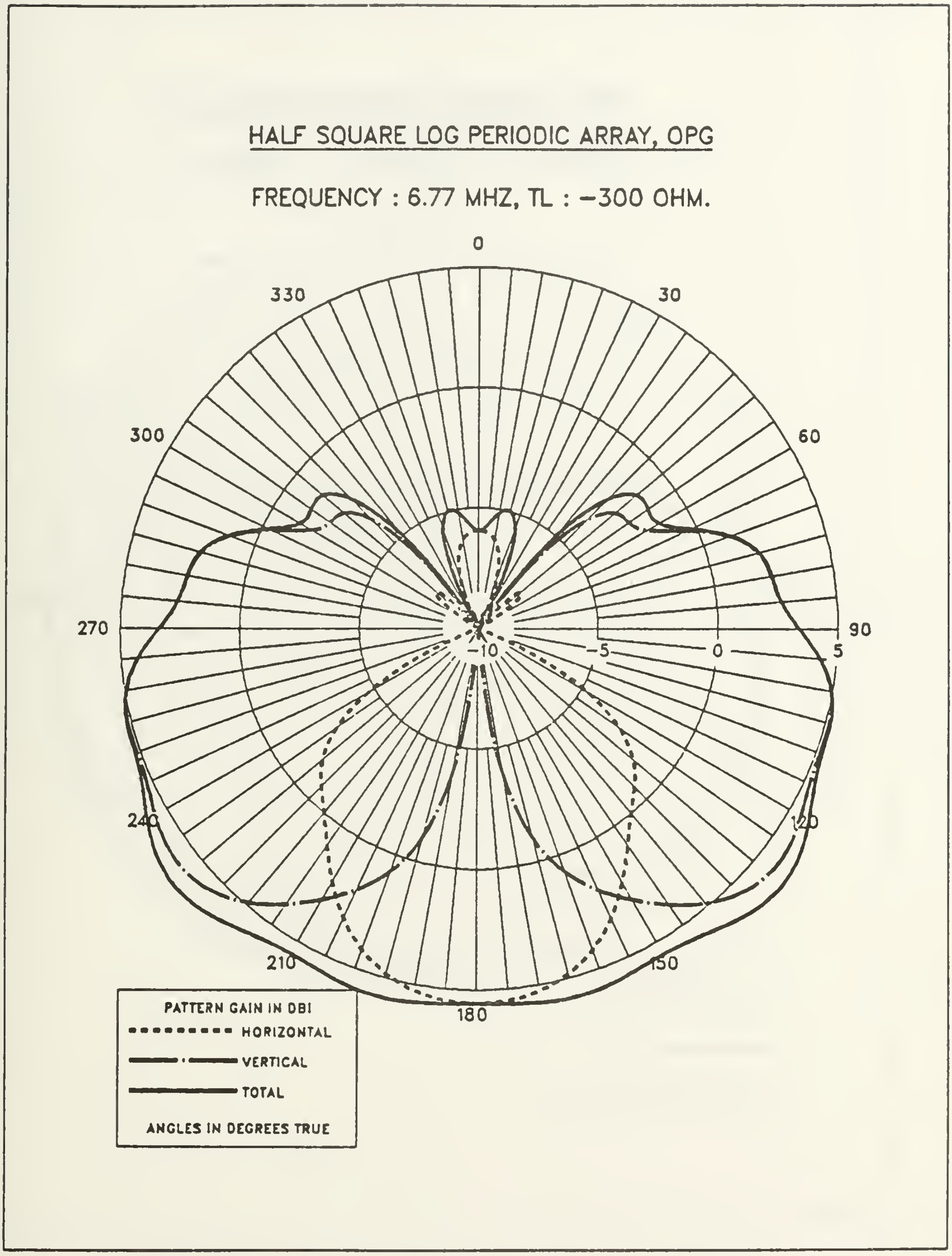

Figure D.8 Horizontal Pattern, Frequency: 6.77 MHz.

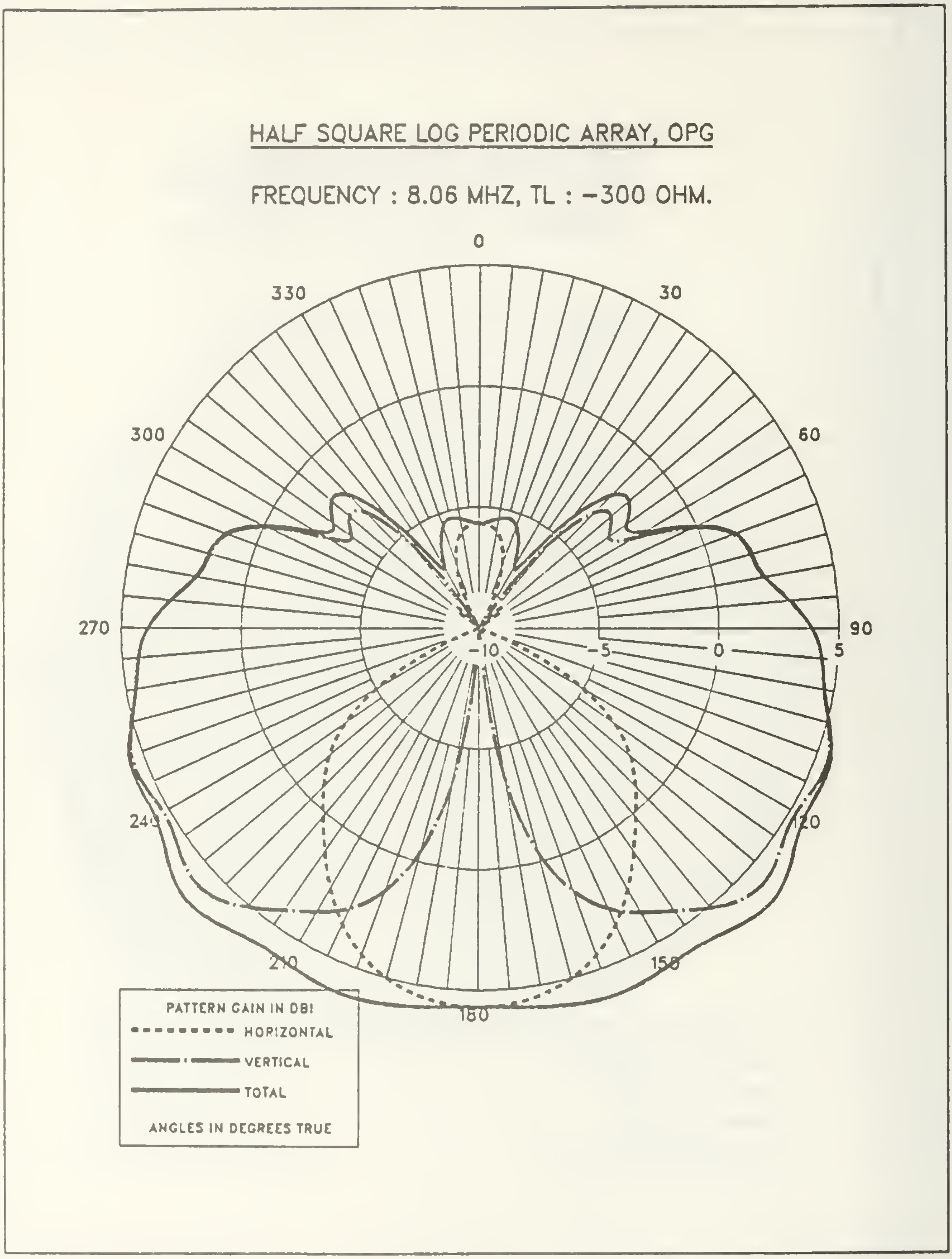

Figure D.9 Horizontal Pattern, Frequency: 8.06 MHz.

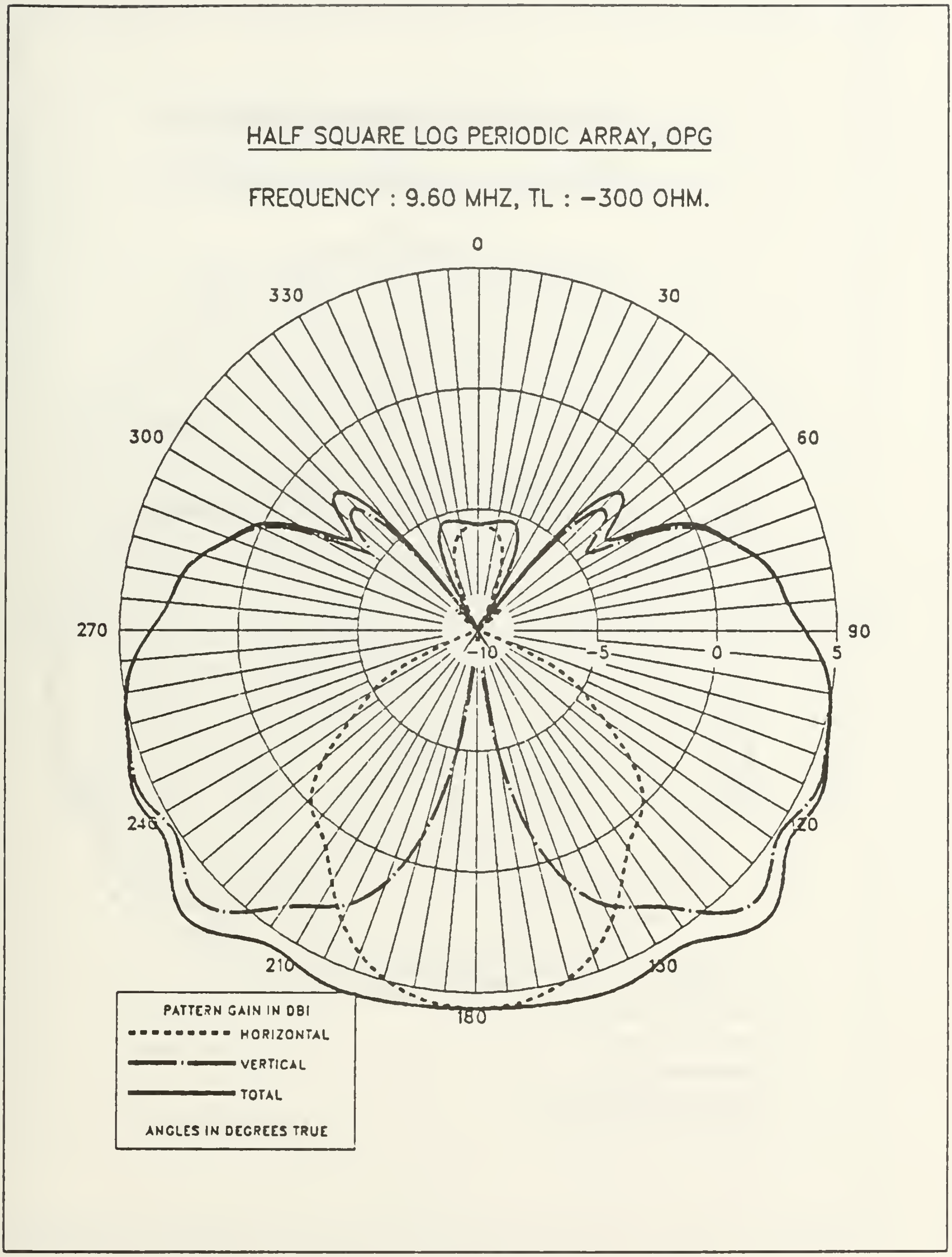

Figure D.10 Horizontal Pattern, Frequency: 9.60 MHz.

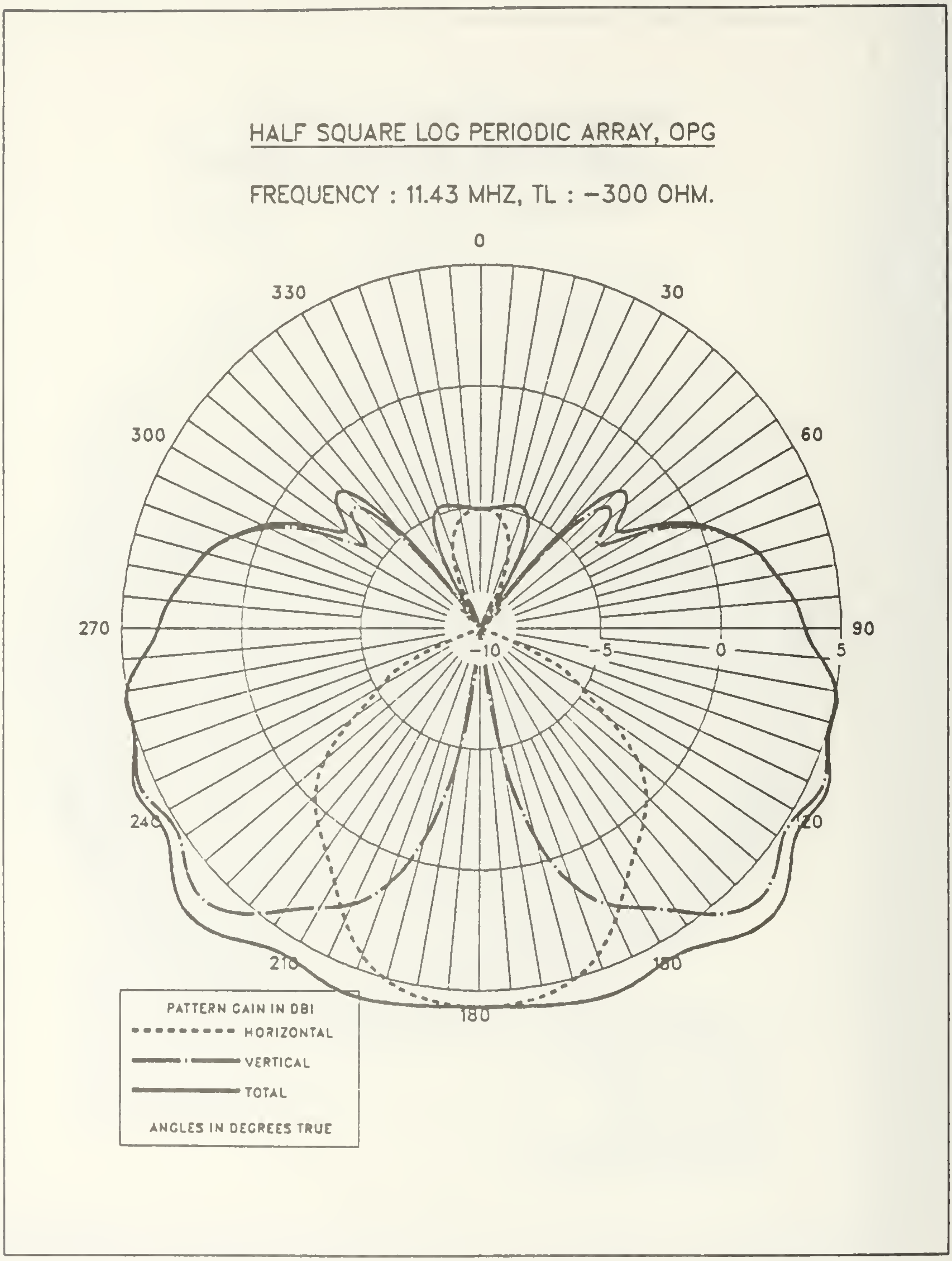

Figure D.11 Horizontal Pattern, Frequency: 11.43 MHz.

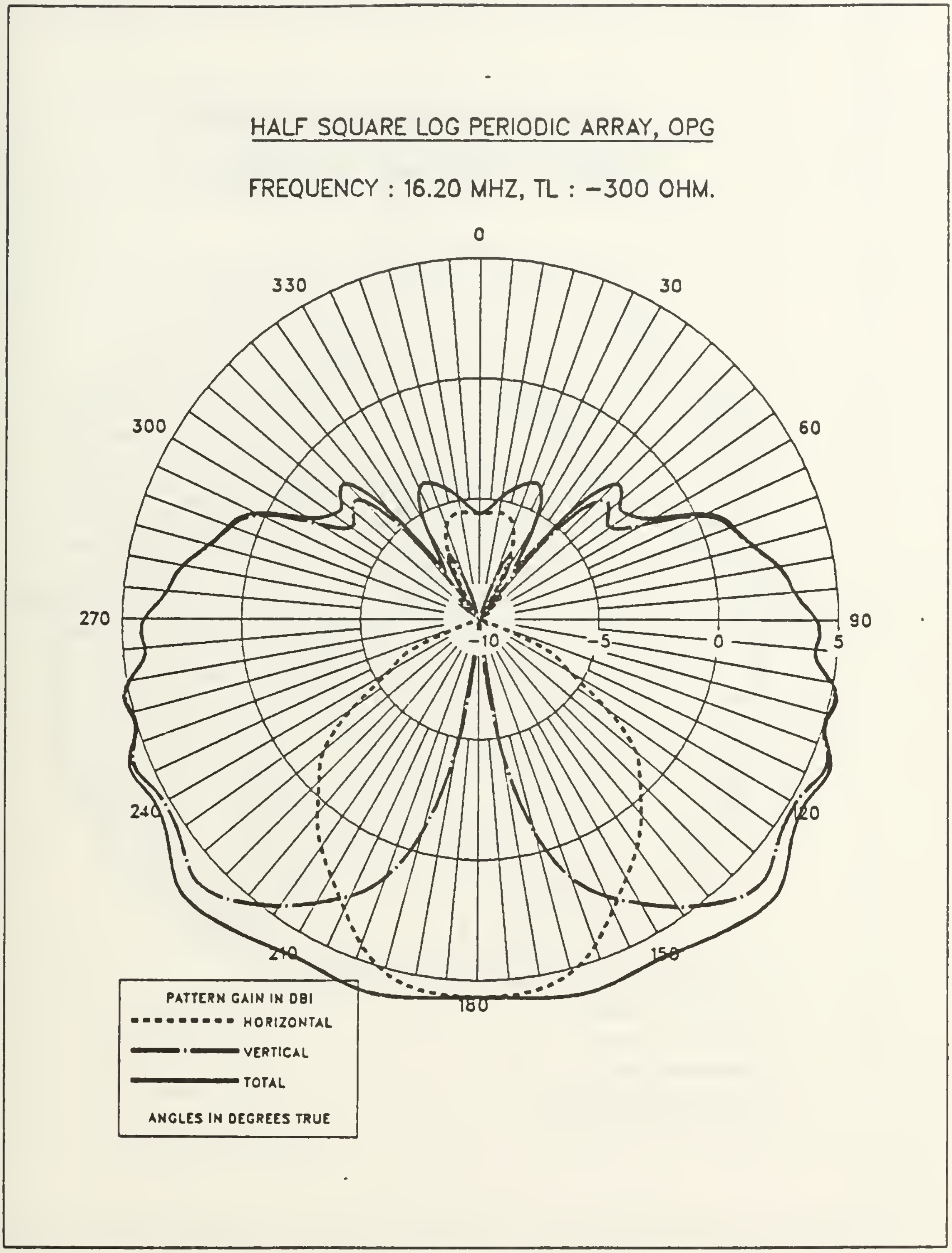

Figure D.12 Horizontal Pattern, Frequency: 16.20 MHz.

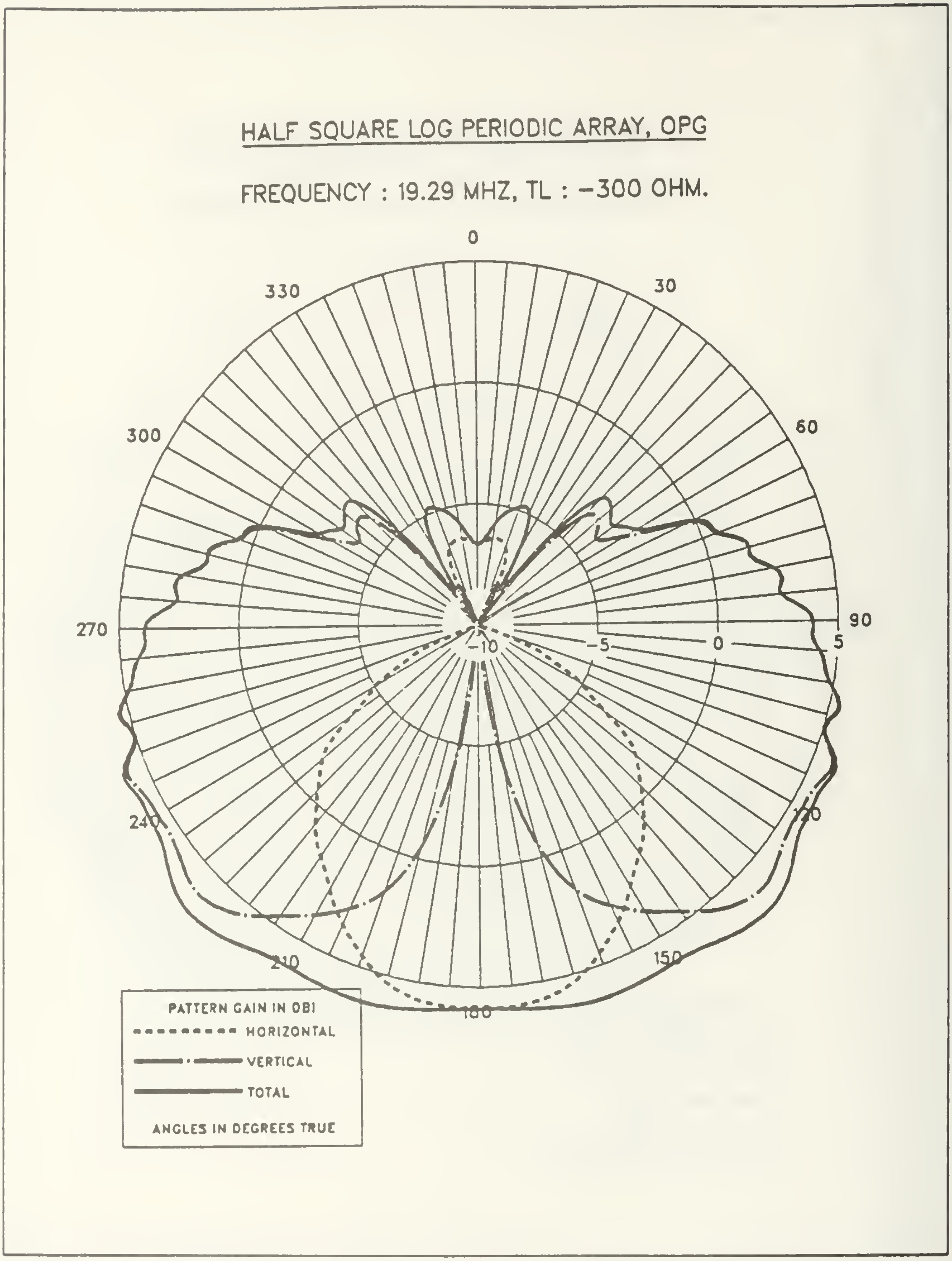

Figure D.13 Horizontal Pattern, Frequency: 19.29 MHz.

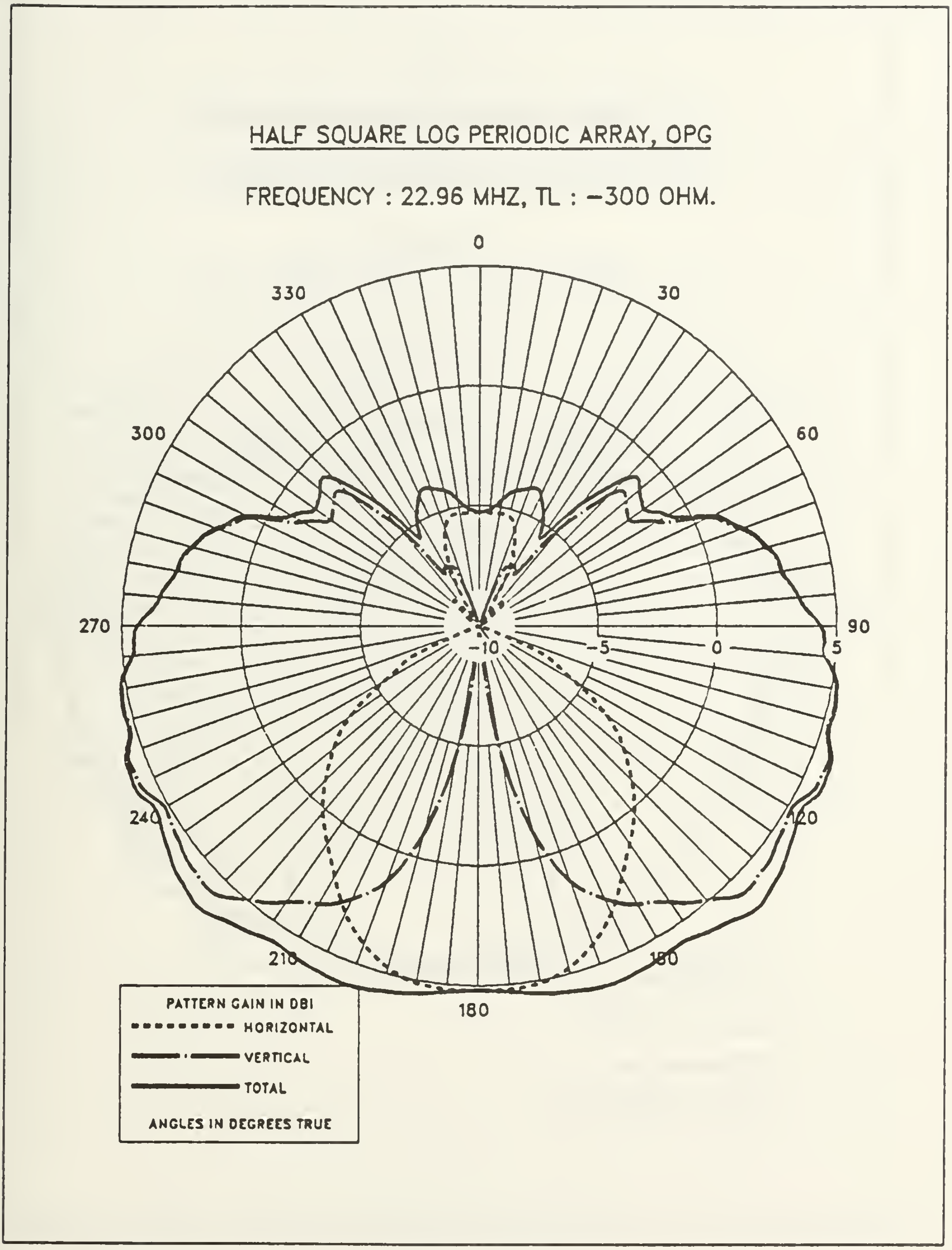

Figure D.14 Horizontal Pattern, Frequency: 22.96 MHz.

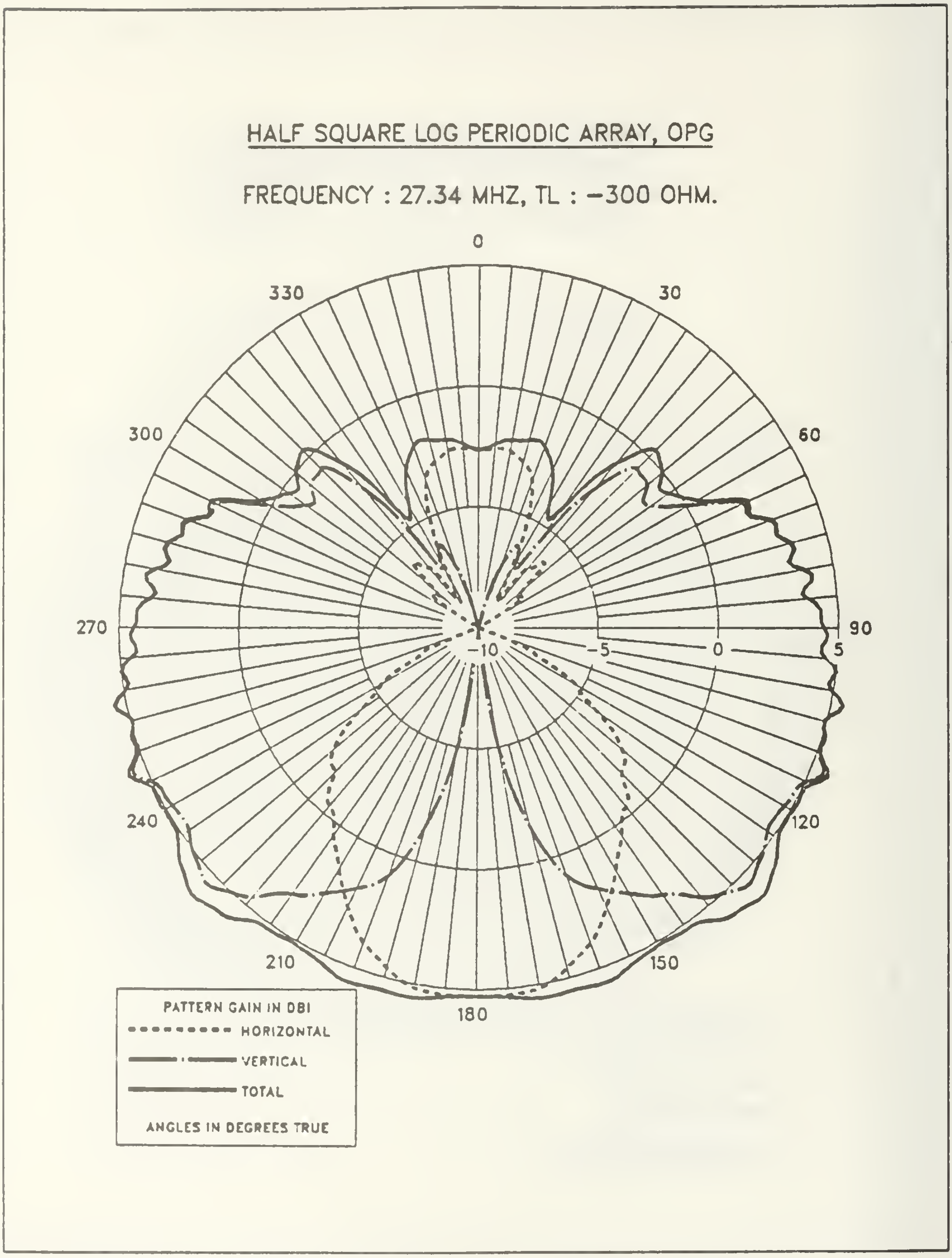

Figure D.15 Horizontal Pattern, Frequency: 27.34 MHz.

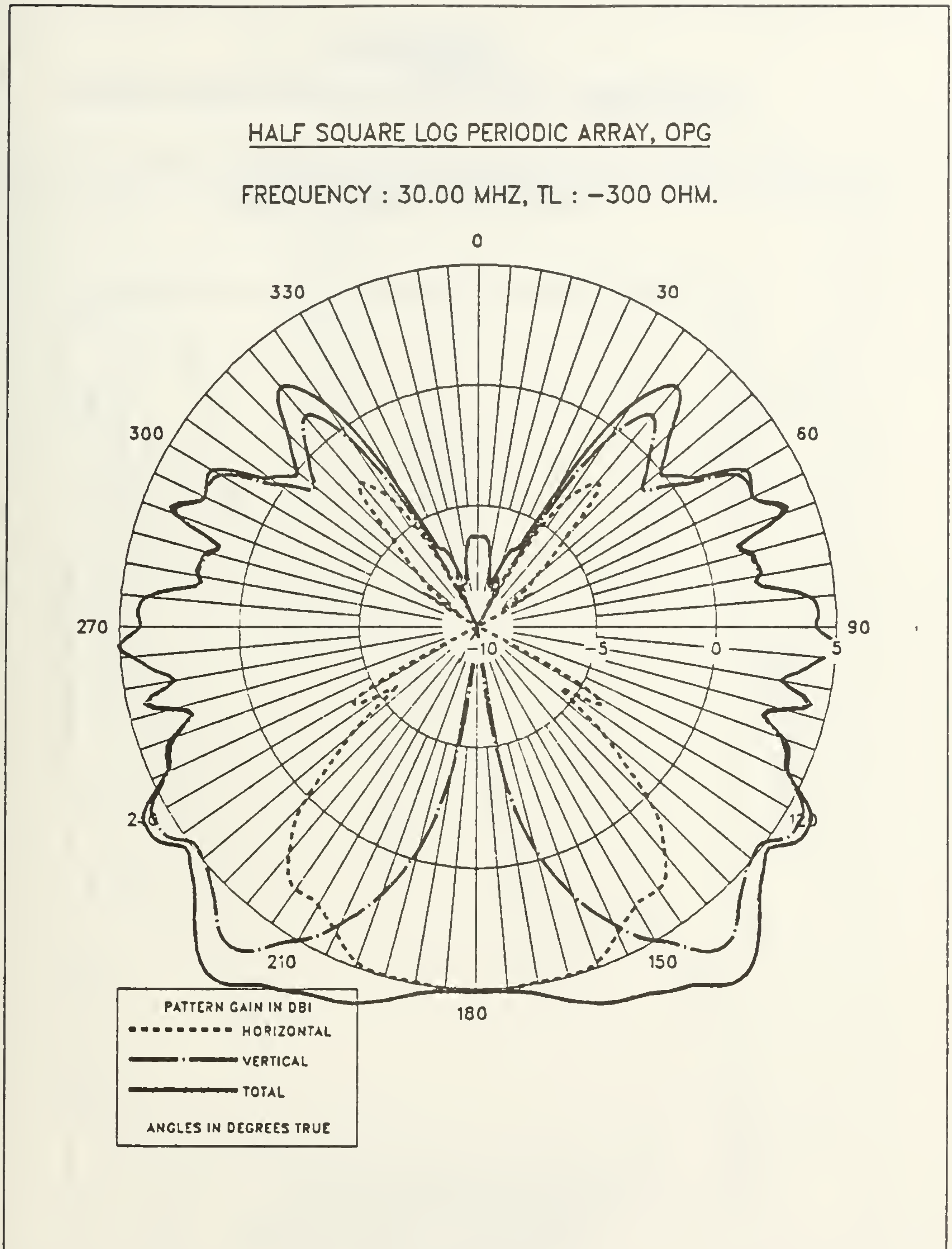

Figure D.16 Horizontal Pattern, Frequency: 30.0 MHz.

APPENDIX E
AMPLITUDE AND PHASE PLOTS IN FREE SPACE

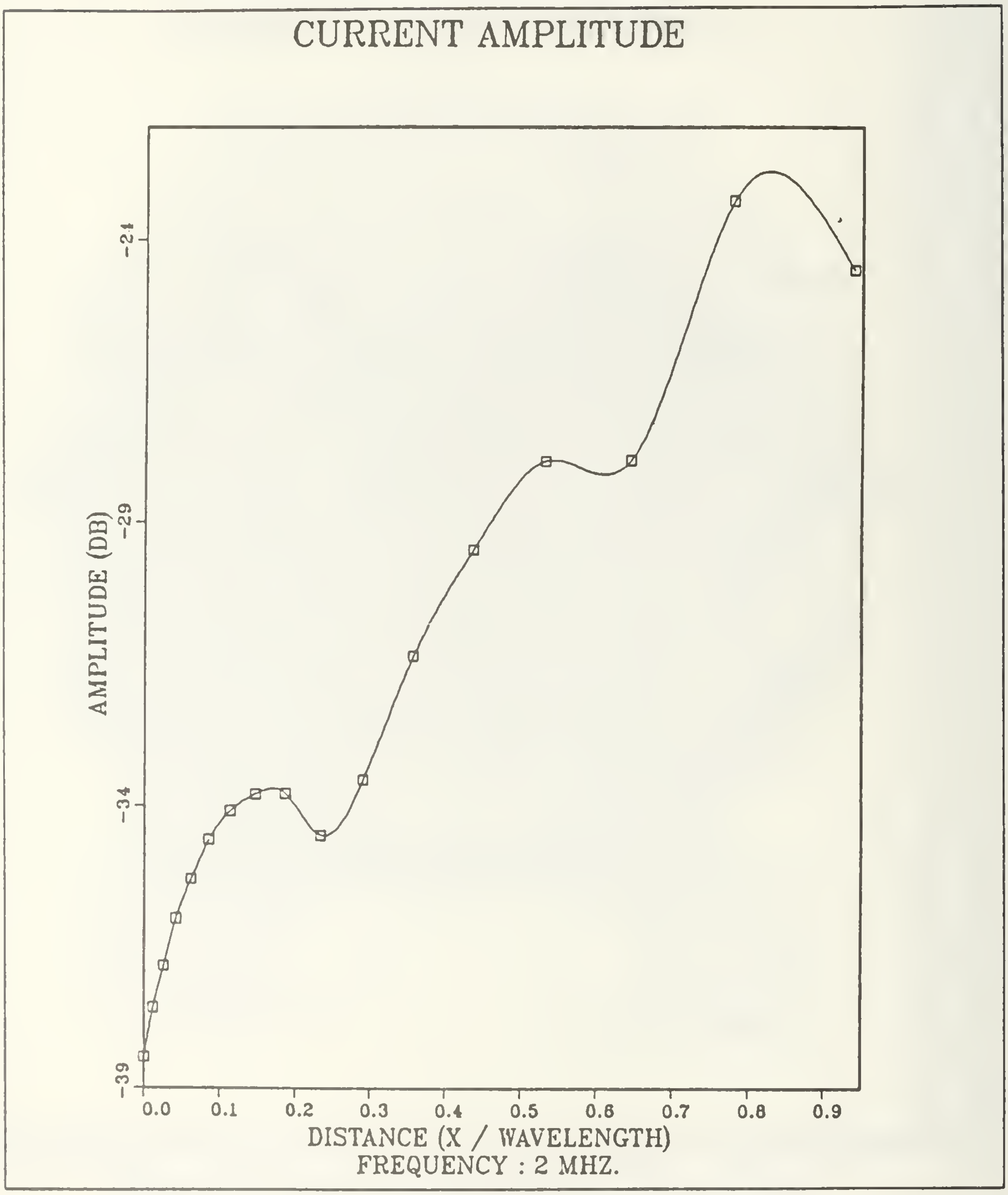

Figure E.1 Current Amplitude, Frequency : 2 MHz.

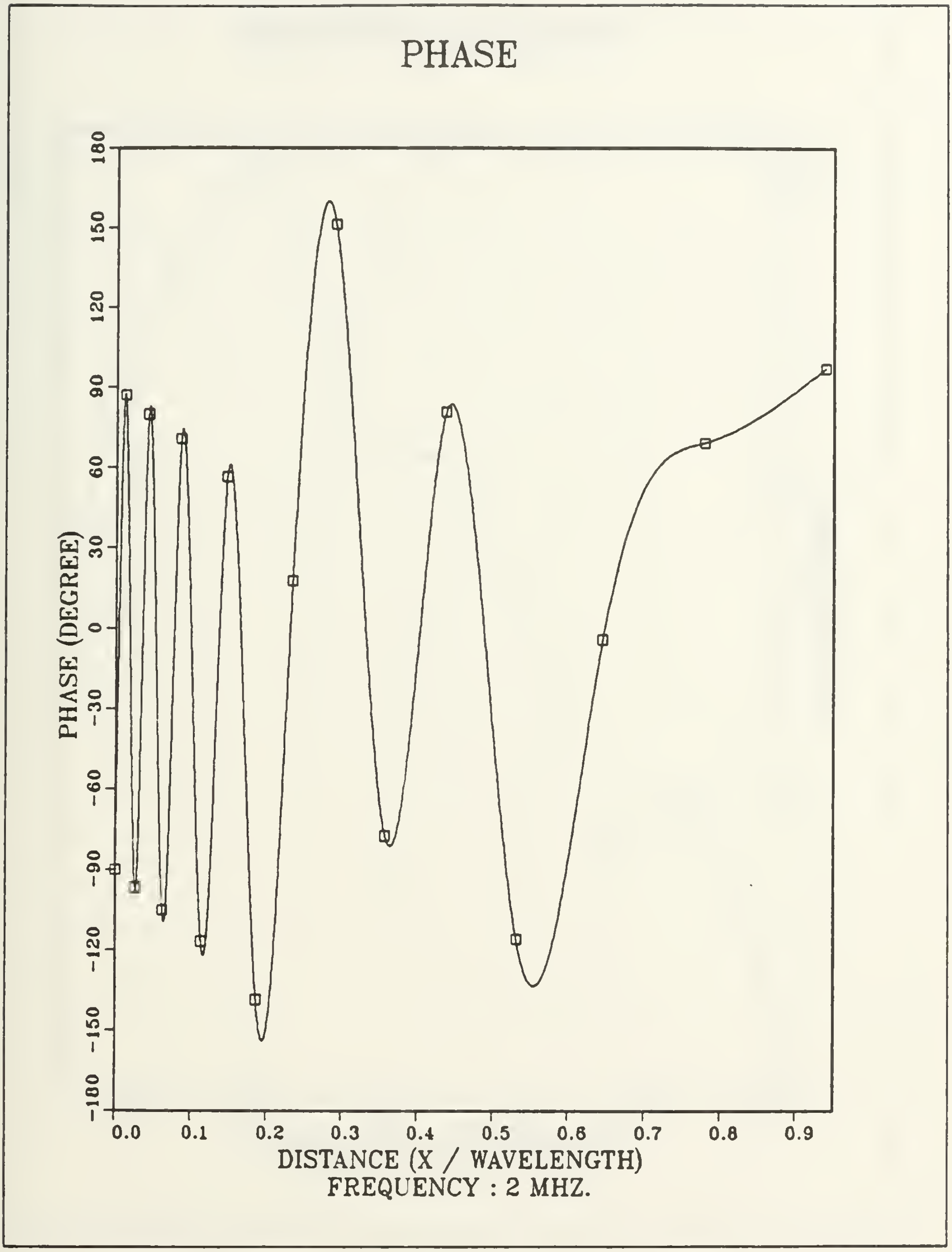

Figure E.2 Current Phase, Frequency : 2 MHz.

Figure E.3 Current Amplitude, Frequency : 2.38 MHz.

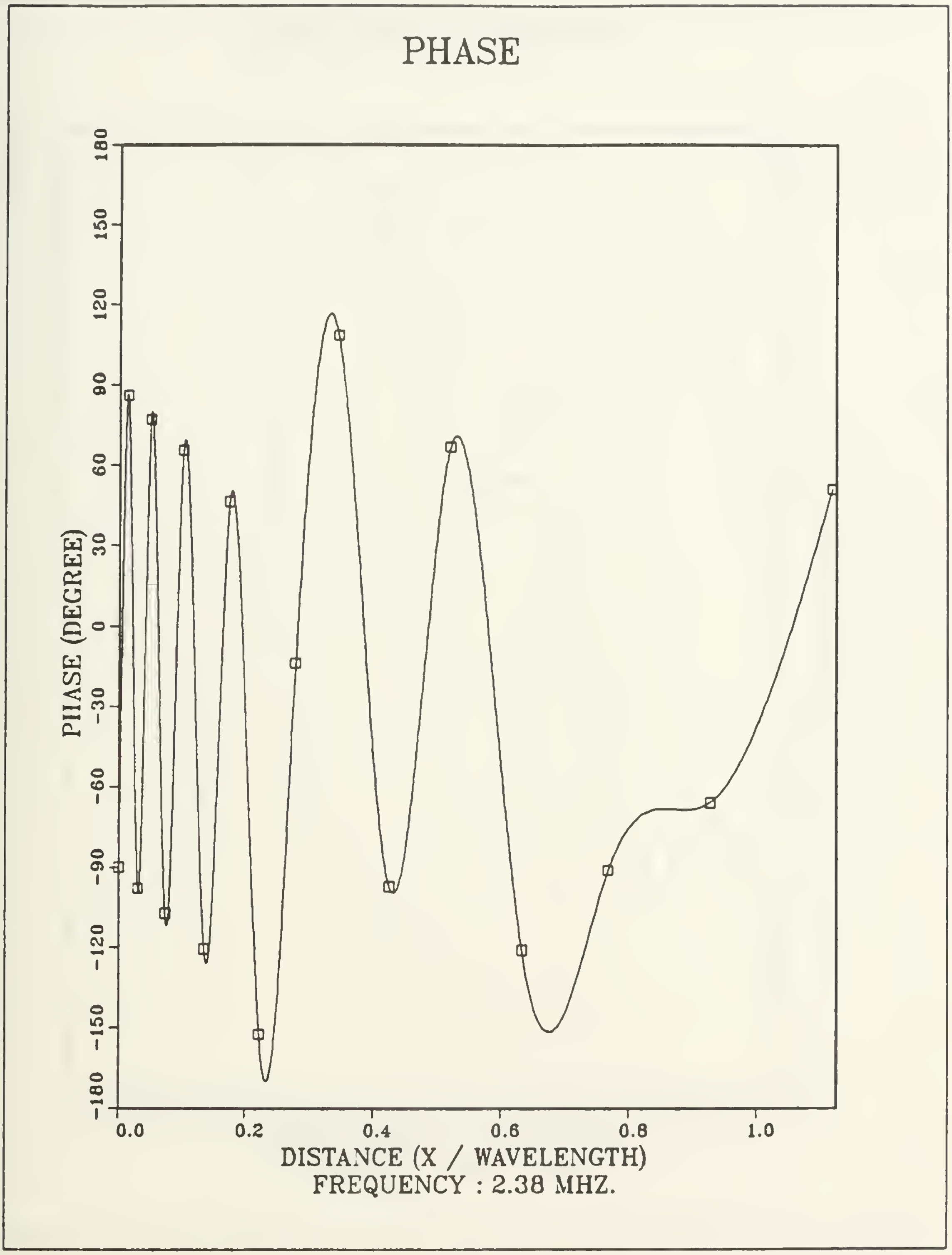

Figure E.4 Current Phase, Frequency : 2.38 MHz.

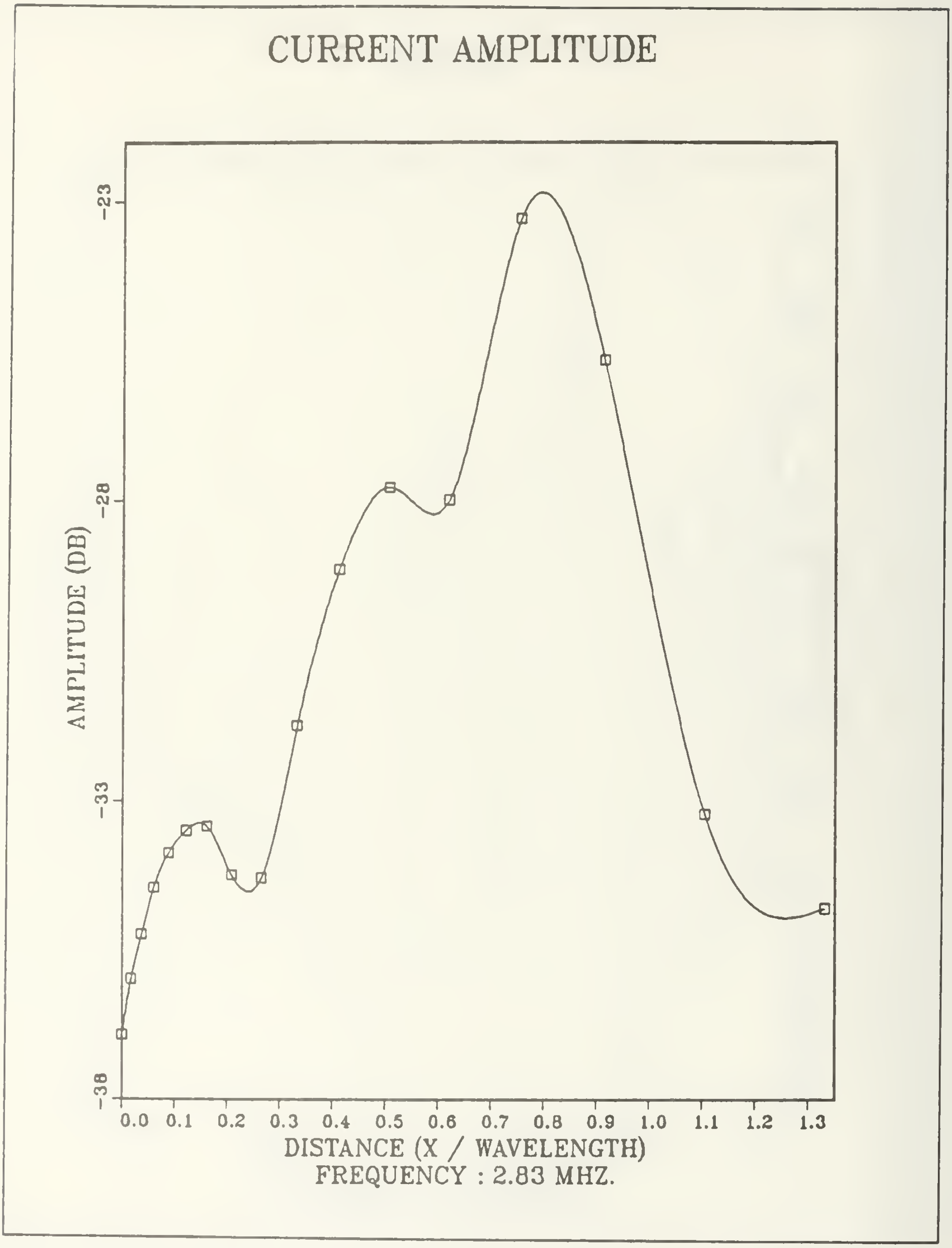

Figure E.5 Current Amplitude, Frequency : 2.83 MHz.

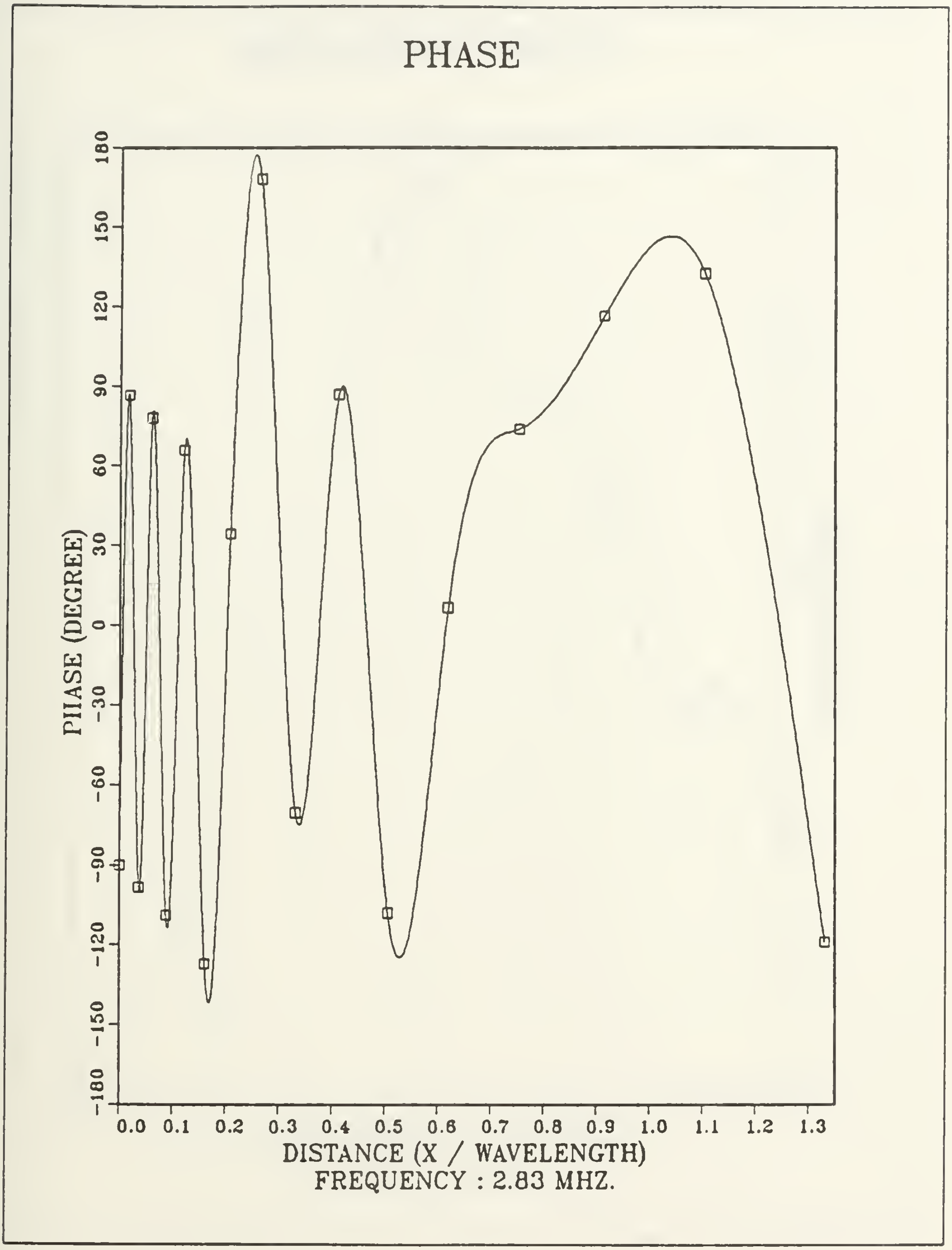

Figure E.6 Current Phase, Frequency : 2.83 MHz.

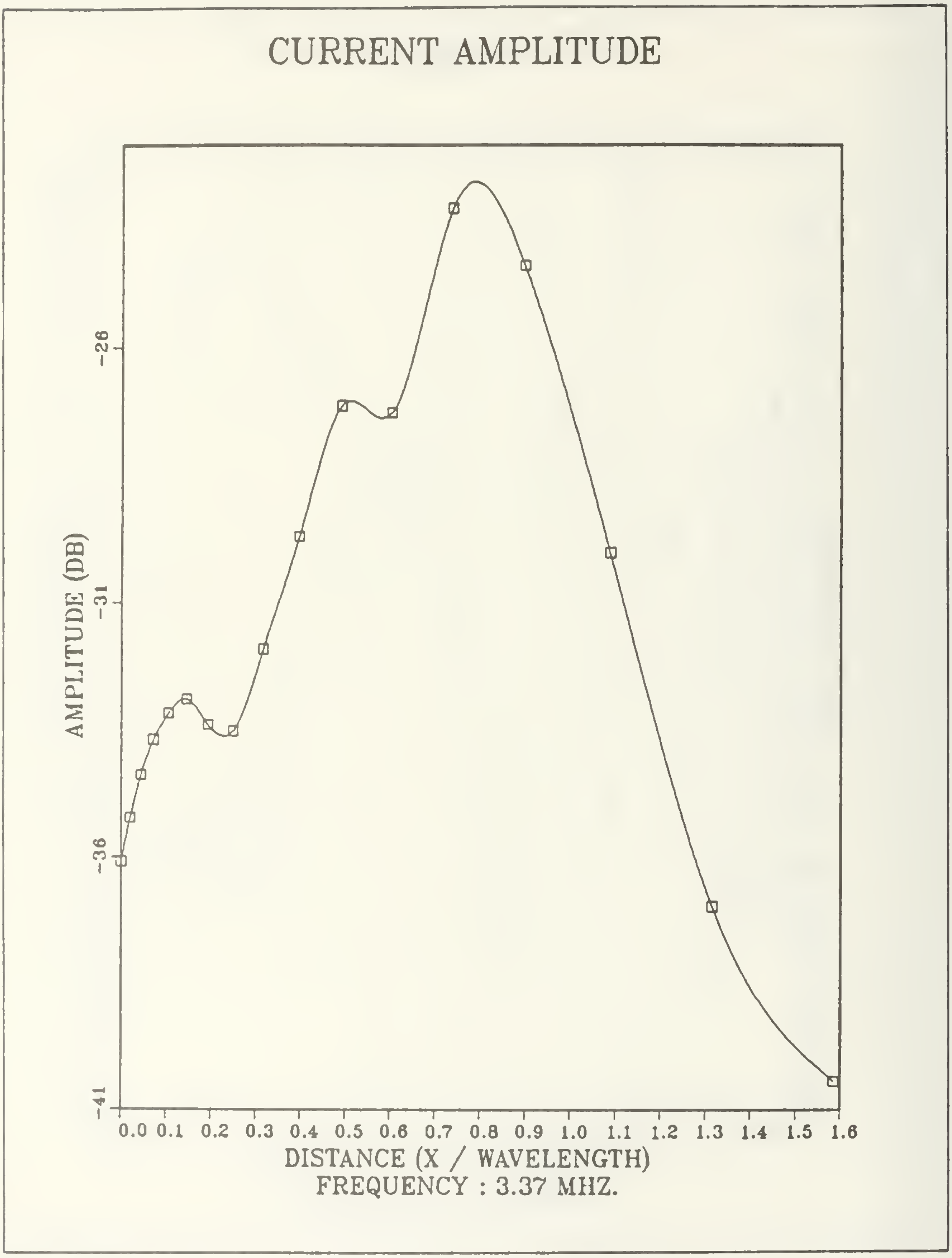

Figure E.7 Current Amplitude, Frequency : 3.37 MHz.

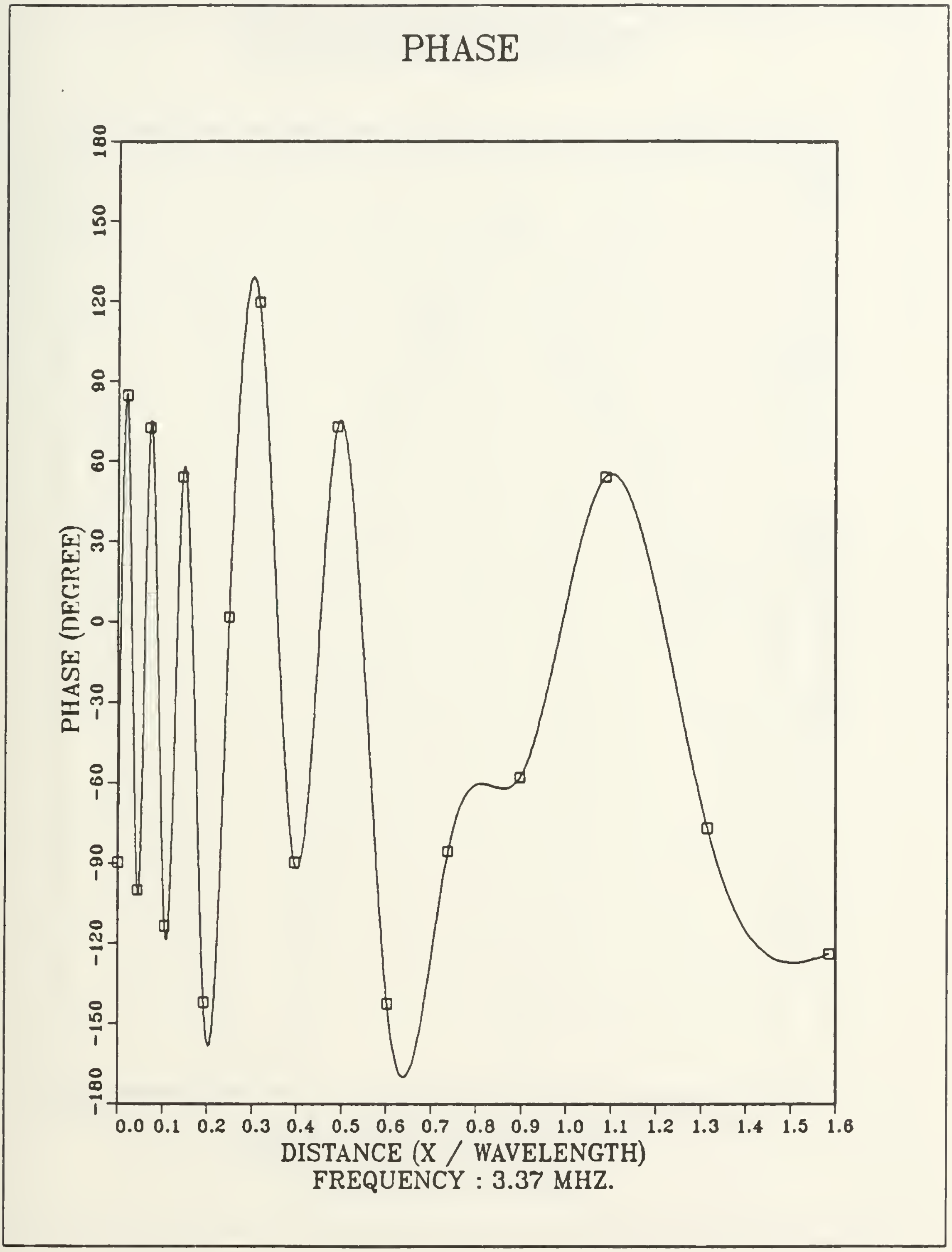

Figure E.8 Current Phase, Frequency : 3.37 MHz.

Figure E.9 Current Amplitude, Frequency : 4.01 MHz.

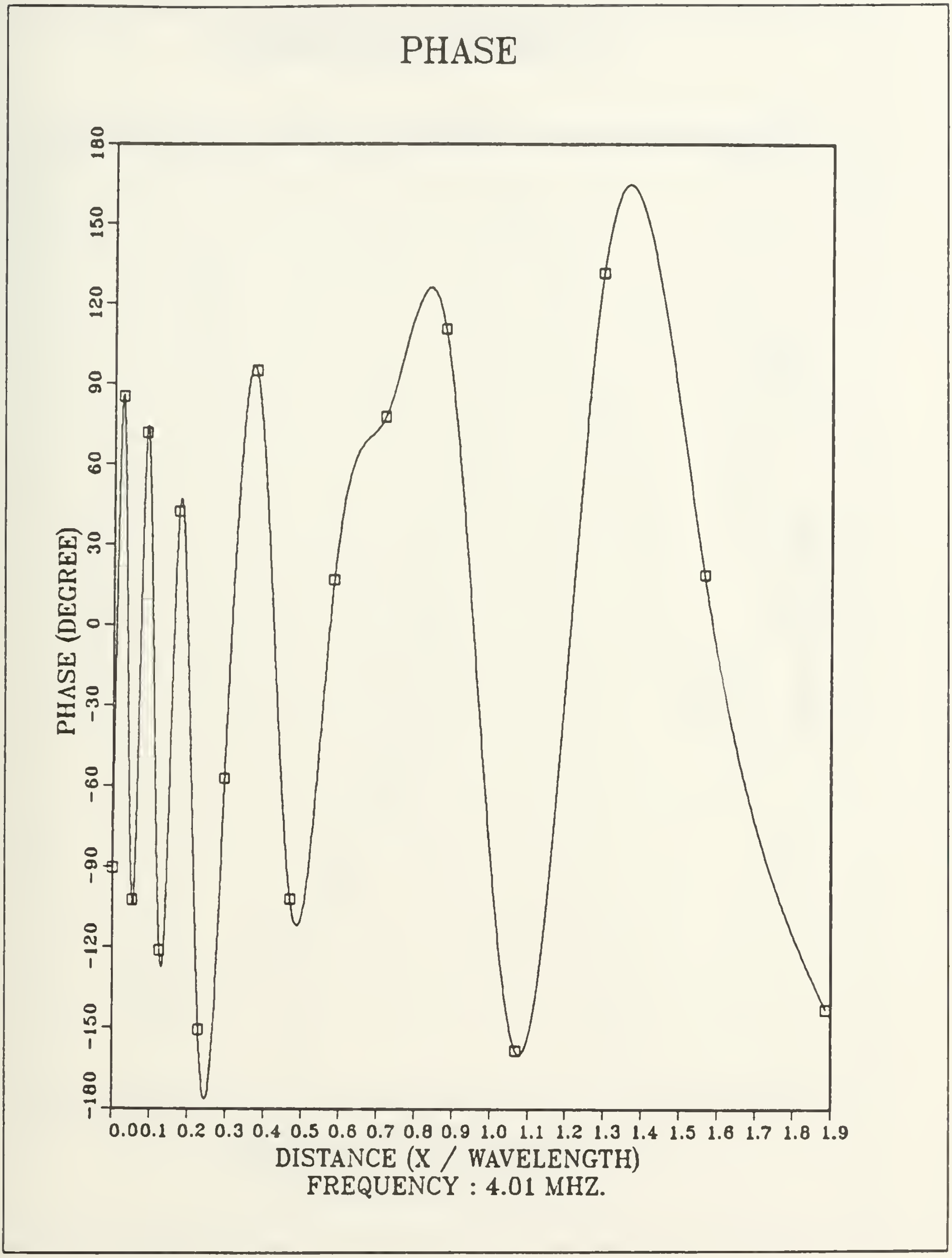

Figure E.10 Current Phase, Frequency : 4.01.

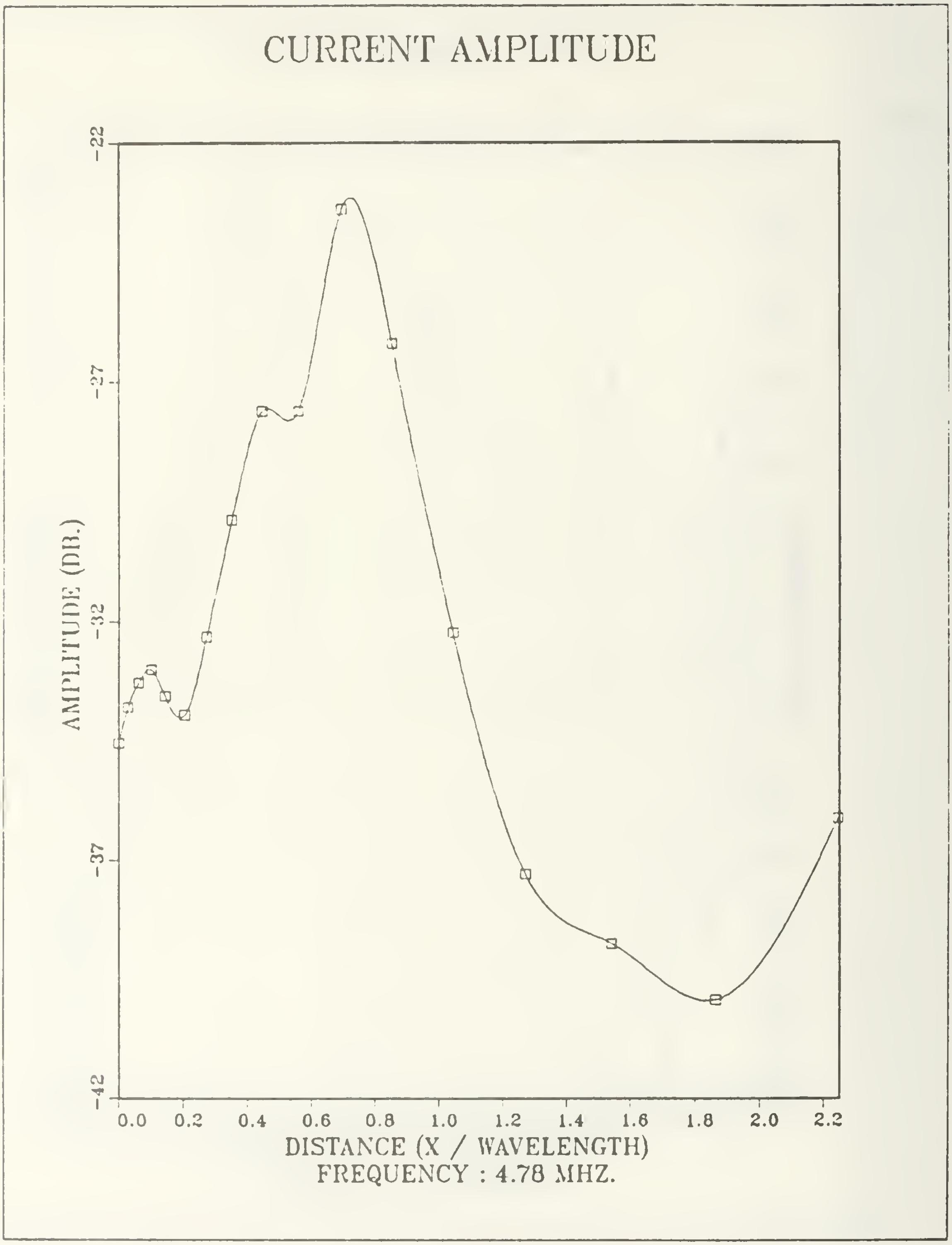

Figure E.11 Current Amplitude, Frequency : 4.78 MHz.

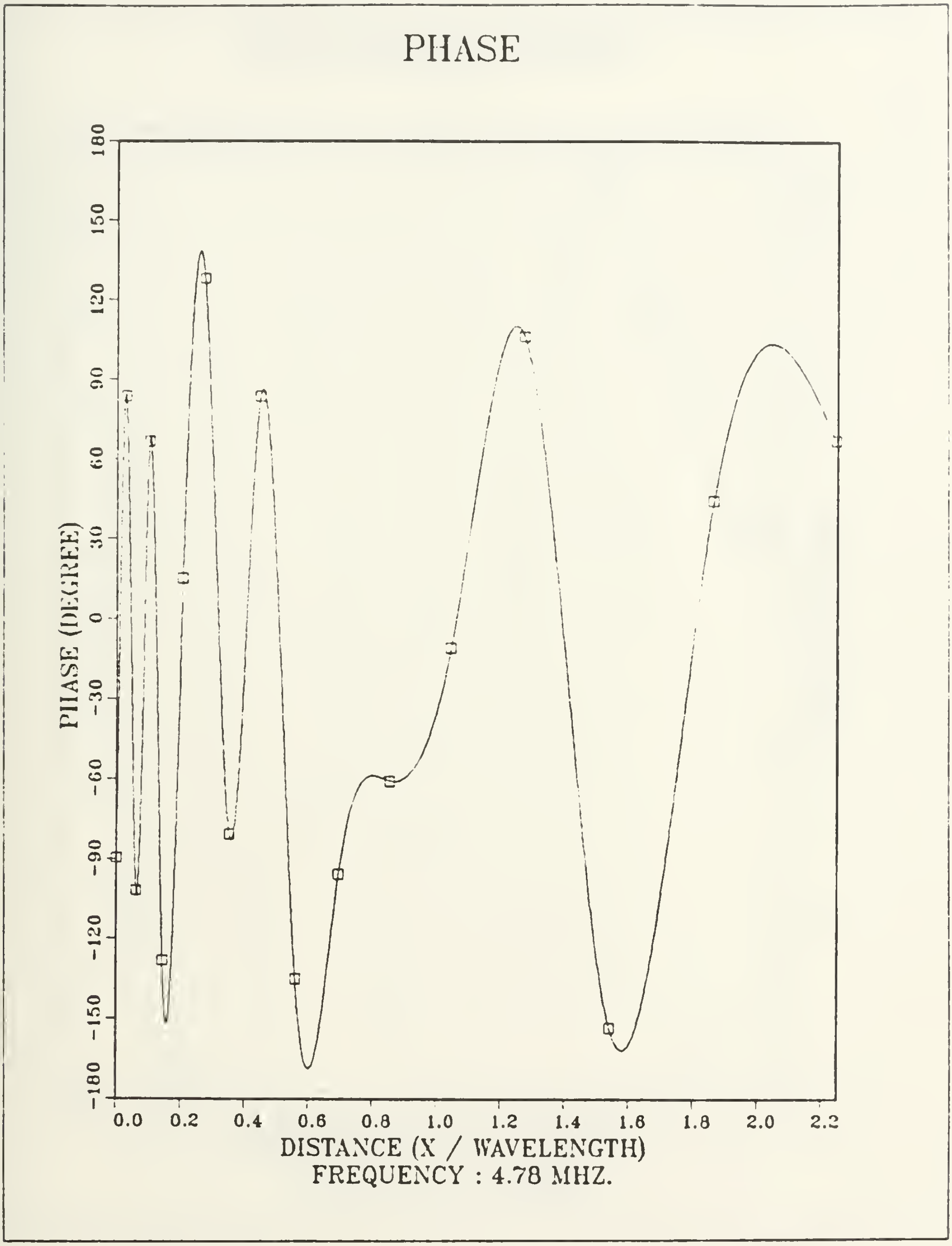

Figure E.12 Current Phase, Frequency : 4.78 MHz.

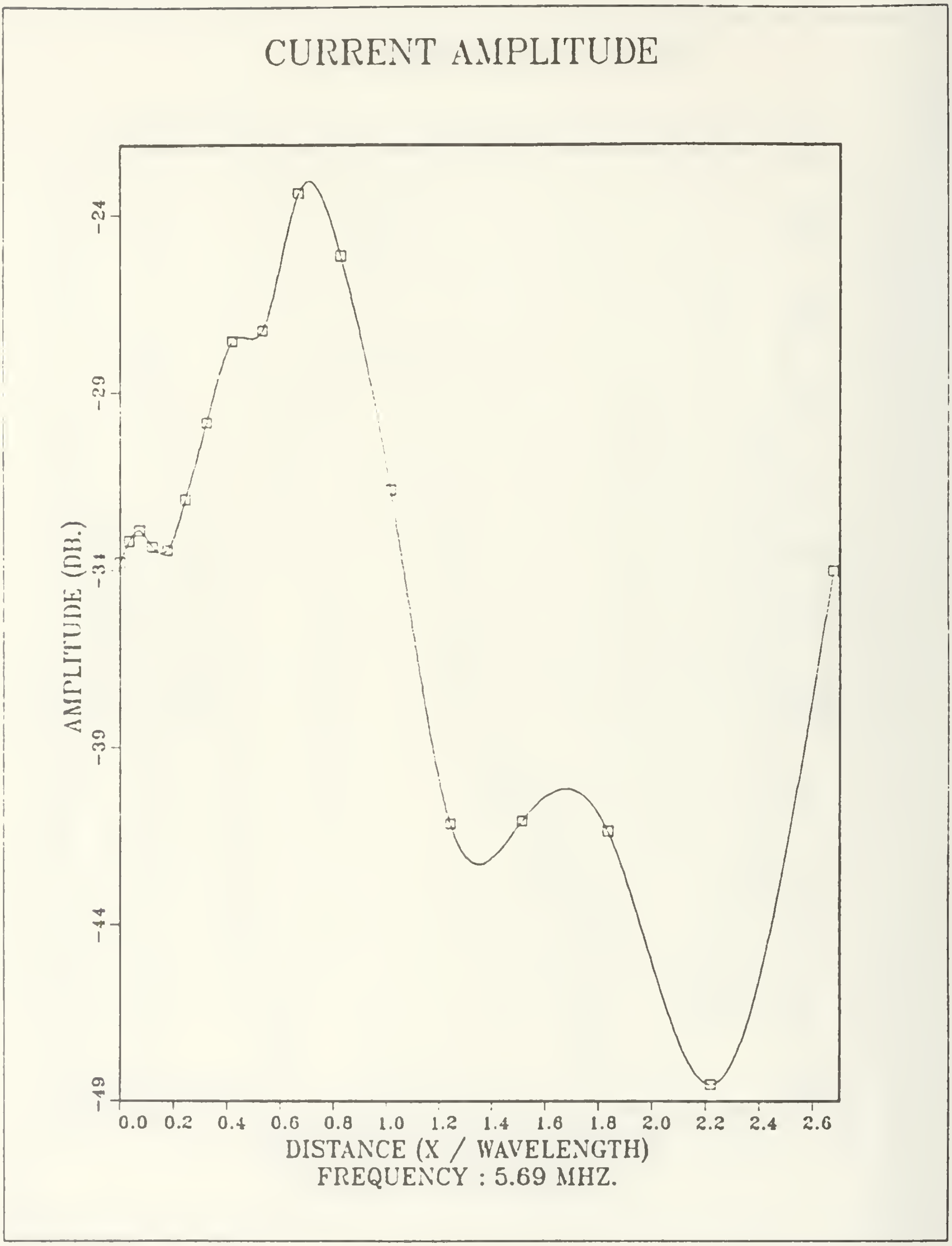

Figure E.13 Current Amplitude, Frequency : 5.69 MHz.

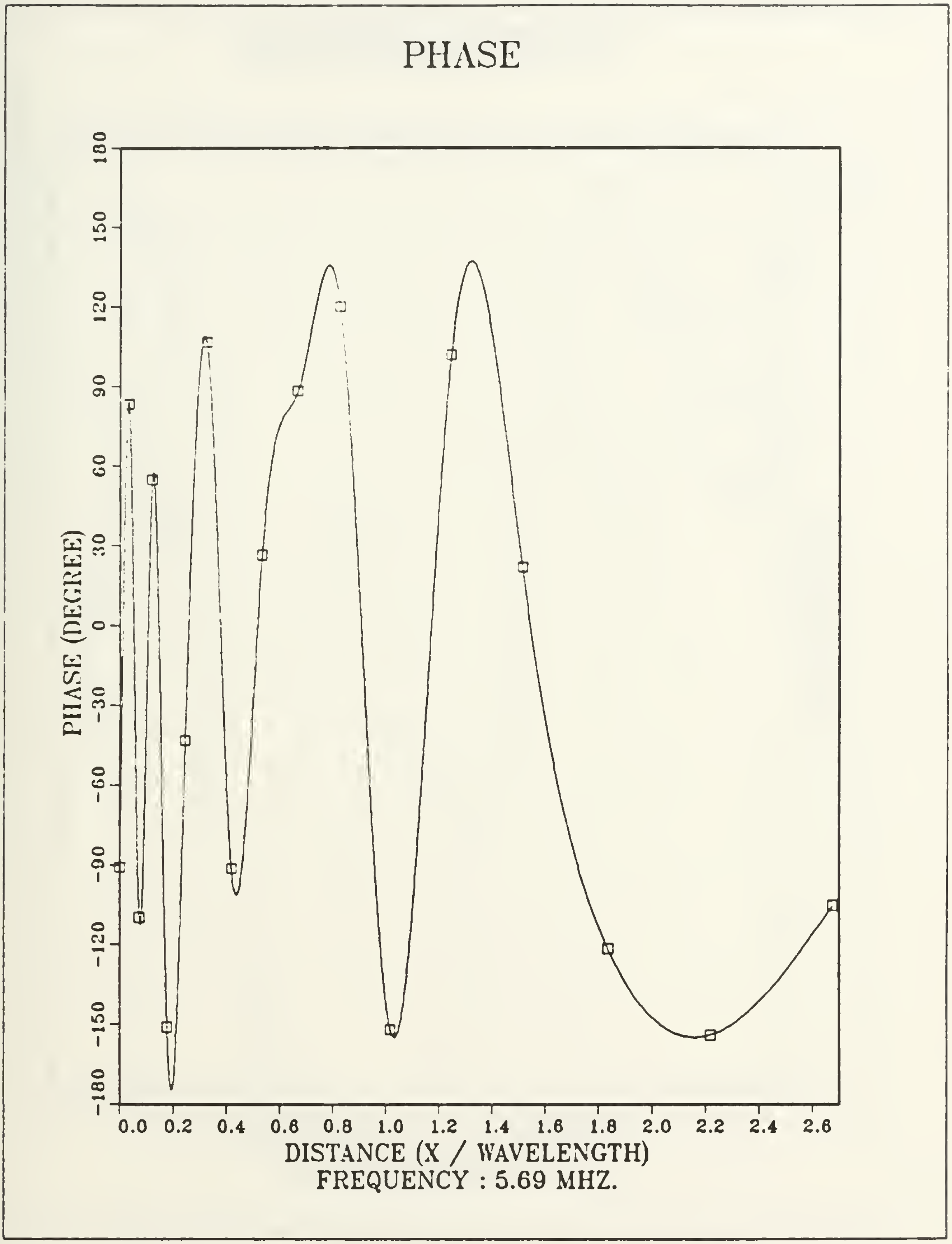

Figure E.14 Current Phase, Frequency : 5.69 MHz.

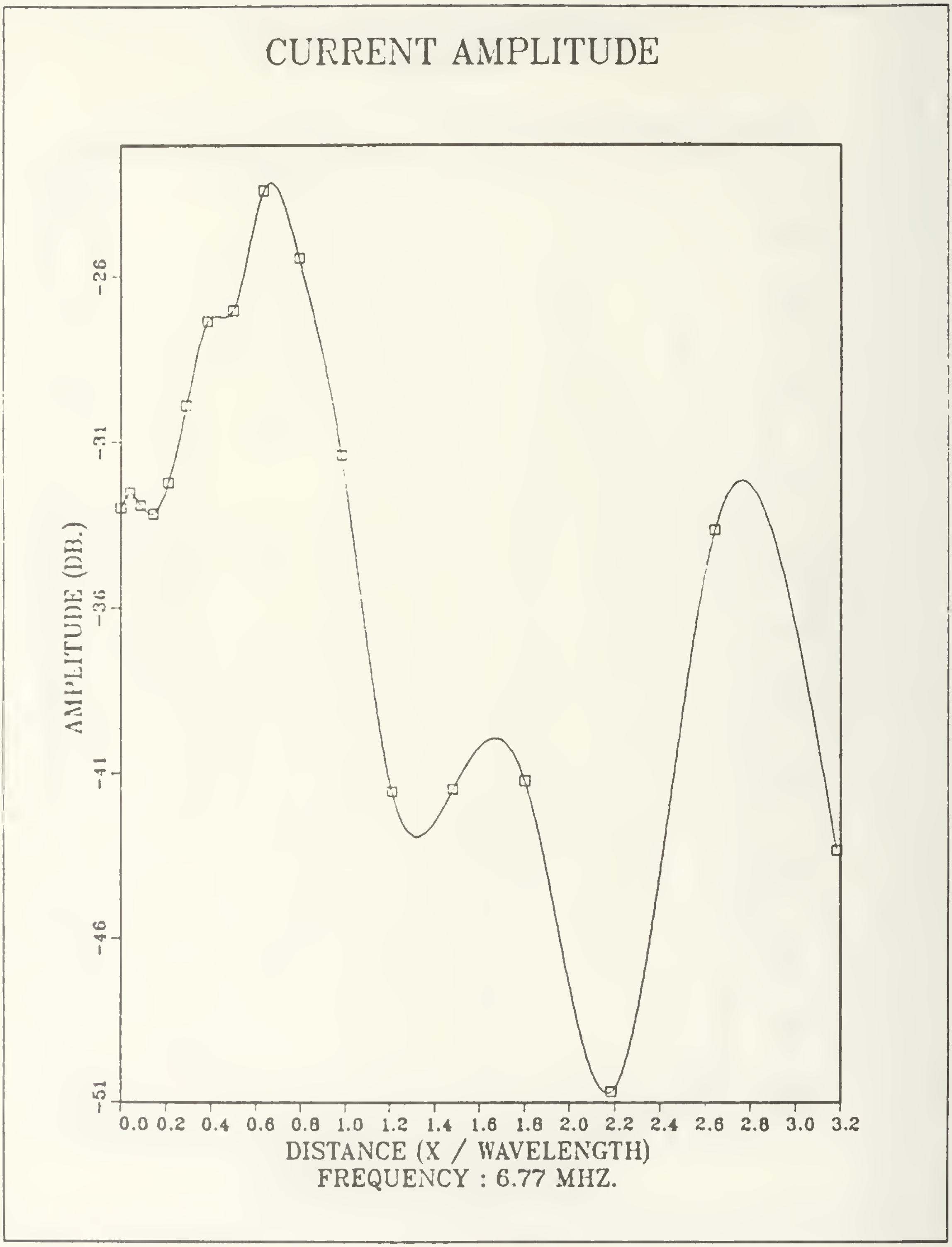

Figure E.15 Current Amplitude, Frequency : 6.77 MHz.

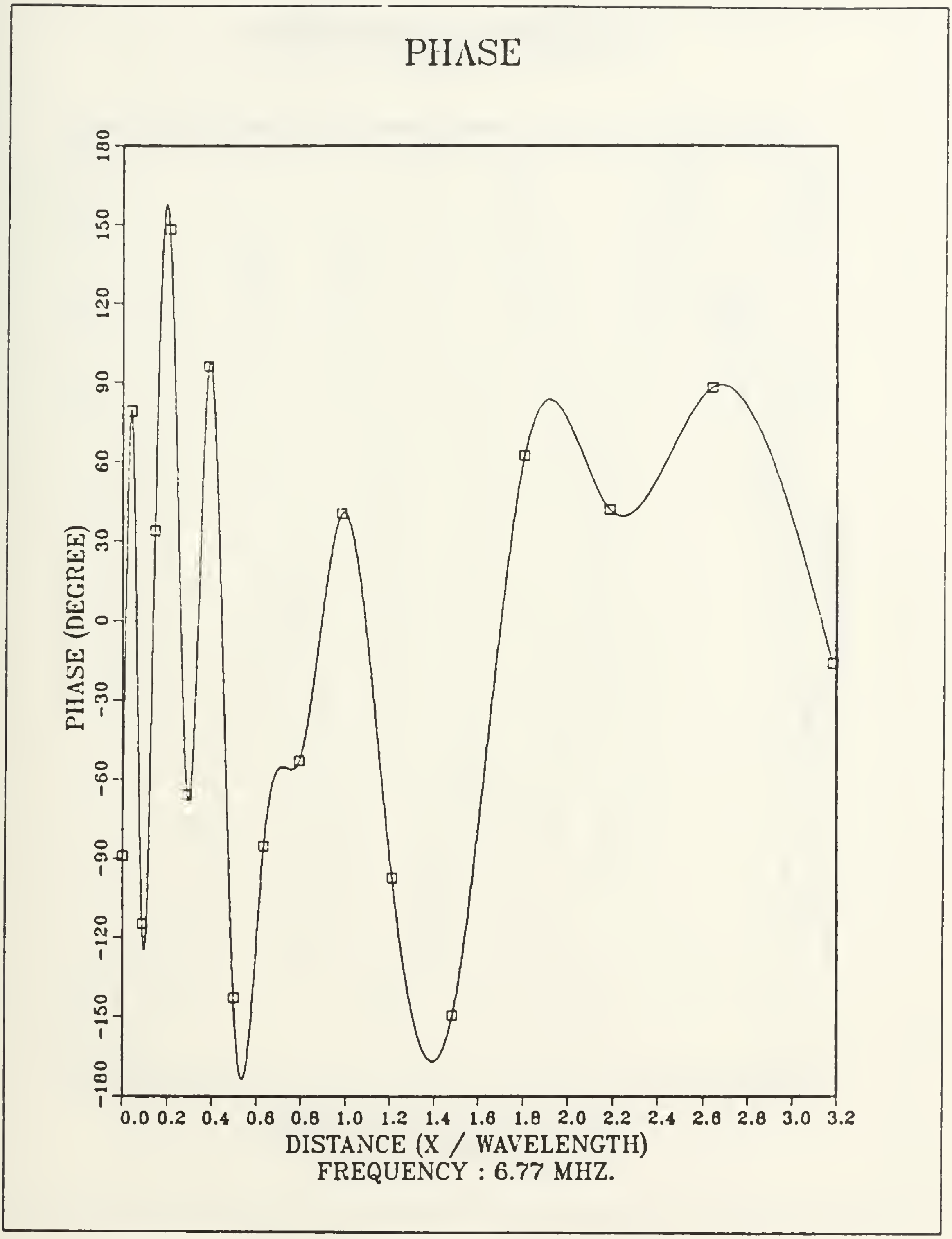

Figure E.16 Current Phase, Frequency : 6.77 MHz.

Figure E.17 Current Amplitude, Frequency : 8.06 MHz.

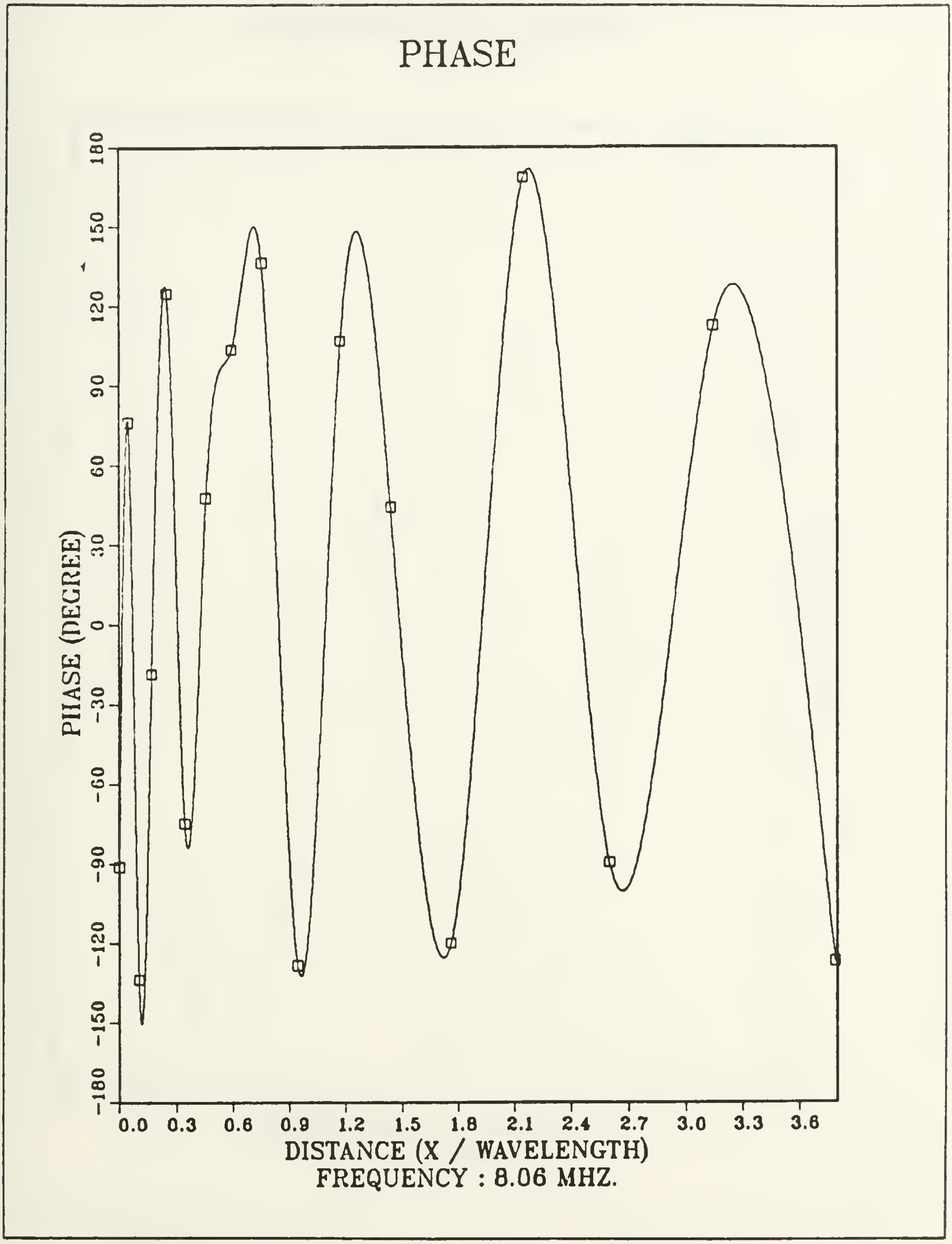

Figure E.18 Current Phase, Frequency : 8.06 MHz.

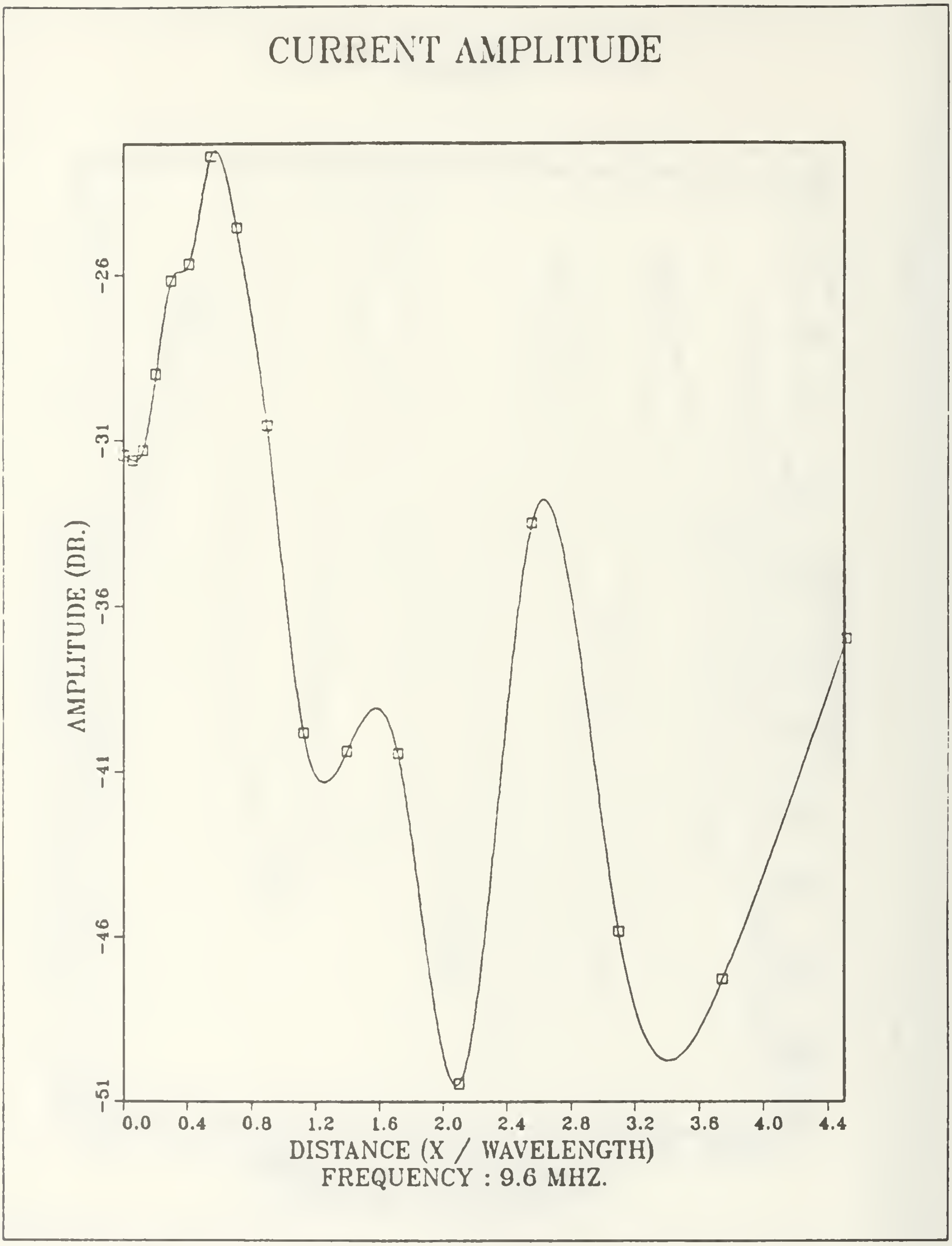

Figure E.19 Current Amplitude, Frequency : 9.6 MHz.

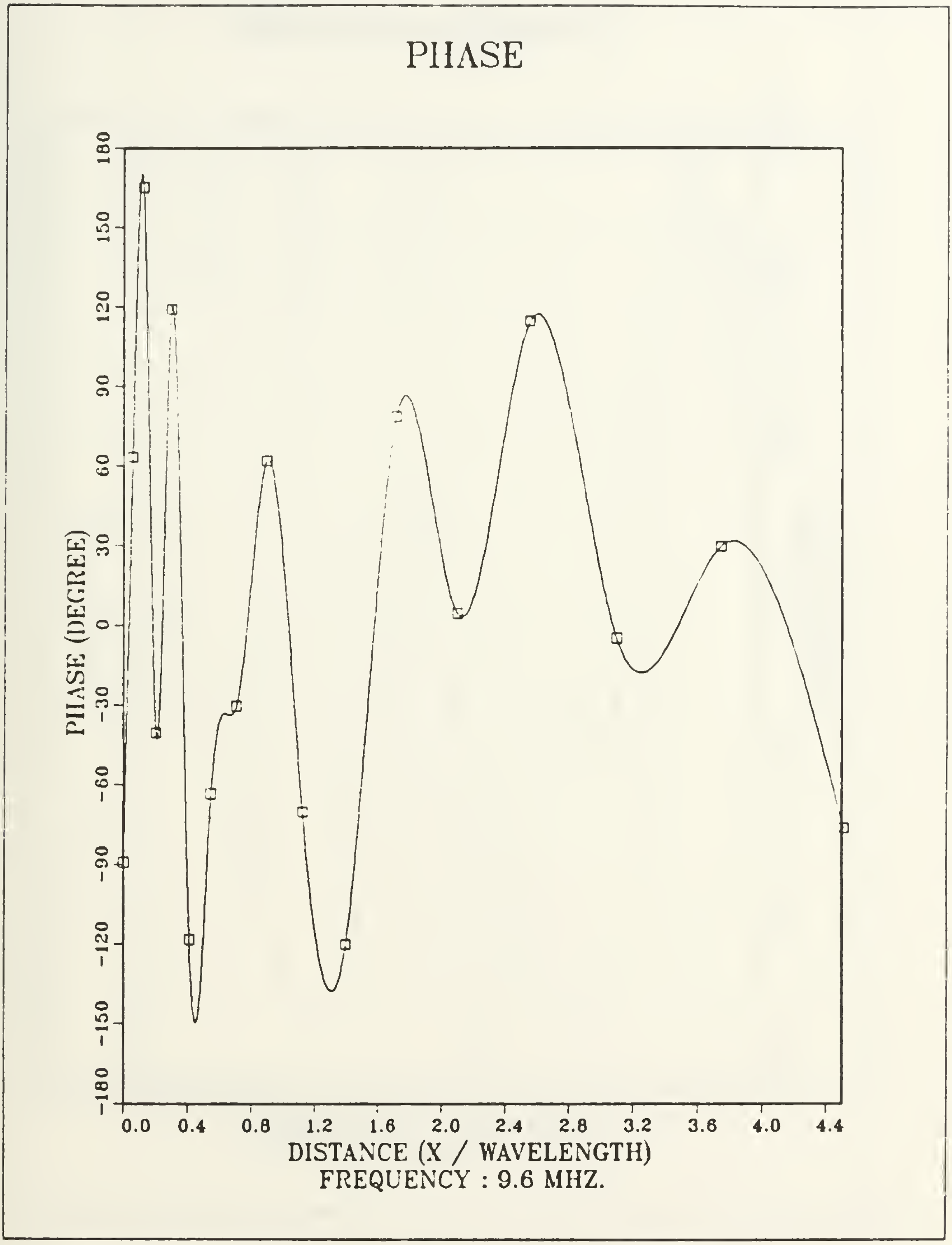

Figure E.20 Current Phase, Frequency : 9.6 MHz.

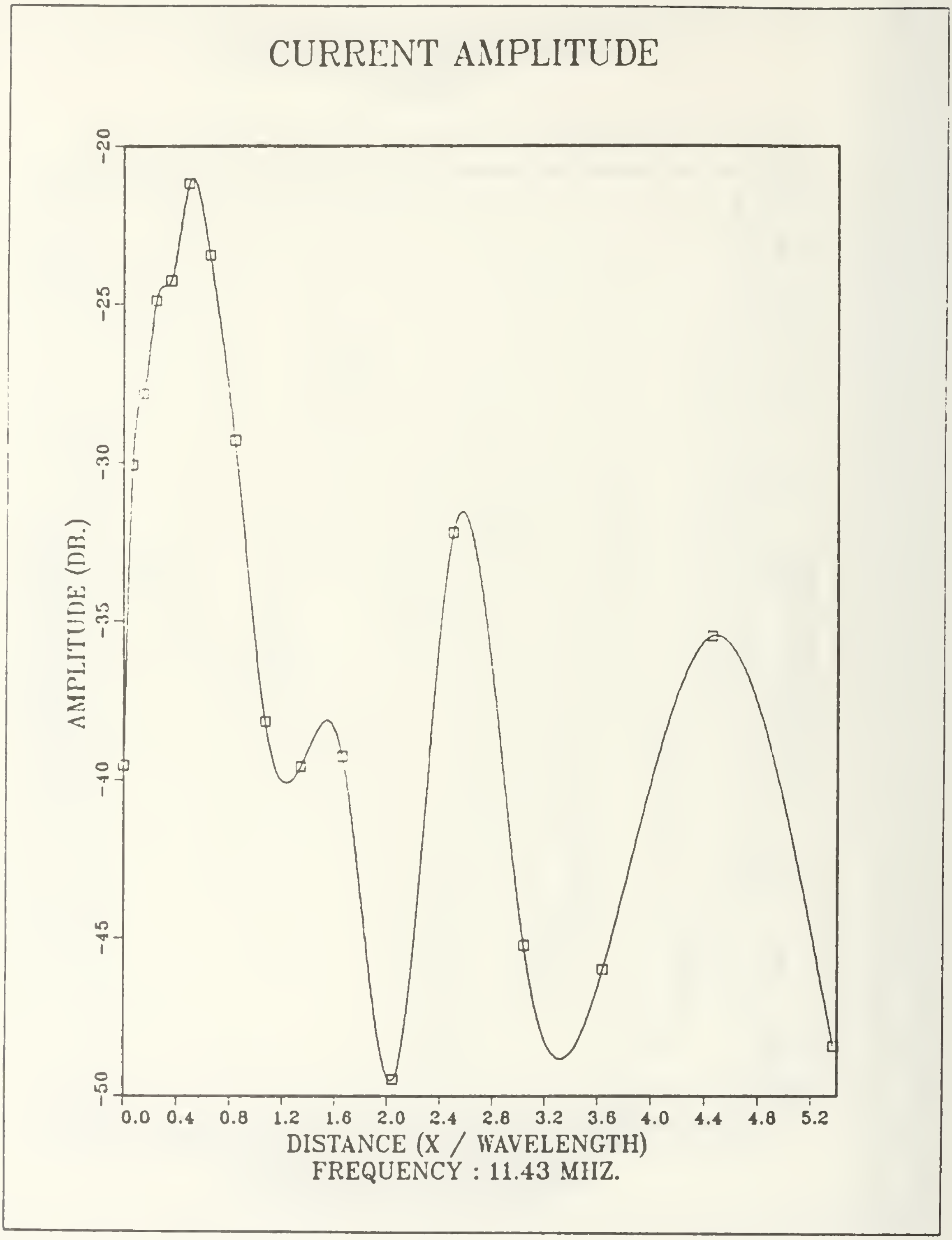

Figure E.21 Current Amplitude, Frequency : 11.43 MHz.

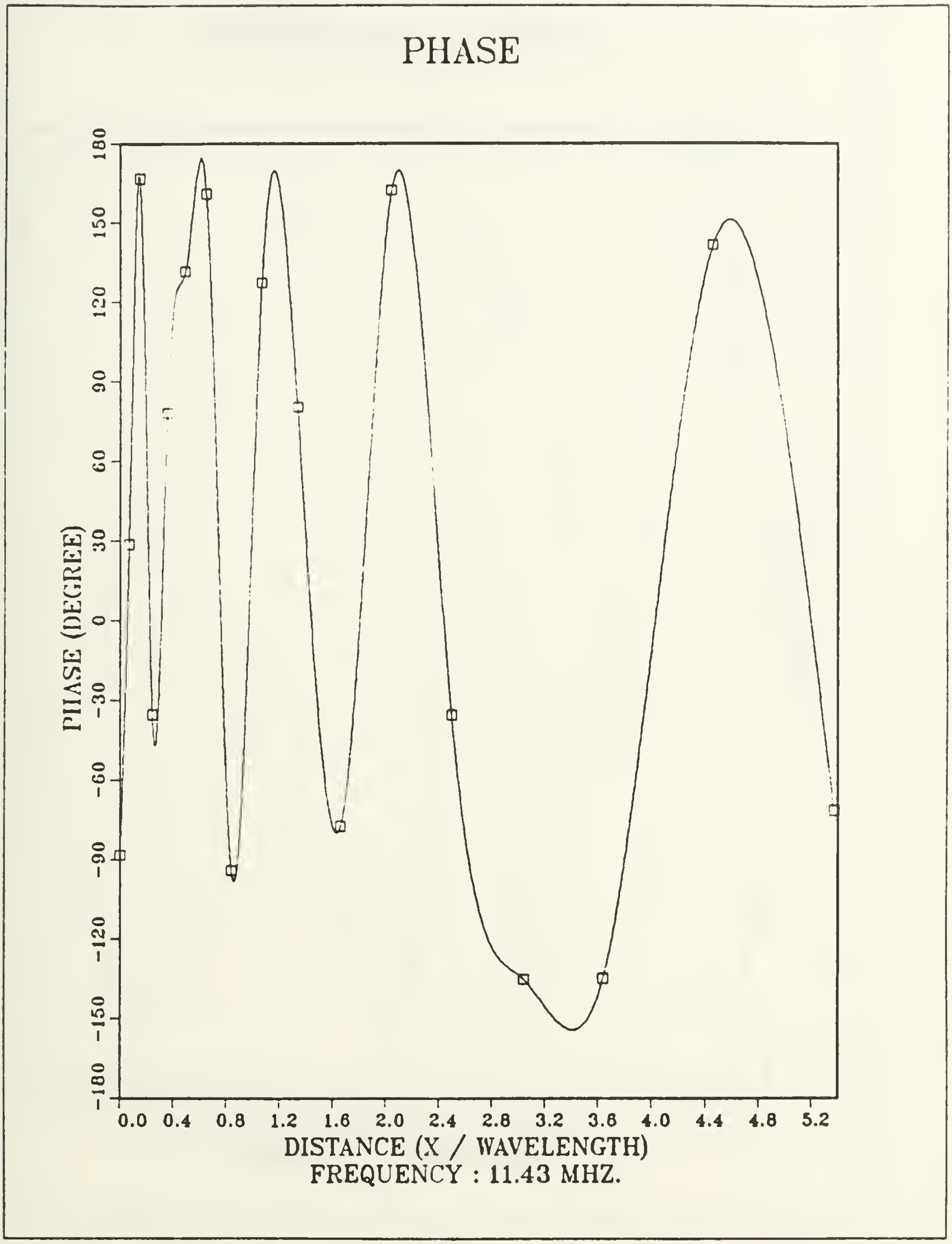

Figure E.22 Current Phase, Frequency : 11.43 MHz.

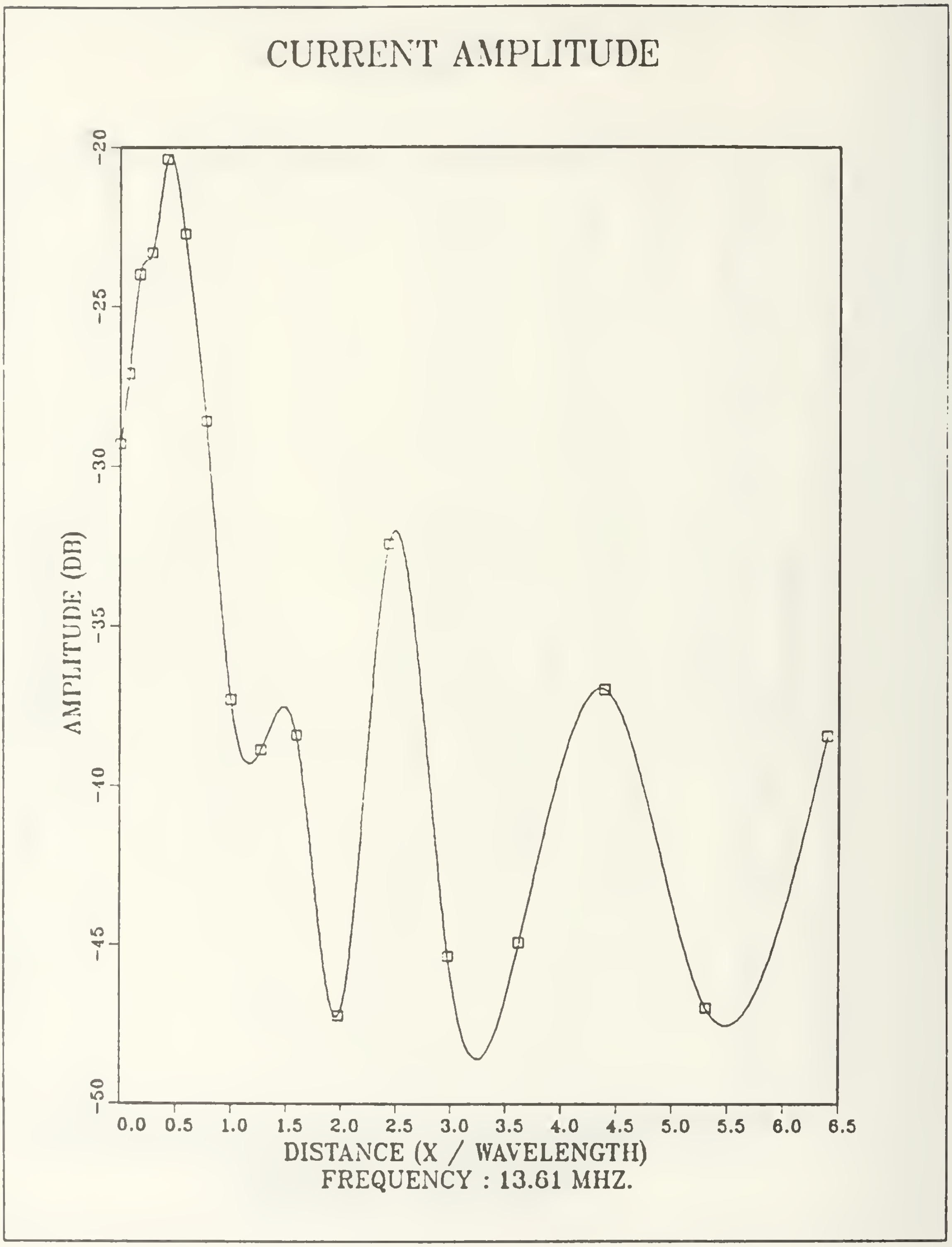

Figure E.23 Current Amplitude, Frequency : 13.61 MHz.

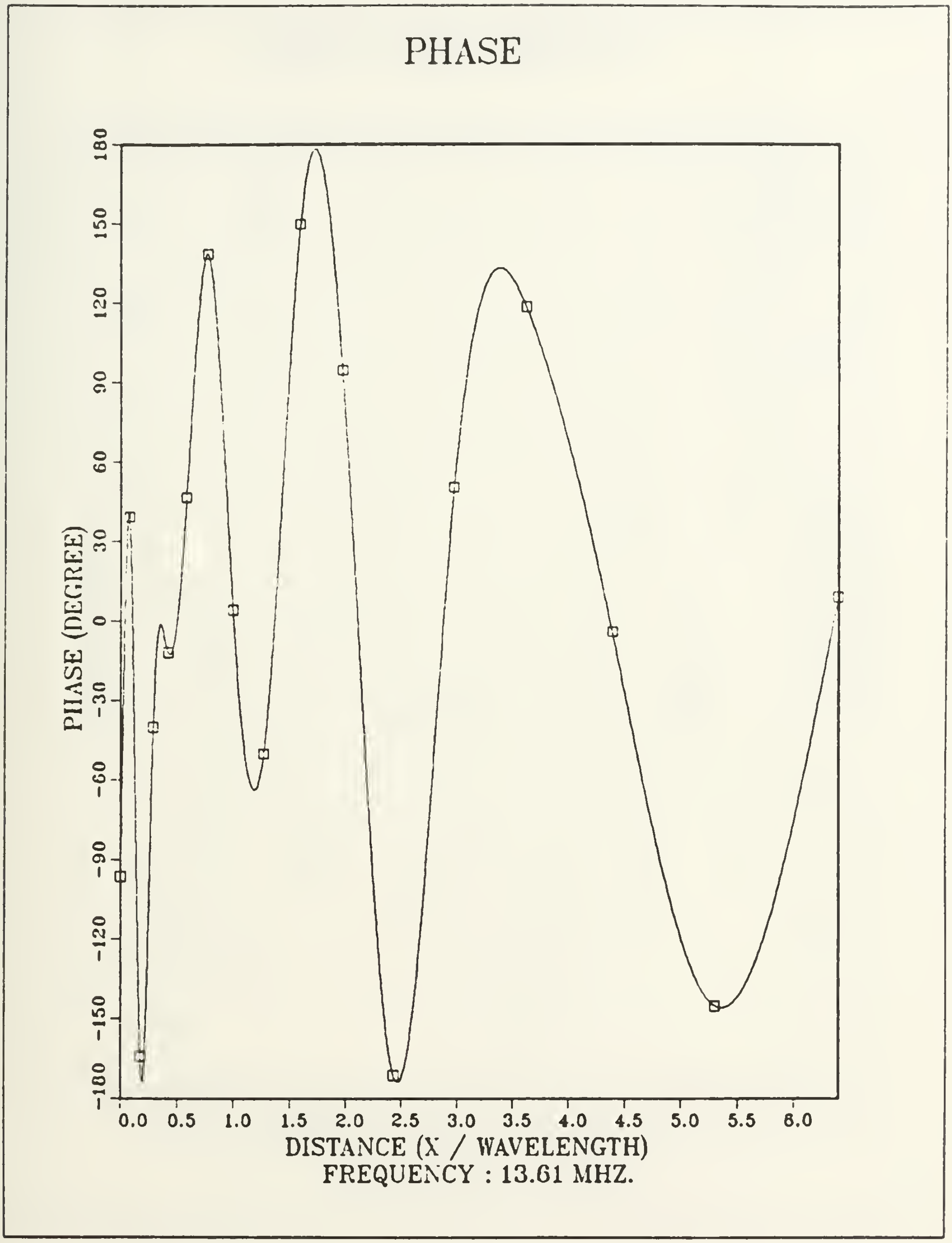

Figure E.24 Current Phase, Frequency : 13.61 MHz.

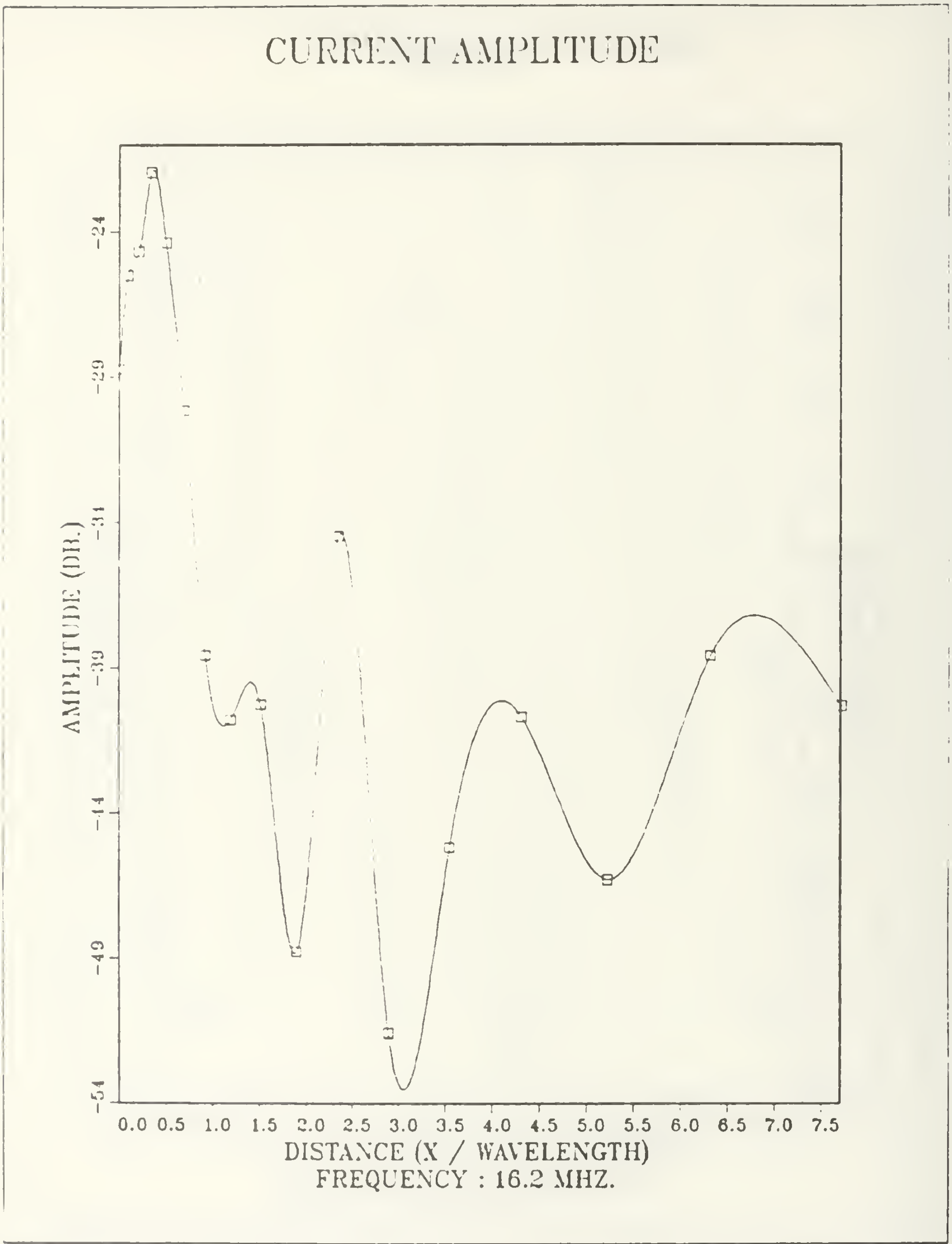

Figure E.25 Current Amplitude, Frequency : 16.2 MHz.

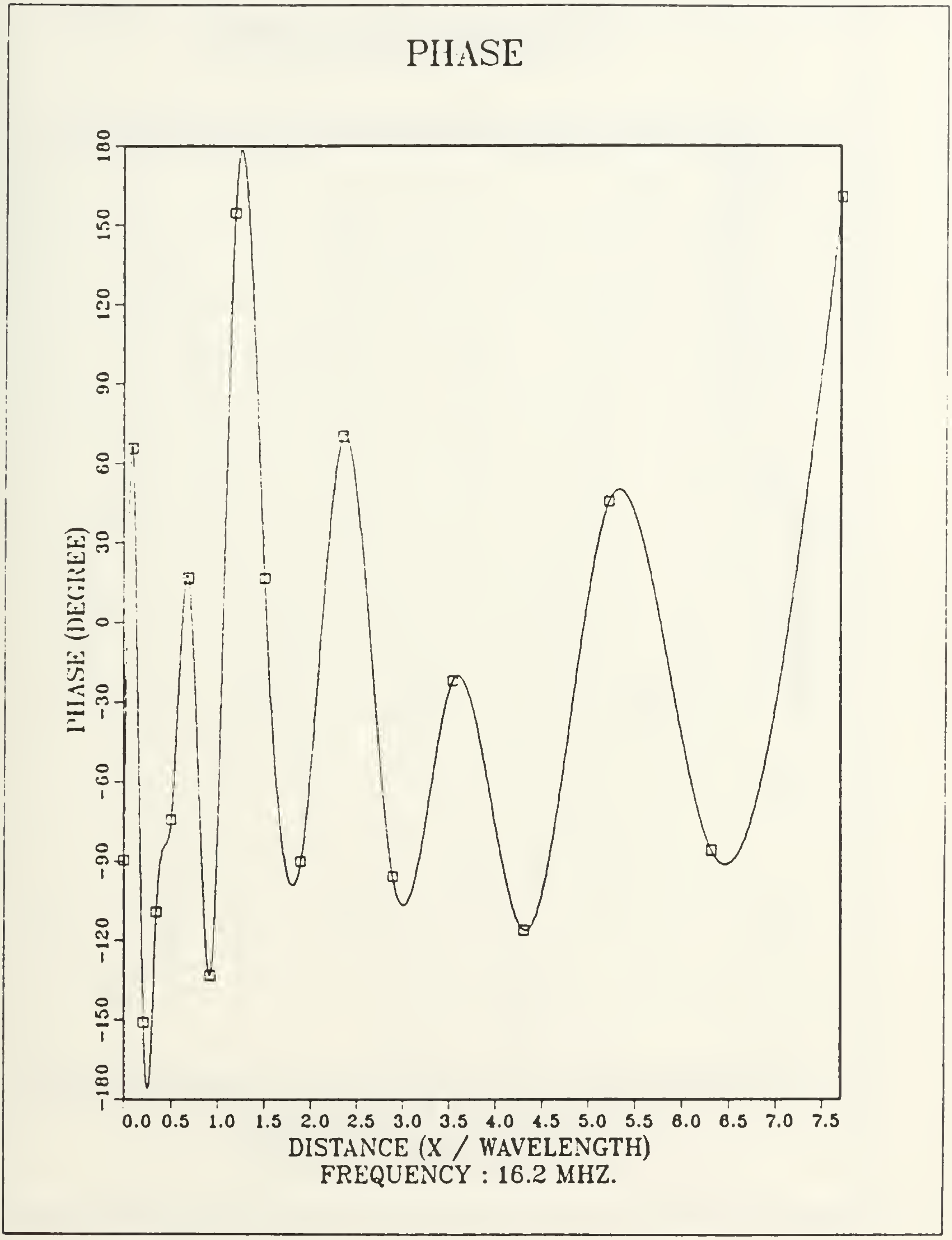

Figure E.26 Current Phase, Frequency : 16.2 MHz.

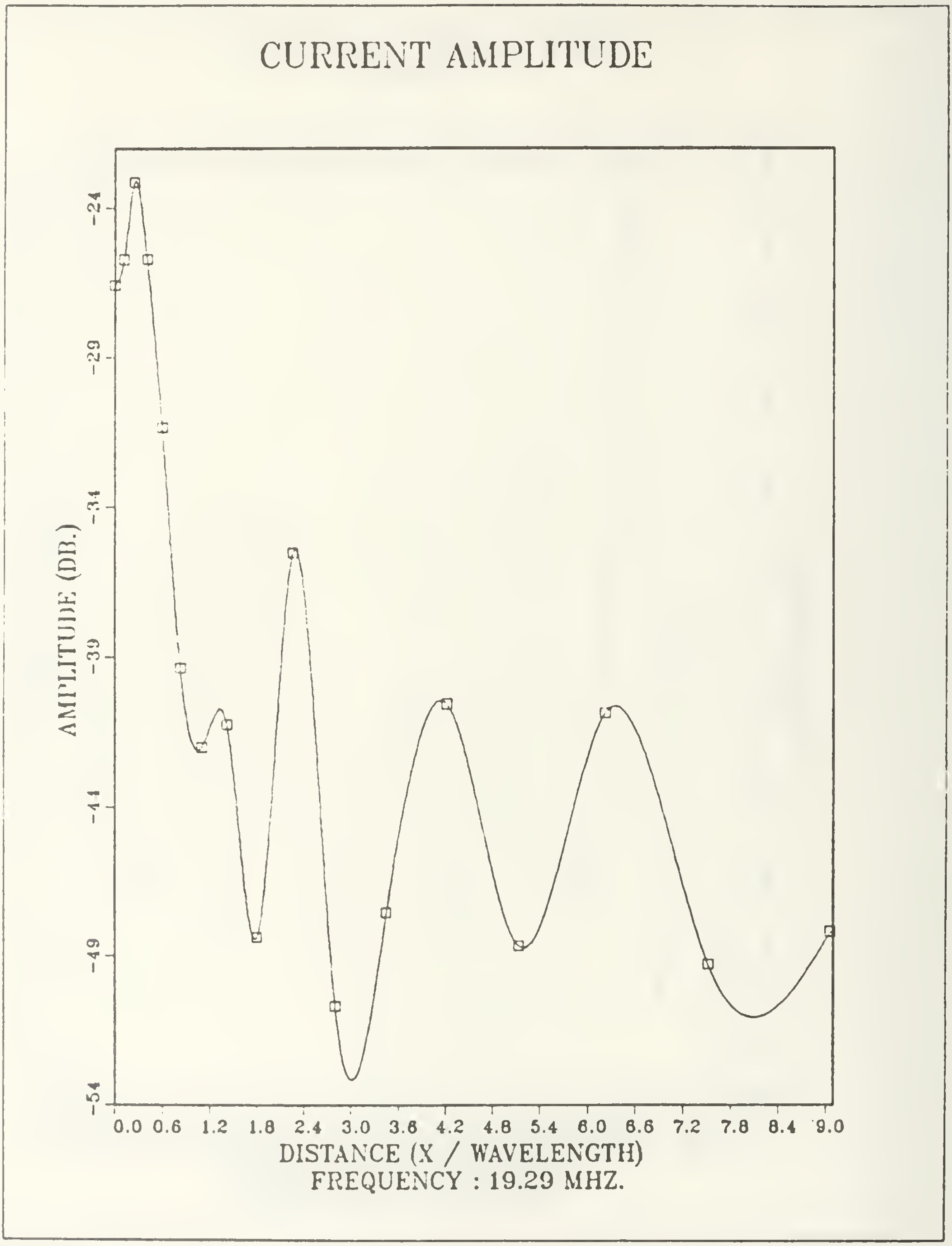

Figure E.27 Current Amplitude, Frequency : 19.29 MHz.

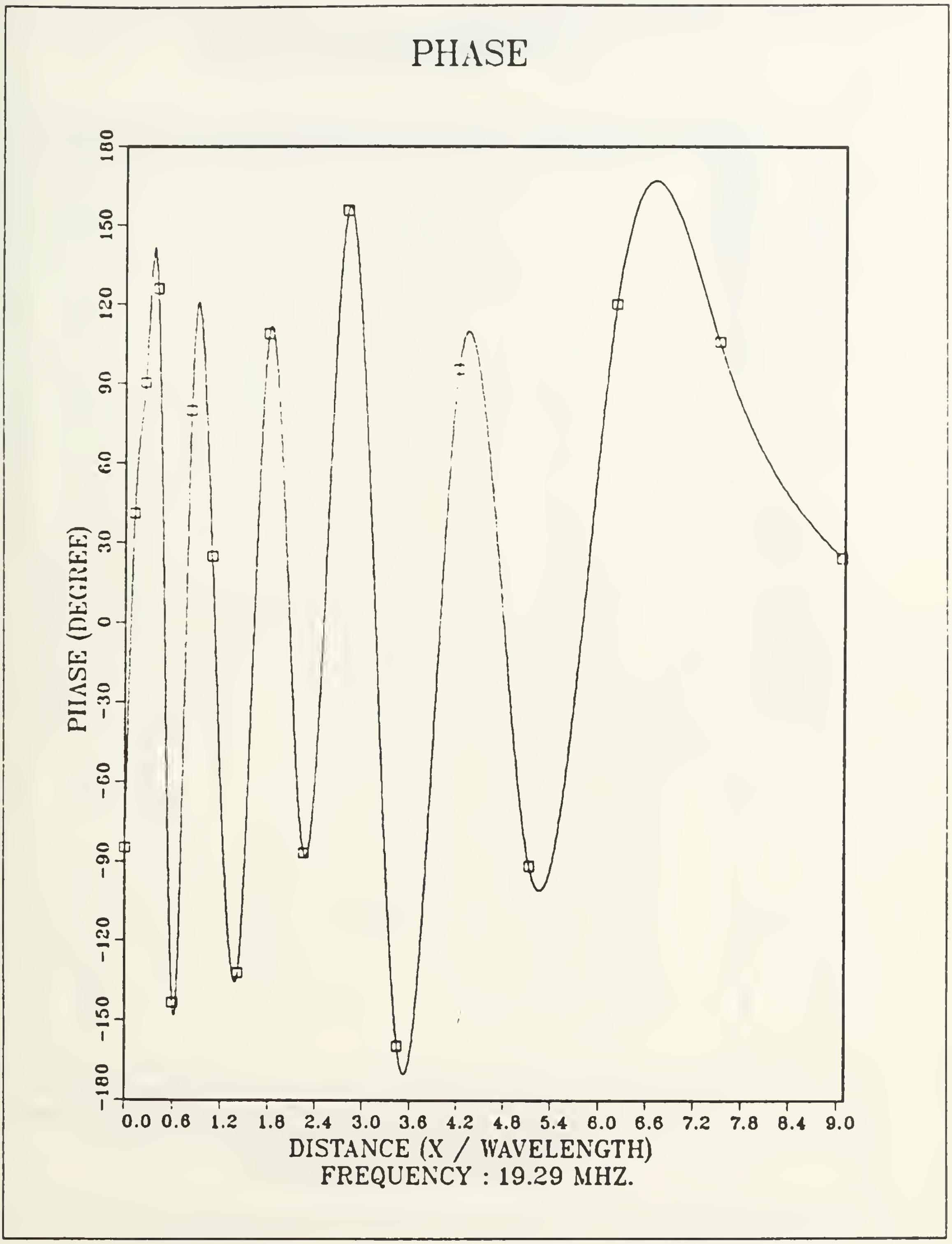

Figure E.28 Current Phase, Frequency : 19.29 MHz.

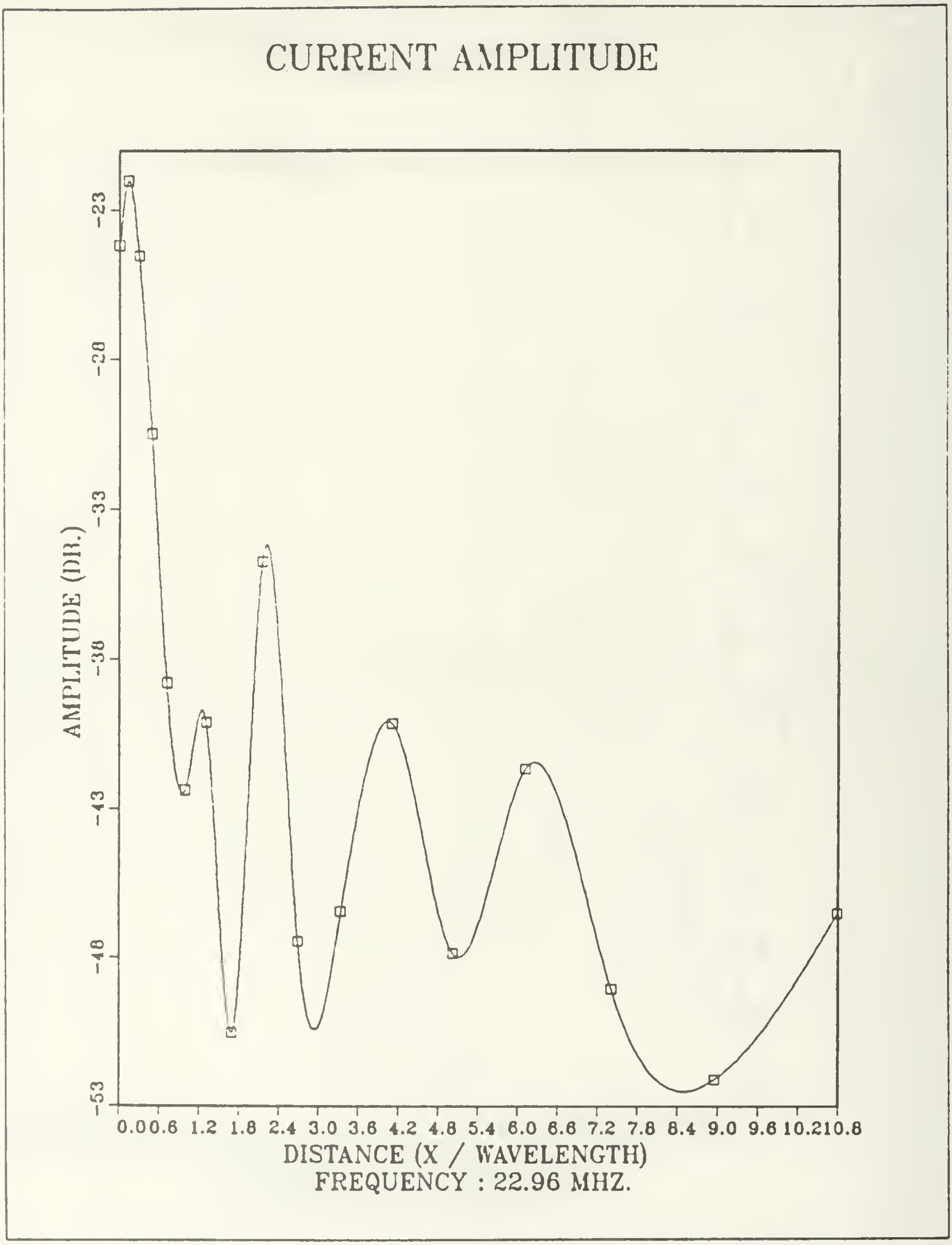

Figure E.29 Current Amplitude, Frequency : 22.96 MHz.

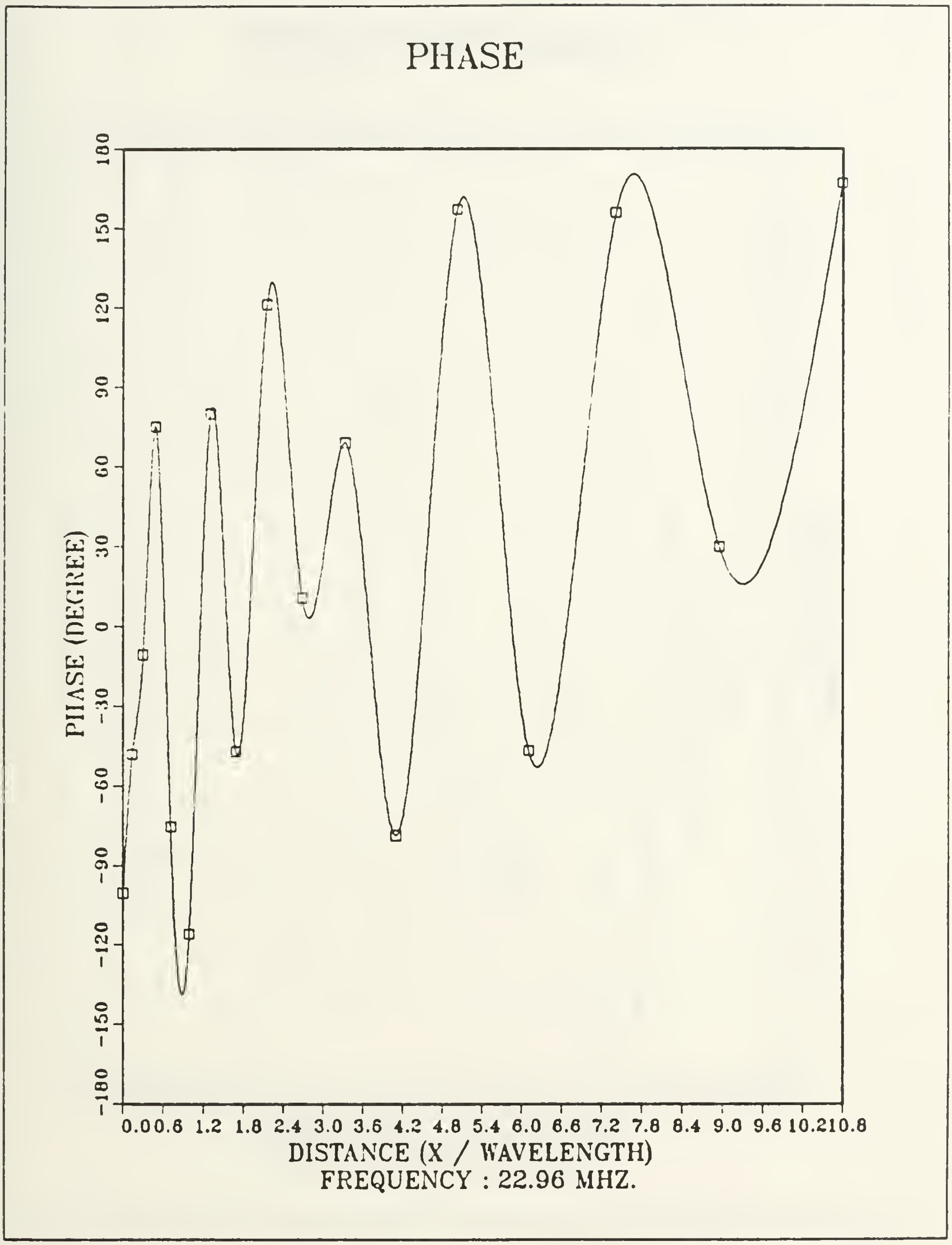

Figure E.30 Current Phase, Frequency : 22.96 MHz.

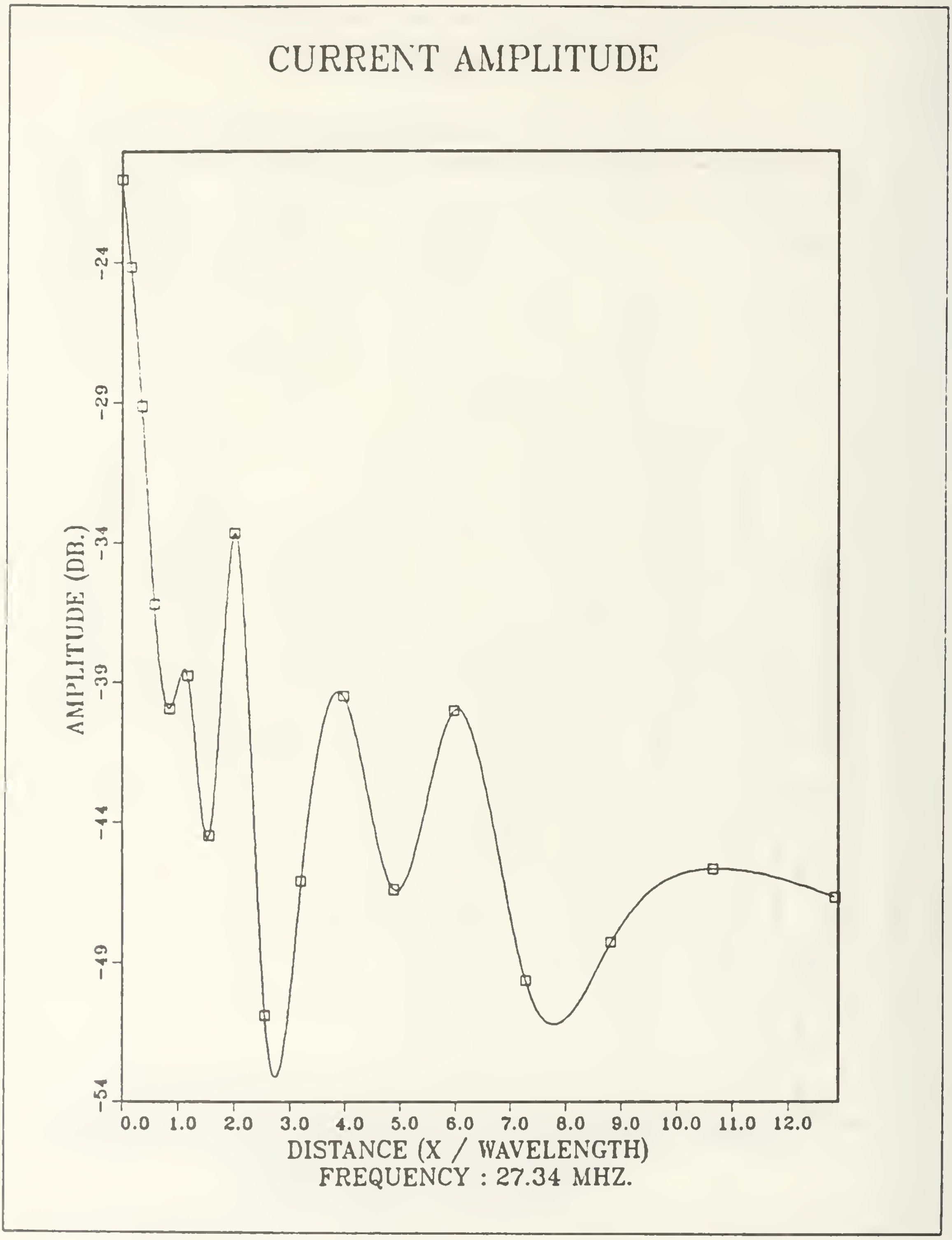

Figure E.31 Current Amplitude, Frequency : 27.34 MHz.

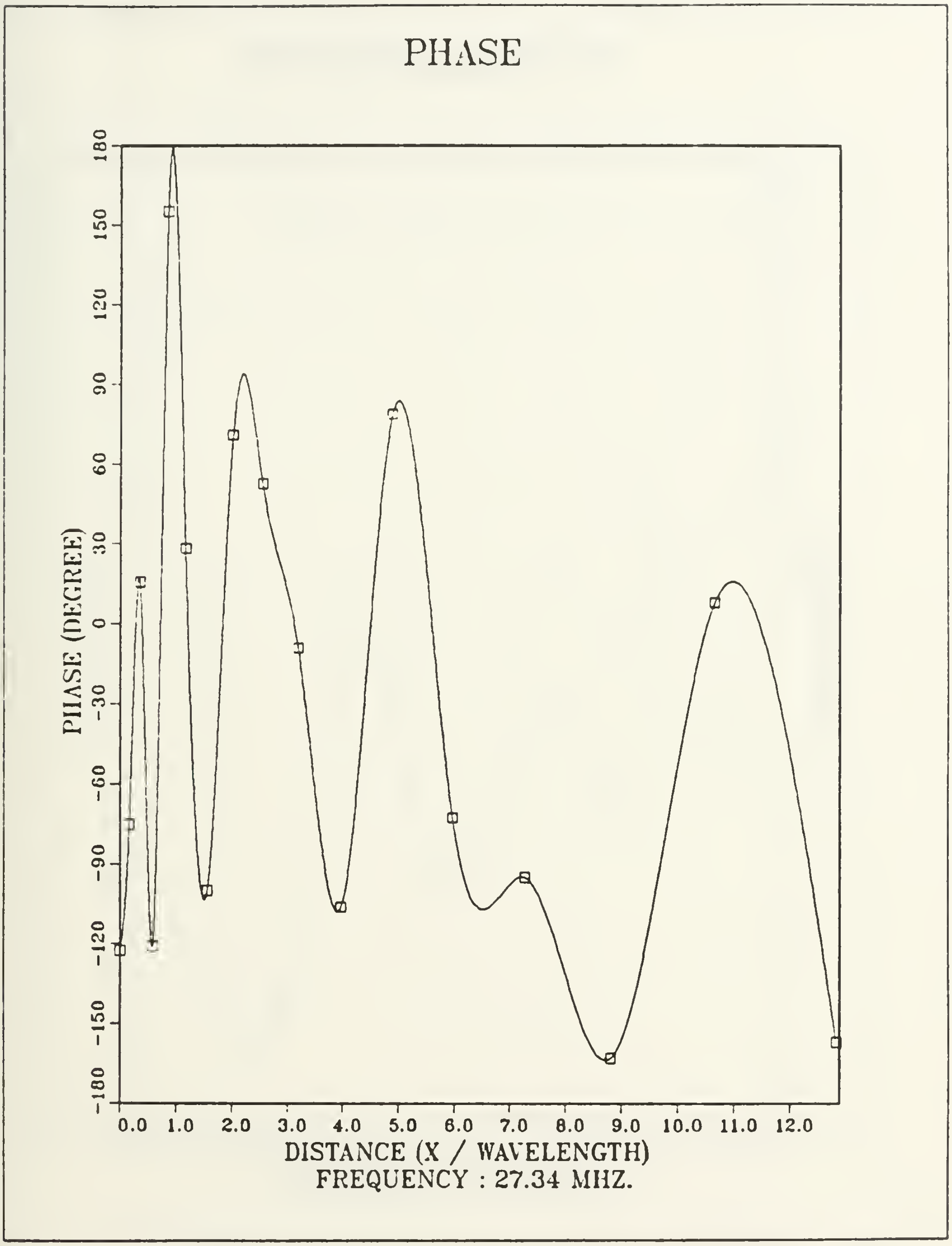

Figure E.32 Current Phase, Frequency : 27.34 MHz.

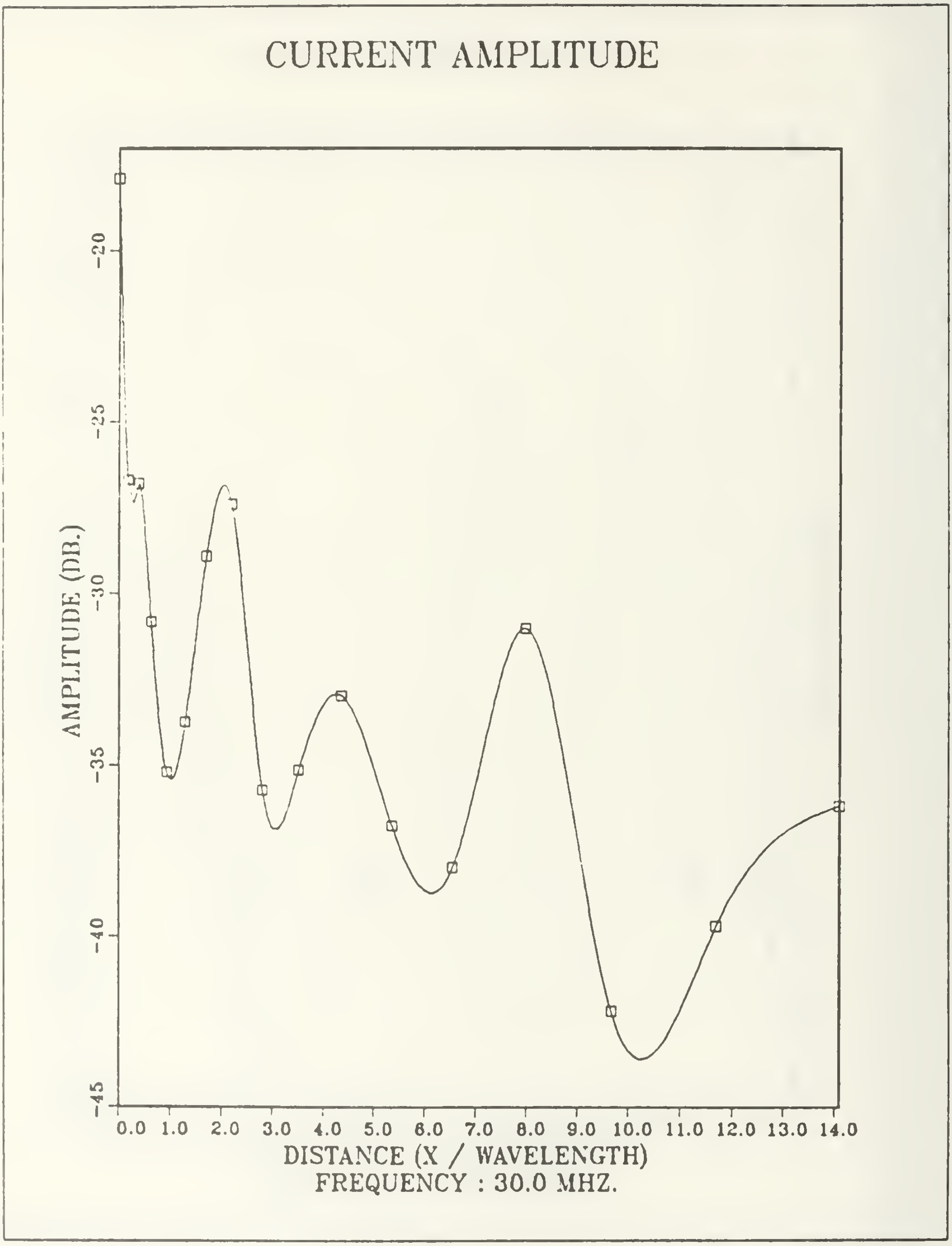

Figure E.33 Current Amplitude, Frequency : 30.0 MHz.

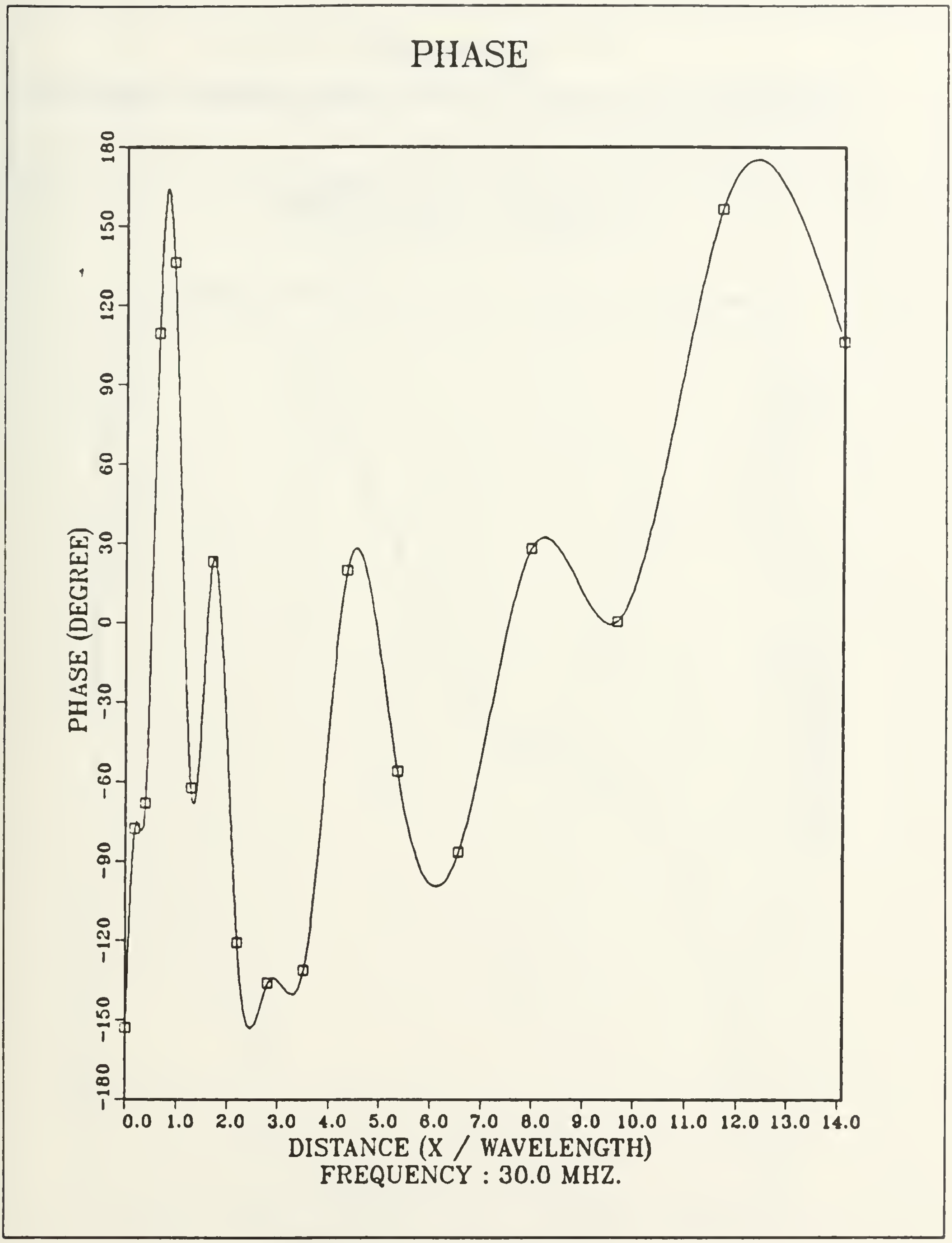

Figure E.34 Current Phase, Frequency : 30.0 MHz.

APPENDIX F
AMPLITUDE AND PHASE PLOTS OVER PERFECT GROUND

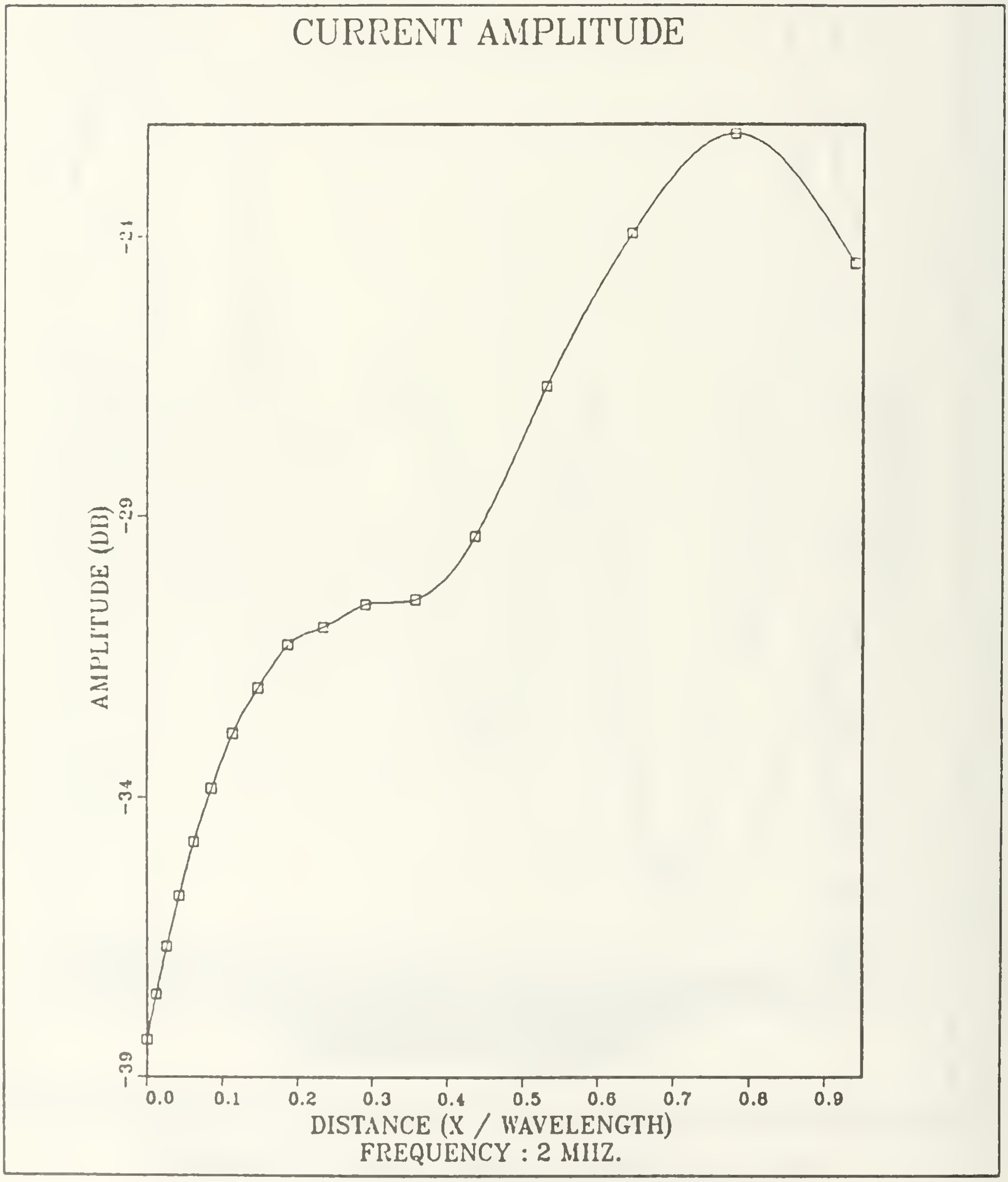

Figure F.1 Current Amplitude, Frequency : 2 MHz.

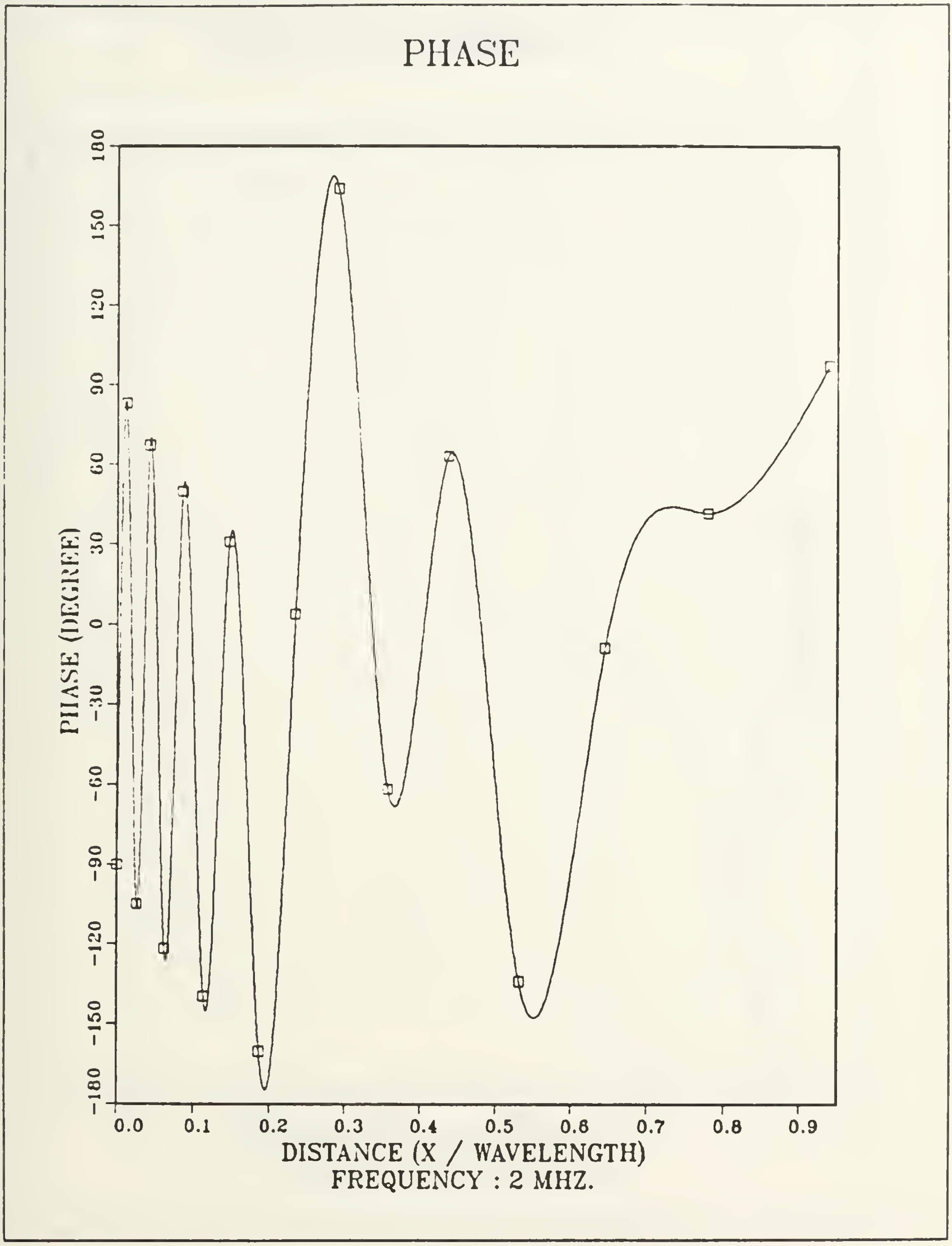

Figure F.2 Current Phase, Frequency : 2 MHz.

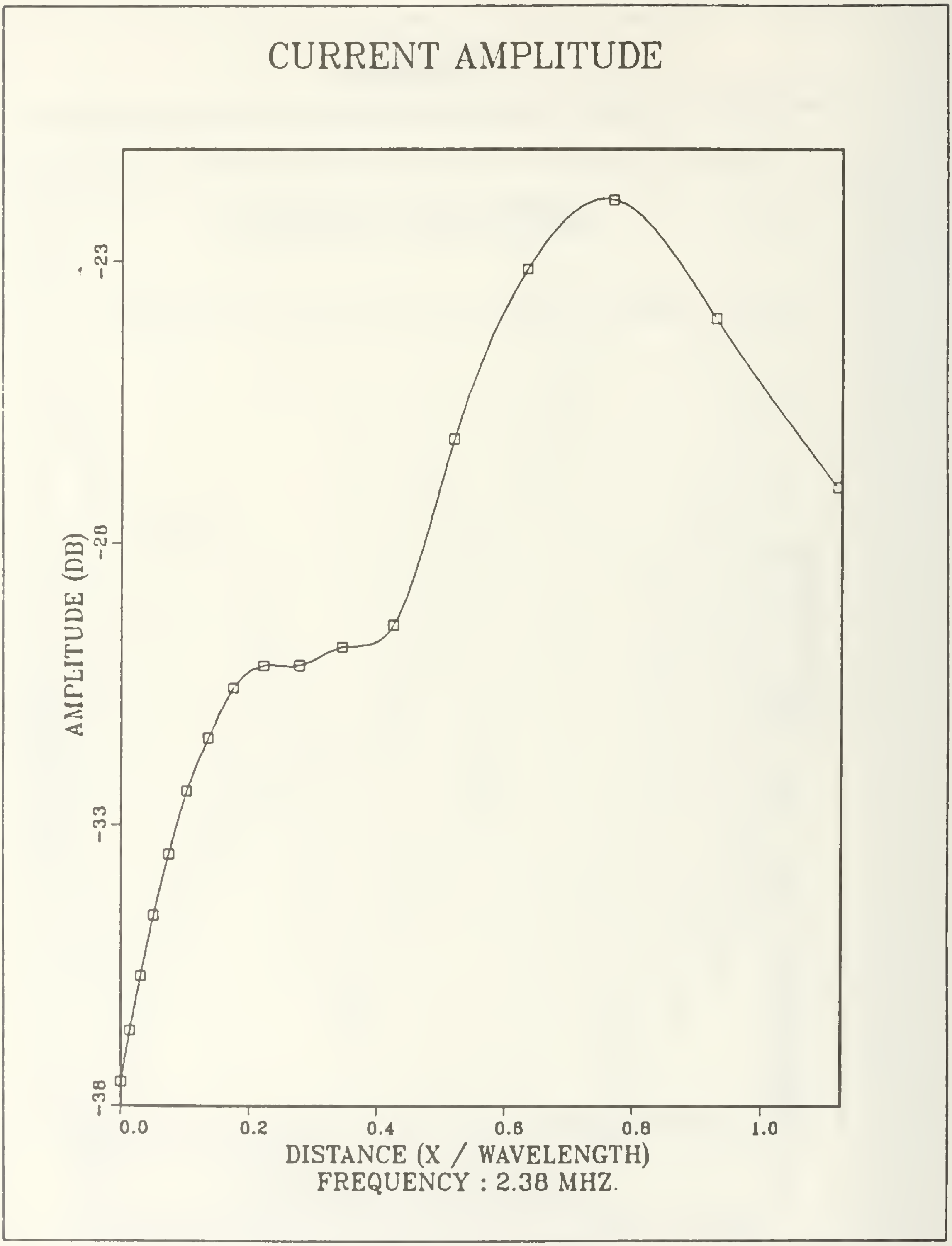

Figure F.3 Current Amplitude, Frequency : 2.38 MHz.

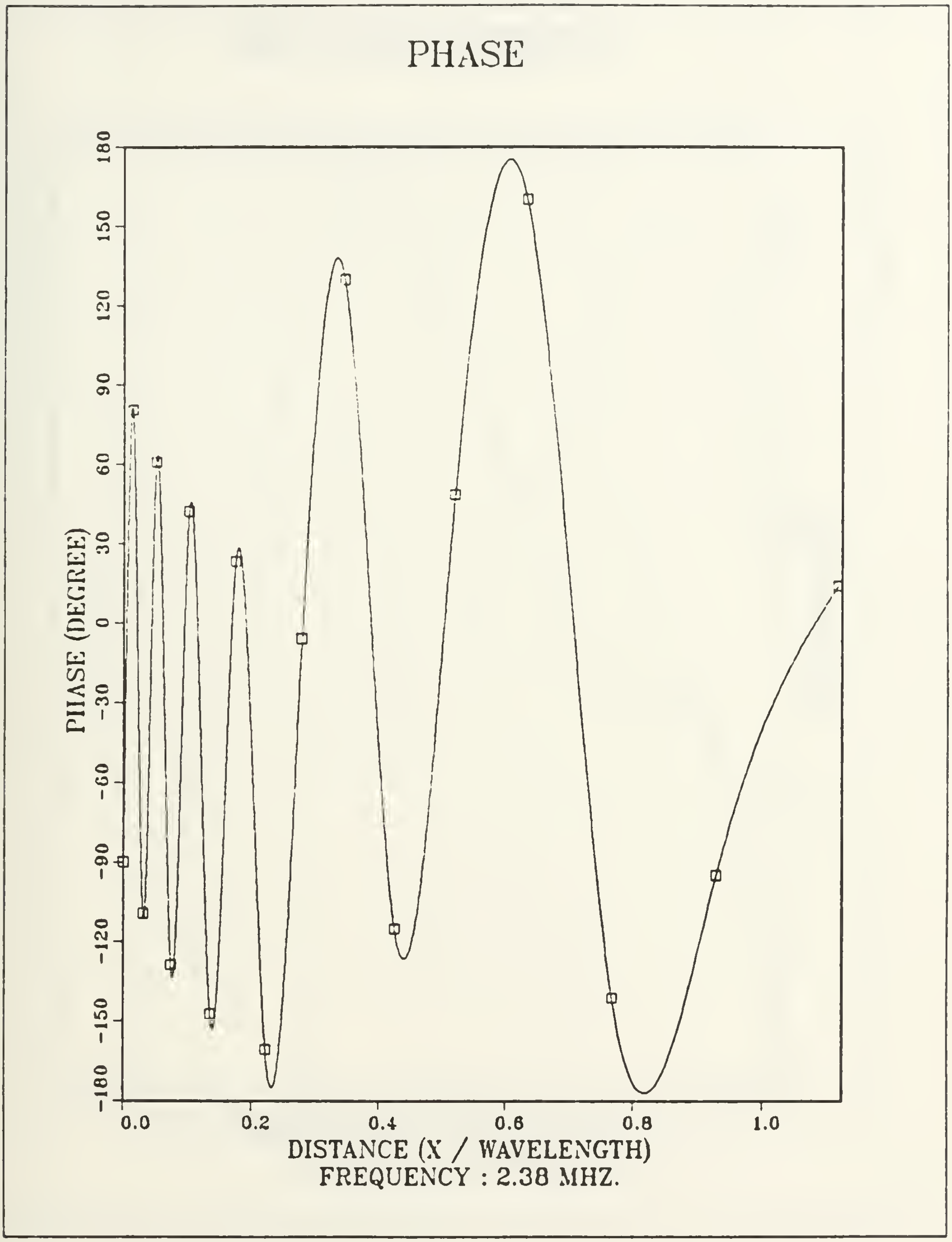

Figure F.4 Current Phase, Frequency : 2.38 MHz.

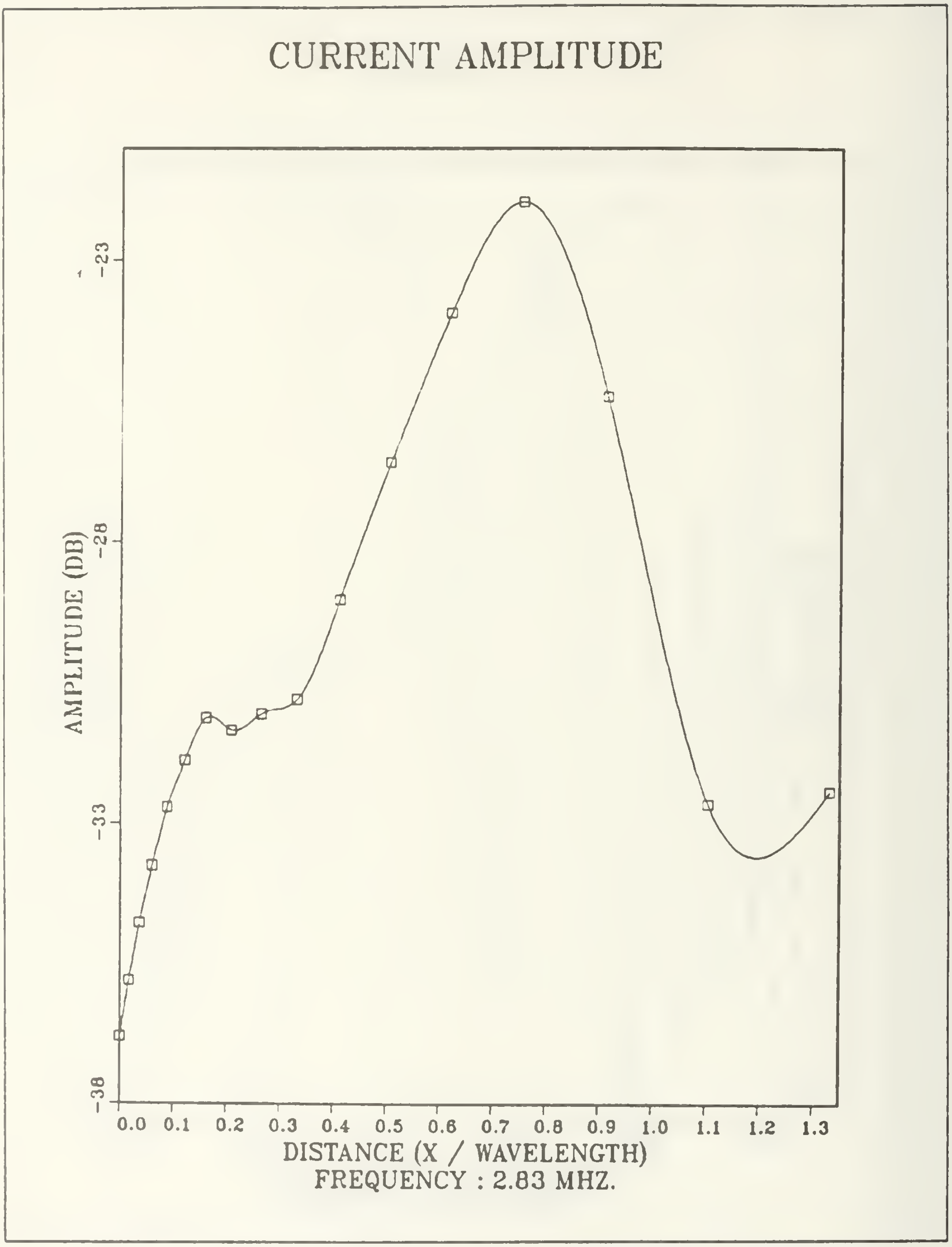

Figure F.5 Current Amplitude, Frequency : 2.83 MHz.

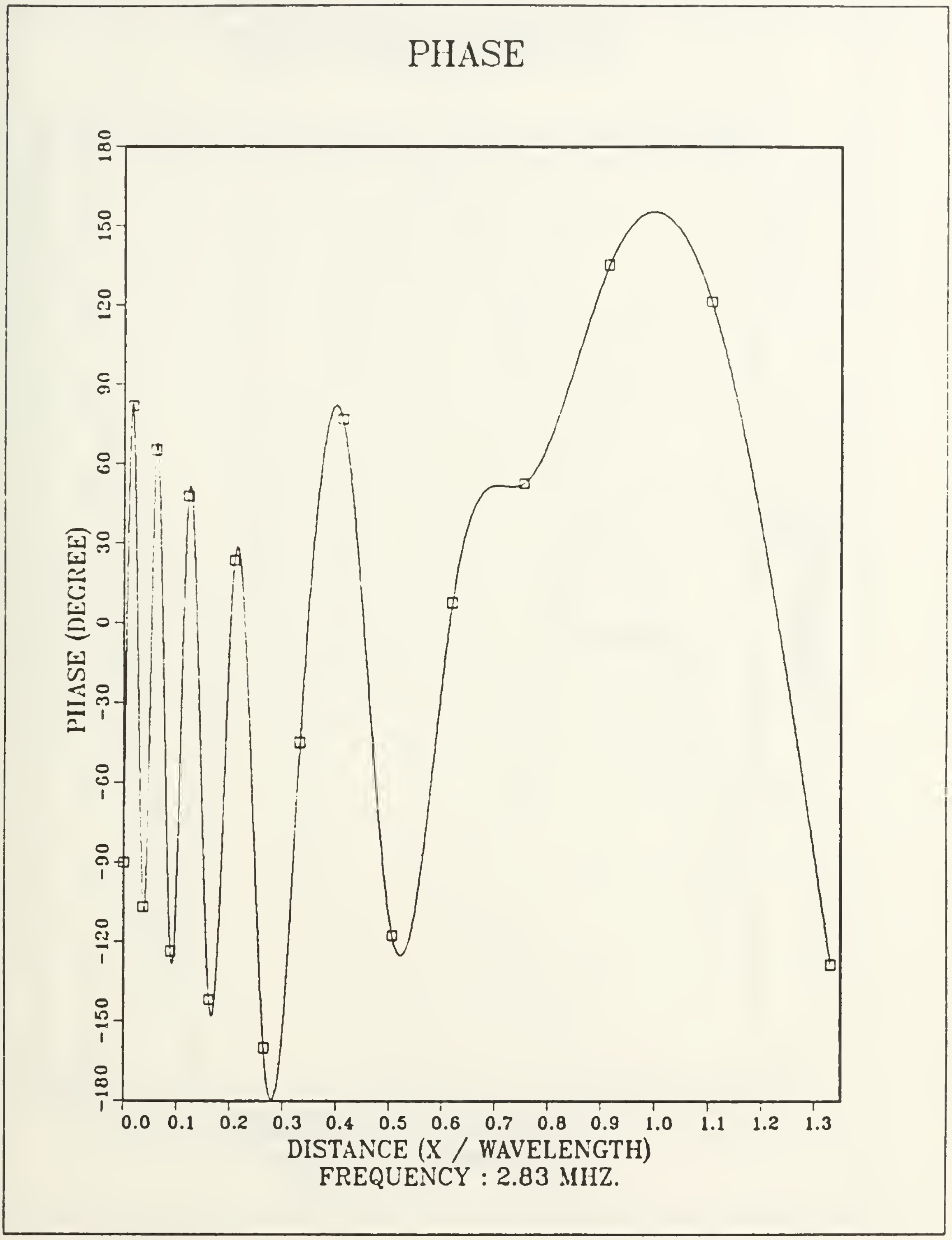

Figure F.6 Current Phase, Frequency : 2.83 MHz.

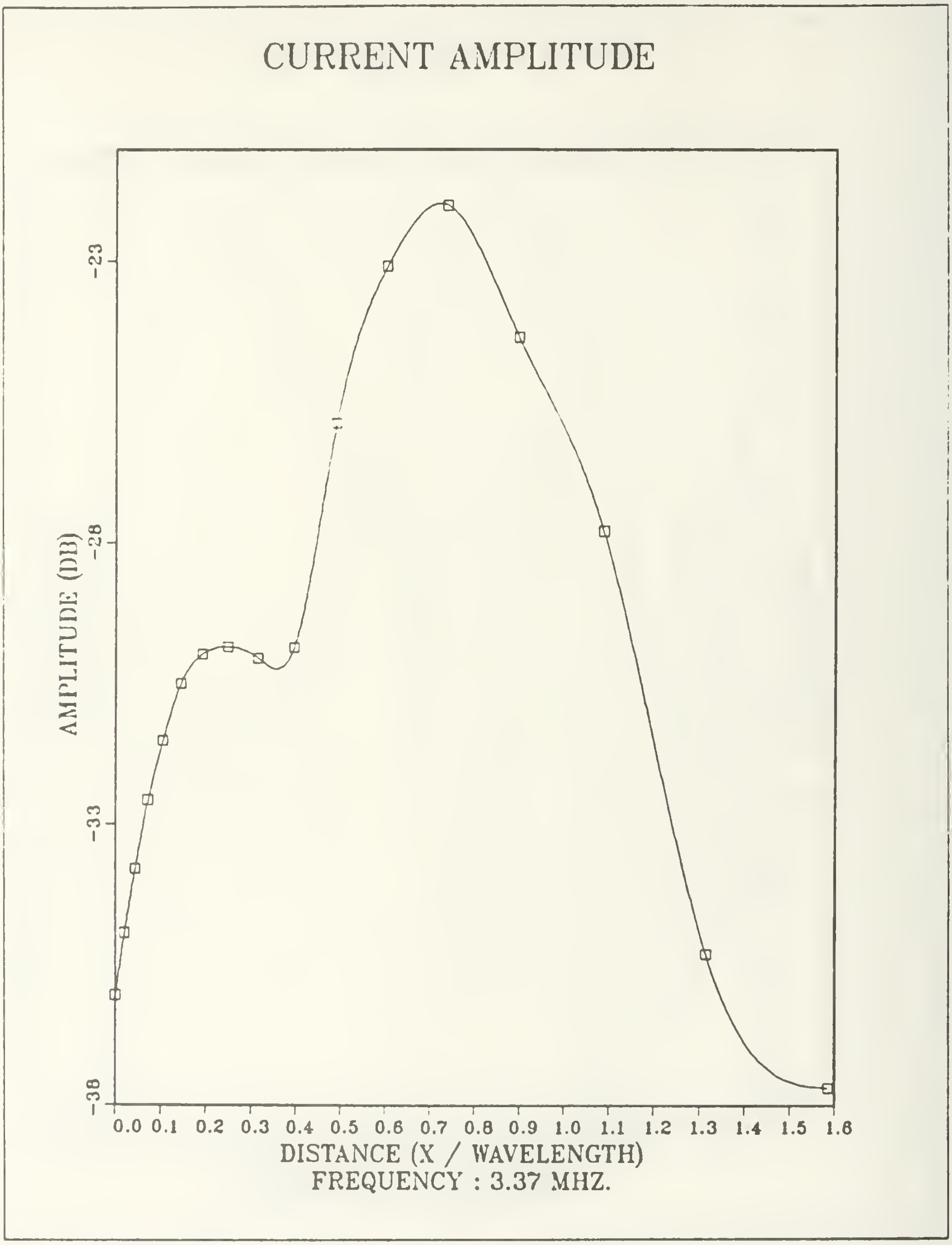

Figure F.7 Current Amplitude, Frequency : 3.37 MHz.

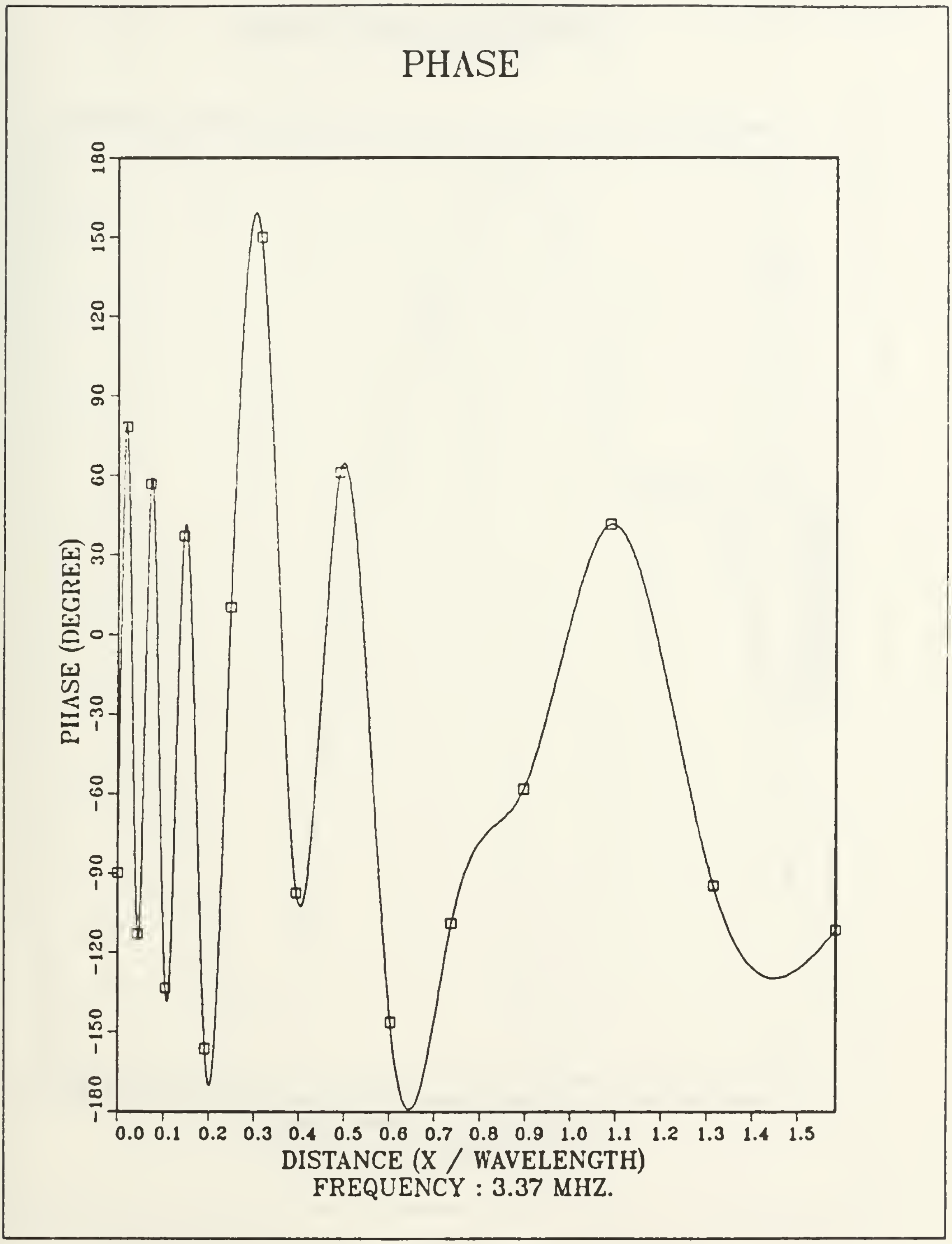

Figure F.8 Current Phase, Frequency : 3.37 MHz.

Figure F.9 Current Amplitude, Frequency : 4.01 MHz.

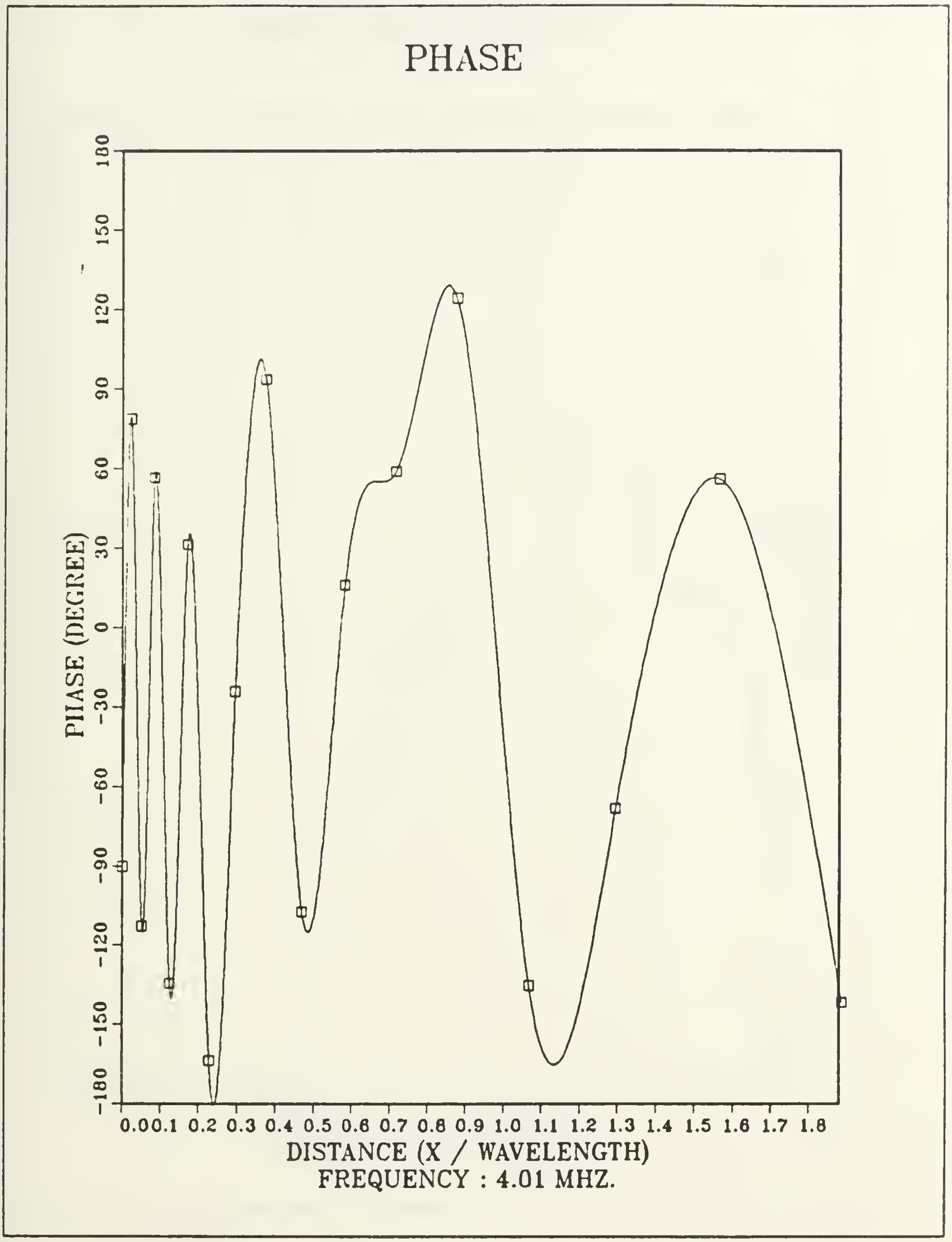

Figure F.10 Current Phase, Frequency : 4.01.

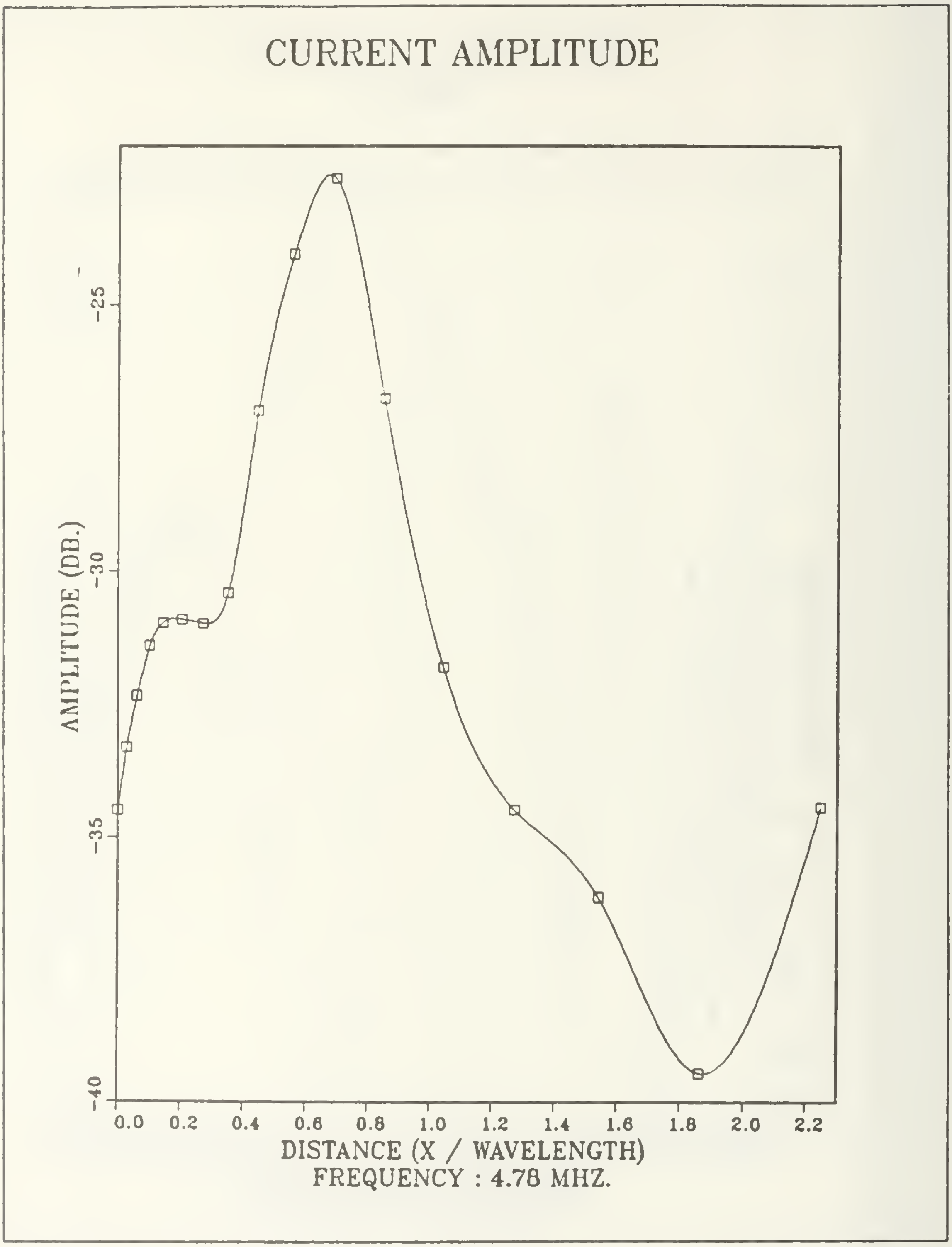

Figure F.11 Current Amplitude, Frequency : 4.78 MHz.

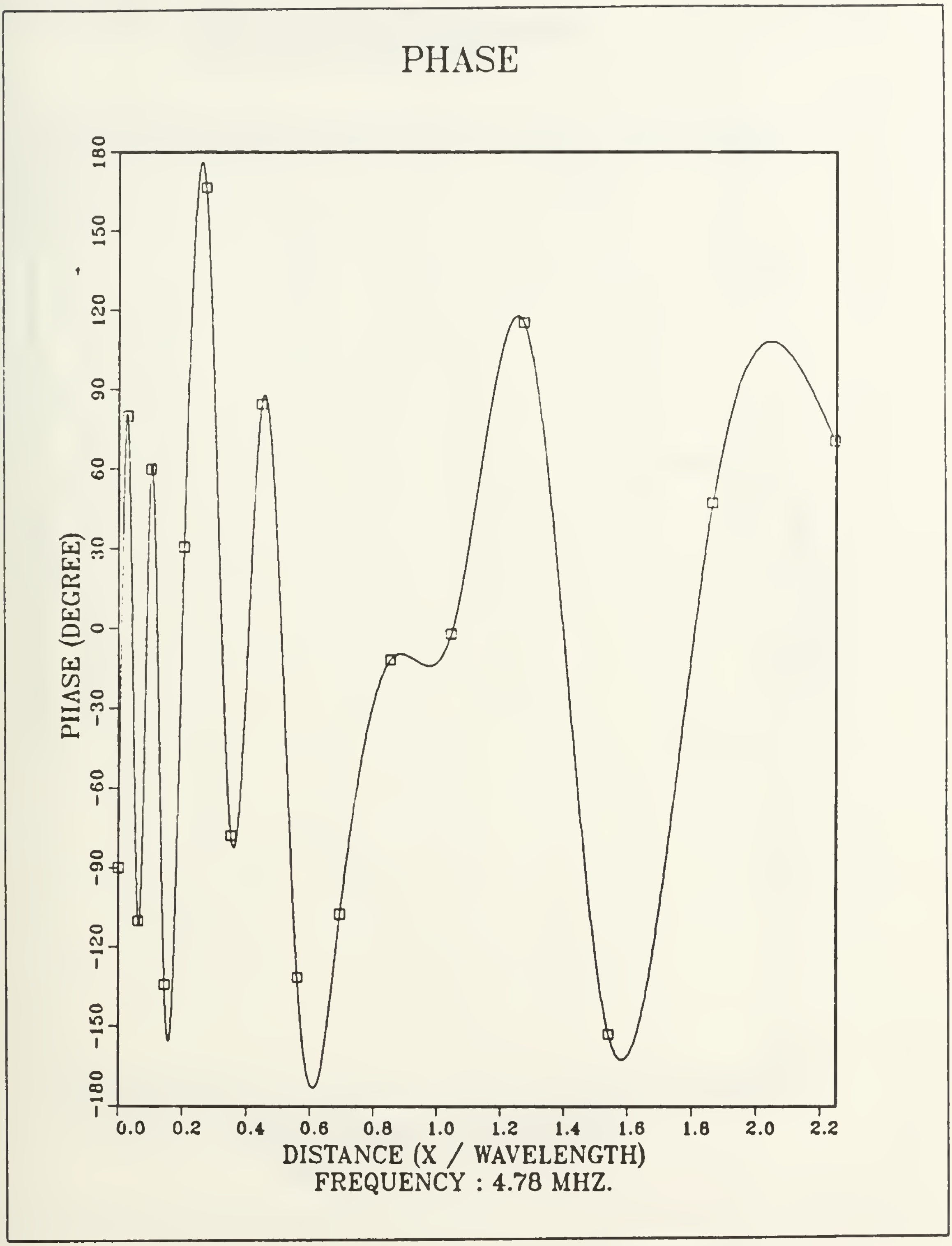

Figure F.12 Current Phase, Frequency : 4.78 MHz.

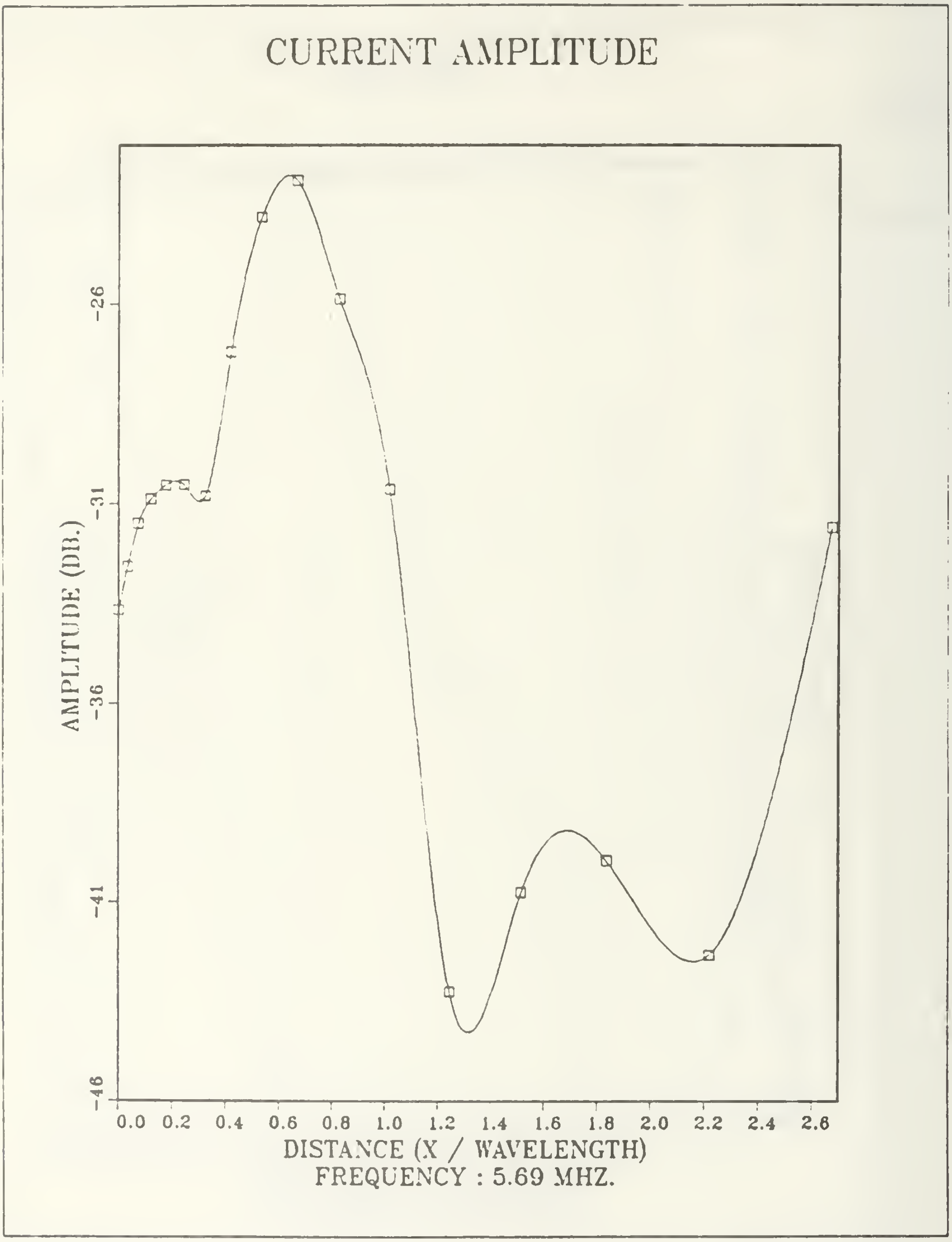

Figure F.13 Current Amplitude, Frequency : 5.69 MHz.

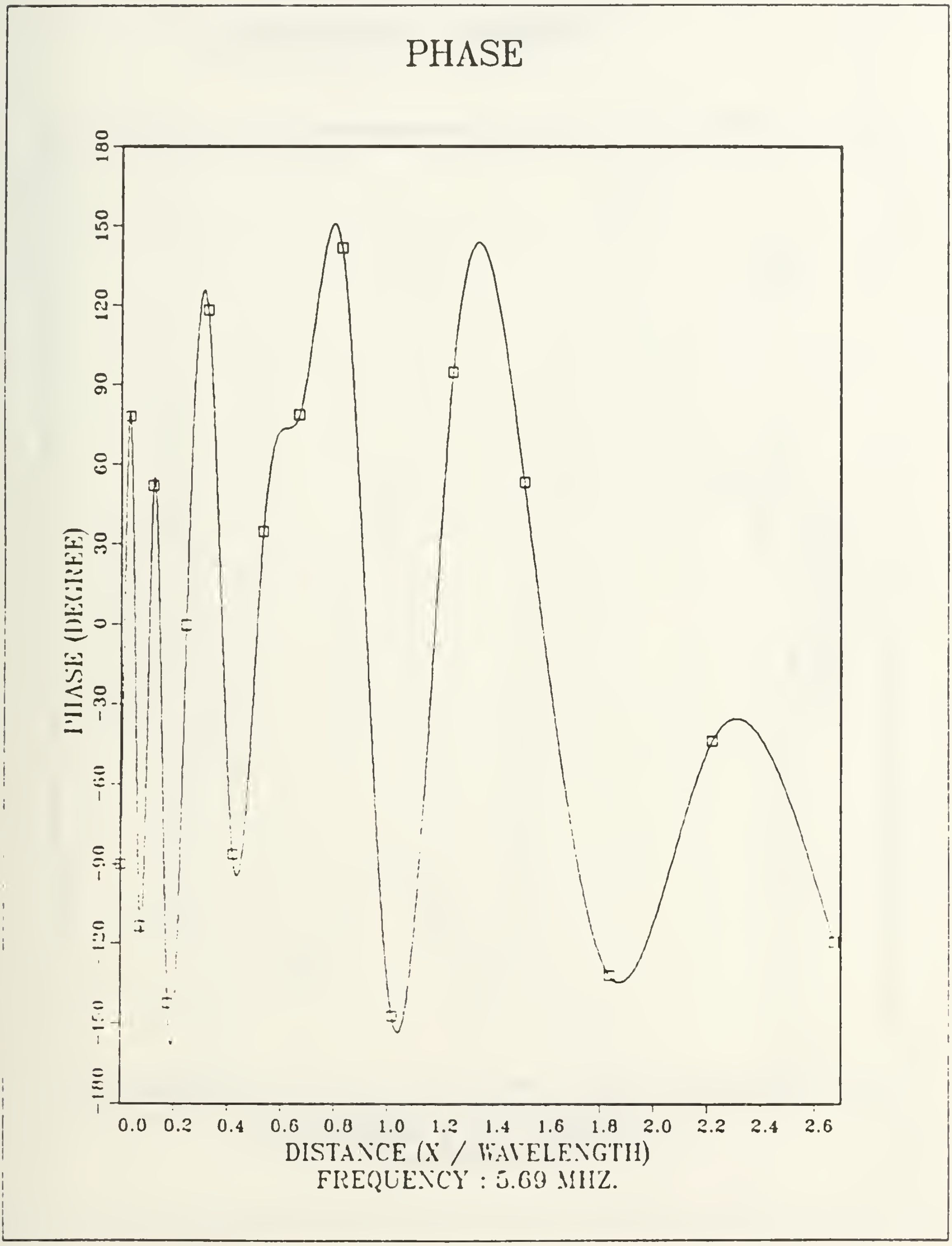

Figure F.14 Current Phase, Frequency : 5.69 MHz.

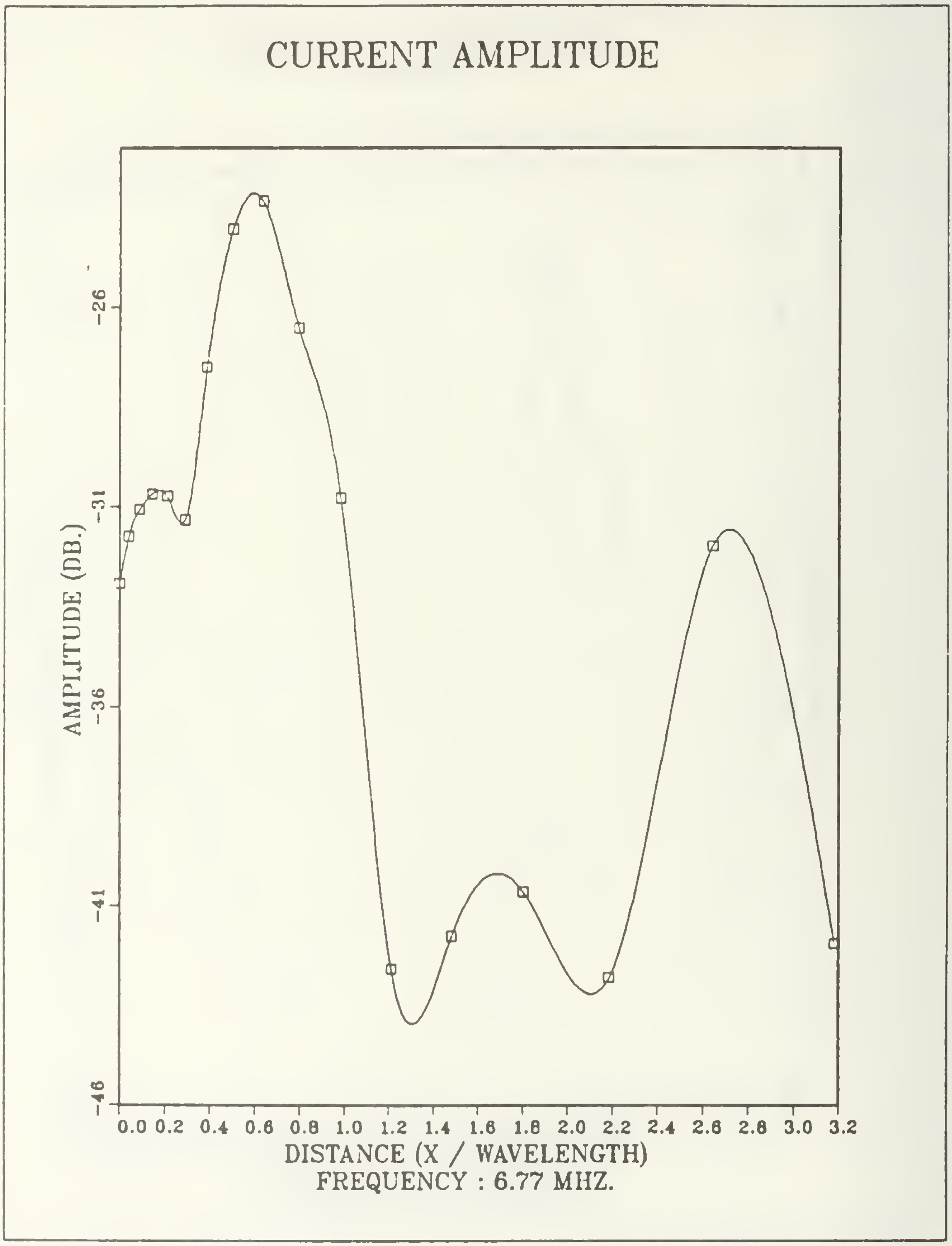

Figure F.15 Current Amplitude, Frequency : 6.77 MHz.

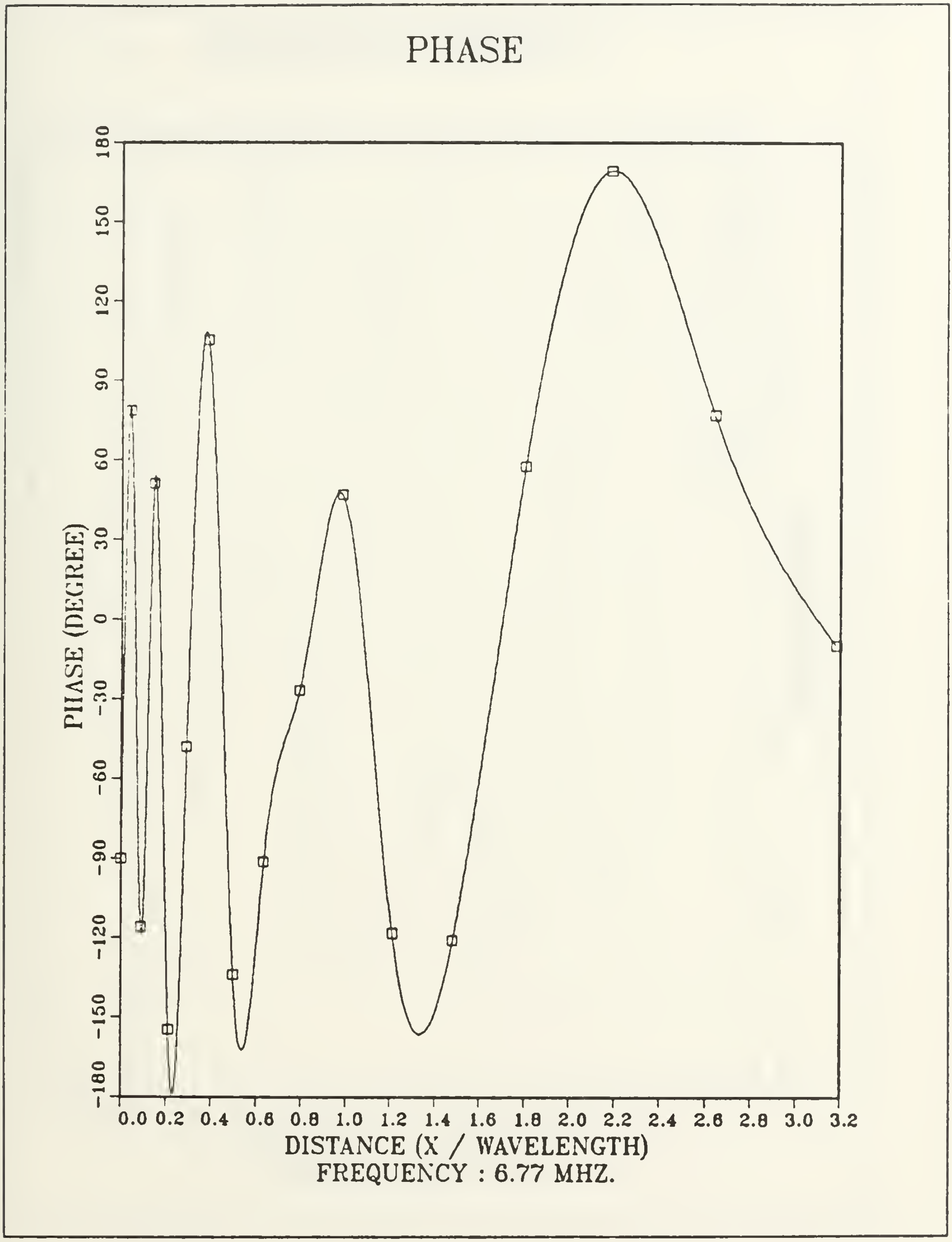

Figure F.16 Current Phase, Frequency : 6.77 MHz.

Figure F.17 Current Amplitude, Frequency : 8.06 MHz.

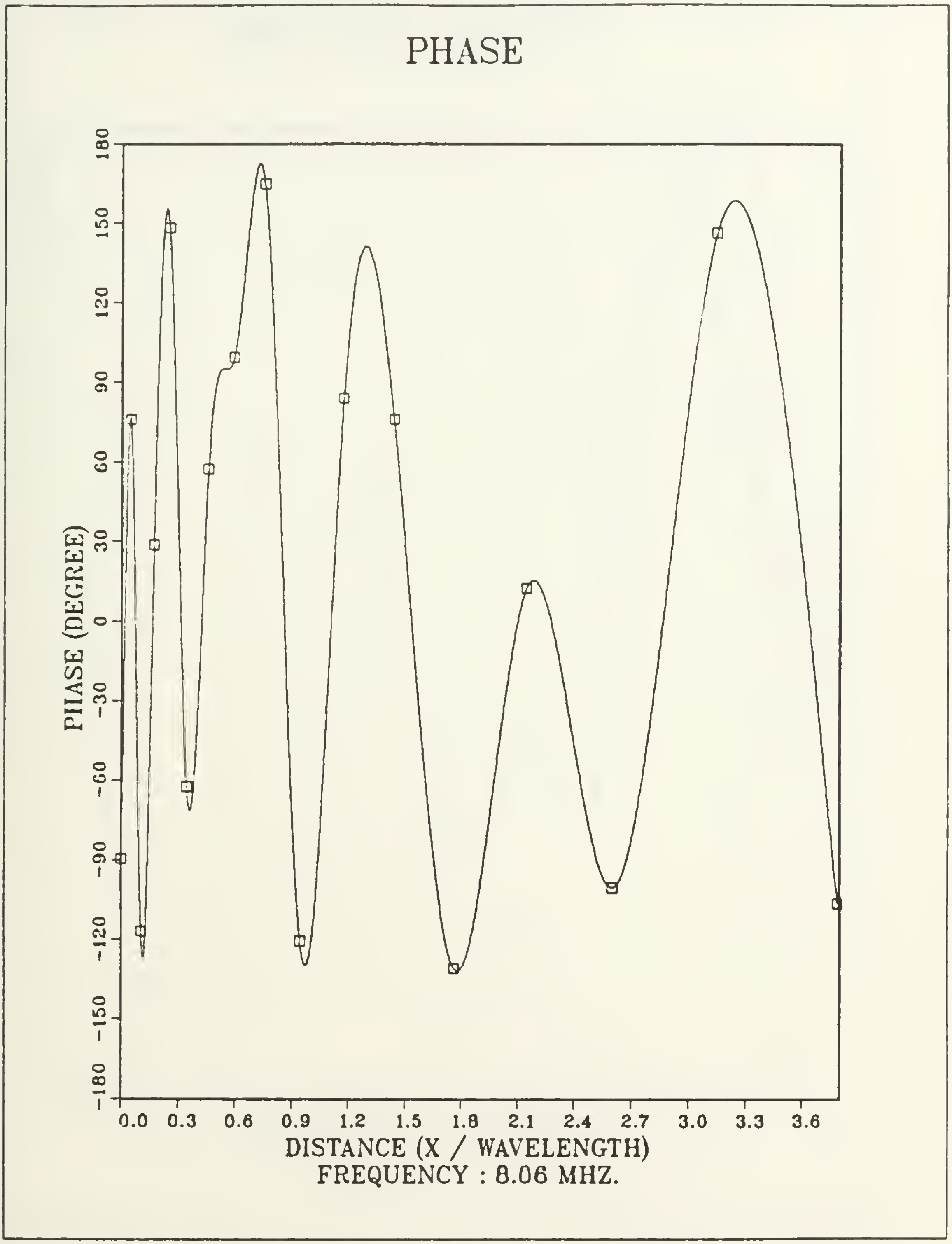

Figure F.18 Current Phase, Frequency : 8.06 MHz.

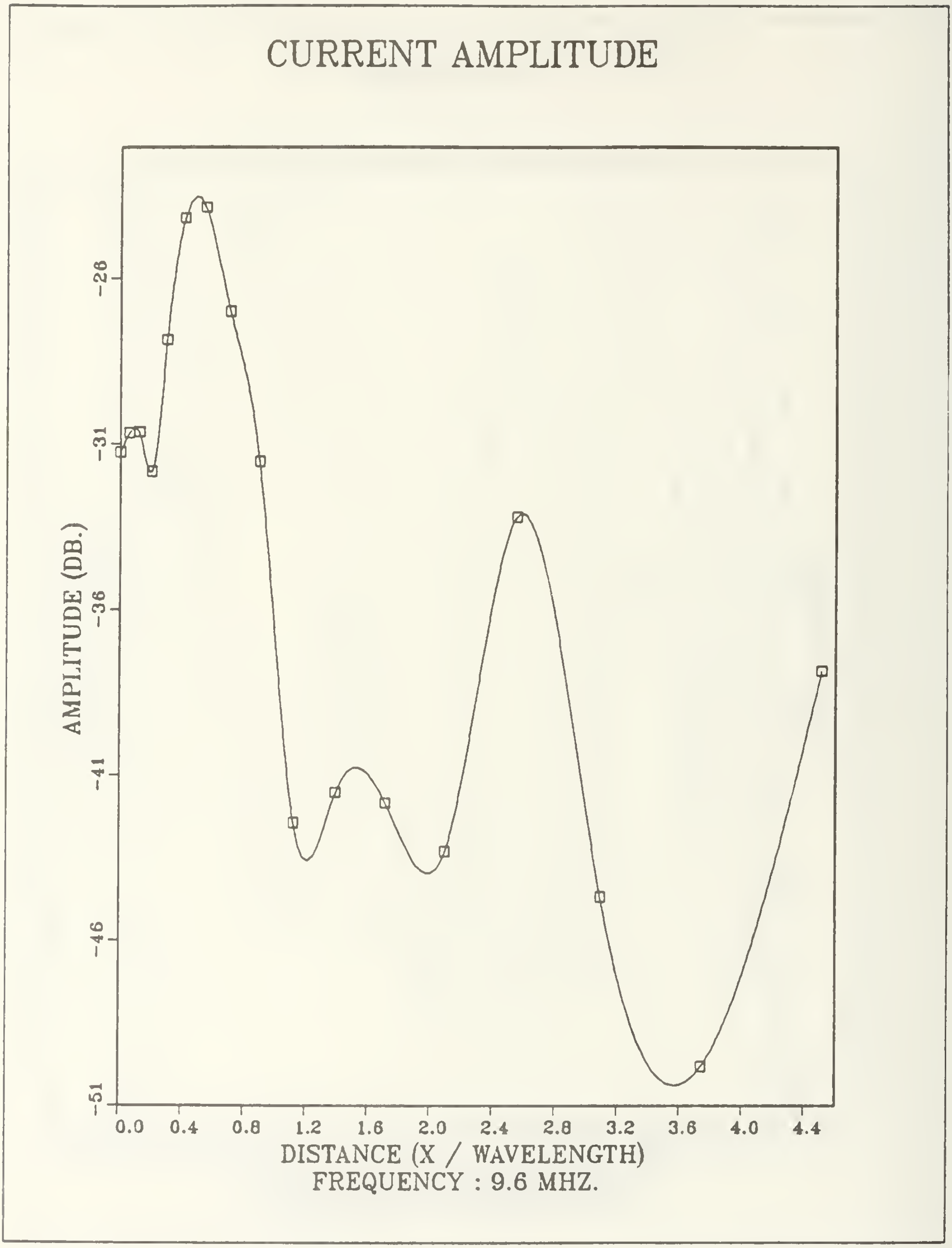

Figure F.19 Current Amplitude, Frequency : 9.6 MHz.

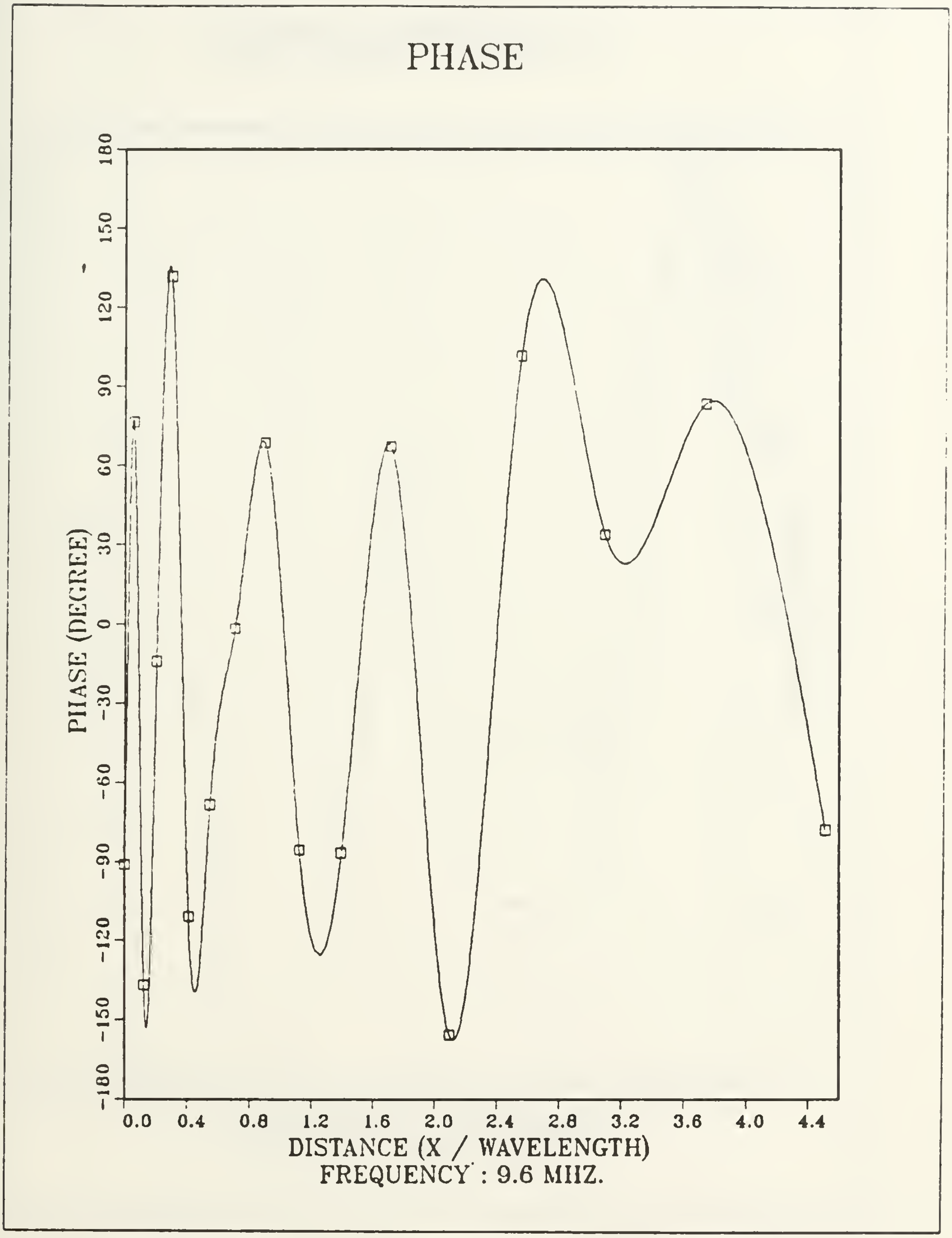

Figure F.20 Current Phase, Frequency : 9.6 MHz.

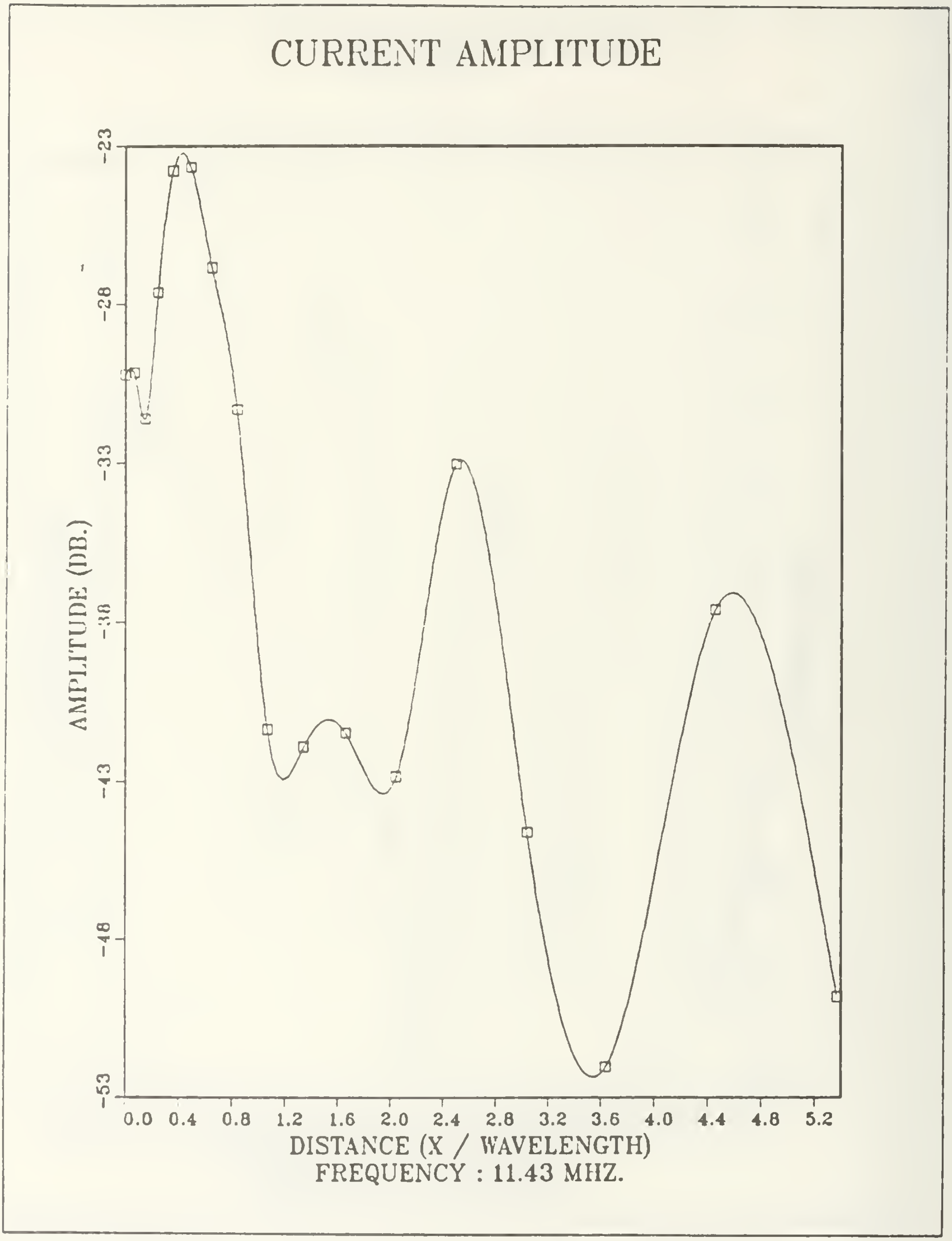

Figure F.21 Current Amplitude, Frequency : 11.43 MHz.

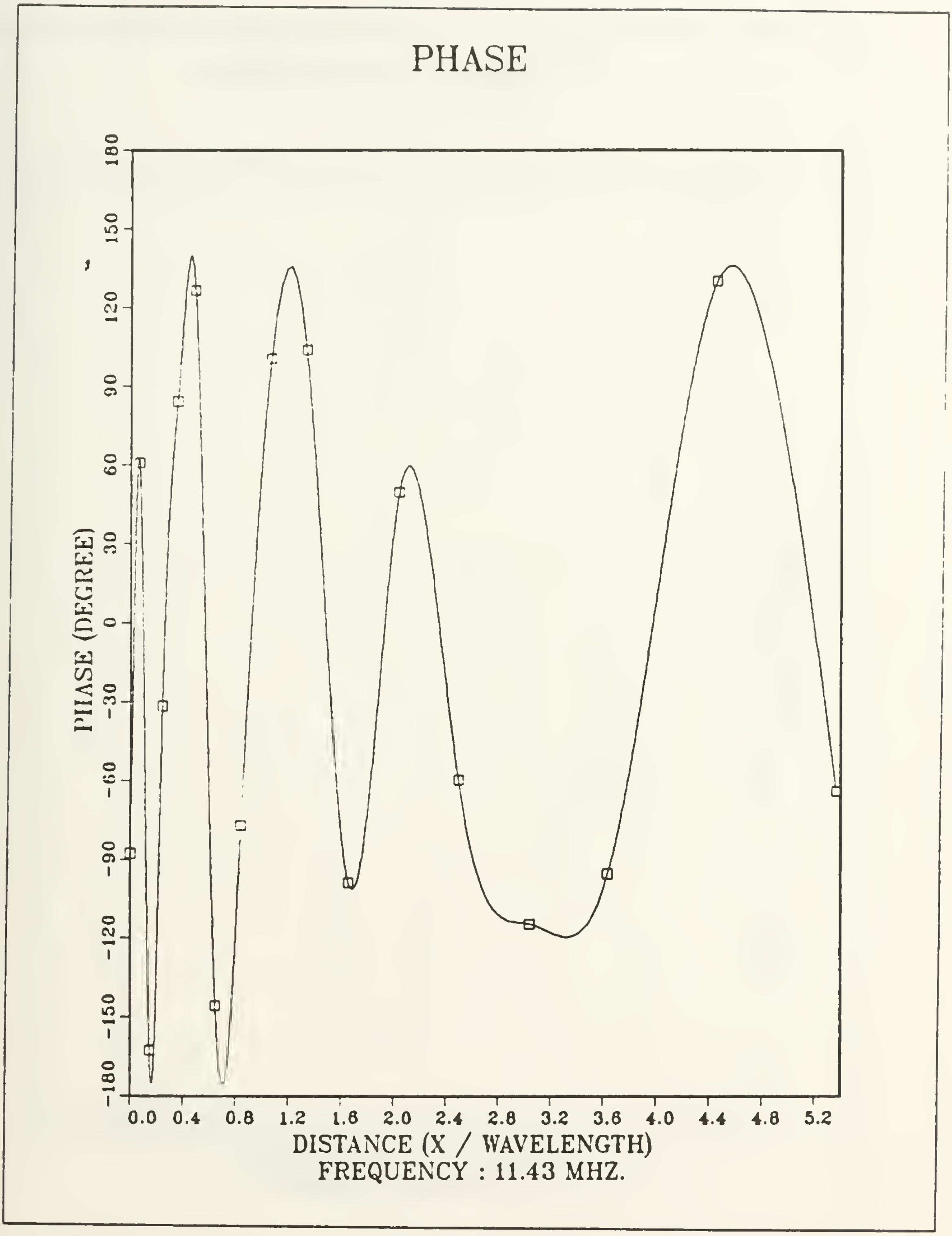

Figure F.22 Current Phase, Frequency : 11.43 MHz.

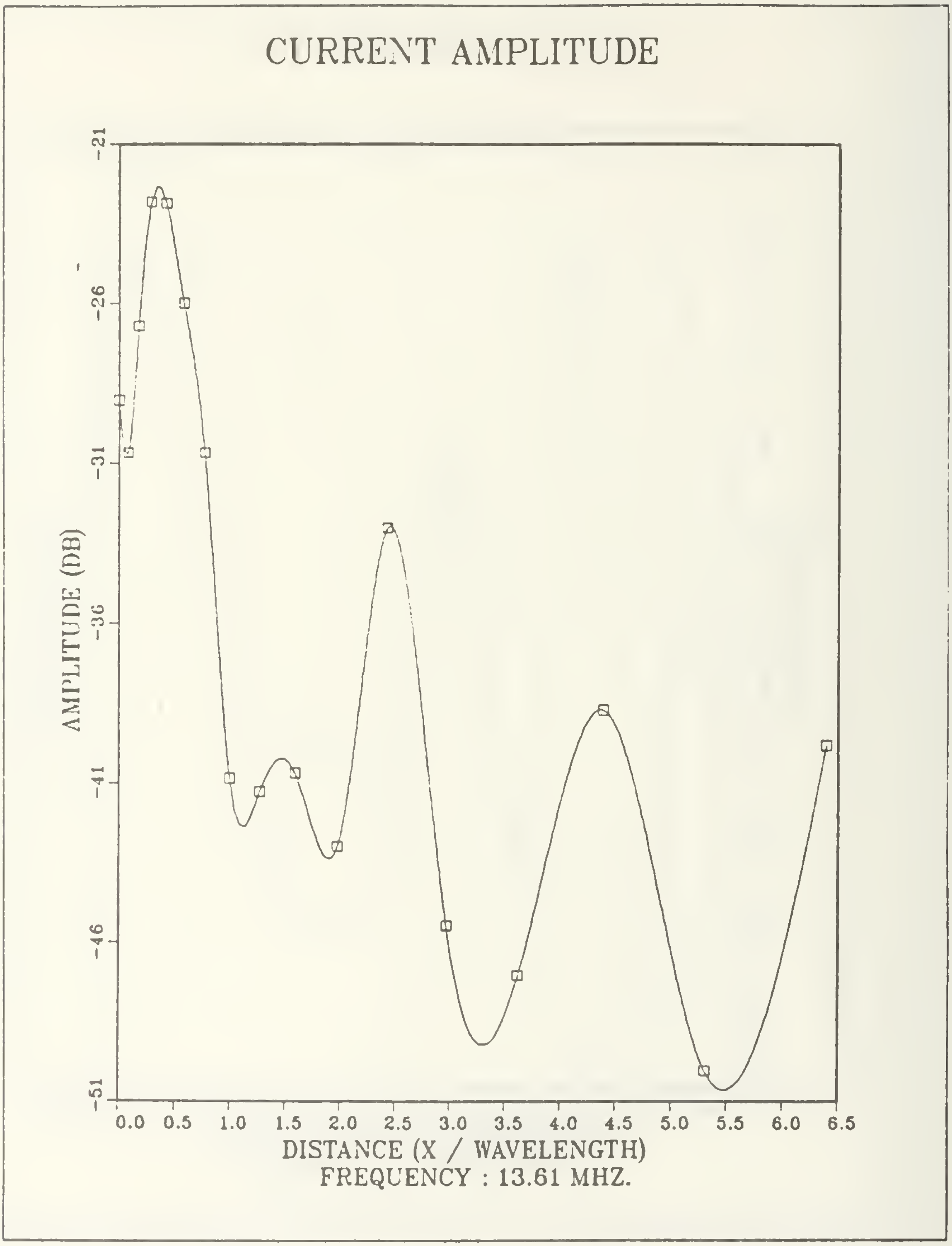

Figure F.23 Current Amplitude, Frequency : 13.61 MHz.

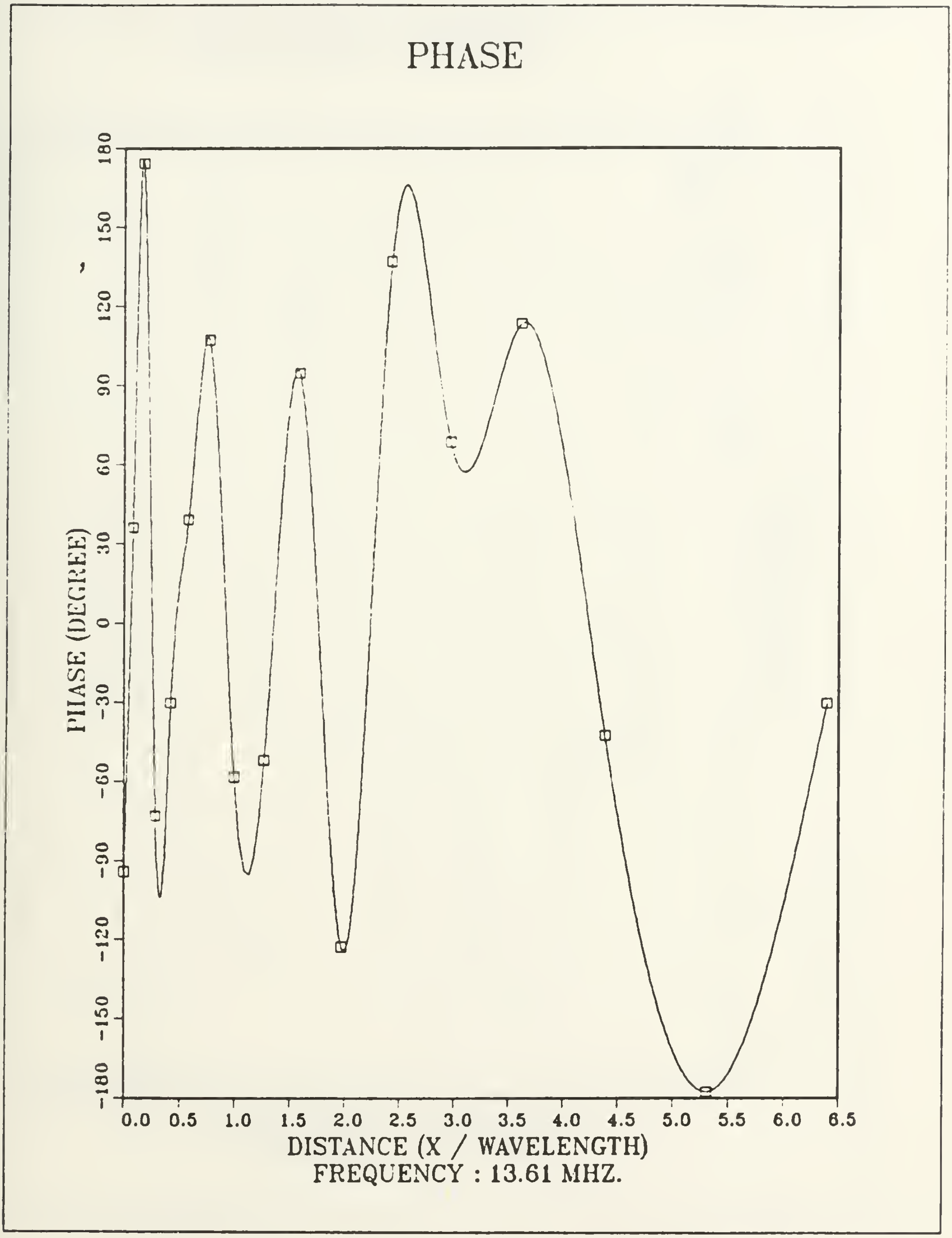

Figure F.24 Current Phase, Frequency : 13.61 MHz.

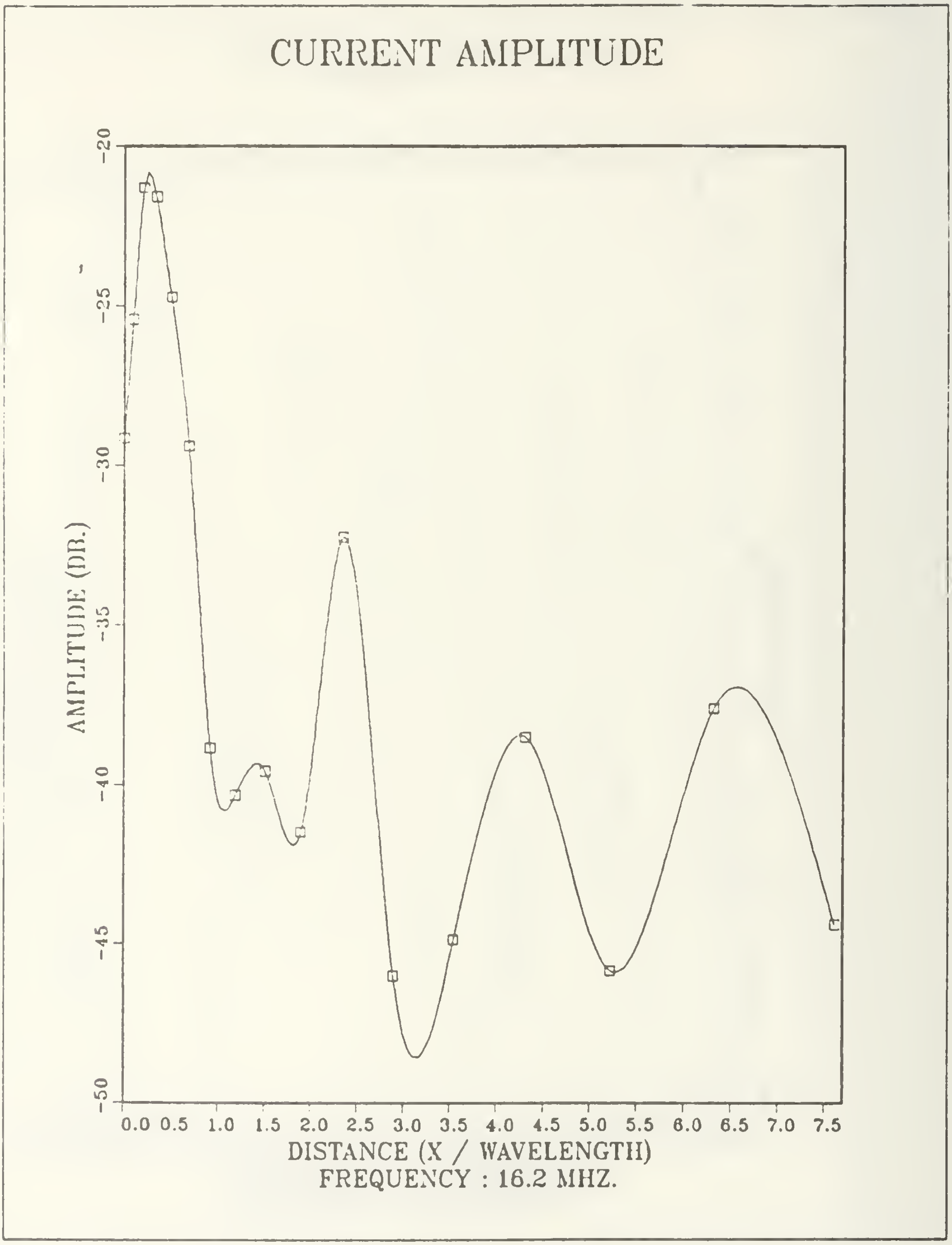

Figure F.25 Current Amplitude, Frequency : 16.2 MHz.

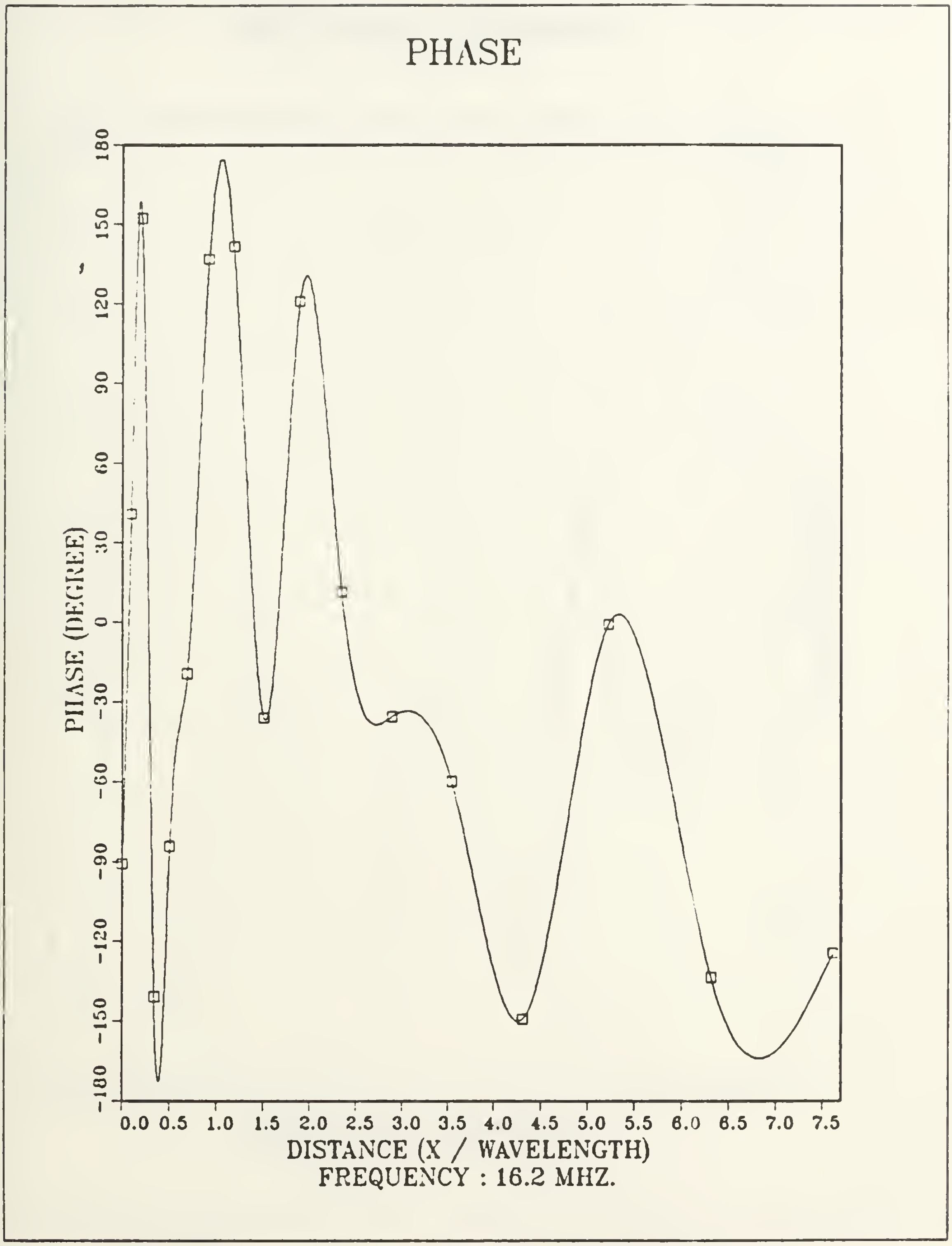

Figure F.26 Current Phase, Frequency : 16.2 MHz.

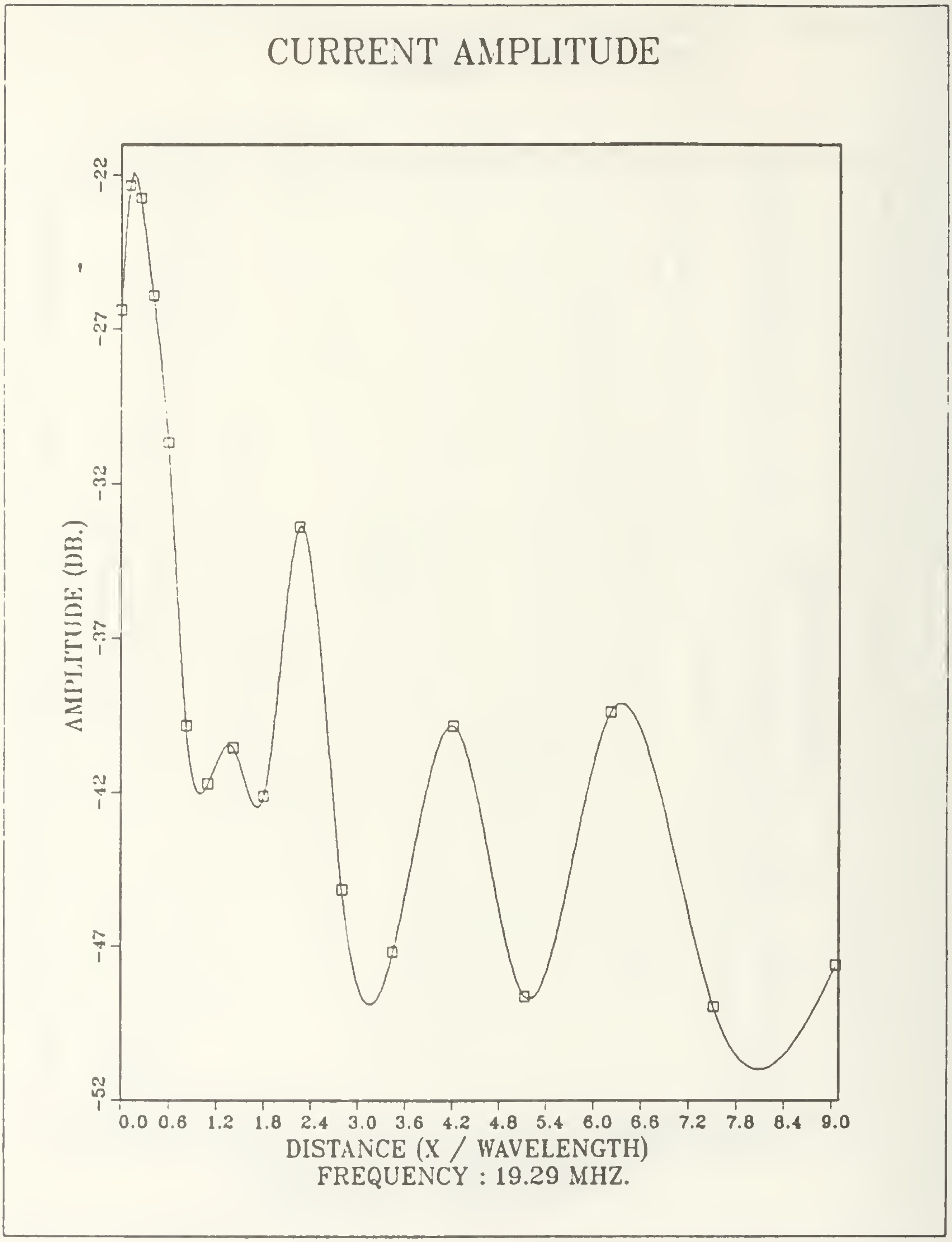

Figure F.27 Current Amplitude, Frequency : 19.29 MHz.

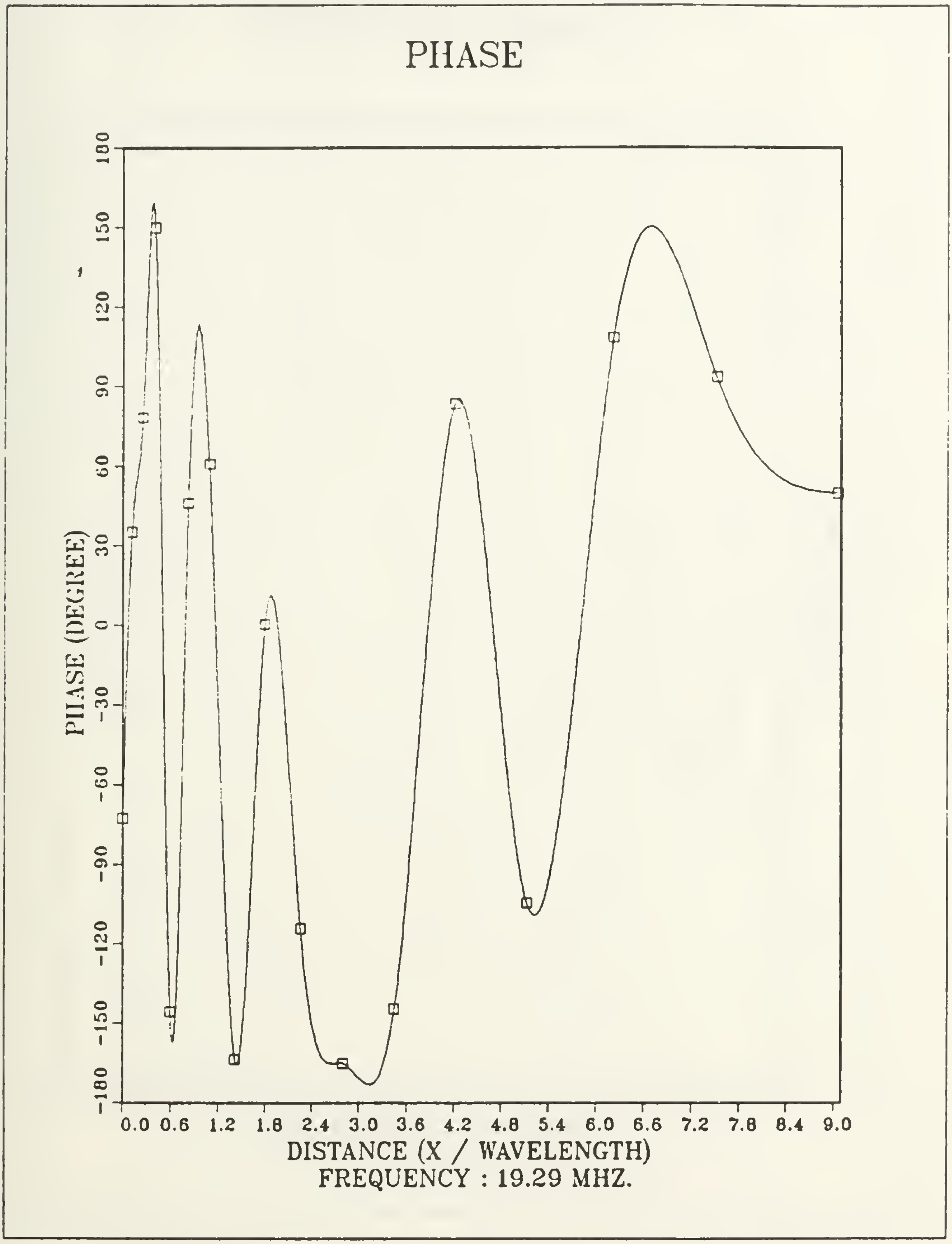

Figure F.28 Current Phase, Frequency : 19.29 MHz.

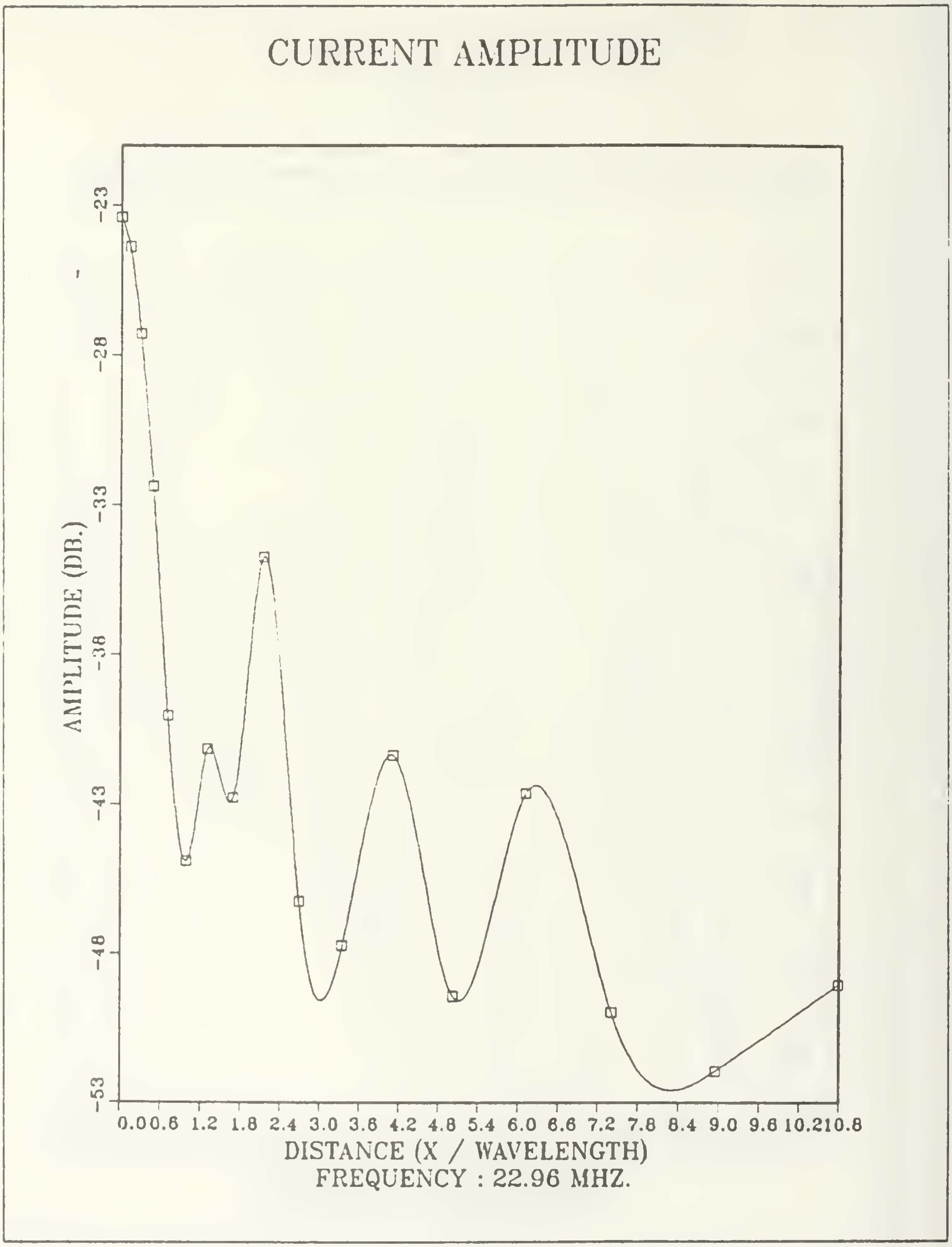

Figure F.29 Current Amplitude, Frequency : 22.96 MHz.

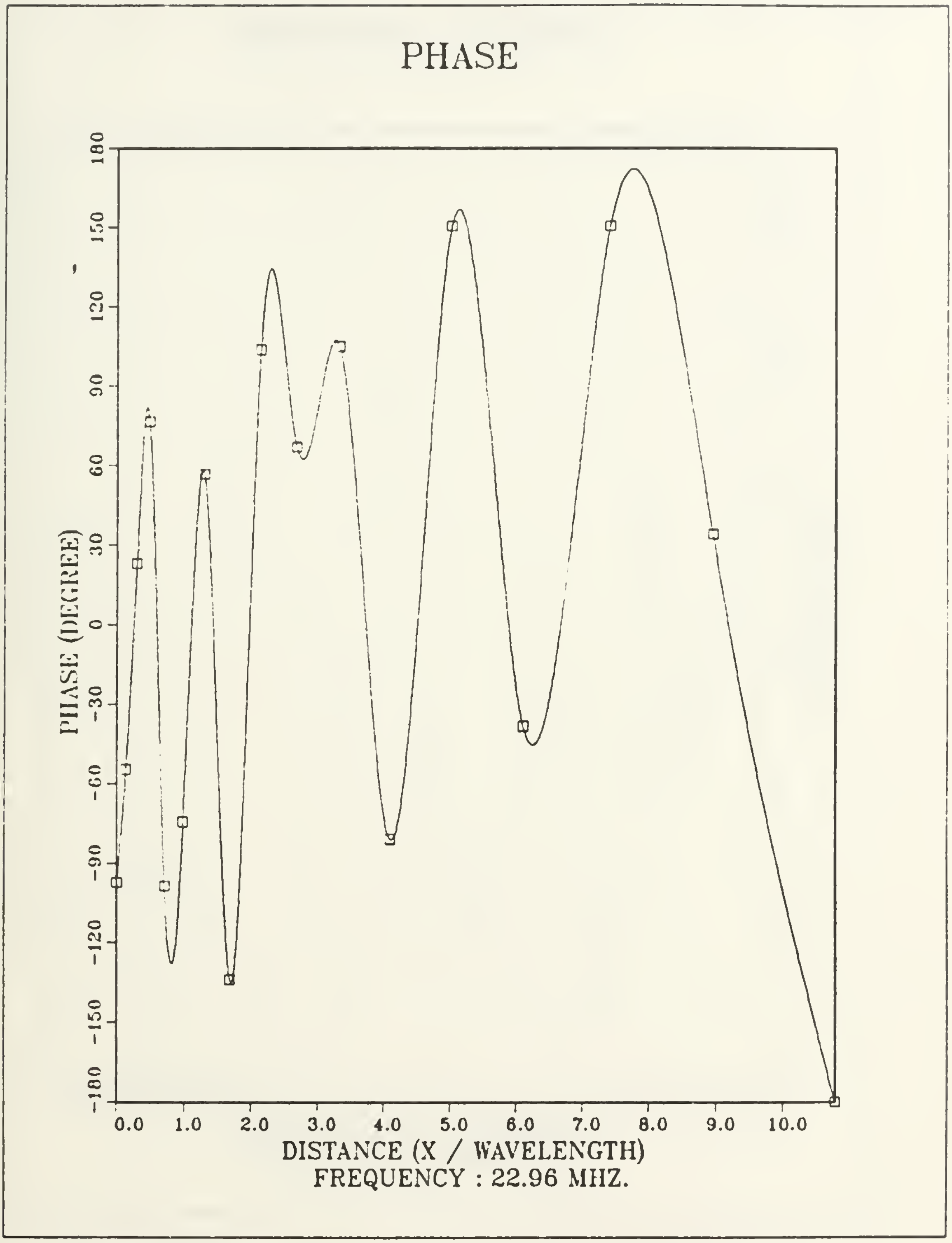

Figure F.30 Current Phase, Frequency : 22.96 MHz.

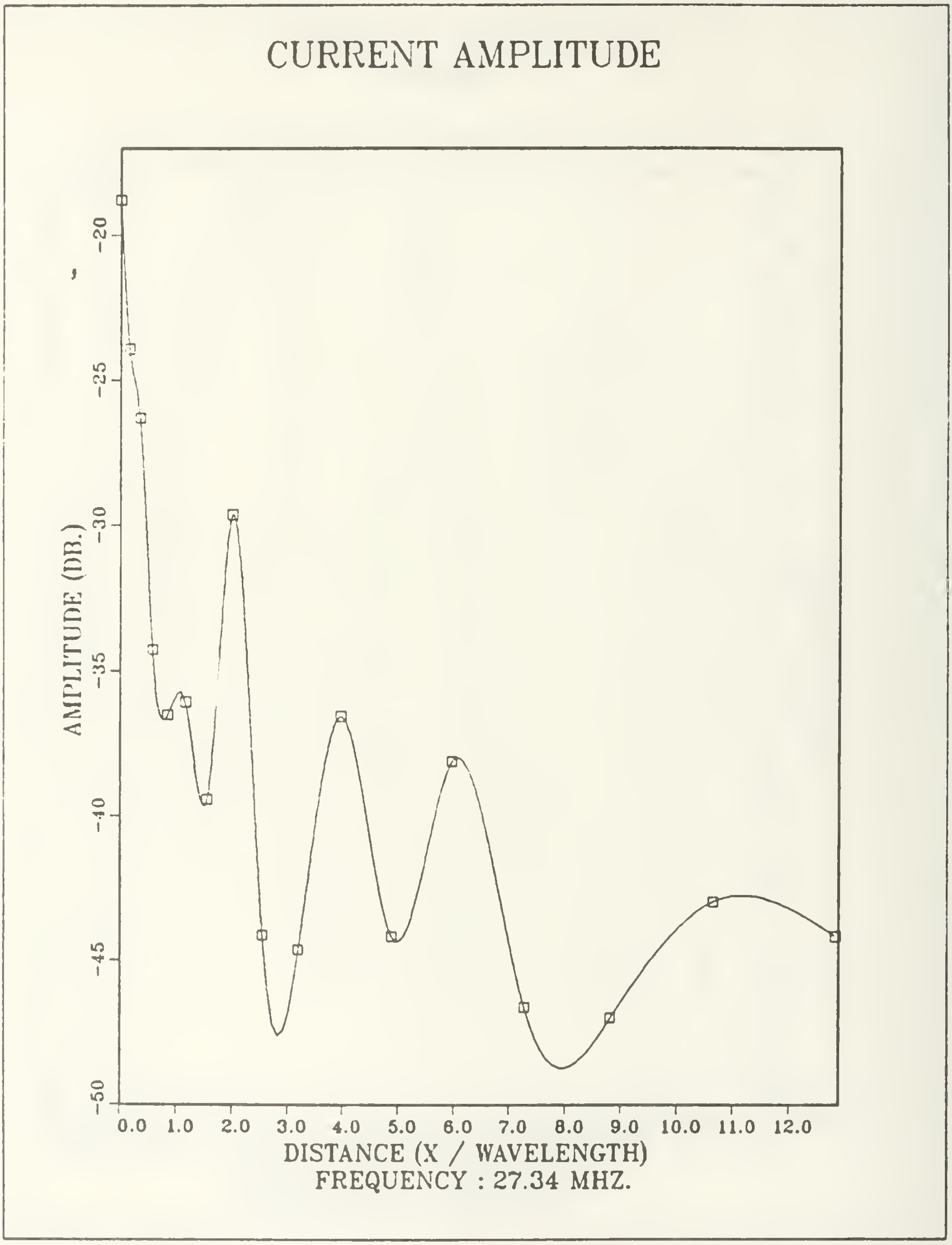

Figure F.31 Current Amplitude, Frequency : 27.34 MHz.

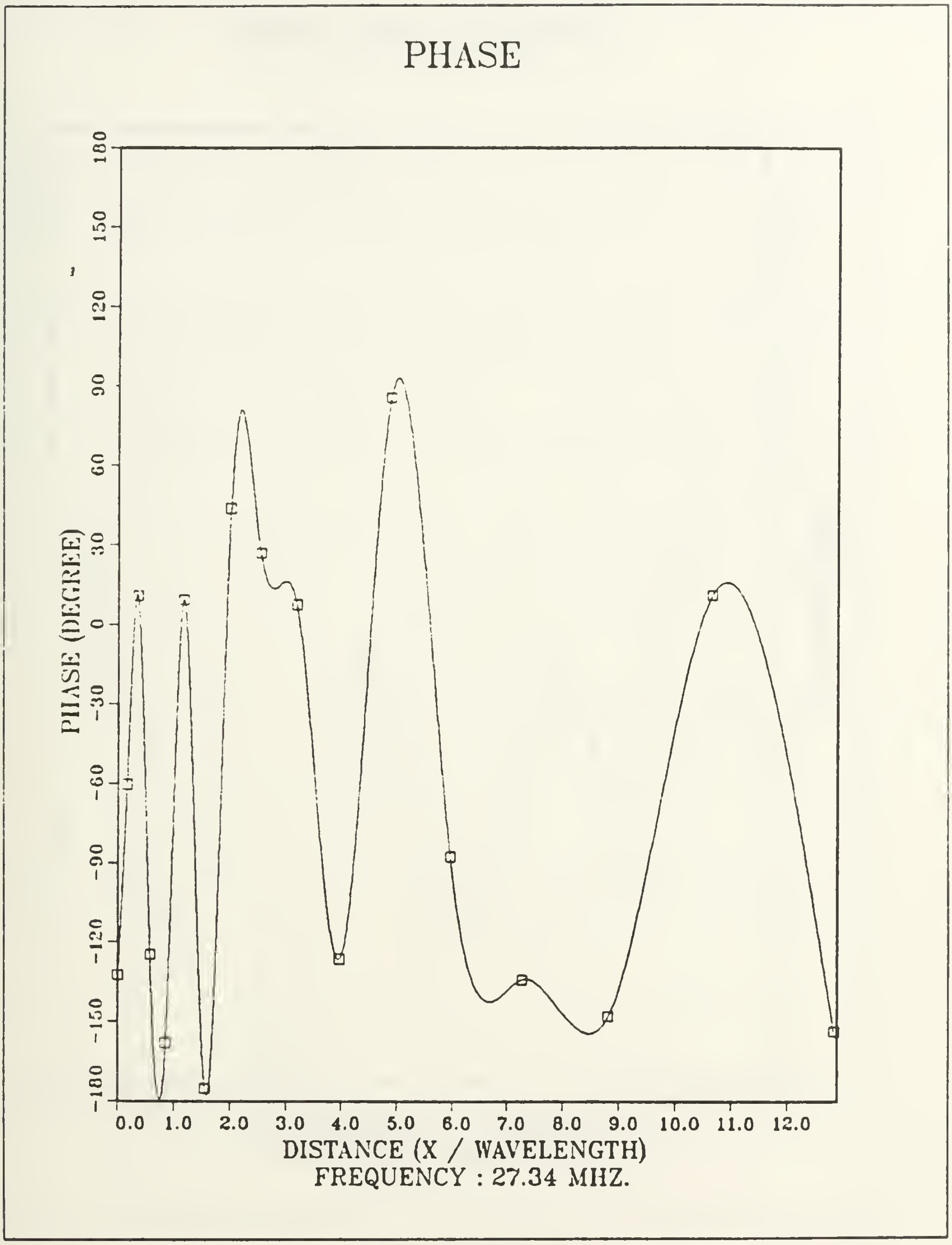

Figure F.32 Current Phase, Frequency : 27.34 MHz.

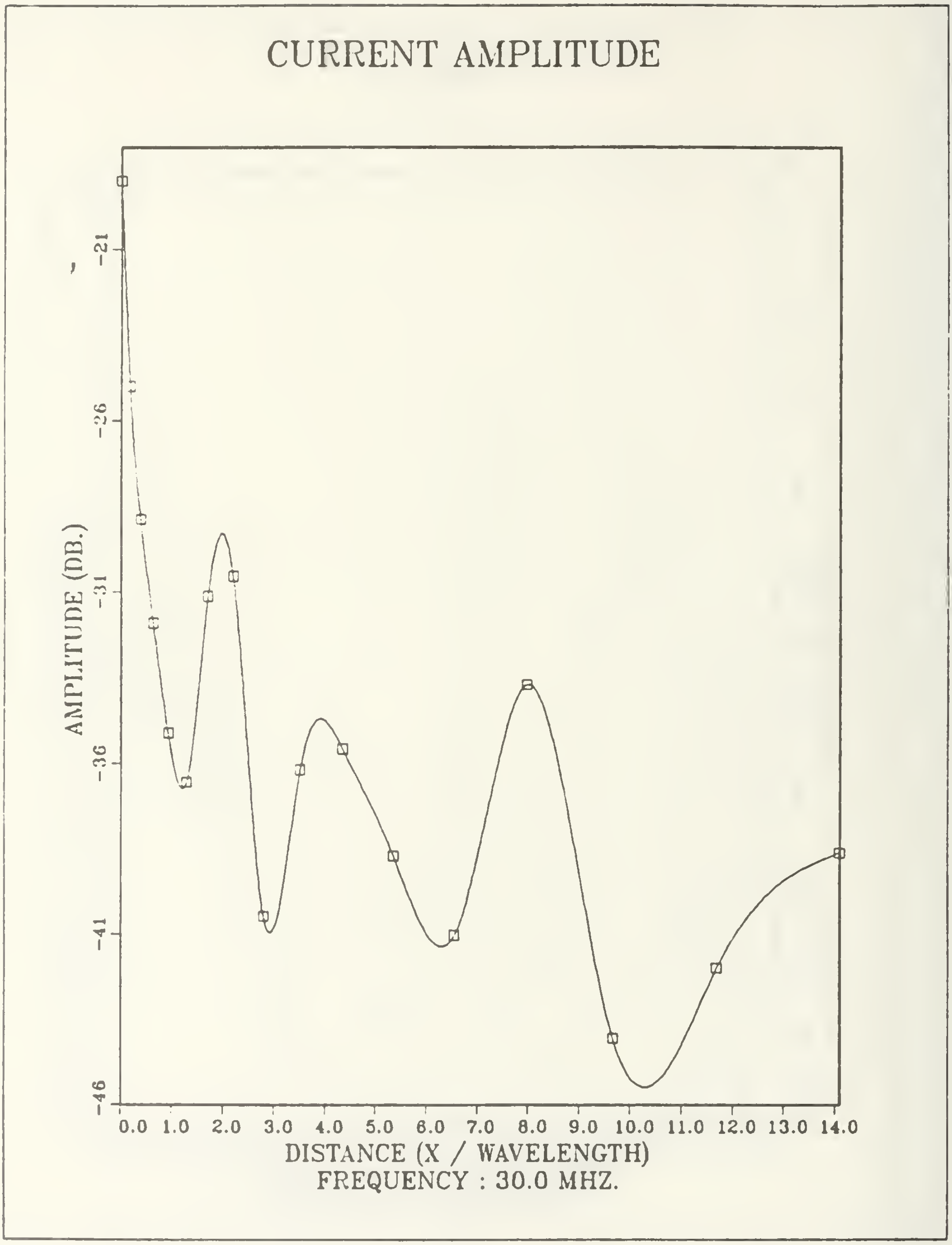

Figure F.33 Current Amplitude, Frequency : 30.0 MHz.

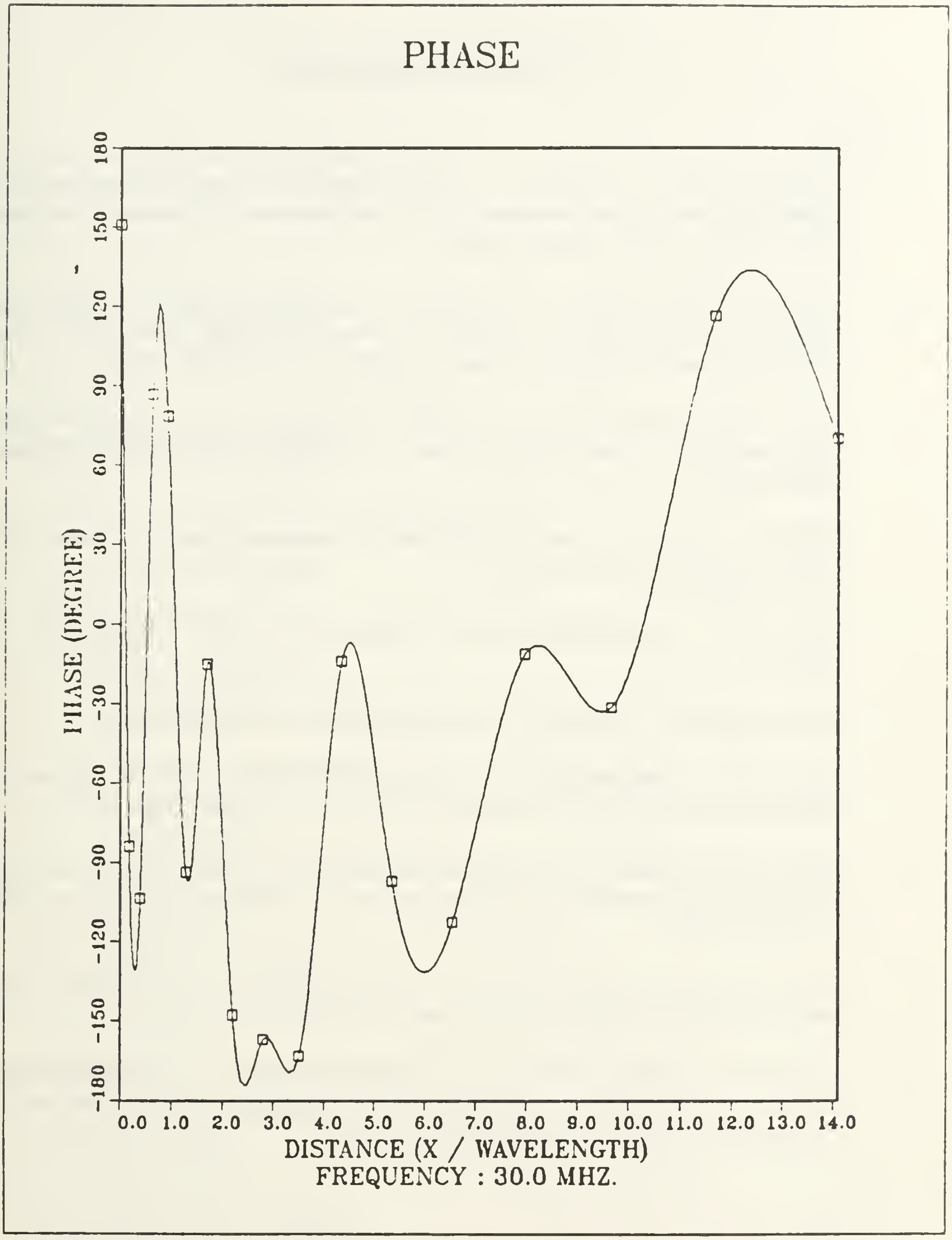

Figure F.34 Current Phase, Frequency : 30.0 MHz.

LIST OF REFERENCES

1. Campbell, D.V., and others, *A Dual Feed-Dual Polarized Log-Periodic HF Antenna System*, paper presented at the 1985 Antenna Applications Symposium, Urbana, Illinois, 18 September 1985.

2. Johnsen, Richard John, *An Investigation into the Potential for Developing A Successful Log-Periodic Half Square Antenna with Dual Feed*, MSEE Thesis, Naval Postgraduate School, Monterey, California, December 1986.

3. Naval Ocean Systems Center Technical Document 116, volume 2, *Numerical Electromagnetics Code (NEC)-Method of Moments*, San Diego, California, January 1981.

4. Stutzman, Warren L., and Thiele, Gary A., *Antenna Theory and Design*, John Wiley and Sons, New York, 1981.

5. Weeks, W.L., *Antenna Engineering*, McGraw Hill Book Company, New York, 1968.

6. Blake, Lamont V., *Antennas*, John Wiley & Sons, New York, 1966.

7. Jordan, E.C., Deschamps, G.A., Dyson, J.D., Mayes, R.E., *Developments In Broadband Antennas*, IEEE spectrum, v. 1, pp. 58-71, April 1964.

8. Hudock, E., Mayes, P.E., *Near-Field Investigation of Uniform Periodic Monopole Arrays*, IEEE Transactions on Antennas and Propagation, v. AP-13, pp.840-885, November 1965.

9. Mitra, R., Jones, E.K., *How to Use k-β Diagrams in Log-Periodic Antenna Design*, MICROWAVES, pp.18-27, June 1965.

10. Greiser J.W., Mayes P.E., *The Bent Backfire Zigzag - A Vertically-Polarized Frequency Independent Antenna*, IEEE Transactions on Antennas and Propagation, v. AP-12, pp. 281-290, May 1964.

INITIAL DISTRIBUTION LIST

		No. Copies
1.	Defense Technical Information Center Cameron Station Alexandria, VA 22304-6145	2
2.	Library, Code 0142 Naval Postgraduate School Monterey, CA 93943-5002	2
3.	Chairman, Code 62 Department of Electrical and Computer Engineering Naval Postgraduate School Monterey, CA 93943-5000	1
4.	Director, Research Administration, Code 012 Naval Postgraduate School Monterey, CA 93943-5000	1
5.	Hermes Elecs. Ltd. Box 1005 Dartmouth, Nova Scotia	1
6.	Ant. Engrg. Austr. Pty. Ltd. Box 191 Croydon Victoria 3136 Australia	1
7.	Sanders Assoc., Inc. Daniel Webster Hwy. Nashua, NH 03061	1
8.	Dayton Granger Inc. P.O. Box 14070 Ft. Lauderdale, FL 33302	1
9.	GTE Government Systems 100 Ferguson Dr. Mountain View, CA 94042	1
10.	HY-GAIN Telex Coms. Inc. 8601 NE Hwy. Six Lincoln, NE 68505	1
11.	CRC/DRC, Bldg 2A, Rm 330 3701 Carling Ave, Box 11490 Sta.H, Ottawa, Ontario Canada K2H 8S2	1

12. R. W. Adler 8
Naval Postgraduate School, Code 62AB
Monterey, CA 93943

13. Richard D. Albus 1
IIT Research Institute
207 Woodloch Ln.
Severna Park, MD 21146

14. J. Ames 1
SRI-G174
333 Ravenswood Ave.
Menlo Park, CA 94025

15. R. Anders 1
Appl. Electromag. Eng.
Vorder Halden 11
D-7777 Salem 1, West Germany

16. Barker & Williamson 1
ATTN: SR Antenna DES ENG
10 Canal St.
Bristol, PA 19007

17. Andrew Corp. 1
ATTN: SR Antenna DES ENG
10500 W 153 St.
Orland Pk., IL 60462

18. Electrospace Systems Inc. 1
ATTN: SR Antenna DES ENG
Box 1359
Richardson, TX 75080

19. DHV/Antenna Prod Div 1
ATTN: SR Antenna DES ENG
Box 520
Mineral Wells, TX 76067

20. Foreign Sci. & Tech. Center 1
ATTN: AIFPM Army Department
220 7th St., NE
Charlottesville, VA 22901-5396

21. Dr. Harold W. Askins, Jr. 1
The Citadel
Department of Electrical Engineering
Charleston, SC 29409

22. Capt. W. P. Averill 1
U.S Naval Academy, Department of Electrical Engineering
Annapolis, MD 21402

23. Dr. Duncan C. Baker 1
University of Pretoria
Electrical and Computer Engineering Department
0002 Pretoria, S. Africa

24. Rajaev Bansal 1
University of Connecticut, EECS, U-157
260 Glenbrook Road
Stors, CT 06268

25. R. L. Bell 1
Antenna Products Corp.
101 S.E. 25th Avenue
Mineral Wells, TX 76067

26. John Belrose 1
CRC/DRC, Bldg. 2A, Rm. 330
3701 Carling Ave. Box 11490
STA.H, Ottawa, Ontario, Canada K2H8S2

27. Richard L. Bibey 1
Communications Engineering Service 1
1600 Wilson Blvd. #1003
Arlington, VA 22209

28. Thomas Birnbaum 1
OAR Corp. Eng. Dept.
10447 Roselle St.
San Diego, CA 92121

29. Comm. Research Center 1
ATTN: Bruce Blevins-DRC
STA.H 3701 Darling Ave. Box 11490
Ottawa, Ontario, Canada

30. Lawrence J. Blum 1
TECH. for COMM. INT'L
1625 Sterlin Road
Mountain View, CA 94043

31. L. Botha 1
NIAST/CSIR
P.O. Box 395
Pretoria, Rep. S.Africa 0001

32. Mr. Edwin Bramel 1
P.O. Box 722
Ft. Huachuca, AZ 85613

33. J. K. Breakall 1
Lawrence Livermore National Lab.
P.O. Box 5504, L-156
Livermore, CA 94550

34. G. Burke 1
Lawrence Livermore National Lab.
P.O. Box 5504, L-156
Livermore, CA 94550

35. J. Cahill 1
Shakespeare, ELEC&FIB DIV.
P.O. Box 733
Newberry, SC 29108

36. TRW Mil. Elex. Div. 1
ATTN: Donn Campbell
RC2/266 7X
San Diego, CA 92128

37. Mr. Brent Campbell 1
ECAC, MS 21
North Severn Naval Base
Annapolis, MD 21401

38. Al Christman 1
Ohio University
Stocker Center
Athens, OH 45701

39. Dawson Coblin 1
Lockheed M & S Co.
0/6242; B/130/ Box 3504
Sunnyvale, CA 94088-3504

40. Lee W. Corrington 1
Commander USAISEIC
ATTN: ASBI-STS
Ft. Huachuca, AZ 85613-7300

41. R. Corry 1
Commander USAISEIC/ASBI-STS
Ft. Huachuca, AZ 85613-7300

42. Roger A. Cox 1
TELEX Communications Inc.
8601 Northeast Hwy 6
Lincoln, NE 68505

43. Pete Cunnigham 1
US ARMY CECOM
ATTN: AMSEL-RD-COM-TA-1
Ft. Monmouth, NJ 07703

44. N. J. Damakos 1
P.O. Box 469
Concordville, PA 19331

45. Robert P. Eckert 1
Fed. Comm. Com.
2025 M Street, NW
Washington DC 20554

46. Wayne A. Essig 1
Naval Electronic Systems Com.
Code 51012
Washington D.C. 20360

47. Robert Everett 1
VOA/ESBA
601 D Street, NW
Washington D.C. 20547

48. Michael F. Evers 1
MFE Associates, Inc.
10403 Courthouse Dr.
Fairfax, VA 22030

49. Dave Faust 1
Eyring Research Institute
1455 W 820 N
Provo, UT 84601

50. Jerry Ferguson 1
Naval Ocean Systems Center
271 Catalina Blvd.
San Diego, CA 92151-5000

51. D. Fessenden 1
Naval Underwater Systems Center
New London Laboratory
New London, CT 06320

52. Mr. Richard G. Fitzgerrell 1
US Department of Commerce
OT/ITS
Boulder, CO 80302

53. Matthew Folkert 1
Radio Free Europe
1201 Conn Ave. NW, 405
Washington D.C. 20036

54. Paul Dean Ford 1
RR 12 Box 379
W. Terre Haute, IN 47885

55. Paul Gailey 1
The EC Corporation
575 Oak Ridge Turnpike
Oak Ridge, TN 37830

56. R. D. Gehring 1
137-124 Collins Rockwell
350 Collins Road NE
Cedar Rapids, IA 52498

57. S. Goodall 1
USA/CECOM/NET RADIO DIV.
Ft. Monmouth, NJ 07703

58. G.H Hagn 1
SRI International
1611 N. Kent Street
Arlington, VA 22209

59. R. C. Hansen 1
Box 215
Tarzana, CA 91336

60. Lawrence Harnish 1
SRI International
1611 N. Kent Street
Arlington, VA 22209

61. J. B. Hatfield 1
Hatfield & Dawson
4266 Sixth Ave., N.W.
Seattle, WA 98107

62. Jackie Ervin Hipp 1
S W Research Institute/EMA
P.O. Drawer 28510
San Antonio, TX 78284

63. H. Hochman/MS 4G12 1
GTE Sylvania
Box 7188
Mountain View, CA 94039

64. R.T. Hoverter 1
U.S. Army CECOM
AMSEL-COM-RN-R
Ft. Monmouth, NJ 07703

65. Fred Hubler 1
Rockwell International
885 35th Street NE
Cedar Rapids, IA 52498

66. D. E. Hudson 1
Lockheed Aircraft Ser. Co. Dept.1-330
P.O. Box 33
Ontario, CA 91761

67. Dwight Isbell 1
Boeing Co.
Box 3999, Mail Stop 47-35
Seattle, WA 98124

68. DELHD-N-EMA/ K. Coburn 1
Harry Diamond Lab.
2800 Powder Mill Rd.
Adelphi, MD 20783

69. S. W. Kershner 1
Kershner & Wright
5730 Gen. Washington Dr.
Alexandria, VA 22312

70. H. Kobayashi 1
Department of Commerce
179 Admiral Cochrane Dr.
Annapolis, MD 21401

71. Jim Lily 1
Litton/Amecon
5115 Calvert Rd.
College Park, MD 20740

72. Mr. Jim Logan 1
NOSC Code 822 (T)
271 Catalina Blvd.
San Diego, CA 92152

73. Janet McDonald 1
Commander USAISEIC/ASBI-STS
Ft. Huachuca, AZ 85613-7300

74. B. John Meloy 1
333 Ravenswood/Bldg. G
Menlo Park, CA 94025

75. E. K. Miller 1
Rockwell Science Center
Box 1085
Thousand Oaks, CA 91365

76. Dr. James Mink/DRXRO-EL 1
U.S. Army Research Office
P.O. Box 12211
Research Tri Pk. NC 27709

77. Lowell C. Minor 1
IIT Research Institute / ECAC
185 Admiral Cohrane Dr.
Annapolis, MD 21401

78. I. C. Olson 1
NOSC Code 822 (T)
271 Catalina Blvd.
San Diego, CA 92152

79. Martin L. Perrine 1
DOD-Radio Science Division
9800 Savage Road
Ft. George G. Meade, MD 20755

80. David J. Pinion 1
1215 S. Alfred Street
Los Angeles, CA 90035

81. Jim Cahill 1
Kershner, Wright & Hagaman
5730 Gen. Washington Dr.
Alexandria, VA 22312

82. J.J. Reaves, Jr. 1
NAVAL ELEC. SYS. ENG. CNTR.
4600 Marriot Drive
N. Charleston, SC 29413

83. Alfred Resnick 1
Capital Cities / ABC Radio
1345 Avenue of Americas / 27F
New York, NY 10105

84. R. B. Riegel 1
NSA
8806 Crandall Rd.
Lanham, MD 20801

85. T. Rouch 1
Microcube Corp.
Box 488
Leesburg, VA 22075

86. Joseph R. Romanosky 1
National Security Agency
R632 Electronic Engineer
Ft. Meade, MD 20755

87. R. Royce 1
Naval Research Lab
Washington D.C. 20375

88. G. M. Royer 1
COMM. Research Center
P.O. Box 11490
STN. H Ottawa, Ontario, Canada K2H8S2

89. D. Rucker 1
ESL
495 Java Drive, MS205
Sunnyvale, CA 94086

90. W. B. Seabreeze 1
202 Fletcher Rd.
Sterling, VA 22170

91. Ed Shea 1
CIA / DIR of COMM
Washington D.C. 20505

92. Kenneth Siarkiewicz 1
Rome Air Development Center, Code RBCT
Griffiss AFB, NY 13441

93. T. Simpson 1
University os S. Carolina
College of Engineering
Columbia, SC 29208

94. W. D. Stuart 1
IIT Research Institute
185 Admiral Cochrane Dr.
Annapolis, MD 21402

95. R. Tanner 1
TechnologyCom. Int'l
1625 Stierlin Rd.
Mountain View, CA 94043

96. Richard Tell 1
USEPA ORP
P.O.Box 18416
Las Vegas, NV 89114

97. Ric Thowless 1
NOSC Code 822 (T)
271 Catalina Blvd.
San Diego, CA 92152

98. Don Uffelman 1
MITRE, C3I Division
7525 Colshire Dr., MS 7405
McLean, VA 22102

99. C. H. Vandament 1
Rockwell International
802 Brentwood
Richardson, TX 75080

100. Dr. Ed Villaseca 1
Hughes Aircraft Co./ GD SYS
P.O. Box 3310
Fullerton, CA 92634

101. W. Perry Wheless Jr. 1
P.O. Box 3 CL
Las Cruces, NM 88003

102. TCI 1
ATTN: Dick Wray
1625 Stierlin Road
Mountain View, CA 94043

103. Mustafa Erdeviren 2
Kizlarpinari, Batman Sok, Bahar Apt. 5/4
Kecioren, Ankara, Turkey

104. K.K.K. ARGE Bsk.ligi 1
Bakanliklar, Ankara, Turkey

105. K.K.K Egitim K.ligi 1
Bakanliklar, Ankara, Turkey

106. Kara Harp Okulu K.ligi 1
Bakanliklar, Ankara, Turkey

107. Baily Aalfs 1
Sabre Comm. Corp.
P.O. Box 536
Sioux City, IO 51102

Thesis
E56625 Erdeviren
c.1 A computer model investigation of a square log-periodic array.